JSCSEN 75(10)1315–1461(2010)

Journal of the Serbian Chemical Society

Electronic version

VOLUME 75

No 10

BELGRADE 2010

Available on line at

www.shd.org.rs/JSCS/

The full search of JSCS is available through

DOAJ DIRECTORY OF OPEN ACCESS JOURNALS

www.doaj.org

Journal of the Serbian Chemical Society
JSCS-info@shd.org.rs • www.shd.org.rs/JSCS

J. Serb. Chem. Soc. Vol. 75, No. 10 (2010)

CONTENTS

Organic Chemistry

A. Zare, A. Hasaninejad, A. Parhami, A. R. Moosavi-Zare, F. Khedri, Z. Parsaee, M. Abdolalipoor-Saretoli, M. Khedri, M. Roshankar and *H. Deisi*: Ionic liquid 1-butyl--3-methylimidazolium bromide ([bmim]Br): a green and neutral reaction media for the efficient, catalyst-free synthesis of quinoxaline derivatives 1315

Y. Xia, Y. Zhang, W. Wang, Y. Ding and *R. He*: Synthesis and bioactivity of *erythro*--nordihydroguaiaretic acid, *threo*-(–)-saururenin and their analogues 1325

Biochemistry and Biotechnology

B. Nikolić, V. Tešević, I. Đorđević, M. Jadranin, M. Todosijević, S. *Bojović* and *P. D. Marin*: *n*-Alkanes in the needle waxes of *Pinus heldreichii* var. *pančići* 1337

J. S. Lazarević, R. M. Palić, N. S. Radulović, N. R. Ristić and *G. S. Stojanović*: Chemical composition and screening of the antimicrobial and antioxidative activity of extracts of *Stachys* species 1347

M. B. Hassanpouraghdam, G. R. Gohari, S. J. Tabatabaei and *M. R. Dadpour*: Inflorescence and leaves essential oil composition of hydroponically grown *Ocimum basilicum* L. 1361

Inorganic Chemistry

D. P. Singh, V. Malik, R. Kumar, K. Kumar and *S. S. Dhiman*: Synthesis, characterization and antibacterial and antifungal studies of some tetraazamacrocyclic complexes 1369

H. de Santana, L. Pelisson, D. R. Janiaski, C. T. B. V. Zaia and *D. A. M. Zaia*: UV Radiation and the reaction between ammonium and thiocyanate under prebiotic chemistry conditions 1381

Theoretical Chemistry

M. Haghdadi and *M. H. Fatemi*: Artificial neural network prediction of the psychometric activities of phenylalkylamines using DFT-calculated molecular descriptors 1391

H. Deng and *H. Xiao*: The Wiener polarity index of molecular graphs of alkanes with a given number of methyl groups 1405

Electrochemistry

V. V. Panić, A. B. Dekanski, V. B. Mišković-Stanković, S. K. Milonjić and *B. Ž. Nikolić*: Differences in the electrochemical behavior of ruthenium and iridium oxide in electrocatalytic coatings of activated titanium anodes prepared by the sol–gel procedure 1413

H. R. Zare, R. Samimi, N. Nasirizadeh and *M. Mazloum-Ardakani*: Preparation and electrochemical application of rutin biosensor for differential pulse voltammetric determination of NADH in the presence of acetaminophen 1421

M. D. Obradović: The electrochemical properties of carbon nanotubes and carbon XC-72R and their application as Pt supports (Extended abstract) 1435

Analytical Chemistry

Lj. Solomun, S. Ibrić, V. Vajs, I. Vučković and *Z. Vujić*: Methylprednisolone and its related substances in freeze-dried powders for injections 1441

Environmental

K. M. Šućur, M. P. Aničić, M. N. Tomašević, D. Z. Antanasijević, A. A. Perić-Grujić and *M. Dj. Ristić*: Urban deciduous tree leaves as biomonitors of trace element (As, V and Cd) atmospheric pollution in Belgrade, Serbia 1453

Published by the Serbian Chemical Society
Karnegijeva 4/III, 11000 Belgrade, Serbia
Printed by the Faculty of Technology and Metallurgy
Karnegijeva 4, P.O. Box 35-03, 11120 Belgrade, Serbia

Journal of the Serbian Chemical Society
JSCS-info@shd.org.rs • www.shd.org.rs/JSCS
J. Serb. Chem. Soc. *75* (10) 1315–1324 (2010)
JSCS–4054
UDC 547.863.11+544.478:544.354.3
Original scientific paper

Ionic liquid 1-butyl-3-methylimidazolium bromide ([bmim]Br): a green and neutral reaction media for the efficient, catalyst-free synthesis of quinoxaline derivatives

ABDOLKARIM ZARE[1]*, ALIREZA HASANINEJAD[2]*, ABOLFATH PARHAMI[1], AHMAD REZA MOOSAVI-ZARE[1], FATEMEH KHEDRI[1], ZAHRA PARSAEE[1], MAASOOMEH ABDOLALIPOOR-SARETOLI[1], MAASOOMEH KHEDRI[1], MEHRNOOSH ROSHANKAR[1] and HANAFIEH DEISI[1]

[1]*Department of Chemistry, Payame Noor University (PNU) and* [2]*Department of Chemistry, Faculty of Sciences, Persian Gulf University, Bushehr 75169, Iran*

(Received 14 October 2009, revised 12 June 2010)

Abstract: Quinoxaline derivatives were produced in excellent yields and short reaction times *via* the condensation of 1,2-diamines with 1,2-diketones in the neutral ionic liquid 1-butyl-3-methylimidazolium bromide ([bmim]Br) under catalyst-free and microwave irradiation conditions.

Keywords: quinoxaline; neutral ionic liquid; catalyst-free; 1,2-diamine; 1,2-diketone; green chemistry.

INTRODUCTION

Currently, catalyst-free reactions are the subject of considerable interest because of advantages such as ease of the experimental procedure as well as work-up, low cost, possibility of using acid- or base-sensitive substrates and environmentally benign processes.[1–21] This valuable technique has been applied in several chemical transformations, such as the self-assembly of carbon nanotubes, carbon nanowires and carbon filaments,[1] conjugate addition of thiols to electron deficient alkenes,[2] synthesis of dithiocarbamates,[3] synthesis of 10-aryl-2,7-dimethyl-4,5-dioxo-3,6,9-trioxa-3,4,5,6,9,10-hexahydroanthracenes,[4] synthesis of 2--substituted benzimidazoles and bis-benzimidazoles,[5] synthesis of di- and tri-substituted thiazoles,[6] synthesis of 2-aryl/alkyl-4(3*H*)-quinazolinones,[7] regioselective conversion of epoxides to vicinal halohydrins,[8] transesterification of triglycerides,[9] conversion of aldehydes to acylals,[10] synthesis of *N*-alkyl and *N*-arylimides,[11] α-amination of nitrogen heterocycles,[12] synthesis of 2-aminothiazoles,[13] *N*-Boc deprotection of *N*-Boc-amines,[14] condensation of indoles with alde-

* Corresponding authors. E-mails: abdolkarimzare@yahoo.com; ahassaninejad@yahoo.com
doi: 10.2298/JSC091014109Z

hydes,[15] synthesis of *N*-sulfonyl imines,[16] dehydration of benzyl alcohols into (*E*)-arylalkenes,[17] chemoselective oxidation of aryl alcohols/acetates,[18] synthesis of furo[2,3-*d*]pyrimidine-2,4(1*H*,3*H*)-diones,[19] synthesis of 3-acetoacetylcoumarin derivatives[20] and synthesis of bis-pyrazolo[3,4-*b*:4',3'-*e*]pyridines.[21]

The elimination of volatile organic solvents in organic synthesis is the most important goal in green chemistry. One of the most efficient protocols to reach this aim is the substitution of volatile solvents with ionic liquids.[22] In recent years, ionic liquids have received increasing attention as benign reaction media in organic synthesis due to their unique properties, including non-volatility, non-flammability, high thermal stability, high polarity because of their ionic nature, recyclability, non-contaminating nature and ability to dissolve a wide range of polar and non-polar materials.[22] The application of microwave irradiation in synthetic chemistry is a fast-growing research area since this method has opened up the possibility of realizing the fast synthesis of organic compounds.[23] From the perspective of microwave chemistry, the strong polar nature of ionic liquids makes them ideal reaction medium in microwave-assisted organic reactions.[15,16,22,23] Many interesting studies have recently been published in which the advantages of microwave irradiation and ionic liquids were combined.[15,16,22,23]

Quinoxalines have attracted great interest as they possess various biological activities, such as antimycobacterial,[24] antibacterial,[25] antifungal,[25] anthelmintic,[26] antidepressant[27] and antitumor.[28] These compounds have also been used for the preparation of various dyes.[29] The condensation of 1,2-diamines with 1,2-diketones has been used as a useful synthetic route toward quinoxalines. For this transformation, several catalysts and reagents have been reported, including *o*-iodoxybenzoic acid,[30] ceric(IV) ammonium nitrate,[31] $Yb(OTf)_3$,[32] zirconium tetrakis(dodecyl sulfate),[33] zeolite,[34] sulfamic acid/MeOH,[35] $(NH_4)_6Mo_7O_{24}\cdot 4H_2O$,[36] $H_6P_2W_{18}O_{62}\cdot 24H_2O$,[37] LiBr,[38] Zn[L-proline],[39] polyaniline-sulfate salt[40] and iodine in DMSO.[41] The condensation of 1,2-diamines with 1,2-diketones has been also realized using the acidic ionic liquid 1-butylimidazolium tetrafluoroborate as the solvent and catalyst.[42] However, in this work, a large amount of the ionic liquid was applied (2 mL of the ionic liquid per mmol of 1,2-diketone). Furthermore, the catalyst used in this study was similar to most employed catalysts, *i.e.*, an acidic catalyst.[42] Quinoxalines have also been prepared from benzene-1,2-diamine and 2-oxo-*N*-phenylalkane-thioamides using the acidic ionic liquid *N*,*N*,*N*-trimethyl-3-sulfo-1-propanaminimum hydrogen sulfate bearing two acidic group. In this work, among the different 1,2-diamines, only benzene-1,2-diamine was employed. Moreover, the preparation of the ionic liquid required a difficult two-steps procedure.[43] Other methods which have been applied for the synthesis of quinoxalines are heteroannulation of the nitroketene *N*,*S*-arylimino-acetals with $POCl_3$,[44] Bi-catalyzed oxidative coupling of epoxides with ene-1,2-diamines,[45] cyclization of 1,2-arylimino oximes of 1,2-dicarbonyl compounds[46]

and from α-hydroxy ketones *via* a tandem oxidation process using $Pd(OAc)_2$ or $RuCl_2(PPh_3)_3$–TEMPO.[47] However, many of the synthetic protocols reported so far suffer from disadvantages such as the use of expensive reagents, the necessity of anhydrous conditions, prolonged reaction times, unsatisfactory yields, difficult experimental as well as workup procedures, the use of expensive and detrimental metal precursors and incompatibility with green chemistry protocols. Moreover, some methods involve multi-steps procedures. Therefore, development of an efficient, novel, safe, simple and catalyst-free method for the preparation of quinoxaline derivatives is desirable.

As a part of our ongoing program to develop the application of catalyst-free techniques in organic synthesis,[15,16] herein, an efficient, green and simple catalyst-free method for the synthesis of quinoxaline derivatives from aromatic and aliphatic 1,2-diamines and 1,2-diketones in the neutral ionic liquid [bmim]Br under microwave irradiation is presented (Scheme 1). This synthesis represents a novelty in the synthesis of quinoxalines in a catalyst-free reaction in the neutral ionic liquid [bmim]Br, which is commercially available or easily prepared.

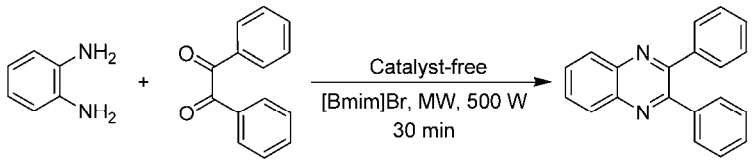

1a
95%

Scheme 1. The condensation of benzene-1,2-diamine with benzil.

RESULTS AND DISCUSSION

The condensation of benzene-1,2-diamine with benzil was selected as the model reaction to provide compound **1a**, for optimizing the reaction conditions (Scheme 1). At first, the model reaction was examined in [bmim]Br without a catalyst in an oil-bath (130 °C). However, under these conditions, the product was obtained in 69 % yield after 180 min. Changing the temperature or the reaction time did not increase the yield. Previously, the combination of microwave irradiation and ionic liquids was applied in several useful organic transformations.[15,16,22,23] Thus, it was decided to use this technique in the catalyst-free synthesis of quinoxalines. For this purpose, a mixture of benzene-1,2-diamine and benzil in [bmim]Br was irradiated in a microwave oven at a maximum of 500 W (130 °C). Interestingly, the reaction yield increased to 95 % under these conditions (Table I). To determine the most suitable media for the reaction, the microwave-assisted synthesis of quinoxaline **1a** was checked in different ionic liquids, 1-methylimidazole (as a precursor of the used ionic liquids) as well as under solvent-free conditions at a maximum of 500 W of microwave power (130

°C). The results are summarized in Table I, from which it can be seen that the highest yield of **1a** was obtained in [bmim]Br. The results showed that Br^- was the best anion part of the ionic liquid for the reaction, and *n*-butyl was the best alkyl chain of the cation part of the ionic liquid. Moreover, 1-methylimidazole cannot efficiently promote the reaction.

TABLE I. The condensation of benzene-1,2-diamine with benzil in some ionic liquids and 1-methylimidazole, as well as under solvent-free conditions

Entry	Solvent	Time, min	Yield[a], %
1	[bmim]Br	30	95
2	[bmim]Cl	30	88
3	[bmim]I	30	84
4	[hmim]Br[b]	30	89
5	[omim]Br[c]	30	82
6	1-Methylimidazole (25 mol %)[d]	30	73
7	Solvent-free	30	67

[a]Isolated yield; [b]1-hexyl-3-methylimidazolium bromide; [c]1-octyl-3-methylimidazolium bromide; [d]increase in amount of 1-methylimidazole did not improve the yield

To assess the generality and efficiency of the catalyst-free protocol, different aromatic and aliphatic 1,2-diamines were reacted with structurally diverse 1,2-diketones. The results are given in Table II, from which it can be seen that all reactions proceeded efficiently and the desired products were obtained in good to excellent yields and in short reaction times. It was observed that electron-releasing substituents on the aromatic ring of the aromatic 1,2-diamines had no significant influence on the reaction results (Table II, entries 7–12); however, electron-withdrawing substituents slightly decreased the yields (Table II, entry 13). Moreover, aliphatic 1,2-diamines afforded the corresponding quinoxaline derivatives in high yields (Table II, entry 16).

TABLE II. The catalyst-free preparation of quinoxaline derivatives from 1,2-diamines and 1,2-diketones

Entry	1,2-Diamine	Product[a]	Time, min	Yield[b], %	M.p., °C
1	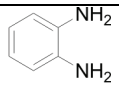	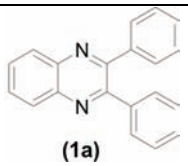 (1a)	30	95	130–131 (128–129)[30]
2		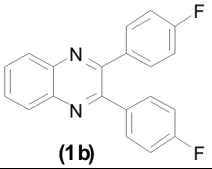 (1b)	30	96	132–134 (135–137)[30]

TABLE II. Continued

Entry	1,2-Diamine	Product[a]	Time, min	Yield[b], %	M.p., °C
3	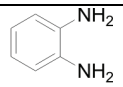	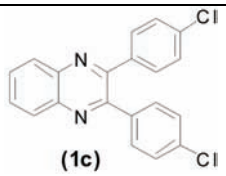 (1c)	30	94	191–193 (195–196)[39]
4		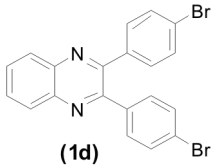 (1d)	32	87	188–190
5		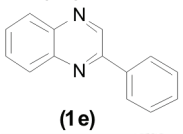 (1e)	35	90	75–77 (78)[35]
6		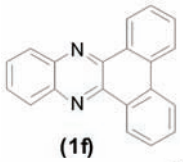 (1f)	30	83	228–230
7	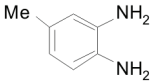	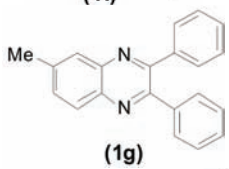 (1g)	30	96	116–117 (117–118)[30]
8		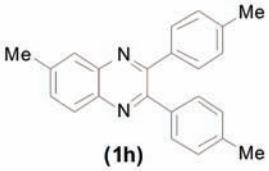 (1h)	35	87	139–140 (139–140)[36]
9		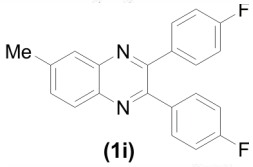 (1i)	30	95	164–166 (163–165)[33]
10		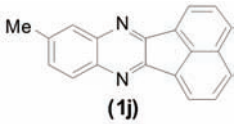 (1j)	30	86	233–235 (233–235)[38]

TABLE II. Continued

Entry	1,2-Diamine	Product[a]	Time, min	Yield[b], %	M.p., °C
11	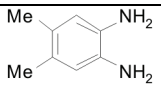	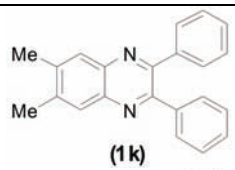 (1k)	25	96	176–178 (172)[35]
12		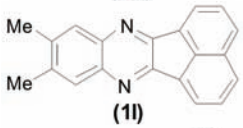 (1l)	30	91	301–303 (302–304)[33]
13	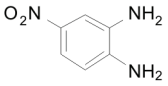	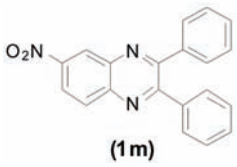 (1m)	30	78	190–192 (193–194)[30]
14	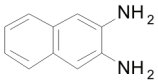	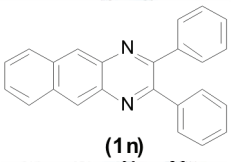 (1n)	30	92	184–186 (187–188)[31]
15		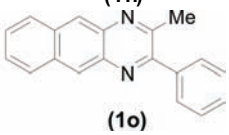 (1o)	40	85	132–134 (134)[31]
16	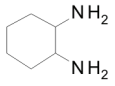	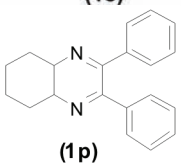 (1p)	40	84	168–170 (168–170)[33]

[a]The structures of known compounds were identified by comparison of their melting points and spectral data with those in the authentic samples; [b]isolated yield

The interesting behavior of ionic liquids lies in the fact that they can be re--used after simple washing with a suitable solvent, thus rendering the process more economical. The yields of compounds **1a** (model compound) in the 2nd, 3rd and 4th uses of [bmim]Br were almost as high as in the first use.

Selected spectral data of the products

*2,3-Diphenylquinoxaline (**1a**)*. White solid; yield: 95 %; m.p. 131–132 °C (lit.[30] m.p. 128–129 °C). Anal. Calcd. for $C_{20}H_{14}N_2$: C, 85.08; H, 5.00; N, 9.92 %. Found: C, 85.31; H, 5.16; N, 9.79 %. ^{1}H-NMR (250 MHz, $CDCl_3$, δ / ppm): 7.29–7.33 (6H, *m*), 7.48–7.54 (4H, *m*), 7.76–7.79 (2H, *m*), 8.20–8.23 (2H, *m*).

^{13}C-NMR (62.5 MHz, $CDCl_3$, δ / ppm): 128.1, 128.7, 129.1, 129.9, 131.0, 139.6, 141.7, 153.2.

*2,3-Bis(4-bromophenyl)quinoxaline (**1d**)*. Pale yellow solid; yield: 87 %; m.p. 188–190 °C. Anal. Calcd. for $C_{20}H_{12}Br_2N_2$: C, 54.58; H, 2.75; N, 6.36 %. Found: C, 54.79; H, 2.65; N, 6.25 %. ^{1}H-NMR (500 MHz, $CDCl_3$, δ / ppm): 7.45 (4H, *dd*, *J* = 8.5, 2.0 Hz), 7.62 (4H, *d*, *J* = 8.5 Hz), 7.88–7.92 (2H, *m*), 8.15–8.18 (2H, *m*). ^{13}C-NMR (125 MHz, $CDCl_3$, δ / ppm): 124.2, 129.7, 130.9, 131.6, 132.2, 138.0, 141.5, 152.9.

*Dibenzo[*a,c*]phenayine (**1f**)*. Pale yellow solid; yield: 83 %; m.p. 228–230 °C. Anal. Calcd. for $C_{20}H_{12}N_2$: C, 85.69; H, 4.31; N, 9.99 %. Found: C, 85.43; H, 4.19; N, 10.14 %. ^{1}H-NMR (500 MHz, $CDCl_3$, δ / ppm): 7.75–7.7.83 (4H, *m*), 7.86–7.89 (2H, *m*), 8.33–8.37 (2H, *m*), 8.54–8.57 (2H, *m*), 9.41 (2H, *dd*, *J* = 7.9, 1.4 Hz). ^{13}C-NMR (125 MHz, $CDCl_3$, δ / ppm): 123.3, 126.7, 128.3, 129.9, 130.2, 130.7, 130.7, 132.4, 142.6, 142.8.

*9-Methylacenaphtho[1,2-*b*]quinoxaline (**1j**)*. Pale yellow solid; yield: 86 %; m.p. 233–235 (lit.: 233–235 °C[38]). Anal. Calcd. for $C_{19}H_{12}N_2$: C, 85.05; H, 4.51; N, 10.44 %. Found: C, 85.23; H, 4.65; N, 10.32 %. ^{1}H-NMR (500 MHz, $CDCl_3$, δ / ppm): 2.60 (3H, *s*), 7.69 (1H, *d*, *J* = 7.8 Hz), 7.93–7.95 (2H, *m*), 8.00 (1H, *s*), 8.09–7.12 (1H, *m*), 8.27–8.31 (2H, *m*), 8.39–8.42 (2H, *m*). ^{13}C-NMR (125 MHz, $CDCl_3$, δ / ppm): 22.3, 121.8, 122.3, 129.0, 129.1, 129.2, 129.5, 129.7, 129.7, 130.4, 131.8, 132.4, 136.7, 140.0, 140.1, 141.8, 153.7, 154.3.

*9,10-Dimethylacenaphtho[1,2-*b*]quinoxaline (**1l**)*. Yellow solid; yield: 91 %; m.p. 301–303 °C (lit.[33] m.p. 302–304 °C). Anal. Calcd. for $C_{20}H_{14}N_2$: C, 85.08; H, 5.00; N, 9.92 %. Found: C, 84.81; H, 5.13; N, 10.09 %; ^{1}H-NMR (250 MHz, $CDCl_3$, δ / ppm): 2.51 (6H, *s*), 7.76–7.80 (2H, *m*), 7.89 (2H, *s*), 8.01–8.05 (2H, *m*), 8.32–8.36 (2H, *m*); ^{13}C-NMR (62.5 MHz, $CDCl_3$, δ / ppm): 20.3, 121.5, 127.8, 128.0, 128.6, 128.9, 129.1, 139.5, 140.00, 148.5, 153.3.

*2,3-Diphenylbenzo[*g*]quinoxaline (**1n**)*. Yellow solid; yield: 92 %; m.p. 184––186 °C (lit.[31] m.p. 187–188 °C). Anal. Calcd. for $C_{24}H_{16}N_2$: C, 86.72; H, 4.85; N, 8.43 %. Found: C, 86.52; H, 4.94; N, 8.31 %. ^{1}H-NMR (250 MHz, $CDC1_3$, δ / / ppm): 7.30–7.34 (6H, *m*), 7.48–7.53 (6H, *m*), 8.01–8.05 (2H, *m*), 8.59 (2H, *s*). ^{13}C-NMR (62.5 MHz, $CDCl_3$, δ / ppm): 126.5, 127.4, 128.0, 128.3, 129.0, 129.7, 133.8, 136.9, 139.4, 153.7.

EXPERIMENTAL

All chemicals were purchased from Merck or Fluka Chemical Companies. The ionic liquids were prepared according to reported methods.[48] All reactions were performed using a laboratory microwave oven (MicroSYNTH, Milestone Company, Italy). The ^{1}H-NMR (250 or 500 MHz) and ^{13}C-NMR (62.5 or 125 MHz) measurements were run on a Bruker Avance DPX-250 FT-NMR spectrometer. The microanalyses were realized on a Perkin-Elmer 240-B microanalyzer. The melting points were recorded on a Büchi B-545 apparatus in open capillary tubes.

General procedure for the catalyst-free preparation of quinoxalines

To a mixture of 1,2-diamine (6 mmol) and 1,2-diketone (6 mmol) in a microwave vessel was added [bmim]Br (2 g) and mixed carefully with a small rod. The resulting mixture was irradiated and stirred in a microwave oven at maximum of 500 W. The microwave oven was programmed to enhance the internal reaction temperature to 130 °C within 5 min, and then continue suitable irradiation (0–500 W) at this temperature, for the appropriate time. The combined times are showed in Table II. Subsequently, the reaction mixture was cooled to room temperature and extracted with Et_2O (3×50 mL). The combined organic extracts were then washed with brine (2×50 mL) and dried over $MgSO_4$. The solvent was evaporated to afford the pure product without any further purification or the crude product was recrystallized from EtOH (96 %) when required to give the pure product. After isolation of the product, the remaining Et_2O in [bmim]Br was evaporated and the ionic liquid was successfully employed for the next run under identical reaction conditions.

Acknowledgement. The authors thank the Payame Noor University (PNU) and the Persian Gulf University Research Councils for the financial support of this work.

ИЗВОД

ЈОНСКА ТЕЧНОСТ 1-БУТИЛ-3-МЕТИЛИМИДАЗОЛИЈУМ-БРОМИД ([bmim]Br): ЕКОЛОШКИ И НЕУТРАЛАН РАСТВАРАЧ ЗА ЕФИКАСНУ СИНТЕЗУ ДЕРИВАТА ХИНОКСАЛИНА БЕЗ КАТАЛИЗАТОРА

ABDOLKARIM ZARE[1]*, ALIREZA HASANINEJAD[2]*, ABOLFATH PARHAMI[1], AHMAD REZA MOOSAVI-ZARE[1], FATEMEH KHEDRI[1], ZAHRA PARSAEE[1], MAASOOMEH ABDOLALIPOOR-SARETOLI[1], MAASOOMEH KHEDRI[1], MEHRNOOSH ROSHANKAR[1] и HANAFIEH DEISI[1]

[1]*Department of Chemistry, Payame Noor University (PNU) и* [2]*Department of Chemistry, Faculty of Sciences, Persian Gulf University, Bushehr 75169, Iran*

Деривати хиноксалина добијени су у кратком реакционом времену и у високом приносу кондензацијом 1,2-диамина и 1,2-дикетона у неутралној јонској течности, без катализатора под условима озрачивања микроталасима.

(Примљено 14. октобра 2009, ревидирано 12. јуна 2010)

REFERENCES

1. a) J. J. Schneider, N. I. Maksimova, J. Engstler, R. Joshi, R. Schierholz, R. Feile, *Inorg. Chim. Acta* **361** (2008) 1770; b) N. J. K. Rantonen, T. Toyabe, T. Maekawa, *Carbon* **46** (2008) 1225
2. B. C. Ranu, S. S. Dey, A. Hajra, *Tetrahedron* **59** (2003) 2417
3. N. Azizi, F. Aryanasab, M. R. Saidi, *Org. Lett.* **8** (2006) 5275
4. Y. Gao, S. Tu, F. Shi, Q. Wang, X. Zhu, D. Shi, *Synth. Commun.* **37** (2007) 1603
5. C. Mukhopadhyay, P. K. Tapaswi, *Tetrahedron Lett.* **49** (2008) 6237
6. D. Zhu, J. Chen, H. Xiao, M. Liu, J. Ding, H. Wu, *Synth. Commun.* **39** (2009) 2895
7. M. Adib, S. Ansari, A. Mohammadi, H. R. Bijanzadeh, *Tetrahedron Lett.* **51** (2010) 30
8. B. C. Ranu, S. Banerjee, *J. Org. Chem.* **70** (2005) 4517
9. J. Geuens, J. M. Kremsner, B. A. Nebel, S. Schober, R. A. Dommisse, M. Mittelbach, S. Tavernier, C. O. Kappe, B. U. W. Maes, *Energy Fuels* **22** (2008) 643
10. J. S. Yadav, B. V. S. Reddy, P. Sreedhar, G. Kondaji, K. Nagaiah, *Catal. Commun.* **9** (2008) 590

11. J. Liang, J. Lv, J.-C. Fan, Z.-C. Shang, *Synth. Commun.* **39** (2009) 2822
12. V. Polshettiwar, R. S. Varma, *Tetrahedron Lett.* **49** (2008) 7165
13. T. M. Potewar, S. A. Ingale, K. V. Srinivasan, *Tetrahedron* **64** (2008) 5019
14. G. Wang, C. Li, J. Li, X. Jia, *Tetrahedron Lett.* **50** (2009) 1438
15. A. Zare, A. Parhami, A. R. Moosavi-Zare, A. Hasaninejad, A. Khalafi-Nezhad, M. H. Beyzavi, *Can. J. Chem.* **87** (2009) 416
16. A. Zare, A. R. Moosavi-Zare, A. Hasaninejad, A. Parhami, A. Khalafi-Nezhad, M. H. Beyzavi, *Synth. Commun.* **39** (2009) 3156
17. R. Kumar, A. Sharma, N. Sharma, V. Kumar, A. K. Sinha, *Eur. J. Org. Chem.* (2008) 5577
18. U. K. Sharma, N. Sharma, R. Kumar, R. Kumar, A. K. Sinha, *Org. Lett.* **11** (2009) 4846
19. A. Shaabani, E. Soleimani, M. Darvishi, *Monatsh. Chem.* **138** (2007) 43
20. D.-Q. Shi, Y. Zhou, S.-F. Rong, *Synth. Commun.* **39** (2009) 3500
21. D.-Q. Shia, F. Yang, *J. Chin. Chem. Soc.* **55** (2008) 755
22. a) P. Wasserscheid, T. Welton, *Ionic Liquids in Synthesis*, Wiley-VCH, Weinheim, 2003; b) K. Mikami, *Green Reaction Media in Organic Synthesis*, Blackwell Publishing, Oxford, 2005; c) T. Welton, *Chem. Rev.* **99** (1999) 2071
23. a) A. Loupy, *Microwaves in Organic Synthesis*, Wiley-VCH, Weinheim, 2006; b) A. Zare, A. Hasaninejad, R. Safinejad, A. R. Moosavi-Zare, A. Khalafi-Nezhad, M. H. Beyzavi, M. Miralai-Moredi, E. Dehghani, P. Kazerooni-Mojarrad, *ARKIVOC* **XVI** (2008) 51; c) A. Zare, A. Hasaninejad, A. R. Moosavi Zare, A. Parhami, H. Sharghi, A. Khalafi--Nezhad, *Can. J. Chem.* **85** (2007) 438; d) A. Zare, A. Hasaninejad, A. Khalafi-Nezhad, A. R. Moosavi Zare, A. Parhami, *ARKIVOC* **XIII** (2007) 105; e) X. Li, W. Eli, G. Li, *Catal. Commun.* **9** (2008) 2264; f) K. G. Mayo, E. H. Nearhoof, J. J. Kiddle, *Org. Lett.* **4** (2002) 1567; g) K. S. A. Vallin, P. Emilsson, M. Larhed, A. Hallberg, *J. Org. Chem.* **67** (2002) 6243; h) Y. Peng, G. Song, *Tetrahedron Lett.* **45** (2004) 5313; i) Y. Peng, G. Song, *Catal. Commun.* **8** (2007) 111; j) H. Berthold, T. Schotten, H. Honig, *Synthesis* (2002) 1607
24. a) K. Waisser, Z. Odlerova, R. Beckert, R. Mayer, *Pharmazie* **44** (1989) 234; b) L. E. Seitz, W. J. Suling, R. C. Reynolds, *J. Med. Chem.* **45** (2002) 5604
25. M. M. Badran, A. A. Moneer, H. M. Refaat, A. A. El-Malah, *J. Chin. Chem. Soc.* **54** (2007) 469
26. G. Sakata, K. Makino, Y. Karasawa, *Heterocycles* **27** (1988) 2481, and references cited therein
27. R. Sarges, H. R. Howard, R. C. Browne, L. A. Label, P. A. Seymour, *J. Med. Chem.* **33** (1990) 2240
28. a) S. T. Hazeldine, L. Polin, J. Kushner, J. Paluch, K. White, M. Edelstein, E. Palomino, T. H. Corbett, J. P. Horwitz, *J. Med. Chem.* **44** (2001) 1758; b) S. T. Hazeldine, L. Polin, J. Kushner, K. White, N. M. Bouregeois, B. Crantz, E. Palomino, T. H. Corbett, J. P. Horwitz, *J. Med. Chem.* **45** (2002) 3130
29. E. D. Brock, D. M. Lewis, T. I. Yousaf, H. H. Harper, (The Procter and Gamble Company, USA), WO Patent 9951688, 1999
30. M. M. Heravi, K. Bakhtiari, M. H. Tehrani, N. M. Javadi, H. A. Oskooie, *ARKIVOC* **XVI** (2006) 16
31. S. V. More, M. N. V. Sastry, C.-F. Yao, *Green Chem.* **8** (2006) 91
32. L. Wang, J. Liu, H. Tian, C. Qian, *Synth. Commun.* **34** (2004) 1349
33. A. Hasaninejad, A. Zare, M. A. Zolfigol, M. Shekouhy, *Synth. Commun.* **39** (2009) 569

34. D. Venugopal, M. Subrahmanmyam, *Catal. Commun.* **2** (2001) 219
35. H. R. Darabi, S. Mohandessi, K. Aghapoor, F. Mohsenzadeh, *Catal. Commun.* **8** (2007) 389
36. A. Hasaninejad, A. Zare, M. R. Mohammadizadeh, Z. Karami, *J. Iran. Chem. Soc.* **6** (2009) 153
37. M. M. Heravi, K. Bakhtiari, F. F. Bamoharram, M. H. Tehrani, *Monatsh. Chem.* **138** (2007) 465
38. A. Hasaninejad, A. Zare, M. R. Mohammadizadeh, M. Shekouhy, *Green Chem. Lett. Rev*. **3** (2010) 143
39. M. M. Heravi, M. H. Tehrani, K. Bakhtiari, H. A. Oskooie, *Catal. Commun.* **8** (2007) 1341
40. C. Srinivas, C. N. S. S. P. Kumar, V. J. Rao, S. Palaniappan, *J. Mol. Catal. A: Chem.* **265** (2007) 227
41. R. S. Bhosale, S. R. Sarda, S. S. Ardhapure, W. N. Jadhav, S. R. Bhusare, R. P. Pawar, *Tetrahedron Lett.* **46** (2005) 7183
42. T. M. Potewar, S. A. Ingale, K. V. Srinivasan, *Synth. Commun.* **38** (2008) 3601
43. F. Dong, G. Kai, F. Zhenghao, Z. Xinli, L. Zuliang, *Catal. Commun.* **9** (2008) 317
44. C. Venkatesh, B. Singh, P. K. Mahata, H. Ila, H. Junjappa, *Org. Lett.* **7** (2005) 2169
45. S. Antoniotti, E. Duńach, *Tetrahedron Lett.* **43** (2002) 3971
46. N. P. Xekoukoulotakis, C. P. Hadjiantoniu-Maroulis, A. J. Maroulis, *Tetrahedron Lett.* **41** (2000) 10299
47. R. S. Robinson, R. J. K. Taylor, *Synlett* (2005) 1003
48. (a) J. Dupont, C. S. Consorti, P. A. Z. Suarez, R. F. de Souza, *Org. Synth.* Coll. Vol. **10** (2004) 184; (b) X. Creary, E. D. Willis, *Org. Synth.* **82** (2005) 166.

Journal of the Serbian Chemical Society
JSCS-info@shd.org.rs • www.shd.org.rs/JSCS
J. Serb. Chem. Soc. *75* (10) 1325–1335 (2010)
JSCS–4055
UDC 542.913+57–188:547.474.4
Original scientific paper

Synthesis and bioactivity of *erythro*-nordihydroguaiaretic acid, *threo*-(–)-saururenin and their analogues

YAMU XIA[1]*, YUANYUAN ZHANG[1], WEI WANG[1], YINING DING[1] and RUI HE[2]

[1]*College of Chemical Engineering, Qingdao University of Science and Technology, Qingdao 266042 and* [2]*College of Mathematics and Physics, Qingdao University of Science and Technology, Qingdao 266042, P. R. China*

(Received 10 April, revised 11 June 2010)

Abstract: Full details of the total syntheses of *erythro*-nordihydroguaiaretic acid, *threo*-(–)-saururenin and their analogues are presented. The syntheses were based on a unified synthetic strategy involving the Stobbe reaction, alkylation to construct the skeleton of lignans and resolution of the *threo*- and *erythro*-isomers. The syntheses were achieved in eight to nine steps from simple aromatic precursors, and by this route 13 lignans were obtained. Among the synthesized lignans, seven lignans were natural products; moreover three of the seven natural products were synthesized for the first time. The effect of 13 lignans was examined on HIV Tat transactivation in human epithelial cells, HSV-1 gene and human leukemic, liver, prostate, stomach and breast cancer cell. Bioactivity results indicated that one product showed activity against the HIV gene and five compounds exhibited anti-HSV activity.

Keywords: synthesis; bioactivity; NDGA; saururenin.

INTRODUCTION

Lignans are a class of naturally occurring plant phenols that formally arise biosynthetically from two cinnamic acid (phenylpropanoid) residues, as defined originally by Howarth in 1936.[1] Lignans are found in all parts of plants, including the roots, stems, leaves, fruit and seeds, and they exhibit a wide range of biological activities, including antitumor, anti-inflammatory, immunosuppressive, cardiovascular, neuroprotective, neurotrophic, antioxidant and antiviral actions.[2] There is a growing interest in lignans and their synthetic derivatives due to applications in cancer chemotherapy and anti-virus therapy.[3,4]

Nordihydroguaiaretic acid (NDGA) is a naturally occurring lignan from the creosote bush (*Larrea tridentata*). NDGA has been utilized in traditional healing practices for a wide range of ailments and was licensed for use as a topical

* Corresponding author. E-mail: xiaym@qust.edu.cn
doi: 10.2298/JSC090410108X

treatment for actinic keratosis (Actinex, Chemex Pharmaceuticals, Denver, CO).[5,6] NDGA is a known antioxidant, a lipoxygenase inhibitor, and has also been shown to inhibit P450.[7–9] (–)-Saururenin is a *threo*-alkene, but different from *erythro*-NDGA, and was isolated from *Saururus cernuus* L., an aquatic weed commonly found in the eastern United States.[10] *Saururus cernuus* L. has been used in folk medicine as a sedative and as poultice for tumors.[11] More recently, much of the interest in NDGA, (–)-saururenin and their analogues centered on their role in anti-virus and anti-tumor activity. Hwu reported that NDGA and its analogues exhibited activity against HIV, and tetramethyl NDGA was a stronger anti-HIV agent.[12] Cheng *et al.* showed that in Vero cells, NDGA and its analogues inhibited the expression of the herpes immediate early gene, which is essential for HSV replication.[13] NDGA, (–)-saururenin and their analogues have also been shown to have cancer chemopreventive properties.[14–16]

NDGA, (–)-saururenin and their analogues have stimulated substantial synthetic efforts due to their biological activity. Lieberman *et al*. used the coupling of two molecules of 1-piperonyl-1-bromoethane as the key step to give the skeleton of NDGA.[17] Son *et al.* developed a modified procedure for the synthesis of NDGA and related lignans.[18] Gezginci and Timmermann reported the synthesis of *meso*-nordihydroguaiaretic acid from (3,4-dimethoxyphenyl)acetone using the low-valent Ti-induced carbonyl-coupling reaction of the ketone as the key step.[19] Rao *et al.* described the synthesis of analogues of (–)-saururenin from *Saururus cernuus*, together with (–)-austrobailignan-5 by regioselective cleavage of the methylenedioxyphenyl groups.[20] A synthetic route to NDGA and machilin A involving two Stobbe condensations to give the skeleton of lignan was reported.[21]

In this paper, an efficient approach for the chiral synthesis of NDGA, (–)-saururenin and their analogues is presented. By this method, 13 lignans were synthesized, among them, seven lignans were natural products and moreover three of the seven natural products were synthesized for the first time. The biological effect of the 13 lignans in their pure form was examined on HIV Tat transactivation in human epithelial cells, the HSV-1 gene and human leukemic, liver, prostate, stomach, and breast cancer cells. The bioactivity results indicated that some compounds exhibited better activities against the HIV and herpes virus. Finally, it should be emphasized that the bioactivity is affected by the skeleton configuration and functional groups.

RESULTS AND DISCUSSION

Synthesis of compounds

The starting materials were piperonal **1a** and veratraldehyde **1b**. Condensation of **1a** or **1b** with diethyl succinate in EtONa/EtOH solution afforded the benzylidene half-ester, which was followed by esterification to produce the diester **2a** or **2b**. Treatment of **2a** or **2b** in THF with LDA and 3,4-methylenedioxybenzyl bromide at –78 °C afforded the diester **3a** or **3b**. Then the compound **3a** or **3b**

was hydrolyzed to form the diacid. At this stage, the diacids were resolved *via* the quinine salt. The quinine salt of diacid (–)-**4a** or (–)-**4b** crystallized first. Concentration of the mother liquors gave a solid, which yielded the quinine salt of (+)-**4a'** or (+)-**4b'**. The diacid **4a** or **4b** was esterified to produce the diester (–)--**5a** or (–)-**5b**. The diester **5a** or **5b** was hydrogenated under a H_2 atmosphere, following by reduction with $LiAlH_4$ in THF to produce a readily separable mixture (approximately 1:1) of diols *threo*-(–)-**6a** and *erythro*-**7a** or *threo*-(–)-**6b** and *erythro*-(–)-**7b**. **7a** was a *meso*-compound and did not have optical rotation (Scheme 1). The spectral data were in agreement with those found in the literature.

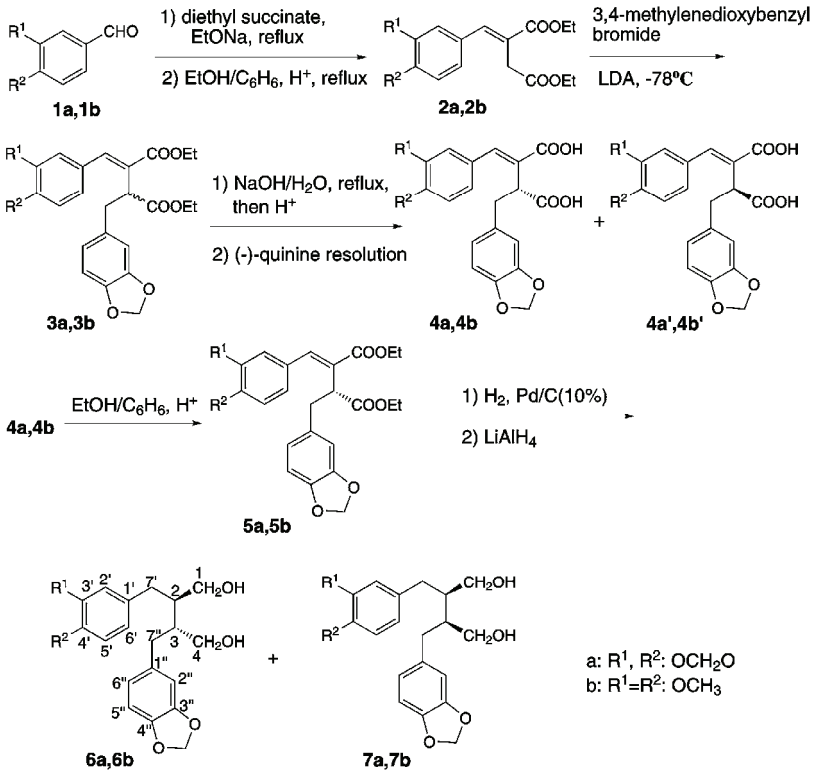

Scheme 1. Synthesis route of the compounds **2**–**7**. The starting materials were piperonal (**1a**) and veratraldehyde (**1b**). Condensation of **1a** or **1b** with diethyl succinate in EtONa/EtOH solution afforded the benzylidene half-ester, which was followed by esterification to produce the diester **2a** or **2b**. Treatment of **2a** or **2b** in THF with LDA and 3,4-methylenedioxybenzyl bromide at –78 °C afforded the diester **3a** or **3b**. Then compound **3a** or **3b** was hydrolyzed to form the diacid. At this stage, the diacids were resolved *via* the quinine salt. The quinine salt of diacid (–)-**4a** or (–)-**4b** crystallized first. Concentration of the mother liquors gave a solid, which yielded the quinine salt of (+)-**4a'** or (+)-**4b'**. The diacid **4a** or **4b** was esterified to produce diester (–)-**5a** or (–)-**5b**. The diester **5a** or **5b** was hydrogenated under an H_2 atmosphere, followed by reduction with $LiAlH_4$ in THF to produce a readily separable mixture (approximately 1:1) of diols *threo*-(–)-**6a** and *erythro*-**7a** or *threo*-(–)-**6b** and *erythro*-(–)-**7b**.

Reaction of diol *threo*-(–)-**6a** or *threo*-(–)-**6b** with equimolar amounts of TsCl in a dilute solution at room temperature gave the corresponding **8a** and **8b**, while diol *threo*-(–)-**6a** or *threo*-(–)-**6b** with TsCl in concentrated solution at 0 °C gave the ditoluenesulfonyl esters, which were reduced with $LiAlH_4$ in THF to provide **10a** and **10b**. On the other hand, etherification of **6a** or **6b** gave the compounds **9a** and **9b**. The compounds **11a**, **11b**, **12a**, **12b**, **13a** and **13b** were prepared in a similar manner. Compound **13a** was refluxed with PCl_5 in anhydrous CCl_4, followed by hydrolysis of the resulting dichloromethylene derivative with water to provide *meso*-nordihydroguaiaretic acid **14** (Schemes 2 and 3).

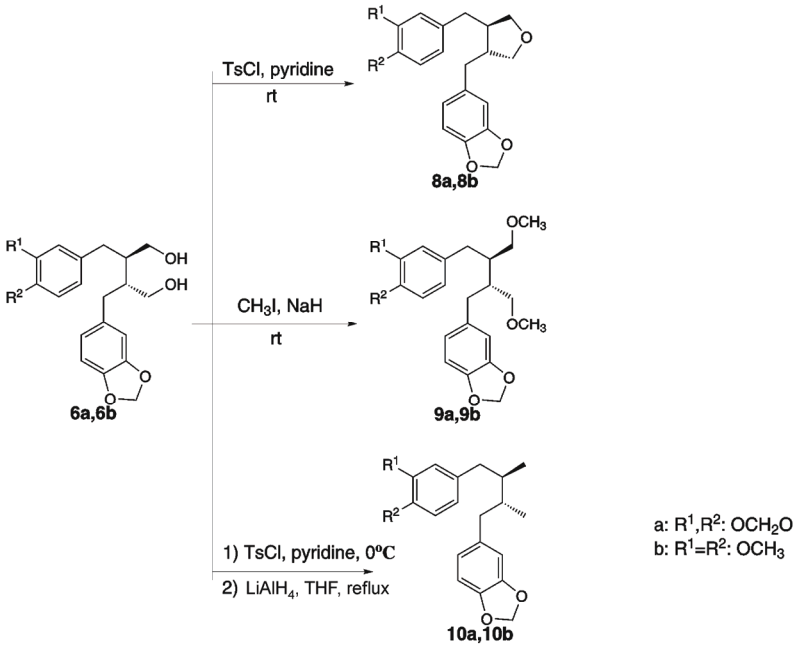

Scheme 2. Synthesis route of the compounds **8**–**10**. Reaction of diol *threo*-(–)-**6a** or *threo*-(–)-**6b** with an equimolar amount of TsCl in dilute solution at room temperature gave the corresponding **8a** and **8b**, while diol *threo*-(–)-**6a** or *threo*-(–)-**6b** with TsCl in concentrated solution at 0 °C gave the ditoluenesulfonyl esters, which were reduced with $LiAlH_4$ in THF to provide **10a** or **10b**. Etherification of **6a** or **6b** gave the compounds **9a** or **9b**.

The compounds **6a**, **6b**, **7b**, **10a**, **10b**, **13a** and **14** are natural products while compounds **7b**, **10b** and **13a** were synthesized for the first time.

Spectroscopic data of the synthesized compounds

The spectral data (Supplementary material) are in agreement with those already reported.[19]

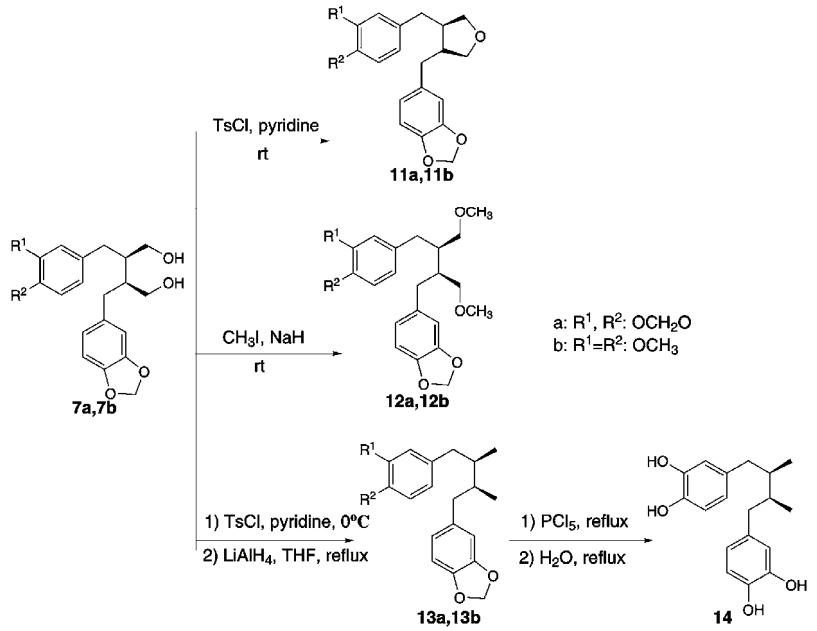

Scheme 3. Synthesis route of the compounds **11**–**14**. Etherification of **6a** or **6b** gave the compounds **9a** or **9b**. Compounds **11a**, **11b**, **12a**, **12b**, **13a** and **13b** were prepared similarly. Compound **13a** was refluxed with PCl5 in anhydrous CCl4, followed by hydrolysis of the resulting dichloromethylene derivative with water to provide *meso*-nordihydroguaiaretic acid (**14**).

Bioactivity

Antitumor activity. NDGA (**14**), (–)-saururenin (**10b**) and their analogues **8a**, **8b**, **9a**, **9b**, **10a**, **11a**, **11b**, **12a**, **12b**, **13a** and **13b** were evaluated *in vitro* against HL-60 human leukemic cells, PC-3MIE8 human prostatic carcinoma cells, BGC--823 human stomach cancer cells and MDA-MB-435 human breast cancer cell, and the assays of the lignans have been previously published.[27] The antitumor test indicated the inhibitory rates of tumor cell were less than 30 %, and the synthesized compounds showed no obvious antitumor activity.

Anti-HIV activity. The synthesized compounds were evaluated for their anti--HIV activity by determining their ability to inhibit the HIV Tat transactivation in *vitro*. The assay method was described previously.[28]

The compounds **8a**, **8b**, **9a**, **9b**, **10a**, **10b**, **11a**, **11b**, **12a**, **12b**, **13a**, **13b** and **14** were tested for their activities against the HIV and herpes viruses. The results showed that **9a** has activity against HIV-RT (IC_{50} = 160 μg ml^{-1}), while the other tested compounds exhibited no obvious activity.

Anti-HSV activity. The activity of the HSV-1 gene inhibitor was examined by measuring the extent of the process of Vero cells transfected with HSV-1 in

vitro. The assays of the compounds NDGA, (–)-saururenin and their analogues reported here were in agreement with those previously reported.[29] The results are given in Table I.

TABLE I. Anti-herpes virus activity of some of the synthesized compounds

Sample code	TC_{50} / μg ml^{-1}	IC_{50} / μg ml^{-1}	*SI*
10a	143.17	68.71	2.08
12a	231.12	143.10	1.61
12b	192.45	53.42	3.6
13a	111.11	111.10	1.0
14	12.35	4.12	3.0
Acyclovir	>250	1.66	>150.6

The compounds **10a**, **12a**, **12b**, **13a** and **14** showed activity against the herpes virus. The IC_{50} values of **10a** and **12b** were less than 100 μg ml^{-1}, and compound **14** with an IC_{50} value of 4.12 μg ml^{-1} exhibited better bioactivity against the herpes virus. The results showed that the *erythro*-structure was good for antiviral activity; however, the compounds with tetrahydrofuran ring did not exhibit activity, which showed that the tetrahydrofuran ring appears suitable for lowering the cytotoxicity. On the other hand, the results showed that the data of *SI* was much lower. Thus, SI should be enhanced in a later study on structure–function relationships in order to increase the selectivity of the activity.

EXPERIMENTAL

The melting points were measured on a Gallenkamp melting point apparatus and are uncorrected. The optical rotation values were determined on a Perkin-Elmer 341 polarimeter. Infrared spectra were recorded on a Nicolet Nexus 670 FT−IR. The ^{1}H-NMR and ^{13}C-NMR spectra were recorded on Brucker AM−400, Mercury Plus−300 and Avance–200 spectrometers. The mass spectra were recorded on a ZAB−HS spectrometer. The HRMS were obtained on a Bruker Daltonics APEXII47e spectrometer. Flash column chromatography was performed on silica gel (200–300 mesh) and TLC inspections on silica gel GF254 plates.

*Diethyl 2-(3,4-methylenedioxybenzylidene)succinate (**2a**)*

Piperonal (**1a**) (15.0 g, 100 mmol) and diethyl succinate (17.4 g, 100 mmol) were added to a solution of NaOEt (13.6 g, 200 mmol) in EtOH (200 ml). After refluxing for 4 h, the EtOH was removed. The residue was cooled and acidified with HCl (5 M). The mixture was extracted with EtOAc (3×80 ml). The EtOAc layer was then re-extracted with a saturated $NaHCO_3$ solution (100 ml). The $NaHCO_3$ extract was acidified with HCl and the pH value was adjusted to 2. Then the obtained oily layer was again extracted with AcOEt (3×100 ml). The combined organic layer was dried and concentrated *in vacuo*. This residue was then added to a mixture of EtOH (250 ml), benzene (100 ml), and H_2SO_4 (2 ml), then refluxed in a Dean Stark apparatus for 24 h. The mixture was concentrated *in vacuo* and extracted with EtOAc (200 ml), then washed with a saturated $NaHCO_3$ solution (3×50 ml). The extract was dried over $MgSO_4$ and concentrated *in vacuo*. Flash column chromatography of the residue afforded compound **2a** as a yellow oil (28.2 g). Yield: 92 %.

*Diethyl 2-(3,4-dimethoxybenzylidene)succinate (**2b**)*

Following the procedure described for the preparation of **2a** but starting with veratraldehyde (**1b**) (16.6 g, 100 mmol), compound **2b** was obtained as a yellow oil (29.6 g). Yield: 92 %.

*Diethyl 2-(3,4-methylenedioxybenzyl)-3-(3,4-methylenedioxybenzylidene)succinate (**3a**)*

To a well-stirred solution of **2a** (24.5 g, 80 mmol) in THF (100 ml) was added dropwise a solution of LDA (80 mmol, 2 M) in THF at –78 °C under a N_2 atmosphere. The mixture was stirred at this temperature for 20 min, then 3,4-methylenedioxybenzyl bromide (17.2 g, 80 mmol) in THF (50 ml) was added. The mixture was stirred at –78 °C for 2 h. The mixture was quenched with a saturated NH_4Cl solution (100 ml). After warming to room temperature, the mixture was extracted with CH_2Cl_2 (3×80 ml) and the organic layer was dried over $MgSO_4$ and concentrated *in vacuo*. Flash chromatography of the residue over silica gel gave compound **3a** as white crystals (31.6 g). Yield: 90 %.

*Diethyl 2-(3,4-dimethoxybenzylidene)-3-(3,4-methylenedioxybenzyl)succinate (**3b**)*

Following the procedure described for the preparation of **3a** but starting with **2b** (25.8 g, 80 mmol), compound **3b** was obtained as a yellowish oil (31.7 g). Yield: 87 %.

*(–)-2-(3,4-Methylenedioxybenzyl)-3-(3,4-methylenedioxybenzylidene)succi-nic acid (**4a**)*

Diester **3a** (26.4 g, 60 mmol) was added to a 20 % aqueous solution of NaOH (250 ml) and refluxed for 3 h. After cooling to room temperature, the mixture was washed with EtOAc (3×30 ml). After decolorizing with active carbon, the mixture was acidified with HCl (2 M) whereby white solids were obtained. The crude product was crystallized from HOAc to give the (±)-diacid **4a**. The (±)-diacid **4a** and (–)-quinine (38.9 g, 120 mmol) in ethanol (120 ml) were refluxed for 1 h. The reaction mixture was allowed to cool slowly to room temperature, whereby fine white crystals were obtained. After two recrystallizations from ethanol, the solid was added to a solution of HCl (2 M, 100 ml) and stirred for 1 h. The mixture was extracted with EtOAc (3×80 ml) and the extract was dried over $MgSO_4$ and the solvent evaporated. The white solid was recrystallized from EtOAc to yield the (–)-diacid **4a** as white crystals (10.1 g). Yield: 44 %.

The white solids obtained by concentrating the mother liquors were recrystallized twice from methanol and water to yield the (+)-diacid **4a'** as white crystals (9.0 g). Yield: 39 %.

*(–)-2-(3,4-Dimethoxybenzylidene)-3-(3,4-methylenedioxybenzyl)succinic acid (**4b**)*

Following the procedure described for the preparation of **4a** but starting with the diester **3b** (27.4 g, 60 mmol), the (–)-diacid **4b** was obtained as white crystals (10.8 g). Yield: 45%.

The (+)-diacid **4b'** was obtained as white crystals (9.2 g). Yield: 38 %.

*(–)-Diethyl 2-(3,4-methylenedioxybenzyl)-3-(3,4-methylenedioxybenzylidene)succinate (**5a**)*

To 151 ml of a mixture of EtOH:benzene:H_2SO_4 (100:50:1) was added **4a** (7.7 g, 20 mmol). The mixture was refluxed in a Dean–Stark apparatus for 36 h to remove the water. The reaction mixture was concentrated *in vacuo*, extracted with EtOAc (100 ml) and then neutralized with a saturated $NaHCO_3$ solution (3×30 ml). The extract was dried over $MgSO_4$ and concentrated *in vacuo*. Flash column chromatography of the residue gave the (–)-diester **5a** as a colorless oil (8. 0 g). Yield: 91 %.

*(–)-Diethyl 2-(3,4-methylenedioxybenzyl)-3-(3,4-dimethoxybenzylidene)succinate (**5b**)*

Following the procedure described for the preparation of **5a** but starting with the diester **4b** (8.0 g, 20 mmol), the diacid **5b** was obtained as a colorless oil (8.2 g). Yield: 90 %.

*(–)-Dihydrocubebin (**6a**) and* meso*-2,3-Bis(3,4-methylenedioxybenzyl)butane-1,4-diol (**7a**)*

The (–)-diester **5a** (7.1 g, 16 mmol) in ethyl acetate (200 ml) was stirred under a hydrogen atmosphere for 12 h in the presence of 10 % Pd/C (0.7 g). The reaction mixture was filtered through a pad of Celite and the solvent was removed *in vacuo* to give a white solid. The solid was dissolved in dry THF (80 ml) and added to a stirred suspension of $LiAlH_4$ (1.4 g, 36 mmol). The mixture was stirred for 10 h. Then the reaction was quenched by ice water and filtered. The filtrate was dried over $MgSO_4$ and concentrated *in vacuo*. Flash column chromatography of the residue gave *threo*-(–)-**6a** (2.7 g, yield: 47 %) as white crystals and *erythro*-**7a** (2.6 g, yield: 46 %) as a colorless oil.

*(2*R*,3*R*)-2-(3,4-Dimethoxybenzyl)-3-(3,4-methylenedioxybenzyl)-1,4-butanediol (**6b**) and (2*R*,3*S*)-2-(3,4-Dimethoxybenzyl)-3-(3,4-methylenedioxybenzyl)-1,4-butanediol (**7b**)*

Following the procedure described for the preparation of **6a** and **7a** but starting with the diester **5b** (7.3 g, 16 mmol), **6b** (2.6 g, yield: 44 %) and **7b** (2.9 g, yield: 48 %) were obtained as colorless oils.

*(–)-Dehydroxycubebin (**8a**)*

To a solution of (–)-diol **6a** (0.36 g, 1 mmol) and pyridine (0.08 g, 1 mmol) in CH_2Cl_2 (25 ml) was added TsCl (0.19 g, 1 mmol) in CH_2Cl_2 (20 ml) at room temperature. The mixture was stirred for 24 h, quenched with HCl (2 M) and extracted with CH_2Cl_2 (3×20 ml). The organic layer was dried over $MgSO_4$ and concentrated *in vacuo*. Flash column chromategraphy of the residue gave (–)-dehydroxycubebin **(8a)** as a colorless oil (0.26 g). Yield: 76 %.

*(–)-5-{[(3*R*,4*R*)-4-(3,4-Dimethoxybenzyl)-tetrahydro-3-furanyl]methyl}-1,3-benzodioxole (**8b**)*

Following the procedure described for the preparation of (–)-dehydroxycubebin (**8a**) but starting with **6b** (0.37 g, 1.0 mmol), compound **8b** was obtained as a colorless oil (0.27 g). Yield: 75 %.

*(+)-5.5'-[(2*R*,3*R*)-2,3-Bis(methoxymethyl)-1,4-butanediyl]bis(1,3-dioxole) (**9a**)*

To a mixture of NaH (1 mmol) and **6a** (0.36g, 1 mmol) in THF (30 ml) was added CH_3I (2 mmol). The mixture was stirred for 7 h at room temperature, quenched with a saturated NH_4Cl solution (20 ml) and then extracted with CH_2Cl_2 (3×20 ml). The organic layer was dried over $MgSO_4$ and concentrated *in vacuo*. Flash column chromatography of the residue gave **9a** as a colorless oil (0.33 g). Yield: 85 %;

*(+)-5-[(2-(2*R*,3*R*)-4-(3,4-Dimethoxybenzyl)-2,3-bis(methoxymethyl)-butyl]-1,3-benzodioxole (**9b**)*

Following the procedure described for the preparation of **9a** but starting with **6b** (0.37 g, 1 mmol), compound **9b** was obtained as a colorless oil (0.35 g). Yield: 88 %.

*(–)-Austrobailignan-5 (**10a**)*

To a solution of (–)-diol **6a** (0.72 g, 2.0 mmol) in pyridine (2.5 ml) was added TsCl (0.76 g, 4 mmol) at 0 °C The mixture was stirred at this temperature for 4 h, acidified with HCl (2 M, 20 ml) and extracted with EtOAc (3×20 ml). The organic layer was washed with a saturated NaCl solution (20 ml), dried over $MgSO_4$ and concentrated *in vacuo* to give the crude ditoluenesulfonyl ester. A mixture of this ditoluenesulfonyl ester and $LiAlH_4$ (0.20 g, 5.0 mmol) in dry THF (30 ml) was refluxed for 6 h, the mixture quenched with ice-water, filtered and then concentrated *in vacuo*. Flash column chromatography of the residue gave **10a** as white crystals (0.56 g). Yield: 86 %.

*(–)-Saururenin (**10b**)*

Following the procedure described for the preparation of **10a** but starting with the diester **6b** (0.75 g, 2 mmol), compound **10b** was obtained as a colorless oil (0.6 g). Yield: 87 %.

meso-*5,5'-[(Tetrahydro-3,4-furandiyl)bis(methylene)]bis(1,3-benzodioxole) (**11a**)*

Following the procedure described for the preparation of **8a**, compound **7a** (0.36 g, 1 mmol) was used as the starting material to give compound **11a** as a colorless oil (0.25 g). Yield: 74 %.

*(+)-5-{[(3*S*,4*R*)-4-[(3,4-Dimethoxyphenyl)methyl]tetrahydro-3-furanyl]methyl}-1,3--benzodioxole (**11b**)*

Following the procedure described for the preparation of **8a** but starting with **7b** (0.37 g, 1 mmol), compound **11b** was obtained as a colorless oil (0.26 g). Yield: 72 %

meso-*5,5'-[Bis(methoxymethyl)-1,4-butanediyl]bis(1,3-benzodioxole) (**12a**)*

Following the procedure described for the preparation of **9a** but starting with **7a** (0.36 g, 1 mmol), compound **12a** was obtained as a colorless oil (0.32 g). Yield: 82 %.

*(+)-5-{[(3*S*,4*R*)-4-[(3,4-Dimethoxyphenyl)-2,3-bis(methoxymetyl)butyl]-1,3-benzodioxole (**12b**)*

Following the procedure described for the preparation of **9a** but starting with **7b** (0.37 g, 1 mmol), compound **12b** was obtained as a colorless oil (0.34 g). Yield: 85 %.

meso-*Machilin A (**13a**)*

Following the procedure described for the preparation of **10a**, compound **7a** (1.07 g, 3 mmol) was used as starting material to give *meso*-machilin A (**4**) as white crystals (0.87 g). Yield: 89 %.

*(–)-Isosaururenin (**13b**)*

Following the procedure described for the preparation of **10a** but starting with **7b** (0.75 g, 2 mmol), compound **13b** was obtained as a colorless oil (0.55 g). Yield: 81 %.

meso-*Nordihydroguaiaretic acid (**14**)*

Compound **13a** (0.65 g, 2 mmol) was dissolved in dry CCl_4 (50 ml), PCl_5 (2.50 g, 12 mmol) was then added. The mixture was refluxed for 10 h under a nitrogen atmosphere. The amber-colored solution was concentrated *in vacuo* and then ice water (15 ml) was added slowly into the residue and refluxed for 5 h under a nitrogen atmosphere. A white solid appeared slowly in the solution, which was collected, washed with water and crystallized from ethanol to give *meso*-nordihydroguaiaretic acid (**14**) as white crystals (0.51 g). Yield: 85 %.

CONCLUSIONS

In summary, an efficient chiral synthetic method was developed to give NDGA, (–)-saururenin and their analogues. With cheap materials, short experimental procedures, mild conditions and simple operations, the route will exhibit more potential value in the future.

SUPPLEMENTARY MATERIAL

Spectroscopic data of the synthesized compounds are available electronically from http://www.shd.org.rs/JSCS/, or from the corresponding author on request.

Acknowledgements. This work was financially supported by the foundation of State Key Laboratory of Applied Organic Chemistry of China (No. 200708) and the National Natural

Science Foundation of Shandong (No. 2006Q02). Peking University School of Pharmaceutical Sciences is kindly acknowledged for evaluation of our compounds in their human tumor cell line screening panel and The National Center for Drug Screening is acknowledged for the anti-HIV and anti-HSV assay of the compounds.

ИЗВОД

СИНТЕЗА И БИОЛОШКА АКТИВНОСТ *erythro*-НОРДИХИДРОГВАЈАРЕТИЧНЕ КИСЕЛИНЕ, *threo*-САУРУРЕНИНА И ЊИХОВИХ АНАЛОГА

YAMU XIA[1], YUANYUAN ZHANG[1], WEI WANG[1], YINING DING[1] и RUI HE[2]

[1]*College of Chemical Engineering, Qingdao University of Science and Technology, Qingdao 266042 и* [2]*College of Mathematics and Physics, Qingdao University of Science and Technology, Qingdao 266042, P. R. China*

У раду је дат детаљан приказ тоталне синтезе *erythro*-нордихидрогвајаретичне киселине, *threo*-(–)-саууренина и њихових аналога. Општа синтетичка стратегија која је примењена заснива се на Stobbe-овој реакцији, алкиловању у циљу изградње лигнанског скелета и раздвајању *threo*- и *erythro*-изомера. Синтеза 13 лигнана је остварена у 8–9 синтетичких фаза коришћењем једноставних ароматичних прекурсора. Од добијених лигнана седам су природни производи од којих је за три урађена прва синтеза у овом раду. Испитан је утицај свих добијених лигнана на HIV Tat трансактивацију у хуманим епителним ћелијама, HSV-1 ген и ћелије хумане леукемије, рака јетре, простате, желуца и дојке. Резултати биолошких испитивања указују да један производ показује активност према HIV-у а пет једињења поседују анти-HSV активност.

(Примљено 10. априла, ревидирано 11. јуна 2010)

REFERENCES

1. R. D. Howarth, *Annu. Rep. Prog. Chem.* **33** (1936) 266
2. M. Saleem, H. J. Kim, M. S. Ali, Y. S. Lee, *Nat. Prod. Rep.* **22** (2005) 696
3. N. Li, J. Wu, T. Hasegawa, J. Sakai, L. Bai, L. Wang, S. Kakuta, Y. Furuya, H. Ogura, T. Kataoka, A. Tomida, T. M. Tsuruo, *J. Nat. Prod.* **70** (2007) 544
4. G. Zhang, N. Li, Y. Wang, Y. Zheng, Z. Zhang, M. Wang, *J. Nat. Prod.* **70** (2007) 662
5. S. Arteaga, A. Andrade-Cetto, R. Cardenas, *J. Ethnopharmacol.* **98** (2005) 231
6. J. D. Lambert, R. T. Dorr, B. N. Timmermann, *Pharm. Biol.* **42** (2004) 149
7. J. L. Billinsky, E. S. Krol, *J. Nat. Prod.* **71** (2008) 1612
8. W. Tong, X. Ding, T. E. Adrian, *Biochem. Biophys. Res. Commun.* **296** (2002) 942
9. R. Agarwal, Z. Y. Wang, D. P. Bik, H. Mukhtar, *Drug Metab. Dispos.* **19** (1991) 620
10. K. V. Rao, N. S. P. Rao, *J. Nat. Prod.* **53** (1990) 212
11. K. V. Rao, F. M. Alvarez, *J. Nat. Prod.* **45** (1982) 393
12. J. R. Hwu, W. N. Tseng, J. Gnabre, P. Giza, R. C. C. Huang, *J. Med. Chem.* **41** (1998) 2994
13. H. S. Cheng, L. Teng, J. N. Li, R. Park, D. E. Mold, J. Gnabre, J. R. Hwu, W. N. Tseng, R. C. C. Huang, *J. Med. Chem.* **41** (1998) 3001
14. S. Whitman, M. Gezginci, B. N. Timmermann, T. R. Holman, *J. Med. Chem.* **45** (2002) 2659
15. T. W. Moody, J. Leyton, A. Martinez, S. Hong, A. Mallkinson, J. L. Mulshine, *Exp. Lung Res.* **24** (1998) 617
16. J. Chang, J. Reiner, J. X. Xie, *Chem. Rev.* **105** (2005) 4581

17. S. V. Lieberman, G. P. Mueller, E. T. Stiller, *J. Am. Chem. Soc.* **69** (1947) 1540
18. J. K. Son, S. H. Lee, L. Nagarapu, Y. Jahng, *Bull. Korean Chem. Soc.* **26** (2005) 1117
19. M. H. Gezginci, B. N. Timmermann, *Tetrahedron Lett.* **42** (2001) 6083
20. K. V. Rao, S. K. Chattopadhyay, *J. Org. Chem.* **55** (1990) 1427
21. Y. M. Xia, Q. Wang, Y. N. Din, F. K. Yang, X. P. Cao, *Chin. J. Org. Chem.* **28** (2008) 1040
22. A. S. R. Anjaneyulu, P. A. Ramaiah, L. R. Row, R. Venkateswarlu, A. Pelter, R. S. Ward, *Tetrahedron* **37** (1981) 3641
23. M. J. Kato, M. Yoshida, O. R. Gottlieb, *Phytochemistry* **31** (1992) 283
24. P. Satyanarayana, S. Venkateswarlu, *Tetrahedron* **47** (1991) 8931
25. S. T. Murphy, E. Ritchie, W. C. Taylor, *Aust. J. Chem.* **28** (1975) 81
26. H. Shimomura, Y. Sashida, M. Oohara, *Phytochemistry* **26** (1987) 1513
27. J. L. Wu, N. Li, T. Hasegawa, J. Sakai, S. Kakuta, W. Tang, S. Oka, M. Kiuchi, H. Ogura, T. Kataoka, A. Tomida, T. Tsuruo, M. Ando, *J. Nat. Prod.* **68** (2005) 1656
28. G. T. Tan, J. M. Pezzuto, A. D. Kinghorn, S. H. Hughes, *J. Nat. Prod.* **54** (1991) 143
29. R. Dulbeccok, *Proc. Natl. Acad. Sci. U.S.A.* **38** (1952) 747.

Journal of the Serbian Chemical Society
JSCS@tmf.bg.ac.rs • www.shd.org.rs/JSCS

J. Serb. Chem. Soc. 75 (10) S1–S6 (2010)

Supplementary material

SUPPLEMENTARY MATERIAL TO

Synthesis and bioactivity of *erythro*-nordihydroguaiaretic acid, *threo*-(–)-saururenin and their analogues

YAMU XIA[1]*, YUANYUAN ZHANG[1], WEI WANG[1], YINING DING[1] and RUI HE[2]

[1]*College of Chemical Engineering, Qingdao University of Science and Technology, Qingdao 266042 and* [2]*College of Mathematics and Physics, Qingdao University of Science and Technology, Qingdao 266042, P. R. China*

J. Serb. Chem. Soc. 75 (10) (2010) 1325–1335

SPECTROSCOPIC DATA OF THE SYNTHESIZED COMPOUNDS

*Diethyl 2-(3,4-methylenedioxybenzylidene)succinate (**2a**)*. ^{1}H-NMR (200 MHz, $CDCl_3$, δ / ppm): 1.22 (3H, *t*, *J* = 7.3 Hz), 1.29 (3H, *t*, *J* = 7.3 Hz,), 3.51 (2H, *s*), 4.16 (2H, *q*, *J* = 7.3 Hz), 4.27 (2H, *q*, *J* = 7.3 Hz), 5.96 (2H, *s*), 6.76−6.87 (3H, *m*), 7.76 (1H, *s*). EI-MS (*m*/*z*, %): 306 (M^+, 70), 261 (20), 232 (34), 203 (52), 175 (59), 159 (100).

*Diethyl 2-(3,4-dimethoxybenzylidene)succinate (**2b**)*. ^{1}H-NMR (200 MHz, $CDCl_3$, δ / ppm): 1.33 (3H, *t*, *J* = 7.3 Hz), 1.26 (3H, *t*, *J* = 7.2 Hz), 3.58 (2H, *s*), 3.87 (3H, *s*), 3.90 (3H, *s*), 4.21 (2H, *q*, *J* = 7.3 Hz), 4.27 (2H, *q*, *J* = 7.3 Hz), 6.86−7.00 (3H, *m*), 7.84 (1H, *s*). EI-MS (*m*/*z*, %): 322 (M^+, 42), 276 (14), 249 (16), 175 (100).

*Diethyl 2-(3,4-methylenedioxybenzyl)-3-(3,4-methylenedioxybenzylidene)succinate (**3a**)*. m.p. 58–59 °C. ^{1}H-NMR (200 MHz, $CDCl_3$, δ / ppm): 1.26 (3H, *t*, *J* = 7.2 Hz, CH_3), 1.34 (3H, *t*, *J* = 7.2 Hz, CH_3), 2.85 (1H, *dd*, *J* = 10.0, 14.2 Hz, H-7"α), 3.34 (1H, *dd*, *J* = 5.0, 14.2 Hz, H-7"β), 3.98 (1H, *dd*, *J* = 5.0, 10.0 Hz, H-3), 4.15−4.32 (4H, *m*, 2×C**H**$_2$CH$_3$), 5.88 (2H, *s*, OCH_2O), 5.97 (2H, *s*, OCH_2O), 6.35−6.73 (6H, *m*, ArH), 7.66 (1H, *s*, H-7'). ^{13}C-NMR (50 MHz, $CDCl_3$, δ / / ppm): 14.4 (2×CH_2**C**H_3), 36.0 (C-3), 45.8 (C-7"), 61.2 (2×O**C**H_2CH_3), 100.9 (OCH_2O), 101.4 (OCH_2O), 108.1 (C-5'), 108.4 (C-5"), 108.7 (C-2'), 109.7 (C--2"), 122.4 (C-6'), 122.7 (C-6"), 129.3 (C-1'), 130.1 (C-1"), 133.2 (C-2), 142.5 (C-7'), 146.1(C-4'), 147.5 (C-4'), 147.8 (C-3', C-3''), 166.9 (C=O), 172.9 (C=O). EI-MS (*m*/*z*, %): 440 (M^+, 4), 395 (1), 306 (5), 231 (40), 137 (100); HRMS Calcd. for $C_{24}H_{25}O_8$ ($M+H^+$): 441.1544. Found: 441.1538.

* Corresponding author. E-mail: xiaym@qust.edu.cn

*Diethyl 2-(3,4-dimethoxybenzylidene)-3-(3,4-methylenedioxybenzyl)succinate (**3b**)*. ^{1}H-NMR (200 MHz, $CDCl_3$, δ / ppm): 1.26 (3H, *t*, *J* = 7.2 Hz, CH_3), 1.35 (3H, *t*, *J* = 7.2 Hz, CH_3), 2.91 (1H, *dd*, *J* = 9.8, 14.2 Hz, H-7''α), 3.34 (1H, *dd*, *J* = 5.0, 14.2 Hz, H-7''β), 3.78 (3H, *s*, OCH_3), 3.88 (3H, *s*, OCH_3), 4.10 (1H, *dd*, *J* = 5.0, 9.8 Hz, H-3), 4.18 (2H, *q*, *J* = 7.2 Hz, C**H**$_2$CH$_3$), 4.30 (2H, *q*, *J* = 7.2 Hz, C**H**$_2$CH$_3$), 5.85 (2H, *s*, OCH_2O), 6.35–6.80 (6H, *m*, ArH), 7.71 (1H, *s*, H-7'). ^{13}C-NMR (50 MHz, $CDCl_3$, δ / ppm): 14.1 (CH$_2$**C**H$_3$), 14.2 (CH$_2$**C**H$_3$), 35.7 (C--3), 45.5 (C-7''), 55.7 (OCH_3), 55.8 (OCH_3), 60.9 (2 × **C**H$_2$CH$_3$), 100.7 (OCH_2O), 107.7 (C-5'), 109.4 (C-5''), 110.7 (C-2'), 111.4 (C-2''), 121.1 (C-6'), 122.0 (C-6''), 127.9 (C-1'), 129.5 (C-1''), 132.9 (C-2), 142.3 (C-7'), 145.7 (C-4'), 147.2 (C-4''), 148.6 (C-3'), 149.1 (C-3''), 166.7 (C=O), 172.7 (C=O). EI-MS (*m*/*z*, %): 456 (M^+, 3), 411 (1), 382 (1), 322 (4), 247 (51), 137 (100). HRMS Calcd. for $C_{25}H_{29}O_8$ ($M+H^+$): 457.1857. Found: 457.1856.

*(–)-2-(3,4-Methylenedioxybenzyl)-3-(3,4-methylenedioxybenzylidene)succinic acid (**4a**)*. M.p. 98–99 °C. ^{1}H-NMR (200 MHz, DMSO-d_6, δ / ppm): 2.85 (1H, *dd*, *J* = 10.2, 13.8 Hz, H-7''α), 3.25 (1H, *dd*, *J* = 4.4, 13.8 Hz, H-7''β), 3.93 (1H, *dd*, *J* = 4.4, 10.2 Hz, H-3), 5.92 (2H, *s*, OCH_2O), 6.04 (2H, *s*, OCH_2O), 6.37−6.90 (6H, *m* , ArH), 7.53 (1H, *s*, H-7'). EI-MS (*m*/*z*, %): 384 (M^+, 1), 366 (1), 244 (1), 203 (3), 159 (2), 135 (100). $[\alpha]_D^{16}$ = –95.3 (*c* 1.0, EtOH).

*(+)-2-(3,4-Methylenedioxybenzyl)-3-(3,4-methylenedioxybenzylidene)succinic acid (**4a'**)*. M.p. 96–97 °C. $[\alpha]_D^{16}$ = +94.8 (*c* 0.8, EtOH). The ^{1}H-NMR, IR and MS data of **4a'** were in agreement with those of **4a**.

*(–)-2-(3,4-Dimethoxybenzylidene)-3-(3,4-methylenedioxybenzyl)succinic acid (**4b**)*. M.p. 159−160 °C. ^{1}H-NMR (200 MHz, DMSO-d_6, δ / ppm): 2.83 (1H, *dd*, *J* = 10.2, 14.0 Hz, H-7''α), 3.18 (1H, *dd*, *J* = 4.8, 14.0 Hz, H-7''β), 3.64 (3H, *s*, OCH_3), 3.73 (3H, *s*, OCH_3), 3.95 (1H, *dd*, *J* = 4.8, 10.2 Hz, H-3), 5.87 (2H, *d*, *J* = 8.2 Hz, OCH_2O), 6.35−6.89 (6H, *m*, ArH), 7.52 (1H, *s*, H-7'). EI-MS (*m*/*z*, %): 400 (M^+, 1), 382 (17), 260 (5), 219 (12), 175 (26), 135 (100); HRMS Calcd. for $C_{21}H_{21}O_8$ ($M+H^+$): 401.1231. Found: 401.1239. $[\alpha]_D^{16}$ = –143.2 (*c* 0.7, EtOH).

*(+)-2-(3,4-Dimethoxybenzylidene)-3-(3,4-methylenedioxybenzyl)succinic acid (**4b'**)*. M.p. 89–91 °C; $[\alpha]_D^{16}$ = +142.6 (*c* 0.6, EtOH). The ^{1}H-NMR, IR and MS of **4b'** were in agreement with those of **4b**.

*(–)-Diethyl 2-(3,4-methylenedioxybenzyl)-3-(3,4-methylenedioxybenzylidene)succinate (**5a**)*. $[\alpha]_D^{16}$ = –68.4 (*c* 1.0, $CHCl_3$). The ^{1}H-NMR, IR, MS and HRMS data of **5a** were in agreement with those of **3a**.

*(–)-Diethyl 2-(3,4-methylenedioxybenzyl)-3-(3,4-dimethoxybenzylidene)succinate (**5b**)*. $[\alpha]_D^{16}$ = –170.1 (*c* 1.0, $CHCl_3$). The ^{1}H-NMR, IR, MS and HRMS data of **5b** were in agreement with those of **3b**.

*(–)-Dihydrocubebin (**6a**)*. M.p. 112–113 °C. ^{1}H-NMR (200 MHz, $CDCl_3$, δ / / ppm): 1.80−1.84 (2H, *m*, H-2, H-3), 2.55−2.81 (4H, *m*, 2×ArCH$_2$), 3.48 (2H, *d*,

J = 11.2 Hz, C**H**$_2$OH), 3.72 (2H, *s*, 2×OH), 3.74 (2H, *d*, *J* = 11.2 Hz, C**H**$_2$OH), 5.91 (4H, *s*, 2×OCH$_2$O), 6.58−6.73 (6H, *m*, ArH). ^{13}C-NMR (100 MHz, CDCl$_3$, *δ* / ppm): 35.8 (C-2, C-3), 44.2 (C-7', C-7''), 59.9 (C-1, C-4), 100.7 (2×OCH$_2$O), 108.1 (C-5', C-5''), 109.2 (C-2', C-2''), 121.8 (C-6', C-6''), 134.3 (C-1', C-1''), 145.6 (C-4', C-4''), 147.5 (C-3', C-3''). EI-MS (*m*/*z*, %): 358 (M$^+$, 2), 340 (0.1), 204 (0.3), 161 (3), 135 (100); HRMS Calcd. for $C_{20}H_{26}NO_6$ (M+NH$_4^+$): 376.1755. Found: 376.1760. $[\alpha]_D^{16}$ = –41.9 (*c* 0.8, CHCl$_3$). The spectral data are in agreement with the literature.[22]

*(2*R*,3*R*)-2-(3,4-Dimethoxybenzyl)-3-(3,4-methylenedioxybenzyl)-1,4-butanediol (**6b**)*. ^{1}H-NMR (200 MHz, CDCl$_3$, *δ* / ppm): 1.85−1.87 (2H, *m*, H-2, H-3), 2.60−2.80 (4H, *m*, 2×H-7', 2×H-7''), 3.50 (2H, *d*, *J* = 11.6 Hz, C**H**$_2$OH), 3.56 (2H, *s*, 2×OH), 3.80 (2H, *d*, *J* = 11.6 Hz, C**H**$_2$OH), 3.82 (3H, *s*, OCH$_3$), 3.84 (3H, *s*, OCH$_3$), 5.90 (2H, *s*, OCH$_2$O), 6.57−6.80 (6H, *m*, ArH). ^{13}C-NMR (100 MHz, CDCl$_3$, *δ* / ppm): 35.7 (C-2), 35.9 (C-3), 43.9 (C-7'), 44.1 (C-7''), 55.8 (OCH$_3$), 55.9 (OCH$_3$), 60.2 (C-1), 60.3 (C-4), 100.7 (OCH$_2$O), 108.0 (C-5'), 109.3 (C-5''), 111.2 (C-2'), 112.1 (C-2''), 121.0 (C-6'), 121.8 (C-6''), 133.1 (C-1'), 134.3 (C-1''), 145.7 (C-4'), 147.3 (C-4''), 147.5 (C-3'), 148.8 (C-3''). EI--MS (*m*/*z*, %): 374 (M$^+$, 4), 356 (0.4), 220 (3), 203 (3), 151 (100). HRMS Calcd. for $C_{21}H_{30}NO_6$ (M+NH$_4^+$): 392.2068. Found: 392.2063. $[\alpha]_D^{16}$ = –36.8 (*c* 0.5, CHCl$_3$). The spectral data are in agreement with the literature.[23]

meso-*2,3-Bis(3,4-methylenedioxybenzyl)butane-1,4-diol (**7a**)*. ^{1}H-NMR (200 MHz, CDCl$_3$, *δ* / ppm): 1.99−2.05 (2H, *m*, H-2, H-3), 2.49−2.63 (4H, *m*, 2×ArCH$_2$), 3.45−3.61 (4H, *m*, 2×C**H**$_2$OH), 3.71 (2H, *s*, 2×OH), 5.92 (4H, *s*, 2×OCH$_2$O), 6.61−6.76 (6H, *m*, ArH). ^{13}C-NMR (50 MHz, CDCl$_3$, *δ* / ppm): 33.4 (C-2, C-3), 45.2 (C-7', C-7''), 62.9 (C-1, C-4), 100.8 (2×OCH$_2$O), 108.1 (C-5', C-5''), 109.2 (C-2', C-2''), 121.8 (C-6', C-6''), 134.1 (C-1', C-1''), 145.8 (C-4', C-4''), 147.6 (C-3', C-3''). EI-MS (*m*/*z*, %): 358 (M$^+$, 3), 340 (0.3), 204 (0.8), 161 (4), 135 (100); HRMS Calcd. for $C_{20}H_{26}NO_6$ (M+NH$_4^+$): 376.1755. Found: 376.1760.

*(2*R*,3*S*)-2-(3,4-Dimethoxybenzyl)-3-(3,4-methylenedioxybenzyl)-1,4-butanediol (**7b**)*. ^{1}H-NMR (200 MHz, CDCl$_3$, *δ* / ppm): 1.84−1.86 (2H, *m*, H-2, H-3), 2.56−2.82 (4H, *m*, 2×H-7', 2×H-7''), 3.50 (2H, *d*, *J* = 11.0 Hz, C**H**$_2$OH), 3.75 (2H, *d*, *J* = 11.0 Hz, C**H**$_2$OH), 3.81 (3H, *s*, OCH$_3$), 3.83 (3H, *s*, OCH$_3$), 3.95 (2H, *s*, 2×OH), 5.89 (2H, *s*, OCH$_2$O), 6.56–6.78 (6H, *m*, ArH). ^{13}C-NMR (100 MHz, CDCl$_3$, *δ* / ppm): 33.1 (C-2), 33.4 (C-3), 45.0 (C-7'), 45.2 (C-7''), 55.8 (OCH$_3$), 55.9 (OCH$_3$), 62.9 (C-1), 63.0 (C-4), 100.8 (OCH$_2$O), 108.1 (C-5'), 109.3 (C-5''), 111.2 (C-2'), 112.1 (C-2''), 121.0 (C-6'), 121.8 (C-6''), 133.0 (C--1'), 134.2 (C-1''), 145.8 (C-4'), 147.3 (C-4''), 147.6 (C-3'), 148.8 (C-3''). EI--MS (*m*/*z*, %): 374 (M$^+$, 4.7), 356 (0.23), 220 (1.8), 203 (2.5), 151 (100). HRMS Calcd. for $C_{21}H_{30}NO_6$ (M+NH$_4^+$): 392.2068. Found: 392.2063. $[\alpha]_D^{16}$ = –1.7 (*c* 0.3, CHCl$_3$). The spectral data were in agreement with the literature.[24]

*(–)-Dehydroxycubebin (**8a**)*. ^{1}H-NMR (200 MHz, $CDCl_3$, δ / ppm): 2.07––2.18 (2H, *m*, H-3, H-4), 2.42–2.59 (4H, *m*, 2×$ArCH_2$), 3.49 (2H, *dd*, *J* = 5.8, 8.6 Hz, 2×H-2), 3.89 (2H, *dd*, *J* = 6.8, 8.8 Hz, 2×H-5), 5.91 (4H, *s*, 2×OCH_2O), 6.51–6.75 (6H, *m*, ArH). ^{13}C-NMR (100 MHz, $CDCl_3$, δ / ppm): 39.1 (C-3, C-4), 46.4 (C-7', C-7''), 73.2 (C-2, C-5), 100.7 (2×OCH_2O), 107.9 (C-5', C-5''), 108.9 (C-2', C-2''), 121.4 (C-6', C-6''), 134.0 (C-1', C-1''), 145.7 (C-4', C-4''), 147.5 (C-3', C-3''). EI-MS (*m*/*z*, %): 340 (M^+, 11), 204 (2), 187 (3), 161 (2), 136 (100). $[\alpha]_D^{16}$ = –54.2 (*c* 0.8, $CHCl_3$).

*(–)-5-{[(3*R*,4*R*)-4-(3,4-Dimethoxybenzyl)-tetrahydro-3-furanyl]methyl}-1,3--benzodioxole (**8b**)*. ^{1}H-NMR (200 MHz, $CDCl_3$, δ / ppm): 2.15−2.18 (2H, *m*, H-3, H-4), 2.45−2.59 (4H, *m*, 2 × $ArCH_2$), 3.46−3.54 (2H, *m*, 2 × H-2), 3.84 (3H, *s*, OCH_3), 3.85 (3H, *s*, OCH_3), 3.89−3.93 (2H, *m*, 2×H-5), 5.91 (2H, *s*, OCH_2O), 6.51–6.78 (6H, *m*, ArH). ^{13}C-NMR (50 MHz, $CDCl_3$, δ / ppm): 39.0 (C-3), 39.1 (C-4), 46.5 (C-7'), 46.6 (C-7''), 55.7 (OCH_3), 55.8 (OCH_3), 73.2 (C-2), 73.3 (C--5), 100.8 (OCH_2O), 108.0 (C-5'), 108.9 (C-5''), 111.1 (C-2'), 111.8 (C-2'), 120.5 (C-6'), 121.4 (C-6''), 132.9 (C-1'), 134.1 (C-1''), 145.8 (C-4'), 147.4 (C-4''), 147.6 (C-3'), 148.8 (C-3''). EI-MS (*m*/*z*, %): 356 (M^+, 15), 220 (3), 177 (6), 151 (100). HRMS Calcd. for $C_{21}H_{25}O_5$ ($M+H^+$): 357.1697. Found: 357.1701. $[\alpha]_D^{16}$ = –104.7 (*c* 0.6, $CHCl_3$).

*(+)-5.5'-[(2*R*,3*R*)-2,3-Bis(methoxymethyl)-1,4-butanediyl]bis(1,3-dioxole) (**9a**)*. ^{1}H-NMR (300 MHz, $CDCl_3$, δ / ppm): 2.00–2.03 (2H, *m*, H-2, H-3), 2.52−2.69 (4H, *m*, 2×$ArCH_2$), 3.28 (10H, *s*, 2×OCH_3, 2×H-1, 2×H-4), 5.92 (4H, *s*, 2×OCH_2O), 6.55−6.71 (6H, *m*, ArH). ^{13}C-NMR (75 MHz, $CDCl_3$, δ / / ppm): 35.1 (C-2, C-3), 41.2 (C-7', C-7''), 58.9 (C-7', C-7''), 72.7 (C-1, C--4), 100.9 (2×OCH_2O), 108.2 (C-5', C-5''), 109.7 (C-2', C-2''), 122.1 (C-6', C--6''), 135.1 (C-1', C-1''), 145.8 (C-4', C-4''), 147.7 (C-3', C-3''). EI-MS (*m*/*z*, %): 386 (M^+, 5), 354 (7), 218 (9), 187 (19), 161 (8), 135 (100). $[\alpha]_D^{16}$ +12.3 (*c* 0.5, $CHCl_3$).

*(+)-5-[(2-(2*R*,3*R*)-4-(3,4-Dimethoxybenzyl)-2,3-bis(methoxymethyl)-butyl]--1,3-benzodioxole (**9b**)*. ^{1}H-NMR (300 MHz, $CDCl_3$, δ / ppm): 2.00–2.03 (2H, *m*, H-2, H-3), 2.61−2.64 (4H, *m*, 2×$ArCH_2$), 3.29 (10H, *s*, 2×OCH_3, 2×H-1, 2×H-4), 3.82 (3H, *s*, $ArOCH_3$), 3.86 (3H, *s*, $ArOCH_3$), 5.92 (2H, *s*, 2×OCH_2O), 6.55−6.78 (6H, *m*, ArH). ^{13}C-NMR (75 MHz, $CDCl_3$, δ / ppm): 34.8 (C-2), 34.9 (C-3), 40.7 (C-7'), 40.9 (C-7''), 55.7 (OCH_3), 55.9 (OCH_3), 58.7 ($ArOCH_3$), 58.8 ($ArOCH_3$), 72.4 (C-1), 72.6 (C-4), 100.7 (OCH_2O), 107.9 (C-5'), 109.4 (C-5''), 110.9 (C-2'), 111.9 (C-2'), 121.1 (C-6'), 121.9 (C-6''), 133.5 (C-1'), 134.9 (C--1''), 145.5 (C-4'), 147.1 (C-4''), 147.4 (C-3'), 148.7 (C-3''). EI-MS (*m*/*z*, %): 402 (M^+, 21), 370 (6), 203 (17), 151 (100). $[\alpha]_D^{16}$ = +14.8 (*c* 0.6, $CHCl_3$).

*(–)-Austrobailignan-5 (**10a**)*. M.p. 44–45 °C. ^{1}H-NMR (200 MHz, $CDCl_3$, δ / / ppm): 0.81 (6H, *d*, *J* = 6.8 Hz, 2×CH_3), 1.67−1.77 (2H, *m*, H-2, H-3), 2.33 (2H, *dd*, *J* = 8.2, 13.6 Hz, $ArCH_2$), 2.55 (2H, *dd*, *J* = 6.0, 13.6 Hz, $ArCH_2$), 5.92 (4H,

s, 2×OCH_2O), 6.52−6.75 (6H, *m*, ArH). ^{13}C-NMR (100 MHz, $CDCl_3$, δ / ppm): 13.9 (C-1, C-4), 38.2 (C-2, C-3), 41.2 (C-7', C-7''), 100.7 (2×OCH_2O), 107.9 (C-5', C-5''), 109.3 (C-2', C-2''), 121.8 (C-6', C-6''), 135.5 (C-1', C-1''), 145.5 (C-4', C-4''), 147.4 (C-3', C-3''). EI-MS (*m*/*z*, %): 326 (M^+, 1), 135 (20), 123 (100). $[\alpha]_D^{16}$ = –36.3 (*c* 0.5, $CHCl_3$). The spectral data are in agreement with the literature.[25]

*(–)-Saururenin (**10b**)*. ^{1}H-NMR (200 MHz, $CDCl_3$, δ / ppm): 0.82 (6H, *d*, *J* = 6.6 Hz, 2×CH_3), 1.71−1.77 (2H, *m*, H-2, H-3), 2.30–2.42 (2H, *m*, $ArCH_2$), 2.49−2.59 (2H, *m*, $ArCH_2$), 3.83 (3H, *s*, OCH_3), 3.85 (3H, *s*, OCH_3), 5.90 (2H, *s*, OCH_2O), 6.51−6.78 (6H, *m*, ArH). ^{13}C-NMR (50 MHz, $CDCl_3$, δ / ppm): 13.7 (C-1), 13.8 (C-4), 37.7 (C-2), 37.9 (C-3), 40.9 (C-7'), 41.1 (C-7''), 55.7 (OCH_3), 55.8 (OCH_3), 100.6 (OCH_2O), 107.8 (C-5'), 109.2 (C-5''), 111.0 (C-2'), 112.0 (C-2''), 120.8 (C-6'), 121.7 (C-6''), 134.1 (C-1'), 135.4 (C-1''), 145.4 (C-4'), 147.0 (C-4''), 147.3 (C-3'), 148.7 (C-3''). EI-MS (*m*/*z*, %): 342 (M^+, 8), 206(2), 151 (100). $[\alpha]_D^{16}$ = –33.0 (*c* 0.8, $CHCl_3$). The spectral data were in agreement with the literature.[10]

meso-*5,5'-[(Tetrahydro-3,4-furandiyl)bis(methylene)]bis(1,3-benzodioxole) (**11a**)*. ^{1}H-NMR (200 MHz, $CDCl_3$, δ / ppm): 2.49−2.53 (4H, *m*, H-3, H-4, $ArCH_2$), 2.75−2.84 (2H, *m*, $ArCH_2$), 3.62 (2H, *dd*, *J* = 5.6, 8.2 Hz, 2×H-2), 3.79 (2H, *dd*, *J* = 5.6, 8.2 Hz, 2×H-5), 5.95 (4H, *s*, 2×OCH_2O), 6.57−6.78 (6H, *m*, ArH). ^{13}C-NMR (50 MHz, $CDCl_3$, δ / ppm): 33.2 (C-3, C-4), 43.6 (C-7', C-7''), 71.9 (C-2, C-5), 100.8 (2×OCH_2O), 108.2 (C-5', C-5''), 108.9 (C-2', C-2''), 121.5 (C-6', C-6''), 134.3 (C-1', C-1''), 145.8 (C-4', C-4''), 147.7 (C-3', C-3''). EI-MS (*m*/*z*, %): 340 (M^+, 9), 204 (5), 187(2), 161 (5), 136 (100). HRMS Calcd. for $C_{20}H_{24}NO_5$ ($M+NH_4^+$): 358.1649. Found: 358.1648. $[\alpha]_D^{16}$ = 0 (*c* 0.8, $CHCl_3$).

*(+)-5-{[(3*S*,4*R*)-4-[(3,4-Dimethoxyphenyl)methyl]tetrahydro-3-furanyl]methyl}-1,3-benzodioxole (**11b**)*. ^{1}H-NMR (200 MHz, $CDCl_3$, δ / ppm): 2.15−2.18 (2H, *m*, H-3, H-4), 2.45−2.59 (4H, *m*, 2×$ArCH_2$), 3.46−3.54 (2H, *m*, 2×H-2), 3.84 (3H, *s*, OCH_3), 3.85 (3H, *s*, OCH_3), 3.89−3.93 (2H, *m*, 2×H-5), 5.91 (2H, *s*, OCH_2O), 6.51−6.78 (6H, *m*, ArH). ^{13}C-NMR (50 MHz, $CDCl_3$, δ / ppm): 39.0 (C-3), 39.1 (C-4), 46.5 (C-7'), 46.6 (C-7''), 55.7 (OCH_3), 55.8 (OCH_3), 73.2 (C--2), 73.3 (C-5), 100.8 (OCH_2O), 108.0 (C-5'), 108.9 (C-5''), 111.1 (C-2'), 111.8 (C-2'), 120.5 (C-6'), 121.4 (C-6''), 132.9 (C-1'), 134.1 (C-1''), 145.8 (C-4'), 147.4 (C-4''), 147.6 (C-3'), 148.8 (C-3''). EI-MS (*m*/*z*, %): 356 (M^+, 15), 220 (3), 177 (6), 151 (100); HRMS Calcd. for $C_{21}H_{25}O_5$ ($M+H^+$): 357.1697. Found: 357.1695. $[\alpha]_D^{16}$ = +2.5 (*c* 0.8, $CHCl_3$).

meso-*5,5'-[Bis(methoxymethyl)-1,4-butanediyl]bis(1,3-benzodioxole) (**12a**)*. ^{1}H-NMR (300 MHz, $CDCl_3$, δ / ppm): 2.04−2.08 (2H, *m*, H-2, H-3), 2.51−2.69 (4H, *m*, 2×$ArCH_2$), 3.26 (6H, *s*, 2×OCH_3), 3.26−3.38 (4H, *m*, H-1, H-4), 5.92 (4H, *s*, 2×OCH_2O), 6.58−6.74 (6H, *m*, ArH). ^{13}C-NMR (75 MHz, $CDCl_3$, δ / ppm): 34.4

(C-2, C-3), 40.9 (C-7', C-7''), 58.6 (C-7', C-7''), 72.7 (C-1, C-4), 100.7 (2×OCH_2O), 107.9 (C-5', C-5''), 109.3 (C-2', C-2''), 121.8 (C-6', C-6''), 134.9 (C-1', C-1''), 145.6 (C-4', C-4''), 147.5 (C-3', C-3''). EI-MS, (*m*/*z*, %): 386 (M^+, 5), 354 (5), 322 (3), 218 (11), 187 (21), 173 (12), 135 (100). HRMS Calcd. for $C_{22}H_{27}O_6$ ($M+H^+$): 387.1802. Found: 387.1812. $[\alpha]_D^{16}$ = 0 (*c* 0.4, $CHCl_3$).

*(+)-5-{[(3*S*,4*R*)-4-[(3,4-Dimethoxyphenyl)-2,3-bis(methoxymetyl)butyl]-1,3--benzodioxole (**12b**)*. ^{1}H-NMR (300 MHz, $CDCl_3$, δ / ppm): 2.07−2.11 (2H, *m*, H--2, H-3), 2.58−2.66 (4H, *m*, 2×$ArCH_2$), 3.29 (6H, *s*, 2×OCH_3), 3.26−3.38 (4H, *m*, 2×$ArCH_2$), 3.85 (3H, *s*, $ArOCH_3$), 3.86 (3H, *s*, $ArOCH_3$), 5.92 (2H, *s*, 2×OCH_2O), 6.60−6.80 (6H, *m*, ArH). ^{13}C-NMR (75 MHz, $CDCl_3$, δ / ppm): 34.8 (C-2), 34.9 (C-3), 40.7 (C-7'), 40.8 (C-7''), 55.6 (OCH_3), 55.8 (OCH_3), 58.7 ($ArOCH_3$), 58.8 ($ArOCH_3$), 72.4 (C-1), 72.6 (C-4), 100.7 (OCH_2O), 107.8 (C-5'), 109.4 (C-5''), 110.9 (C-2'), 120.0 (C-2'), 121.0 (C-6'), 121.9 (C-6''), 133.5 (C--1'), 134.8 (C-1''), 145.5 (C-4'), 147.1 (C-4''), 147.4 (C-3'), 148.7 (C-3''). HRMS Calcd. for $C_{23}H_{34}NO_6$ ($M+NH_4^+$): 420.2381. Found: 420.2384. $[\alpha]_D^{16}$ = = +2.7 (*c* 0.8, $CHCl_3$).

meso-*Machilin A (**13a**)*. M.p. 47–48 °C. ^{1}H-NMR (200 MHz, $CDCl_3$, δ / / ppm): 0.83 (6H, *d*, *J* = 6.6 Hz, 2×CH_3), 1.72−1.76 (2H, *m*, H-2, H-3), 2.26 (2H, *dd*, *J* = 9.4, 13.4 Hz, $ArCH_2$), 2.72 (2H, *dd*, *J* = 4.8, 13.4 Hz, $ArCH_2$), 5.93 (4H, *s*, 2×OCH_2O), 6.58−6.76 (6H, *m*, ArH). ^{13}C-NMR (100 MHz, $CDCl_3$, δ / ppm): 16.1 (C-1, C-4), 39.0 (C-2, C-3), 39.3 (C-7', C-7''), 100.6 (2×OCH_2O), 107.9 (C-5', C-5''), 109.2 (C-2', C-2''), 121.8 (C-6', C-6''), 135.6 (C-1', C-1''), 145.4 (C-4', C-4''), 147.4 (C-3', C-3''). EI-MS (*m*/*z*, %): 326 (M^+, 3), 135(58), 123 (100). $[\alpha]_D^{16}$ = 0 (*c* 0.4, $CHCl_3$). The spectral data are in agreement with the literature.[26]

*(–)-Isosaururenin (**13b**)*. ^{1}H-NMR (200 MHz, $CDCl_3$, δ / ppm): 0.82 (3H, *d*, *J* = 6.6 Hz, CH_3), 0.85 (3H, *d*, *J* = 6.6 Hz, CH_3), 1.62−1.79 (2H, *m*, H-2, H-3), 2.20−2.35 (2H, *m*, $ArCH_2$), 2.68−2.78 (2H, *m*, $ArCH_2$), 3.86 (6H, *s*, 2×OCH_3), 5.90 (2H, *s*, OCH_2O), 6.59−6.81 (6H, *m*, ArH). ^{13}C-NMR (50 MHz, $CDCl_3$, δ / / ppm): 16.0 (C-1), 16.2 (C-4), 38.7 (C-2), 39.0 (C-3), 39.1 (C-7'), 39.3 (C-7''), 55.7 (OCH_3), 55.9 (OCH_3), 100.6 (OCH_2O), 107.9 (C-5'), 109.3 (C-5''), 111.0 (C-2'), 112.2 (C-2''), 120.9 (C-6'), 121.7 (C-6''), 134.4 (C-1'), 135.6 (C-1''), 145.4 (C-4'), 147.0 (C-4''), 147.4 (C-3'), 148.7 (C-3''). EI-MS (*m*/*z*, %): 342 (M^+, 6), 206(10), 151 (100). $[\alpha]_D^{16}$ = –1.9 (*c* 0.8, $CHCl_3$).

meso-*Nordihydroguaiaretic acid (**14**)*. M.p. 184–185 °C. ^{1}H-NMR (300 MHz, acetone-d_6, δ / ppm): 0.86 (6H, *d*, *J* = 6.3 Hz, 2×CH_3), 1.80−1.85 (2H, *m*, H-2, H-3), 2.49 (2H, *dd*, *J* = 9.6, 12.9 Hz, $ArCH_2$), 2.96 (2H, *dd*, *J* = 5.4, 12.9 Hz, $ArCH_2$), 7.14−7.33 (6H, *m*, ArH). ^{13}C-NMR (75 MHz, acetone-d_6, δ / ppm): 16.1 (C-1, C-4), 39.5 (C-2, C-3), 40.3 (C-7', C-7''), 110.6 (C-5', C-5''), 111.5 (C-2', C-2''), 126.1 (C-6', C-6''), 140.2 (C-1', C-1''), 142.4 (C-4', C-4''), 144.3 (C-3', C-3''). EI–MS (*m*/*z*, %): 302 (M^+, 4), 178 (1), 151 (2), 137 (4), 123 (100).

Journal of the Serbian Chemical Society
JSCS-info@shd.org.rs • www.shd.org.rs/JSCS
J. Serb. Chem. Soc. *75* (10) 1337–1346 (2010)
JSCS–4056
UDC 547.21:665.944.55:633.94
Original scientific paper

n-Alkanes in the needle waxes of *Pinus heldreichii* var. *pančići*

BILJANA NIKOLIĆ[1*#], VELE TEŠEVIĆ[2#], IRIS ĐORĐEVIĆ[3#], MILKA JADRANIN[4#], MARINA TODOSIJEVIĆ[4], SRĐAN BOJOVIĆ[5#] and PETAR D. MARIN[6#]

[1]*Institute of Forestry, Kneza Višeslava 3, 11000 Belgrade,* [2]*Faculty of Chemistry, University of Belgrade, Studentski trg 16, 11000 Belgrade,* [3]*Faculty of Veterinary Medicine, University of Belgrade, Bulevar oslobođenja 18, 11000 Belgrade,* [4]*Institute for Chemistry, Technology and Metallurgy, University of Belgrade, Njegoševa 12, 11000 Belgrade,* [5]*Institute for Biological Research "Siniša Stanković", Bulevar despota Stefana 142, 11000 Belgrade and* [6]*Faculty of Biology, Institute of Botany and Botanical Garden "Jevremovac", University of Belgrade, Studentski trg 16, 11000 Belgrade, Serbia*

(Received 22 March, revised 14 June 2010)

Abstract: This is the first report of *n*-alkanes in needle epicuticular waxes of the variety Bosnian pine, *Pinus heldreichii* var. *pančići*. *n*-Hexane extracts of needle samples, originating from seven isolated localities in Serbia, were analysed by gas chromatography (GC) and gas chromatography–mass spectrometry (GC–MS). The results evidenced *n*-alkanes ranging from C_{18} to C_{33} in epicuticular waxes. The most abundant alkanes were C_{27}, C_{23}, C_{25} and C_{29} (12.53 %, 12.46 %, 12.00 % and 10.38 % on average, respectively). The carbon preference index (CPI_{total}) of *Pinus heldreichii* var. *pančići* ranged from 1.1 to 2.1 (1.6 on average), while the average chain length (ACL_{total}) ranged from 25.0 to 25.8 (25.3 on average). A high level of individual quantitative variation in all of these hydrocarbon parameters was also found. The obtained results were compared with the bibliographic references for *Pinus heldreichii* var. *leucodermis* and other species of the *Pinus* genus.

Keywords: Bosnian pine; Pinaceae; needles; *n*-alkanes.

INTRODUCTION

Bosnian pine, *Pinus heldreichii* Christ. (Pinaceae family), is a relict and subendemic tree species naturally distributed in fragmented areas in Italy, Bosnia and Herzegovina, Serbia, Montenegro, Albania, Macedonia, Bulgaria and Greece. The Bosnian pines, which grow in southwestern Serbia and northern Montenegro, are regarded as *Pinus heldreichii* var. *pančići* Fukarek.[1–3] These trees grow individually or in smaller groups, in relict and geographically isolated popula-

* Corresponding author. E-mail: smikitis@gmail.com
# Serbian Chemical Society member.
doi: 10.2298/JSC100322089N

tions (mainly up to 10 trees). Concerning the site and morphology of the branches, needles and/or cones, var. *pančići* is similar to *Pinus nigra* Arn. and partially to two natural hybrids: *Pinus x mugodermis* Fukarek[4] and *Pinus x nigradermis* Fukarek and Vidaković,[5] and one intermedial form, *Pinus nigra* f. *leucodermoides* Fukarek and Nikolić,[6] but differs clearly from other *Pinus heldreichii* varieties: *Pinus heldreichii* var. *typica* Markgraf, *Pinus heldreichii* var. *leucodermis* (Ant.) Markgraf and *Pinus heldreichii* var. *longiseminis* Papaioannou.[1] Differences between populations of Bosnian Pine from Serbia and Montenegro (regarded as *Pinus heldreichii* var. *pančići* and *Pinus heldreichii* var. *leucodermis*,[2] respectively) in the compositions of the essential oil have also been noticed.[7]

n-Alkanes are among the most common hydrocarbons in cuticular waxes of numerous higher plants. In leaf waxes, they show abundances up to 73 %.[8] In waxes of conifers, polar lipids are dominant (above 90 %), whereas there is often a small percentage of non-polar lipids, particularly leaf *n*-alkanes (up to 4.5 %),[9] with the exception of *Wollemia nobilis* Jones, Hill and Allen (up to 22 %).[10]

Hitherto, the research of *n*-alkanes has most frequently been used in chemotaxonomic studies of trees[11–16] and herbaceous plants.[17–22] *n*-Alkanes in plants, in combination with other chemical markers, are also valuable objects for analyses in other fields: phylogenetic studies,[23] hybrid detection,[24] air pollution studies,[25,26] studies of nutrition,[27,28] *etc*.

The parameters which are often used for the description of the *n*-alkane distribution patterns are: abundance of long-chain *n*-alkanes (LNAs), carbon preference index (*CPI*)[29] and average chain length (*ACL*).[30] They can be used as chemotaxonomic markers at the genus level,[31] in environmental studies,[30] in palaeoenvironmental reconstructions,[32] *etc*.

The *n*-alkanes in conifer trees have been most extensively researched in *Picea*[11,33] and *Pinus*[11] genera. The *n*-alkanes in pines are present as mixtures with chain lengths ranging from 18 to 34 carbon atoms, whereby odd-numbered alkanes are dominant.[11]

The composition of the epicuticular wax of needles of *Pinus heldreichii* var. *leucodermis* has already been studied[11] but, to the best of our knowledge, this is the first report of the composition and variability of *n*-alkanes in the needles of Bosnian pine from natural populations. In addition, this is the first report of the composition of pine needle epicuticulal wax from the variety *pančići*.

EXPERIMENTAL

Plant material

The population density of Bosnian pine in Serbia is low, *ca*. 200 trees, which are very old (up to 400 years) and tall (10–20 m). These trees grow individually or in small groups,[2] mainly on difficult to access terrains. In order to cover the altitudinal range of Bosnian pine in Serbia, seven trees were selected from seven natural sites, *i.e*., from Mt. Zlatibor to Mt. Pešter,

at the following localities: 1) Negbina (village, Mt. Zlatibor), 2) Sjeništa (village, Mt. Zlatibor), 3) Kamena gora (Mt. near Prijepolje), 4) Lastva (Milakovići village near Brodarevo, Mt. Ozren), 5) Trijebine (Prijevorac village, located between Mt. Ozren and Mt. Giljeva), 6) Bare (Krajinovići village, Mt. Giljeva), and 7) Lokva (Krajinovići Village, Mt. Giljeva) (Table I).

TABLE I. Geographic and geologic characteristics of the study area of *Pinus heldreichii* var. *pančići*

Localities	Negbina	Sjeništa	Kamena gora	Lastva	Trijebine	Bare	Lokva
	1	2	3	4	5	6	7
Latitude (N)	43°32’	43°32’	43°20’	43°16’	43°16’	43°10’	43°10’
Longitude (E)	19°47’	19°47’	19°33’	19°42’	19°55’	19°52’	19°52’
Altitude, m	1206	982	1273	1430	1313	1360	1335
Exposition	SE	NE	E	SW	E	SW	S
Geological substratum	Lime-stone	Serpen-tinite	Limestone	Serpen-tinite	Neogene sediments	Limestone horno-stone tuff	Serpen-tinite

Two-year-old needles were collected at the end of the photosynthetic active season, around the lower third of the unshaded tree crown, to ensure comparability of the sample collections. The second, more practical reason for this kind of plant collection, is the fact that climbing and collecting of needles from the higher parts of crown could be very difficult and unsafe, since many of the investigated trees from natural populations were located on difficult to access terrains. The needles were kept in polyethylene bags (with the labels of the sample plot, date of collection and age of the needles) in a hand fridge and transported to a freezer (–20 °C).

Extraction and isolation of needle wax

The total wax of each sample was extracted by immersing 3 g of needles in 10 ml of *n*-hexane for 45 s. After extraction, the solvent was removed under vacuum at 60 °C. The concentrated extracts were chromatographed on a small-scale column using a Pasteur pipette filled with silica gel 60, previously activated at 120 °C.[34] The wax was obtained by elution with 5 ml of *n*-hexane. The wax samples were stored at –20 °C until further analysis.

Chemicals and reagents

n-Hexane (HPLC grade) and silica gel 60 (0.2–0.5 mm) were purchased from Merck (Darmstadt, Germany).

GC and GC–MS analysis

Gas chromatography (GC) and gas chromatography–mass spectrometric (GC–MS) analyses were performed using an Agilent 7890A GC equipped with an inert 5975C XL EI/CI mass spectrometer detector (MSD) and flame ionisation detector (FID) connected by capillary flow technology 2-way splitter with make-up. A HP-5MS capillary column (30 m×0.25 mm×0.25 μm) was used. The GC oven temperature was programmed from 60 to 300 °C at a rate of 3 °C min^{-1} and held for 10 min. Helium was used as the carrier gas at 16.255 psi (constant pressure mode). An auto-injection system (Agilent 7683B Series Injector) was employed to inject 1 μL of sample. The sample was analysed in the splitless mode. The injector temperature was 250 °C and the detector temperature 300 °C. MS data was acquired in the EI mode with scan range 30–550 *m*/*z*, source temperature 230 °C, and quadrupole temperature 150 °C; the solvent delay was 3 min.

The components were identified based on their retention index and comparison with reference spectra (Wiley and NIST databases) as well as by the retention time locking (RTL) method and the RTL Adams database. The retention indices were experimentally determined using the standard method of Van Den Dool and Kratz[35] involving retention times of *n*-alkanes, injected after the sample under the same chromatographic conditions. The relative abundance of the *n*-alkanes (Table II) was calculated from the signal intensities of the homologues in the GC-FID traces.

Calculations of the CPI *and* ACL *values*

Carbon preference index of total odd-numbered and even-numbered LNAs (CPI_{total}) was calculated by formula of Mazurek and Simoneit[36] (Table III). The average chain length of the total odd-numbered and even-numbered LNAs (ACL_{total}) was calculated by the Poynter and Eglington method.[37] In order to compare the obtained results with those from literature sources,[9,38,39] $CPI_{25\text{-}33}$, $CPI_{20\text{-}36}$, $CPI_{15\text{-}21}$ and $CPI_{25\text{-}31}$ were also calculated using the formula of Bray and Evans,[40] as well as $ACL_{23\text{-}35}$ value using the formula of Poynter and Eglington.[37] The relative proportions of short, mid and long chain n-alkanes[39] (*n*-$C_{18\text{-}20}$, *n*-$C_{21\text{-}24}$ and *n*-$C_{25\text{-}33}$, respectively) were also calculated.

RESULTS AND DISCUSSION

In the epicuticular waxes of two-year old needles of *Pinus heldreichii* var. *pančići*, the *n*-alkanes ranged from C_{18} to C_{33} (Fig. 1, Tables II and III). It can be noticed that the trees at the northernmost sites, Negbina (No. 1) and Sjeništa (No. 2), had a narrower range of *n*-alkanes (C_{18} to C_{31}), as well as *Pinus heldreichii* var. *leucodermis*.[11] Some pines from the section Sylvester (*Pinus sylvestris* L., *Pinus sylvestris* var. *iberica* Svoboda, *Pinus mugo* var. *pumilio* (Haenke) Zenari, *Pinus mugo* Haenke, *Pinus thunbergii* Parl., *Pinus engelmannii* Carr. and *Pinus montezumae* Lamb.) and the section Strobus (*Pinus cembra* L. and *Pinus wallichiana* A. B. Jacks.).[9,11,38] also had the same or a narrower range of needle *n*-alkanes than *Pinus heldreichii* var. *pančići*.

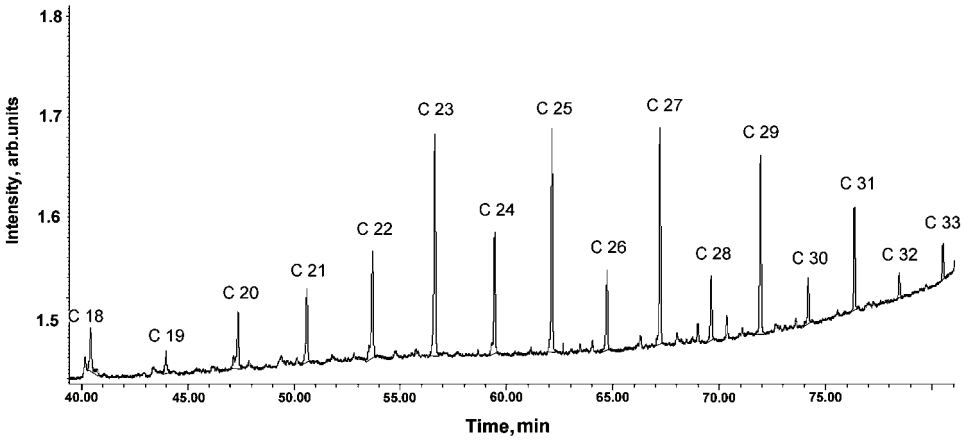

Fig. 1. *n*-Alkanes in needle wax of *Pinus heldreichii* var. *pančići*, Lastva locality (No. 4).

TABLE II. Chemical composition of needle *n*-alkanes of *Pinus heldreichii* var. *pančići*

n-Alkane	Localities							Statistical parameters	
	1	2	3	4	5	6	7	X^a	SD^b
C_{18}	2.41	4.21	4.36	3.19	6.58	3.94	4.84	4.22	1.32
C_{19}	0.00	0.00	1.31	0.89	1.24	1.23	0.88	0.79	0.57
C_{20}	0.00	7.10	3.90	4.03	5.28	3.83	3.63	3.97	2.14
C_{21}	4.48	4.77	4.91	5.21	6.22	5.90	4.51	5.14	0.68
C_{22}	9.11	10.40	7.20	7.80	8.94	10.57	8.49	8.93	1.25
C_{23}	13.43	11.50	9.51	14.44	10.90	14.23	13.21	12.46	1.85
C_{24}	8.58	9.74	8.85	8.17	6.73	7.15	7.57	8.11	1.04
C_{25}	13.12	10.90	10.45	14.03	9.13	12.76	13.64	12.00	1.85
C_{26}	4.89	5.41	7.08	5.10	4.55	4.57	4.37	5.14	0.93
C_{27}	15.16	10.93	11.39	12.49	11.40	12.61	13.76	12.53	1.50
C_{28}	3.76	4.56	5.77	3.51	3.97	3.53	3.83	4.13	0.80
C_{29}	12.50	8.10	10.11	9.77	12.13	9.59	10.47	10.38	1.52
C_{30}	2.49	3.21	4.14	2.31	2.86	2.19	2.51	2.82	0.68
C_{31}	5.94	4.90	5.59	5.47	5.54	4.90	5.41	5.39	0.38
C_{32}	1.50	1.99	2.66	1.53	1.64	1.46	1.16	1.71	0.49
C_{33}	2.63	2.28	2.77	2.06	2.89	1.54	1.72	2.27	0.52

[a]Mean value; [b]standard deviation

In *Pinus heldreichii* var. *pančići* needles, the most abundant alkanes were the four odd-numbered *n*-alkanes: C_{27}, C_{23}, C_{25} and C_{29} (12.53, 12.46, 12.00 and 10.38 % on average, respectively, Table II). Most trees had a maximal abundance at C_{23} (four trees). *n*-Alkane C_{27} was first-ranked at the localities Kamena gora and Lokva (No. 3 and No. 7, respectively). *n*-Alkane C_{29} was first-ranked only in the tree which grows in the southernmost part of the research altitudinal range (Trijebine, No. 5). Two even-numbered *n*-alkanes, C_{22} and C_{24}, were also abundant (8.93 and 8.11 % on average, respectively). Variation of each *n*-alkane is listed as the value of the standard deviation (*SD*, Table II). The most variable were C_{20}, C_{23}, C_{25}, C_{29} and C_{27} (*SD* values: 2.14, 1.85, 1.85, 1.52 and 1.50, respectively). According to literature sources, other pine species are often rich only in one *n*-alkane, C_{31},[11] rarely C_{33}.[9] However, in *Pinus heldreichii* var. *pančići*, no correlation between the C_{max} values of needle *n*-alkanes and the distances of the trees from villages or adjacent roads was found.

For the calculation of the *CPI* and *ACL* values of *n*-alkanes of *Pinus heldreichii* var. *pančići* (Table III), the relative values from Table II were used. CPI_{total} of *Pinus heldreichii* var. *pančići* (from 1.1 to 2.1; 1.6 on average) was a little higher than in wood smoke particular matter of *Pinus elliottii* Engelm.[41] The maximum *CPI* values of long chain *n*-alkanes of *Pinus heldreichii* var. *pančići* (Table III) were 2.2 ($CPI_{20–36}$), 3.0 ($CPI_{25–31}$) and 3.1 ($CPI_{25–33}$), while the short chain *n*-alkanes ($CPI_{15–21}$) ranged from 0.3 to 1.1 (0.6 on average) and exhibited an even/odd predominance (*EOP*) (because $CPI < 1$ indicates *EOP*, $CPI > 1$ denotes *OEP*[39]). The ACL_{total} values of *Pinus heldreichii* var. *pančići*

TABLE III. Analytical data for *n*-alkanes in needles of *Pinus heldreichii* var. *pančići*

No. of tree	C_{range}	C_{max}	CPI_{total}[c]	CPI_{25-33}[d]	CPI_{20-36}[e]	CPI_{15-21}[f]	CPI_{25-31}[g]	ACL_{total}[h]	ACL_{23-35}[i]	In % of total		*n*-alkanes (C 18-33)	
										n-C 18-20	*n*-C 21-24	*n*-C 25-33	
1		23	2.1	3.1	2.2	1.1	3.0	25.8	26.8	2.4	35.6	62.0	
2	18, 20 – 33	23	1.1	2.0	1.4	0.3	1.9	25.0	26.6	11.3	36.4	52.3	
3	18 – 33	27	1.3	1.7	1.5	0.6	1.7	25.6	27.0	9.6	30.5	60.0	
4	18 – 33	23	1.8	2.8	2.1	0.6	2.8	25.2	26.5	8.1	35.6	56.3	
5	18 – 33	29	1.5	2.6	1.9	0.5	2.5	25.1	27.0	13.1	32.8	54.1	
6	18 – 33	23	1.7	2.9	2.0	0.7	2.8	25.0	26.4	9.0	37.9	53.2	
7	18 – 33	27	1.7	3.1	2.1	0.5	3.0	25.2	26.5	9.4	33.8	56.9	
Range	18 – 33	23 – 29	1.1 – 2.1	1.7 – 3.1	1.4 – 2.2	0.3 – 1.1	1.7 – 3.0	25.0 – 25.8	26.4 – 27.0	2.4 – 13.1	32.8 – 37.9	52.3 – 62.0	
Average	18 – 33	27	1.6	2.6	1.9	0.6	2.5	25.3	26.7	9.0	34.6	56.4	

[c] CPI_{total} = Σodd C_n/Σeven C_n (ref. 36); C_n is the concentration of *n*-alkane containing *n* carbon atoms;

[d] CPI_{25-33} = [Σ(C_{25}–C_{33})odd/ΣC_{24}–C_{32})even+Σ(C_{25}–C_{33})odd/ΣC_{26}–C_{34})even]/2 (ref. 40);

[e] CPI_{20-36} = [Σ(C_{20}–C_{36})odd/Σ(C_{19}–C_{35})even+Σ(C_{20}–C_{36})odd/Σ(C_{21}–C_{37})even]/2 (ref. 40);

[f] CPI_{15-21} = [Σ(C_{15}–C_{21})odd/Σ(C_{14}–C_{20})even+Σ(C_{15}–C_{21})odd/Σ(C_{16}–C_{22})even]/2 (ref. 40);

[g] CPI_{25-31} = [Σ(C_{25}–C_{31})odd/Σ(C_{24}–C_{30})even+Σ(C_{25}–C_{31})odd/Σ(C_{26}–C_{32})even]/2 (ref. 40);

[h] ACL_{total} = nΣC_n/ΣC_n (ref. 37);

[i] ACL_{23-35} = (23C_{23}+25C_{25}+27C_{27}+29C_{29}+31C_{31}+33C_{33}+35C_{35})/(C_{23}+C_{25}+C_{27}+C_{29}+C_{31}+C_{33}+C_{35}) (ref. 37)

ranged from 25.0 to 25.8 and the $ACL_{23–35}$ values ranged from 26.4 to 27.9 (Table III).

The relative proportion of short chain *n*-alkanes of *Pinus heldreichii* var. *pančići* (*n*-$C_{18–20}$ = 9.0 %) is significant (Table III) and similar to that in the leaves of *Acacia* sp. ($C_{14–20}$ = 10.1 %).[40] There is no great dominance of long chain (*n*-$C_{25–33}$ = 56.4 %) over mid chain *n*-alkanes (*n*-$C_{21–24}$ = 34.6 %), which could explain lower *CPI* and *ACL* values of *Pinus heldreichii* var. *pančići* (Table III) compared to those of some other species of the section *Pinus*.[9,38]

The differences in the composition, abundance, C_{max} values and other characteristics of *n*-alkanes between *Pinus heldreichii* var. *pančići* and other pines from the literature can be the consequence of the time of the needle sampling. In this research, the needles were sampled in the autumn, whereas some authors sampled the needles in the spring.[9,11,38] The crown exposition and illumination can also be a cause of the differences between *Pinus heldreichii* var. *pančići* and other pines. A large number of factors including light intensity, humidity, use of recycled CO_2, osmotic stress, CO_2 concentration, temperature, altitude and plant age influence the carbon isotopic composition of *n*-alkanes,[32,42,43] which is often regarded together with *ACL* values.[43] Trends to longer *n*-alkane chains and less negative carbon isotopic values are evident from rain forest over C_3 savanna to C_4 vegetation.[43] Lipids from inner shade leaves of *Quercus robur* L. and *Fagus sylvatica* L. were consistently more depleted in ^{13}C than those from the corresponding sun-lit leaves.[32] In contrast, in the case of *Quercus castaneifolia* C. A. Mey., the concentrations of C_{27} and C_{31} *n*-alkanes remained at constant levels throughout the whole growing season.[44] As the amount of seasonal variation is unknown for *Pinus* needles, the influence of different sampling season on sample comparison is unknown.

It is important to emphasize that in many other studies, chloroform[9] and not *n*-hexane was used as the dissolving agent.

CONCLUSIONS

According to the dominant *n*-alkanes, *Pinus heldreichii* var. *pančići* differs clearly from *Pinus heldreichii* var. *leucodermis*. The fact that *n*-alkanes can be successfully used in the determination of the variety of conifers has already been proved for *Juniperus communis* L.[16] and *Picea omorika* (Pančić) Purkyne.[45]

According to several alkane patterns, it was found that *Pinus heldreichii* var. *pančići* is more similar to some pines from subsections *Ponderosae* (section Pinus), *Cembrae* and *Strobi* (section Strobus) than to some of closely related pines (subsection *Sylvestres*, section Pinus).[9,11,38,39,41] Low values of odd/even predominance of *Pinus heldreichii* var. *pančići* leaf *n*-alkanes as well as low *CPI* and *ACL* values are the consequence of large amounts of short and mid chain *n*-al-

kanes, which are not typical for most pines and other C_3 gymnosperm and angyosperm plants, where long-chain *n*-alkanes strongly dominate.[46]

Populations adapted to warmer and more arid conditions have higher proportions of alkanes with longer chains in their waxes than those adapted to cooler and more humid conditions.[47] It is presumed that a strong genetic influence on the adaptation of hydrocarbons to environmental conditions exists (in the Cupressaceae family).[48] Similarly to the composition and variability of essential oils,[7] the specific profile of *n*-alkanes of *Pinus heldreichii* var. *pančići* could also be explained by the relict character of this species, the variability and genetic adaptation of which was expressed during great tectonic changes and glaciations.

Although in this paper the composition of alkanes in *Pinus heldreichii* on the different natural sites were analysed for the first time, the study of a small number of samples cannot give the complete picture on the variability at the species level, but only a picture of its variety *pančići*. Due to this fact, more detailed population research is recommended to be conducted in the future outside the borders of Serbia.

Acknowledgment. This research was supported by a grant from the Ministry of Science and Technological Development of the Republic of Serbia.

И З В О Д

n-АЛКАНИ У ВОСКОВИМА ИГЛИЦА *Pinus heldreichii* var. *pančići*

БИЉАНА НИКОЛИЋ[1], ВЕЛЕ ТЕШЕВИЋ[2], ИРИС ЂОРЂЕВИЋ[3], МИЛКА ЈАДРАНИН[4], МАРИНА ТОДОСИЈЕВИЋ[4], СРЂАН БОЈОВИЋ[5] и ПЕТАР Д. МАРИН[6]

[1]Институт за шумарство, Кнеза Вишеслава 3, 11000 Београд, [2]Хемијски факултет, Универзитет у Београду, Студентски трг 16, 11000 Београд, [3]Факултет ветеринарске медицине, Универзитет у Београду, Булевар ослобођења 18, 11000 Београд, [4]Институт за хемију, технологију и металургију, Универзитет у Београду, Његошева 12, 11000 Београд, [5]Институт за биолошка истраживања "Синиша Станковић", Булевар деспота Стефана 142, 11000 Београд и [6]Биолошки факултет, Институт за ботанику и Ботаничка башта "Јевремовац", Студентски трг 16, 11000 Београд

Ово је прво саопштење о *n*-алканима у восковима иглица варијетета мунике, *Pinus heldreichii* var. *pančići*. *n*-Хексански екстракти узорака иглица који потичу са седам изолованих локалитета у Србији анализирани су гасном хроматографијом (GC) и гасном хроматографијом–масеном спектрометријом (GC–MS). Резултати су показали да се *n*-алкани налазе у опсегу од C_{18} до C_{33}. Међу њима су најобилнији C_{27}, C_{23}, C_{25} и C_{29} (12,53, 12,46, 12,00 и 10,38 % у просеку, редом). Угљенични преференцијални индекс (CPI_{total}) *Pinus heldreichii* var. *pančići* је био у опсегу од 1,1 до 2,1 (просечно 1,6), а дужина низа угљеникових атома (ACL_{total}) у опсегу од 25,0 до 25,8 (просечно 25,3). Такође је утврђен висок ниво индивидуалне квантитативне варијабилности у свим анализираним параметрима ових угљоводоника. Добијени резултати су упоређени са литературним подацима који се односе на *Pinus heldreichii* var. *leucodermis* и друге врсте рода *Pinus*.

(Примљено 22. марта, ревидирано 14. јуна 2010)

REFERENCES

1. M. Vidaković, *Conifers. Morphology and Variabilities*, JAZU i Sveučilišna naklada Liber, Zagreb, 1982, p. 710 (in Croatian)
2. P. Fukarek, *Godišnjak Biološkog Instituta (Sarajevo)* **4/1** (1951) 41 (in BHS)
3. M. Tošić, *Šumarstvo (Beograd)* **7**–**8** (1960) 383 (in Serbian)
4. P. Fukarek, *Šumarski list (Zagreb)* **5**–**6** (1960) 152 (in Croatian)
5. P. Fukarek, M. Vidaković, *Naučno društvo Bosne i Hercegovine, Radovi (Sarajevo)* **28** (1965) 68 (in BHS)
6. P. Fukarek, M. Nikolić, *Zbornik SANU i ANUBiH (Beograd)* **1** (1974) 20 (in BHS)
7. B. Nikolić, M. Ristić, S. Bojović, P. D. Marin, *Chem. Biodiv.* **4** (2007) 905
8. F. Gniwotta, G. Vogg, V. Gartmann, T. L. W. Carver, M. Riederer, R. Jetter, *Plant Physiol.* **139** (2005) 519
9. D. R. Oros, L. J. Standley, X. Chen, B. R. T. Simoneit, *Z. Naturforsch.* **54c** (1999) 117
10. S. Dragota, M. Riederer, *Ann. Bot.* **100** (2007) 225
11. M. Maffei, S. Badino, S. Rossi, *J. Biol. Res. – Thessaloniki* **1** (2004) 3
12. G. A. Herbin, P. A. Robins, *Phytochemistry* **7** (1968) 1325
13. G. A. Herbin, P. A. Robins, *Phytochemistry* **7** (1968) 267
14. W. Tin, F. C. Vasek, R. W Scora, *Am. J. Bot.* **58** (1971) 255
15. K. D. Cameron, M. A. Teece, E. Bevilacqua, B. Lawrence, *Phytochemistry* **60** (2000) 715
16. R. S. Dodd, M. M. Poveda, *Biochem. Syst. Ecol.* **31** (2003) 1257
17. A. P. Tulloch, *Can. J. Bot.* **59** (1981) 1213
18. J. F. Stevens, H. Hart, A. Bolck, J. H. Zwaving, T. M. Malingre, *Phytochemistry* **35** (1994) 389
19. M. Maffei, *Biochem. Syst. Ecol.* **22** (1994) 711
20. M. Maffei, in *Compositae: Systematics*, D. J. N. Hind, H. J. Beentje, Eds., Royal Botanic Gardens, Kew, UK, 1969, p. 141
21. G. A. Herbin, P. A. Robins, *Phytochemistry* **7** (1968) 239
22. N. Simić, R. Palić, S. Milosavljević, V. Vajs, D. Djoković, N. Randjelović, *Facta Univ. Ser. Phys. Chem. Tech. (Niš)* **2** (1999) 27
23. R. N. Bowman, *Am. J. Bot.* **67** (1980) 671
24. T. G. Knight, M. A. B. Wallwork, M. Sedgley, *Int. J. Plant Sci.* **165** (2004) 27
25. C. Lutz, V. Heinzmann, P. G. Gülz, *Environ. Pollut.* **64** (1990) 313
26. K. E. Percy, E. A. Baker, *New Phytol.* **116** (1990) 79
27. G. Bianchi, C. Murelli, E. Ottaviano, *Phytochemistry* **29** (1990) 739
28. K. N. Gaind, R. L. Gupta, *Phytochemistry* **11** (1972) 1500
29. D. Sachse, J. Radke, G. Gleixner, *EOS Trans.* **85** Fall Meet. Suppl. (2004) 80
30. K. E. Percy, R. Jagels, S. Marden, C. K. McLaughlin, J. Carlisle, *Can. J. Forest Res.* **23** (1993) 1472
31. G. A. Herbin, P. A. Robins, *Phytochemistry* **7** (1969) 1985
32. M. J. Lockheart, I. Poole, P. F. Van Bergen, R. P. Evershed, *Org. Geochem.* **29** (1998) 1003
33. D. Corrigan, R. F. Timoney, D. M. X. Donnelly, *Phytochemistry* **17** (1978) 907
34. M. R. M. Mimura, M. L. F. Salatino, A. Salatino, J. F. A. Baumgratz, *Biochem. Syst. Ecol.* **26** (1998) 581
35. H. Van Den Dool, P. D. Kratz, *J. Chromatogr.* **11** (1963) 463

36. M. A. Mazurek, B. R. T. Simoneit, in *Molecular Markers in Environmental Geochemistry*, R. P. Eganhouse, Ed., Am. Chem. Soc. Symp. Series 671, ACS, Washington, DC, 1997, p. 92
37. J. Poynter, G. Eglington, in *Molecular composition of three sediments from Hole 717C: the Bengal Fan*, J. R. Cochran, D. A. V. Stow, Eds., Proc. ODP Sci. Results 116, Ocean Drilling Program, College Station, TX, 1990, p. 155
38. Y. Chikaraishi, H. Naraoka, *Phytochemistry* **63** (2003) 361
39. T. K. Kuhn, E. S. Krull, A. Bowater, K. Grice, G. Gleixner, *Org. Geochem.* **41** (2010) 88
40. E. E. Bray, E. D. Evans, *Geochim. Cosmochim. Acta* **22** (1961) 2
41. B. R. T. Simoneit, W. F. Rogge, Q. Lang, R. Jaffé, *Chemosphere – Global Change Science (Amsterdam)* **2** (2000) 107
42. N. C. Arens, A. H. Jahren, R. Amundson, *Paleobiology* **26** (2000) 137
43. A. Vogts, H. Moossen, F. Rommerskirchen, J. Rullkötter, *Org. Geochem.* **40** (2009) 1037
44. M. J. Lockheart, P. F. Van Bergen, R. P. Evershed, *Org. Geochem.* **26** (1997) 137
45. B. Nikolic, V. Tesevic, I. Djordjević, M. Jadranin, S. Bojovic, P. D. Marin, *Chem. Nat. Compd.* **45** (2009) 697
46. F. Rommerskirchen, A. Plader, G. Eglinton, Y. Chikaraishi, J. Rullkötter, *Org. Geochem.* **37** (2006) 1303
47. R. S. Dodd, Z. Afzal-Rafii, A. B. Power, *New Phytol.* **138** (1998) 699
48. R. S. Dodd, Z. Afzal-Rafii, *Evolution* **54** (2000) 1438.

Journal of the Serbian Chemical Society
JSCS-info@shd.org.rs • www.shd.org.rs/JSCS
J. Serb. Chem. Soc. 75 (10) 1347–1359 (2010)
JSCS–4057
UDC 582.623–035.27:547.384:
547.431.4:615.28
Original scientific paper

Chemical composition and screening of the antimicrobial and antioxidative activity of extracts of *Stachys* species

JELENA S. LAZAREVIĆ[1]*, RADOSAV M. PALIĆ[2#], NIKO S. RADULOVIĆ[2], NOVICA R. RISTIĆ[3] and GORDANA S. STOJANOVIĆ[2]

[1]*Department of Pharmacy, Faculty of Medicine, University of Niš, Bul. Dr Zorana Đinđića 81, 18000 Niš,* [2]*Department of Chemistry, Faculty of Science and Mathematics, University of Niš, Višegradska 33, 18000 Niš and* [3]*Department of Chemistry, Faculty of Science and Mathematics, University of Priština, Kosovska Mitrovica, Serbia*

(Received 3 June, revised 24 August 2010)

Abstract: GC and GC/MS analyses of the diethyl ether and ethyl acetate extracts obtained from the aerial parts of *Stachys germanica* subsp. *heldreichii* (Boiss) Hayek, *Stachys iva* Griseb., *Stachys plumosa* Griseb. and *Stachys scardica* Griseb., Balkan peninsula endemics, were performed. One hundred and seventy-nine constituents, accounting for 88.8–98.1% of the total composition of the extracts, were identified. The common feature of the diethyl ether extracts was the high content of terpenoids and fatty acid-derived compounds, while the common feature of the ethyl acetate extracts was the prevalence of fatty acid-derived compounds. A disk diffusion method was used for the evaluation of the antimicrobial activities of the extracts against a panel of microorganisms (bacteria: *Staphylococcus aureus*, *Escherichia coli*, *Klebsiella pneumoniae*, *Pseudomonas aeruginosa*, and *Salmonella enteritidis*; fungi: *Aspergillus niger* and *Candida albicans*). The total antioxidant capacity of the extracts was evaluated by the phosphomolybdenum method. The preliminary bioassay results indicated that the diethyl ether extract of *S. plumosa* could be a possible source of antioxidant and antimicrobial compounds.

Keywords: *Stachys*; Lamiaceae; diethyl ether and ethyl acetate extracts; antimicrobial activity, antioxidant capacity.

INTRODUCTION

Stachys L., one of the largest genera of the Lamiaceae family, contains more than 270 species. This sub-cosmopolitan genus has two main centers of diversity in the Old World area.[1] One is confined to S. and E. Anatolia, Caucasia, N.W.

* Corresponding author. E-mail: jelena217@yahoo.com
# Serbian Chemical Society member.
doi: 10.2298/JSC100601117L

Iran and N. Iraq, and the other to the Balkan Peninsula. Serbia is an area that is moderately rich in taxa belonging to the genus (seventeen species are acknowledged), however, eight species are recognized as endemic to the Balkans, or even narrower regions.[2]

Although genus *Stachys* is considered to be one of the largest genera in the Lamiaceae family, little attention has been paid to the elucidation of its pharmacological properties. These facts stand as a surprise, especially when it is known that data exist concerning the traditional application of many *Stachys* species for genital and inflammatory tumors, cancerous ulcers and sclerosis of the spleen.[3] Teas prepared from the whole part or leaves are used in phytotherapy, possessing sedative, antispasmodic, diuretic and emmenagogue activities. In Turkish folk medicine, species of the *Stachys* genus are used in the same way as sage.[4] Several *Stachys* species are recognized in Iranian folk medicine,[5] especially *S. inflata* which is used to treat various inflammatory disorders.[6] In hitherto undertaken pharmacological studies, *Stachys* species showed a variety of effects (anti-allergic,[7] anti-anoxic,[8] antibacterial,[9–12] anxiolytic,[13] anti-inflammatory,[6,14] antinephritic,[15] antioxidant,[16–19] antihepatitis and choleretic[20,21]), confirming a wide spectrum of application and an extensive range of traditional usage. The compositions of essential oils, as well as the preliminary screening using disk diffusion method for the *Stachys* species under study (*S. germanica* subsp. *heldreichii* (Boiss) Hayek, *S. iva* Griseb., *S. plumosa* Griseb. and *S. scardica* Griseb.) have been the subject of several previous publications,[10,22–25] but to the best of our knowledge, the chemical composition of extracts and the evaluation of their antimicrobial and antioxidant activities have never been studied previously (except for the antioxidant activities of a methanol extract of *S. plumosa*[16]).

In view of the growing interest in the application of natural products in the food, cosmetics and pharmaceutical industries and bearing in mind the scarcity of previous work on the bioassay of Balkan *Stachys* species, the subject of this study was to determine the chemical composition of diethyl ether and ethyl acetate extracts and to evaluate the antimicrobial and antioxidant activities of four Balkan endemic *Stachys* species: *S. germanica* subsp. *heldreichii* (Boiss) Hayek, *S. iva* Griseb., *S. plumosa* Griseb. and *S. scardica* Griseb.

EXPERIMENTAL

Plant material

The plant material of the four species was collected in June 2003 from natural populations, in the blooming stage as follows: *S. germanica* subsp. *heldreichii*, Galičica Mountain pastures at an altitude of 1600 m, Former Yugoslavian Republic of Macedonia; *S. iva*, Bislim-Kumanovo, the slopes of the Pčinja Gorge, Former Yugoslavian Republic of Macedonia; *S. plumosa*, along the road side Bosilegrad–Izvor, Serbia and *S. scardica*, Kozjak Mountain, Former Yugoslavian Republic of Macedonia. The material was air-dried until constant weight. Voucher specimens are deposited in the Herbarium of the Faculty of Biology, University of

Belgrade, under the accession numbers: BEOU 16024, 16017, 16018 and 16063, respectively. The plant species were identified by Dr Vladimir Ranđelović, Department of Biology and Ecology, Faculty of Science and Mathematics, University of Niš.

Preparation of the extracts

Ground samples of air-dried aerial parts (50 g per extract preparation) were extracted in sealed vessels with 250 ml of the appropriate solvent (diethyl ether or ethyl acetate) in an ultrasonic bath (Bandelin Electronics, Germany) for 5 h at room temperature. The obtained extracts were gravity filtered through small columns packed with 1 g of Celite® (Merck, Germany) in order to remove all the insoluble material and then concentrated to 10 mL using a steam of nitrogen before GC and GC/MS analysis. The yields of the dry extracts (% w/w, dry plant material), obtained by complete evaporation of the solvents *in vacuo* are given in Table I-S in the Supplementary material. The dried extracts were dissolved in the solvents used for extraction to a final concentration of 1 mg mL^{-1} and used as such for the antimicrobial and antioxidant testing.

Gas chromatography and gas chromatography/mass spectrometry

The GC/MS analyses (three repetitions for each sample) were preformed using a Hewlett Packard gas chromatograph, Model 5890, Series II equipped with an SPB-1 capillary column (Supelco Inc., Bellfonte, PA; 30 m×0.25 mm, film thickness 0.25 μm) directly coupled to a mass selective detector MSD 5971A of the same company operated in the EI mode (70 eV). Helium was used as the carrier gas at a flow rate of 1 mL min^{-1}. The operating conditions were injector temperature 250 °C and the oven temperature program: isothermal at 50 °C for 3 min, then ramped to 250 °C at a rate of 5 °C min^{-1}, and finally isothermal at 250 °C for 15 min. The injection volume for all samples was 1 μL (prepared as mentioned previously), and the injector split ratio was 1:10. The extract constituents were identified by comparison of their linear retention indices (relative to C8–C31 alkanes[26] on the SPB-1 column) with literature values[27] and their mass spectra with those of authentic standard, as well as those from Wiley 6, NIST02, MassFinder 2.3 and a home-made MS library with spectra corresponding to pure substances and components of known oils. Wherever possible, the identity of the constituents was verified by co-injection with an authentic sample. GC (FID) analysis was performed under the same experimental conditions using the same column as described for the GC/MS measurements, except that H_2 was used as the carrier gas. The FID temperature was 300 °C. Percentage area values were obtained electronically from the GC–FID response, without the use of an internal standard or correction factors.

Antimicrobial activity

The *in vitro* antimicrobial activity of the extracts against a panel of laboratory control strains belonging to the American Type Culture Collections, Maryland, USA; Gram-positive: *Staphylococcus aureus* (ATCC 6538), Gram-negative: *Klebsiella pneumoniae* (ATCC 10031), *Pseudomonas aeruginosa* (ATCC 9027), *Salmonella enteritidis* (ATCC 13076); fungal organisms *Aspergillus niger* (ATCC 16404) and *Candida albicans* (ATCC 10231) and the Gram-negative bacteria *Escherichia coli* 95 (Institute of Immunology and Virology "Torlak", Serbia) was determined using the disc diffusion assay recommended by NCCLS.[28]

The following nutrition media were used: Antibiotic Medium 1 (Difco Laboratories, Detroit, MI, USA) for growing the Gram-positive and Gram-negative bacteria and Tripton soy agar (TSA, Torlak, Belgrade, Serbia) for *A. niger* and *C. albicans*. The nutrition media were prepared according to the instructions of the manufacturers. All agar plates were prepared in 90 mm Petri dishes with 22 mL of agar, giving the final depth of 4 mm. A suspension of the

tested microorganisms (0.1 mL, 10^8 cells per mL) was spread on the solid media plates. Sterile filter paper disks ("Antibiotica Test Blättchen", Schleicher and Schuell, Dassel, Germany, 6 mm in diameter) were impregnated with 20 μL of the extracts and placed on the inoculated plates. These plates, after standing at 4 °C for 2 h, were incubated at 37 °C for 24 h for the bacteria, and at 30 °C for 48 h for the fungi. Standard disks of tetracycline, gentamicin, ampicillin and nystatin (Institute of Immunology and Virology "Torlak", 30 μg of the active component, diameter 6 mm) were individually used as the positive controls, while disks imbued with 20 μL of pure diethyl ether or ethyl acetate were used as the negative controls. The diameters of the inhibition zones were measured in millimeters using a "Fisher-Lilly Antibiotic Zone Reader" (Fisher Scientific Co., USA). Each test was performed in triplicate. Mean values are presented.

Antioxidant capacity

The total antioxidant capacity of the extracts was evaluated by the method of Prieto, Pineda, and Aguilar.[29] The antioxidant capacity of the extracts was measured spectrophotometrically using the phosphomolybdenum method, based on the reduction of Mo(VI) to Mo(V) by the sample analyte and the subsequent formation of green phosphate/Mo(V) compounds with a maximum absorption at λ = 695 nm. A 0.1 mL aliquot of sample solution (100 μg mL^{-1}) was combined in an Eppendorf tube with 1 mL of the reagent solution (0.6 M sulfuric acid, 28 mM sodium phosphate and 4 mM ammonium molybdate). The tubes were capped and incubated in a boiling water bath at 95 °C for 90 min. After the samples had cooled to room temperature, the absorbance of each aqueous solution was measured at 695 nm against a blank solution, using a Perkin-Elmer Lambda 15 UV-VIS spectrophotometer. A typical blank solution contained 1 mL of reagent solution and 0.1 mL of the solvent used for the extraction (diethyl ether or ethyl acetate), which was incubated under the same conditions as for the other samples. Stock solutions of α-tocopherol acetate were prepared in diethyl ether and in ethyl acetate just prior to use. The total antioxidant capacity is expressed as equivalents of α-tocopherol acetate (l μmol g^{-1} of extract) using a standard curve at five concentrations covering the range 50–1.600 μmol. The exact concentrations were determined spectrophotometrically based on the absorption coefficients from the literature. The determination of the total antioxidant capacity was performed in triplicate.

RESULTS AND DISCUSSION

The GC and GC/MS analyses of the diethyl ether (DE) and ethyl acetate (EA) extracts of *S. germanica* subsp. *heldreichii*, *S. iva*, *S. plumosa* and *S. scardica* enabled the overall identification of 179 components, listed in Table I-S (Supplementary material). In each instance, the fraction of extracted compounds consisted of a complex mixture of different classes of compounds the identities of which are presented as a separate column in Tables I and I-S. Generally, two main classes dominated the composition of the DE extract: terpenoids (from 36.5 to 64.9%) and fatty acid derived compounds (FADs, from 33.3 to 59.9 %). The main characteristic of the EA extracts was the prevalence of FADs (from 68.4 to 85.9 %) among other classes. The common feature of the DE extracts was a relatively high content of oxygenated sesquiterpenes (from 12.2 to 33.1 %, except for *S. plumosa*, 2.1 %) and *n*-alkanes (from 14.1 to 39.3 %). *n*-Alkanes (ranging from 43.2 to 79.3 %), together with branched alkanes (from 5.9 to

17.0%) constitute considerable portions of the EA extracts. (*Z*)-Nuciferyl isobutyrate (*S. iva* DE, 15.3 %), spathulenol and caryophyllene oxide (3.8 % DE and 4.3 % EA for *S. germanica*, and 3.8 % DE and 3.6 % EA *S. iva*, respectively) and abieta-8,11,13-triene (13.6 % DE and 17.8 % EA for *S. plumosa* and 5.0 % DE *S. scardica*, Table I) were compounds of terpenoid origin detected in significant amounts. Monoterpenoids, aliphatic alcohols and aldehydes represented residual portions of the analyzed extracts, or were not even detected.

TABLE I. Chemical composition (%) of four *Stachys* species extracts

RI[a]	Compounds[b]	Class	Method[c]	*S. germanica*		*S. iva*		*S. plumosa*		*S. scardica*	
				DE[d]	EA[e]	DE	EA	DE	EA	DE	EA
947	α-Pinene	T	a,b,c	–[f]	–	–	0.1	0.1	1.4	0.1	–
1375	β-Bourbonene	T	a,b	2.2	–	–	–	–	–	0.2	–
1409	β-Caryophyllene	T	a,b,c	0.7	–	0.9	tr[g]	0.1	–	1.3	tr
1459	γ-Muurolene	T	a,b	0.6	–	–	–	–	–	2.0	–
1464	Germacrene D	T	a,b,c	1.5	–	0.3	–	–	–	–	–
1491	γ-Cadinene	T	a,b	–	–	–	–	–	–	2.0	–
1498	δ-Cadinene	T	a,b	–	–	2.7	–	0.2	–	1.4	–
1563	Spathulenol	T	a,b,c	3.8	–	3.8	–	–	–	0.4	–
1571	Caryophyllene oxide	T	a,b,c	4.3	–	3.6	0.1	0.7	–	3.1	–
1580	4(14)-Salvialen-1-one	T	a,b	1.4	–	–	–	–	–	1.3	–
1583	Viridiflorol	T	a,b	2.5	–	1.1	–	–	–	–	–
1601	Copaborneol	T	a,b	–	–	2.0	–	–	–	–	–
1623	Isospathulenol	T	a,b	–	–	–	–	–	–	1.9	–
1625	1-*epi*-Cubenol	T	a,b	–	–	1.2	–	–	–	–	–
1637	τ-Muurolol	T	a,b	0.3	–	1.2	–	0.3	–	1.6	–
1651	α-Cadinol	T	a,b	0.5	–	–	–	0.2	–	2.1	–
1669	Valeranone	T	a,b	2.1	–	1.4	0.1	–	–	–	–
1678	Cadalene	T	a,b	–	–	–	–	–	–	1.9	–
1692	3-Hydroxy-5,6-epoxy--β-ionone	CR	a,b	1.5	–	–	–	0.5	–	–	–
1731	7,8-Dihydro-3--oxo-α-ionol	CR	a,b	1.0	–	–	–	–	–	0.3	–
1844	Neophytadiene, isomer I	T	a,b	–	1.1	1.4	0.3	2.7	0.6	2.6	2.8
1845	Hexahydrofarne-sylacetone	CR	a,b	3.5	–	–	–	–	–	–	–
1900	Nonadecane	FAD	a,b,c	1.2	–	0.3	–	0.1	–	0.2	–
1910	Methyl hexadeca-noate (*syn.*[h] methyl palmitate)	FAD	a,b	1.2	0.2	0.1	–	0.3	–	0.5	–
1929	1-Methylphenantrene	O	a,b	–	–	–	–	–	1.2	–	–
1944	(*Z*)-Nuciferyl isobutyrate	T	a,b	4.5	0.2	15.3	1.2	0.1	–	–	–
1968	*n*-Hexadecanoic acid	FAD	a,b,c	–	–	–	–	6.0	–	–	–

TABLE I. Continued

RI[a]	Compounds[b]	Class	Method[c]	*S. germanica*		*S. iva*		*S. plumosa*		*S. scardica*	
				DE[d]	EA[e]	DE	EA	DE	EA	DE	EA
1979	Ethyl hexadecanoate (*syn.* ethyl palmitate)	FAD	a,b	1.7	0.1	0.3	–	6.1	–	4.8	–
2000	Eicosane	FAD	a,b,c	0.5	–	–	–	–	–	1.9	–
2007	13-*epi*-Manoyl oxide	T	a,b	–	–	–	–	2.4	–	–	–
2039	Abieta-8,11,13-triene	T	a,b	0.3	–	0.1	–	13.6	17.8	5.0	0.8
2073	Methyl-(*Z*,*Z*,*Z*)--9,12,15-octadecatrienoate (*syn.* methyl linolenate)	FAD	a,b	1.5	–	0.1	–	1.1	–	0.8	–
2083	(*Z*)-9-Octadecenoic acid (*syn.* oleic acid)	FAD	a,b	–	0.6	–	–	1.7	–	0.2	0.5
2084	Methyl-(*Z*)-9-octadecenoate (*syn.* methyl oleate)	FAD	a,b	1.0	–	0.2	–	–	–	0.4	–
2093	Isoabienol	T	a,b	–	–	3.6	1.2	–	–	–	–
2100	Heneicosane	FAD	a,b,c	2.2	0.4	–	0.4	0.2	–	0.5	0.1
2105	*trans*-Phytol	T	a,b	5.2	0.7	4.0	0.8	7.9	–	3.8	0.9
2127	Methyl octadecanoate (*syn.* methyl stearate)	FAD	a,b	1.5	–	3.2	–	0.4	0.9	0.4	0.1
2140	Ethyl (*Z*,*Z*)-9,12-octadecadienoate (*syn.* ethyl linoleate)	FAD	a,b	1.4	–	0.3	–	2.9	–	0.4	–
2145	Ethyl (*Z*,*Z*,*Z*)-9,12,15--octadecatrienoate (*syn.* ethyl linolenate)	FAD	a,b	0.5	–	0.3	–	4.4	–	0.2	–
2170	Thunbergol	T	a,b	–	–	–	–	2.3	–	0.9	–
2178	Ethyl octadecanoate	FAD	a,b	0.2	–	0.2	–	1.5	–	0.4	–
2200	Docosane	FAD	a,b,c	1.6	0.6	0.3	tr	–	–	0.6	0.2
2209	Sclareol	T	a,b	–	–	0.3	0.1	–	1.5	–	–
2223	*cis*-Totarol	T	a,b	–	–	–	0.9	3.0	–	–	–
2270	Dehydroabietal	T	a,b	–	–	–	–	3.5	–	0.9	–
2271	1-Eicosanol	FAD	a,b	2.8	0.4	–	–	–	–	–	–
2300	Tricosane	FAD	a,b,c	5.5	1.8	3.8	0.5	6.6	–	17.6	1.4
2328	11-Methyltricosane	FAD	a,b	–	–	–	–	–	–	–	4.4
2338	Dehydroabietic acid methyl ester	T	a,b	–	–	–	–	2.8	–	1.4	1.2
2347	Dehydroabietol	T	a,b	–	–	–	–	1.3	6.2	–	–
2361	Butyl octadecanoate	FAD	a,b	–	–	0.5	0.2	1.4	–	0.8	–
2378	Ethyl eicosanoate	FAD	a,b	0.6	–	tr	–	0.4	–	2.1	–
2398	Labd-13(*E*)-en--8α,15-diol	T	a,b	–	–	14.3	–	–	–	–	–
2400	Tetracosane	FAD	a,b,c	1.0	0.6	tr	–	0.9	–	0.8	0.5
2431	Methyl neoabietate	T	a,b	–	–	0.3	9.6	0.2	–	–	–
2468	1-Docosanol	FAD	a,b	1.2	0.4	–	–	–	–	–	–

TABLE I. Continued

RI[a]	Compounds[b]	Class	Method[c]	*S. germanica*		*S. iva*		*S. plumosa*		*S. scardica*	
				DE[d]	EA[e]	DE	EA	DE	EA	DE	EA
2500	Pentacosane	FAD	a,b,c	3.6	2.5	0.6	0.8	1.2	2.6	1.3	1.4
2564	2-Methylpentacosane	FAD	a,b	0.1	–	–	–	–	13.2	–	–
2573	3-Methylpentacosane	FAD	a,b	–	0.3	–	1.5	–	–	–	–
2576	Ethyl docosanoate	FAD	a,b	–	–	–	–	0.8	6.1	0.2	–
2700	Heptacosane	FAD	a,b,c	4.9	7.2	2.9	5.3	4.3	27.7	4.3	5.0
2771	3-Methylheptacosane	FAD	a,b	0.2	1.0	–	0.1	0.1	–	–	–
2800	Octacosane	FAD	a,b,c	0.8	1.9	0.8	1.4	0.5	2.8	0.3	1.1
2808	Squalene	T	a,b	0.8	1.1	0.1	0.2	0.2	–	0.5	1.6
2859	10-Demethylsqualene	T	a,b	0.1	0.2	0.5	–	0.3	–	1.0	0.4
2900	Nonacosane	FAD	a,b,c	17.0	36.9	18.0	28.3	–	6.5	3.6	19.3
2934	10-Methylnonacosane	FAD	a,b	–	2.7	–	12.0	–	–	–	–
2973	3-Methylnonacosane	FAD	a,b	–	0.3	–	–	–	3.2	–	0.6
3000	Triacontane	FAD	a,b,c	0.6	2.1	–	2.1	–	3.6	8.0	5.9
3100	Hentriacontane	FAD	a,b	–	20.9	–	23.3	–	–	–	43.7
Total				96.4	88.8	98.1	93.2	91.9	96.7	97.5	94.7
Yield, % (w/w)				1.4	10.0	1.5	4.0	1.4	8.0	1.5	5.8
Grouped components											
Terpenoids (T)				36.5	3.9	64.7	14.7	47.3	28.3	43.0	8.8
Monoterpene hydrocarbons				–	–	tr	0.1	0.6	2.2	0.3	–
Oxygenated monoterpenes				0.4	–	–	–	2.5	–	0.1	–
Sesquiterpene hydrocarbons				6.5	–	6.0	tr	0.8	–	12.6	tr
Oxygenated sesquiterpenes				22.5	0.2	32.9	1.4	2.1	–	12.7	0.1
Diterpenes				6.0	2.4	25.2	13.0	40.8	26.1	15.7	6.5
Triterpenes				1.1	1.3	0.6	0.2	0.5	–	2.1	2.2
Fatty acid derived compounds (FAD)				59.9	84.9	33.4	78.5	44.6	68.4	54.5	85.9
n-Alkanes				39.2	74.9	26.9	62.1	14.1	43.2	39.3	79.3
Branched alkanes				0.3	7.1	–	15.4	0.2	17.0	0.8	5.9
Alcoholes				4.0	0.8	–	–	–	–	–	–
Aldehydes				–	–	tr	0.1	0.5	–	–	0.1
Fatty acids and fatty acid esters				10.4	1.7	6.4	0.9	28.3	7.0	13.8	0.6
Carotenoid derived compounds				6.0	0.4	0.1	–	1.3	–	0.3	–
Others (O)				–	–	–	–	0.2	1.2	0.3	–

[a]Components listed in order of elution from SPB-1 column (RI – experimentally determined retention indices on the mentioned column by co-injection of a homologous series of *n*-alkanes C_8–C_{31}); [b]major components are given in Table I (components having relative abundances ≥1.0 % in at least one sample), while the other identified components (minor) can be found in Supplementary material (see Supplementary material for detail composition on extracted volatiles); [c]a – constituent identified by retention index matching; b – constituent identified by mass spectra comparison; c – constituent identified by co-injection of an authentic sample; [d]diethyl ether extract; [e]ethyl acetate extract; [f]not detected; [g]trace (<0.05 %); [h]synonym

As already mentioned, an interesting feature of the extracts was the occurrence of branched alkanes, detected in relatively significant amounts in the EA

extracts (from 5.9 to 17.0 %) and as minor constituents in the DE extract (from 0.2 to 0.4 %). Until now, branched alkanes were considered to have limited occurrence in the plant kingdom, and their distribution was assumed to be a characteristic of evolutionary primitive and old higher plant taxa.[30] However, it might be just as possible that these compounds may be taken into account as common constituents of epicuticular waxes of evolutionary and philogenetically more complex plants, although present in lower amounts (distribution of long chain *n*-alkanes is dominant[31]). Publications dealing with other members of the Lamiaceae family, *i.e.*, *Marrubium*,[32] *Micromeria*[33] and *Scutellaria*,[34] also reported the identification of branched alkenes among the components detected during analyses of epidermal tissue hydrocarbons. This provides more reason to speculate and employ this observation as a hypothesis for future work (extending analyzes to related families).

An additional characteristic of the analyzed extracts was the ubiquitous presence of diterpenoids in all samples. Among the samples analysed, *S. plumosa* contained the highest portion (DE 40.8 % and EA 26.1 %), while *S. germanica* (DE 6 % and EA 2.4 %) had the smallest portion of the diterpene moieties detected. The distribution of the extractable compounds within the diterpenoid fraction was in favor of abietanes, labdanes and phytanes. Conservation of the diterpenoid skeleton has proven to be useful in reflecting chemotaxonomic features within the Lamiaceae family.[35,36] Concerning the taxonomical problems within the *Stachys* genus and several papers dealing this matter,[37–40] it might be valuable to perceive if diterpenes (and if, which of the skeletal types is the most prominent one) can be considered as biomarkers reflecting potential infrageneric chemotaxonomic relations.

Comparing the composition of the obtained extracts (DE and EA, present study) with previously published results for the essential oils[22] of the *Stachys* species under study (collected from the same localities), it can be observed that FAD constituents were present in high amounts in the extracts (Table I), while only in the oil of *S. germanica* subsp. *heldreichii* were FADs identified (*n*-alkanes 0.2 %).

The results of the antimicrobial assay showed that the DE extracts of *Stachys* inhibited the growth of all the tested bacteria (Table II), but only *S. plumosa* exhibited significant antimicrobial activity against the most persistent human pathogens *E. coli*, *P. aeruginosa* and *S. aureus* (comparable to antibiotics used as the positive controls). The obtained results seem to be in agreement with the activity that can be expected when referring to the chemical composition of the extracts, since *S. plumosa* DE components (oxygenated [3.1.1] bicyclic (pinane type) monoterpenoides *cis*/*trans*-verbenol, myrtenal, pinocarvone) have been shown to act as good antimicrobial agents.[41] However, concerning the hitherto reported publications, diterpenes (identified in the present extracts in significant amounts,

TABLE II. The antimicrobial activity (diameters of growth inhibition zones measured in mm) of the extracts of four *Stachys* species

Sample	Microorganism										
	E. coli[a]		*S. enteritidis*	*P. aeruginosa*		*K. pneumoniae*		*S. aureus*		*C. albicans*	*A. niger*
	C[b]	S[b]	S	C	S	C	S	C	S	S	S
						S. iva					
DE	–	22.7±0.09	22.7±0.67	–	–	19.9±0.16	21.1±0.64	–	–	–	–
EA	–	19.0±0.11	15.8±0.15	–	17.8±0.11	–	15.8±0.23	–	17.9±0.66	–	–
						S. germanica					
DE	–	24.1±0.19	24.0±0.84	–	29.4±0.28	–	20.7±0.05	–	22.0±0.61	–	28.6±0.37
EA	–	15.6±0.23	15.4±0.61	–	15.8±0.10	–	–	–	–	–	–
						S. plumosa					
DE	23.8±0.04	31.8±0.13	31.8±1.23	20.4±0.10	31.0±0.01	–	20.2±0.35	23.1±0.84	30.0±0.61	–	24.1±0.10
EA	–	15.8±0.31	16.2±0.37	–	16.1±0.51	–	–	–	14.8±0.03	–	–
						S. scardica					
DE	–	23.8±0.09	25.9±0.07	–	25.0±0.08	–	–	–	27.0±0.94	23.0±0.77	24.7±0.70
EA	–	15.2±0.08	17.8±0.12	–	14.7±0.26	–	–	–	14.9±0.21	–	–
Tetracycline[c]	30.6±0.53		31.3±0.73	29.3±0.63		30.3±0.77		30.7±0.42		nt[d]	nt
Gentamicine[c]	24.2±0.99		22.2±0.35	19.8±0.87		16.5±0.62		19.2±1.23		nt	nt
Ampicillin[c]	12.2±0.61		11.2±0.14	–		14.1±0.09		–		nt	nt
Nystatin[c]	nt		nt	nt		nt		nt		17.2±0.34	19.0±0.27

[a] Mean value ±*SD* (in mm) of 5 experiments, including disk diameter, 6 mm (20 μg of extract per disk). Values for static zones represent the extra millimeters around the cidal zone (or the sole disk if no cidal activity) in which the growth of microorganisms was inhibited but in which the microorganisms were not killed; [b] bacteri- and fungicidal zones; [c] positive control cidal activity (30 μg per disk); [d] not tested

Table I) might be acting as antimicrobial agents in these plants as well.[42,43] Labdane type diterpenes detected in the DE extracts of *S. iva* and *S. plumosa*, 13--*epi*-manoyl oxide (*S. plumosa* DE, Table I) and labd-13(*E*)-ene-8*α*,15-diol (*S. iva* DE, Table I), have been tested previously and found to possess significant antimicrobial activity.[44,45] However, although *S. iva* contained significant amount of labd-13(*E*)-ene-8*α*,15-diol (14.3 %), the activity of the extract was a selective one and affected the growth of *K. pneumoniae* only. The EA extracts exhibited no significant antimicrobial activity. The low activity could be correlated with the high content of alkane fraction (alkanes are known as substances that are not active against microorganisms).

The results of the total antioxidant capacity assay (Table III) showed that the extracts possessed antioxidant activity. The antioxidant capacity of the DE extracts was approximately ten times higher than the capacity of the EA extracts. The values for the capacity of EA extracts were comparable for all species under study, ranging between 4 and 5 μmol g^{-1} of the EA extracts (expressed as equivalents of *α*-tocopherol acetate, rounded numbers). The highest antioxidant capacity was measured for the DE extract of *S. plumosa*, and was approximately two times higher than the activity of DE extracts of the other examined species (Table II). A previously published paper reported significant antioxidant activities for the methanol extract of *S. plumosa* (tested for its ferric reducing antioxidant power assay, 1,1-diphenyl-2-picryl-hydrazyl free radical and OH radical scavenging activity, and in lipid peroxidation assays), which were attributed to the large amount of total phenolics in the methanol extract of the examined species (reported in this paper as well).[16] The value obtained in the total antioxidant capacity assay for the DE extract of *S. plumosa* (present work, no polyphenols detected) indicates that apart from polyphenols, this species might be having other

TABLE II. The total antioxidant capacity of the extracts of *Stachys* species from the Balkans expressed as equivalents of *α*-tocopherol acetate (μmol g^{-1} of extract)

Sample	Antioxidant activity (the mean values±*SD* of five experiments)
S. iva	
DE	38.1±0.35
EA	4.4±0.77
S. germanica	
DE	47.0±0.31
EA	4.0±0.11
S. plumosa	
DE	75.3±1.94
EA	5.1±0.59
S. scardica	
DE	34.0±0.54
EA	4.9±0.51

compound(s) that could act as antioxidant agent(s). However, due to the complexity of the extract analyzed (more than 80 compounds detected), it seems difficult to explain which component of this complex mixture may be responsible for the expressed activity.

CONCLUSIONS

The performed GC and GC/MS analyses enabled the identification of 179 components obtained from four Balkan endemic *Stachys* species (*S. germanica* subsp. *heldreichii* (Boiss) Hayek, *S. iva* Griseb., *S. plumosa* Griseb. and *S. scardica* Griseb) extracts. Terpenoids (from 36.5 to 64.9 %) and fatty acid derived-compounds (FADs from 33.4 to 59.9 %) were the main compound classes detected among the extractable matter obtained when diethyl ether was used as the extracting solvent. The main characteristic of the ethyl acetate extracts was the prevalence of FADs (from 68.4 to 85.9 %), with its most dominant subfraction represented by *n*- and branched alkanes. An additional characteristic of the analyzed extracts was the presence of diterpenoids in all samples (from 40.8 to 2.4 %). The results of the antimicrobial assay showed that DE extracts of *Stachys* inhibited the growth of all tested bacteria (*S. plumosa* activity was comparable to those of the antibiotics used as positive controls), while the activities of the EA extracts could be considered weak. The results of the total antioxidant capacity assay showed that the studied species possessed antioxidant activity, which was found to be the greatest in the case of the DE extract of *S. plumosa*.

In conclusion, the DE extract of *S. plumosa* exhibited good antimicrobial and antioxidant activity and could be considered as a good candidate for raw material phyto-preparations.

SUPPLEMENTARY MATERIAL

The yields of the dry extracts of plant material are available electronically from http://www.shd.org.rs/JSCS/, or from the corresponding author on request.

Acknowledgement. This work was funded by the Ministry of Science and Technological Development of the Republic of Serbia, Project No. 142054B.

И З В О Д

ХЕМИЈСКИ САСТАВ, АНТИМИКРОБНА И АНТИОКСИДАНТНА АКТИВНОСТ ЕКСТРАКАТА ОДАБРАНИХ БИЉНИХ ВРСТА РОДА *Stachys*

ЈЕЛЕНА С. ЛАЗАРЕВИЋ[1], РАДОСАВ М. ПАЛИЋ[2], НИКО С. РАДУЛОВИЋ[2], НОВИЦА Р. РИСТИЋ[3] и ГОРДАНА С. СТОЈАНОВИЋ[2]

[1]*Одсек Фармација, Медицински факултет, Универзитет у Нишу, Бул. Др. Зорана Ђинђића 81, 18000 Ниш,* [2]*Одсек за Хемију, Природно-математички факултет, Универзитет у Нишу, Вишеградска 33, 18000 Ниш и* [3]*Одсек за Хемију, Природно-математички факултет, Универзитет у Приштини са седиштем у Косовској Митровици, Косовска Митровица*

Диетил-етарски и етил-ацетатни екстракти надземних делова ендемичних балканских биљних врста, *Stachys germanica* ssp. *heldreichii* (Boiss) Hayek, *Stachys iva* Griseb., *Stachys*

plumosa Griseb. и *Stachys scardica* Griseb, анализирани су комбинацијом GC и GC/MS. У испитиваним екстрактима идентификовано је укупно 179 компонената, које су чиниле од 88,8 до 98,1 % екстраката. Етарски екстракти анализираних биљака садрже висок проценат терпеноида (од 36,5 до 64,7 %) и деривата масних киселина (од 33,4 до 59,9 %), док су се етил-ацетатни одликовали високим процентом деривата масних киселина (од 68,4 до 85,9 %). Антимикробна активност добијених екстраката испитана је диск дифузионом методом користећи лабораторијски контролисане сојеве бактерија (*Staphylococcus aureus*, *Escherichia coli*, *Klebsiella pneumonia*, *Pseudomonas aeruginosa* и *Salmonella enteritidis*) и гљивица (*Aspergillus niger* и *Candida albicans*). Антиоксидантни капацитет екстраката одређен је фосфомолибденском методом. Прелиминарни резултати in vitro спроведених биотестова указују на значајну антимикробну активност и антиоксидантни капацитет етарског екстракта биљне врсте *S. plumosa*, те да ову биљну врсту треба узети у обзир за даља испитивања у циљу практичне примене.

(Примљено 3. јуна, ревидирано 24. августа 2010)

REFERENCES

1. D. J. Mabberly, *The Plant Book*, Cambridge University Press, Cambridge, 1997, p. 678
2. N. R. Diklic, in *Flora of SR Serbia*, M. Josifović, Ed., SANU, Belgrade, 1974, p. 408 (in Serbian)
3. H. D.Skaltsa, D. M. Lazari, I. B. Chinou, A. E. Loukis, *Planta Med*. **65** (1999) 255
4. E. Sezik, A. Bascaran, *J. Fac. Pharm.* **21** (1985) 98
5. A. Zargari, *Medicinal Plants*, Vol. 4, Teheran University Publications, Teheran, 1990, p. 123
6. N. Maleki, A. Garjani, H. Nazemiyah, N. Nilfouroushan, A. T. Eftekhar Sadat, Z. Allameh, N. Hasannia, *J. Ethnopharmacol*. **75** (2001) 213
7. K. Suk-Hyun, K. Dae-Keun, E. Dong-Ok, P. Jeong-Suk, L. Jong-Pil, K. Sang-Yong, S. Hye-Young, K. Sang-Hyun, S. Tae-Yong, *Nat. Prod. Sci.* **9** (2003) 44
8. J. Yamahara, T. Kitani, H. Kobayashi, Y. Kawahara, *Yakugaku Zasshi* **110** (1990) 932 (in Japanese)
9. G. Stamatis, P. Kyriazopoulos, S. Golegou, A. Basayannis, S. Skaltsas, H. Skaltsa, *J. Ethnopharmacol*. **88** (2003) 175
10. S. Grujić-Jovanović, H. D. Skaltsa, P. Marin, M. Soković, *Flavour Fragrance J.* **19** (2004) 139
11. A. I. Derkach, *Rastitel'nye Resursy* **34** (1998) 57 (in Russian)
12. R. M. Palić, J. S. Lazarević, G. S. Stojanović, V. N. Randjelović, *J. Essent. Oil Res.* **18** (2006) 290
13. M. Rabbani, S. E. Sajjadi, H. R. Zarei, *J. Ethnopharmacol*. **89** (2003) 271
14. T. V. Zinchenko, G. N. Voitenko, G. N. Lipkan, *Farmakol. Toksikol.* **44** (1981) 191
15. K. Hayashi, T. Nagamatsu, M. Ito, H. Yagita, Y. Suzuki, *Jpn. J. Pharmacol.* **70** (1996) 157
16. J. Kukić, S. Petrović, M. Niketić, *Biol. Pharm. Bull.* **29** (2006) 725
17. M. Couladis, O. Tzakou, E. Verykokidou, C. Harvala, *Phytother. Res.* **17** (2003) 194
18. D. Mantle, F. Eddeb, A. T. Pickering, *J. Ethnopharmacol.* **72** (2000) 47
19. F. Conforti, F. Menichini, C. Formisano, D. Rigano, F. Senatore, N. A. Arnold, F. Piozzi, *Food Chem.* **116** (2009) 898
20. 21. I. Kh. Pasechnik, *Farmakol. Toksikol.* **32** (1969) 575

21. I. Kh. Pasechnik, T. V. Zinchenko, M. A. Garbarets, V. Y. Gorodinskaya, *Farma. Zhur.* **26** (1971) 64 (in Russian)
22. N. Radulović, J. Lazarević, N. Ristić, R. Palić, *Biochem. Syst. Ecol*. **35** (2007) 196
23. N. Ristić, J. Lazarević, N. Radulović, R. Palić, *Chem. Nat. Compd.* **44** (2008) 522
24. H. D. Skaltsa, C. Demetzos, D. Lazari, M. Sokovic, *Phytochemistry* **64** (2003) 743
25. S. Petrović, M. Ristić, M. Milenković, J. Kukić, J. Antić Stanković, M. Niketić, *Flavour Fragrance J*. **21** (2006) 250
26. H. Van Den Dool, P. D. Kratz, *J. Chromatogr*. **11** (1963) 463
27. R. P. Adams, *Identification of Essential Oil Components by Gas Chromatography and Mass Spectroscopy*, Allured Publishing Corporation, Carol Stream, IL, 2007
28. *Performance Standards for Antimicrobial Disk Susceptibility Test*, 6th ed., National Committee for Clinical Laboratory Standards, approved standard: P. A. Wayne, M100-S9, 1997
29. P. Prieto, M. Pineda, M. Aguilar, *Anal. Biochem*. **269** (1999) 337
30. N. S. Radulović, P. D. Blagojević, R. M. Palić, B. K. Zlatković, B. M. Stevanović, *J. Serb. Chem. Soc*. **74** (2009) 35
31. G. Eglington, R. J. Hamilton, *Science* **156** (1967) 1322
32. C. H. Brieskorn, K. Feilner, *Phytochemistry* **7** (1968) 485
33. C. Reddy, T. Elinton, R. Palić, B. Benitez-Nelson, G. Stojanović, I. Palić, *Org. Geochem.* **31** (2000) 331
34. S. Yaghmai, M. H. Khayat, *J. Chem. Chem. Eng.* **9** (1987) 26
35. P. D. Cantino, in *Advances in Labiatae Science*, R. M. Harley, T. Reynolds, Eds., RBG Kew, Richmond, UK, 1992, p. 27
36. P. D. Cantino, R. M. Harley, S. J. Wagstaff, in *Advances in Labiatae Science*, R. M. Harley, T. Reynolds, Eds., RBG Kew, Richmond, UK, 1992, p. 511
37. H. Skaltsa, P. Georgakopoulos, D. Lazari, A. Karioti, J. Heilmann, O. Sticher, T. Constantinidis, *Biochem. Syst. Ecol*. **35** (2007) 317
38. P. D. Marin, R. J. Grayer, S. Grujić Jovanović, G. C. Kite, N. C. Veitch, *Phytochemistry* **65** (2004) 1247
39. H. D. Skaltsa, A. Mavrommati, T. Constantinidis, *Phytochemistry* **57** (2001) 235
40. F. A. Tomas Barberan, M. I. Gil, F. Ferreres, F. Tomas Lorente, *Phytochemistry* **31** (1992) 3097
41. S. G. Griffin, S. G. Wyllie, J. L. Markham, D. N. Leach, *Flavour Fragrance J*. **14** (1999) 322
42. M .J. Alcarez, S. G. Ochoa, M. J. Jimenez, S. Valverde, A. Villar, *Phytochemistry* **28** (1989) 1267
43. M. Singh, M. Pal, R. P. Sharma, *Planta Med*. **65** (1999) 2
44. I. Chinou, C. Demetzos, C. Harvala, C. Roussakis, J. F. Verbist, *Planta Med*. **60** (1994) 34
45. E. Kalpoutzakis, I. Chinou, S. Mitaku, A. L. Skaltsounis, C. Harvala, *Nat. Prod. Lett.* **11** (1998) 173.

Journal of the Serbian Chemical Society
JSCS@tmf.bg.ac.rs • www.shd.org.rs/JSCS

J. Serb. Chem. Soc. 75 (10) S7–S12 (2010)

Supplementary material

SUPPLEMENTARY MATERIAL TO

Chemical composition and screening of the antimicrobial and anti-oxidative activity of extracts of *Stachys* species

JELENA S. LAZAREVIĆ[1]*, RADOSAV M. PALIĆ[2#], NIKO S. RADULOVIĆ[2], NOVICA R. RISTIĆ[3] and GORDANA S. STOJANOVIĆ[2]

[1]*Department of Pharmacy, Faculty of Medicine, University of Niš, Bul. Dr Zorana Đinđića 81, 18000 Niš,* [2]*Department of Chemistry, Faculty of Science and Mathematics, University of Niš, Višegradska 33, 18000 Niš and* [3]*Department of Chemistry, Faculty of Science and Mathematics, University of Priština, Kosovska Mitrovica, Serbia*

J. Serb. Chem. Soc. 75 (10) (2010) 1347–1359

TABLE I-S. Chemical composition (%) of the extracts of four *Stachys* species

RI[a]	Compound	Class	Method[b]	*S. germanica*		*S. iva*		*S. plumosa*		*S. scardica*	
				DE[c]	EA[d]	DE	EA	DE	EA	DE	EA
841	2-Isopropyl-5-methylfuran	O	a,b	–[e]	–	–	–	tr[f]	–	tr	–
939	*α*-Thujene	T	a,b	–	–	–	–	0.1	–	tr	–
947	*α*-Pinene	T	a,b,c	–	–	–	0.1	0.1	1.4	0.1	–
969	*β*-Thujene	T	a,b	–	–	–	–	0.1	–	0.1	–
994	*β*-Myrcene	T	a,b	–	–	–	–	–	–	tr	–
996	*β*-Pinene	T	a,b,c	–	–	tr	tr	0.2	0.8	0.1	–
1051	1,8-Cineole	T	a,b,c	0.1	–	–	–	0.1	–	–	–
1098	Terpinolene	T	a,b	–	–	–	–	0.1	–	–	–
1110	*α*-Pinene epoxide	T	a,b	–	–	–	–	tr	–	–	–
1113	1-Octen-3-yl acetate	FAD	a,b	–	–	–	–	tr	–	–	–
1118	*cis*-Limonene oxide	T	a,b	–	–	–	–	0.3	–	tr	–
1130	*α*-Campholenal	T	a,b	–	–	–	–	0.1	–	–	–
1131	Nopinone	T	a,b	–	–	–	–	tr	–	–	–
1140	Camphor	T	a,b,c	0.3	–	–	–	–	–	tr	–
1144	*trans*-Pinocarveol	T	a,b,c	–	–	–	–	0.3	–	–	–
1149	*cis*-Verbenol	T	a,b,c	–	–	–	–	0.4	–	0.1	–
1154	Pinocarvone	T	a,b,c	–	–	–	–	0.3	–	–	–
1158	*trans*-Verbenol	T	a,b,c	–	–	–	–	0.1	–	–	–
1176	Myrtenal	T	a,b,c	–	–	–	–	0.2	–	–	–
1185	Verbenone	T	a,b,c	–	–	–	–	0.4	–	–	–
1192	3-Thujen-10-al	T	a,b	–	–	–	–	0.1	–	–	–

* Corresponding author. E-mail: jelena217@yahoo.com
# Serbian Chemical Society member.

TABLE I-S. Continued

RI[a]	Compound	Class	Method[b]	*S. germanica*		*S. iva*		*S. plumosa*		*S. scardica*	
				DE[c]	EA[d]	DE	EA	DE	EA	DE	EA
1236	Linalyl acetate	T	a,b	–	–	–	–	0.1	–	–	–
1256	Bornyl acetate	T	a,b,c	–	–	–	–	0.1	–	–	–
1319	Bicycloelemene	T	a,b	–	–	0.1	–	–	–	–	–
1321	δ-Elemene	T	a,b	–	–	–	–	–	–	tr	–
1322	Dihydrocarveol acetate[g]	T	a,b	–	–	–	–	tr	–	–	–
1337	α-Cubebene	T	a,b	tr	–	–	–	–	–	0.2	–
1355	Cyclosativene	T	a,b	–	–	0.2	–	–	–	–	–
1361	α-Yangene	T	a,b	–	–	–	–	–	–	0.1	–
1367	α-Copaene	T	a,b	0.5	–	0.9	–	0.1	–	0.3	–
1375	β-Bourbonene	T	a,b	2.2	–	–	–	–	–	0.2	–
1378	β-Cubebene	T	a,b	–	–	–	–	–	–	0.4	–
1380	β-Elemene	T	a,b	–	–	0.2	–	–	–	–	–
1386	1,5-di-*epi*-β-Bourbonene	T	a,b	tr	–	–	–	–	–	–	–
1392	β-Longipinene	T	a,b	–	–	–	–	–	–	tr	–
1395	Italicene	T	a,b	–	–	–	–	tr	–	–	–
1401	α-Gurjunene	T	a,b	–	–	0.1	–	–	–	–	–
1402	6-*epi*-α-Cubebene	T	a,b	–	–	–	–	–	–	tr	–
1409	β-Caryophyllene	T	a,b,c	0.7	–	0.9	tr	0.1	–	1.3	tr
1418	β-Copaene	T	a,b	0.2	–	–	–	–	–	0.2	–
1422	Calarene	T	a,b	–	–	–	–	–	–	0.1	–
1429	Aromadendrene	T	a,b	–	–	–	–	–	–	0.2	–
1432	Isogermacrene D	T	a,b	0.2	–	0.1	–	–	–	–	–
1440	α-Humulene	T	a,b,c	–	–	0.2	–	0.1	–	0.1	–
1448	*cis*-Muurola-4(15),5-diene	T	a,b	0.3	–	0.1	–	0.1	–	0.1	–
1452	*trans*-β-Ionone-5,6-epoxide	CR	a,b	–	–	0.1	–	0.1	–	tr	–
1454	(*E*)-β-Farnesene	T	a,b	0.3	–	tr	–	–	–	–	–
1457	(*E*)-β-Ionone	CR	a,b	–	–	–	–	0.2	–	–	–
1459	*epi*-(*E*)-β-Caryophyllene	T	a,b	–	–	0.2	–	–	–	–	–
1459	γ-Muurolene	T	a,b	0.6	–	–	–	–	–	2.0	–
1463	*ar*-Curcumene	T	a,b	–	–	–	–	0.2	–	–	–
1464	Germacrene D	T	a,b,c	1.5	–	0.3	–	–	–	–	–
1469	*cis*-β-Guaiene	T	a,b	–	–	–	–	–	–	0.2	–
1475	γ-Amorphene	T	a,b	–	–	–	–	–	–	0.6	–
1476	*epi*-Cubebol	T	a,b	–	–	0.4	–	–	–	tr	–
1482	β-Curcumene	T	a,b	tr	–	–	–	–	–	–	–
1491	γ-Cadinene	T	a,b	–	–	–	–	–	–	2.0	–
1492	Cubebol	T	a,b	–	–	0.9	–	–	–	–	–
1495	*cis*-Calamenene	T	a,b	–	–	–	–	–	–	tr	–
1498	δ-Cadinene	T	a,b	–	–	2.7	–	0.2	–	1.4	–
1510	Dihydroactinidiolide	CR	a,b	–	–	–	–	0.3	–	–	–
1518	α-Calacorene	T	a,b	–	–	–	–	–	–	0.7	–
1539	α-Agarofuran	T	a,b	–	–	–	–	–	–	0.5	0.1
1542	β-Calacorene	T	a,b	–	–	–	–	–	–	0.6	–
1554	1,8-Oxidocadin-4-ene	T	a,b	–	–	–	–	0.1	–	–	–

TABLE I-S. Continued

RI[a]	Compound	Class	Method[b]	*S. germanica*		*S. iva*		*S. plumosa*		*S. scardica*	
				DE[c]	EA[d]	DE	EA	DE	EA	DE	EA
1563	Spathulenol	T	a,b,c	3.8	–	3.8	–	–	–	0.4	–
1571	Caryophyllene oxide	T	a,b,c	4.3	–	3.6	0.1	0.7	–	3.1	–
1580	4(14)-Salvialen-1-one	T	a,b	1.4	–	–	–	–	–	1.3	–
1583	Viridiflorol	T	a,b	2.5	–	1.1	–	–	–	–	–
1587	*β*-Oplopenone	T	a,b	–	–	–	–	0.4	–	–	–
1597	Humulene epoxide II	T	a,b	–	–	–	–	–	–	0.5	–
1601	Copaborneol	T	a,b	–	–	2.0	–	–	–	–	–
1603	*epi*-Marsupellol	T	a,b	–	–	–	–	–	–	0.1	–
1608	1,10-di-*epi*-Cubenol	T	a,b	–	–	–	–	–	–	0.5	–
1623	Isospathulenol	T	a,b	–	–	–	–	–	–	1.9	–
1625	1-*epi*-Cubenol	T	a,b	–	–	1.2	–	–	–	–	–
1632	10-*epi*-Italicen-4-one	T	a,b	–	–	–	–	–	–	0.3	–
1637	*τ*-Muurolol	T	a,b	0.3	–	1.2	–	0.3	–	1.6	–
1651	*α*-Cadinol	T	a,b	0.5	–	–	–	0.2	–	2.1	–
1660	10*β*-Hydroxy-*cis*--calamenene	T	a,b	–	–	–	–	0.1	–	–	–
1665	10*α*-Hydroxy-*cis*-calamenene	T	a,b	–	–	–	–	0.1	–	0.4	–
1669	Valeranone	T	a,b	2.1	–	1.4	0.1	–	–	–	–
1675	3-Oxo-*α*-damascone	CR	a,b	–	–	–	–	0.2	–	–	–
1678	Cadalene	T	a,b	–	–	–	–	–	–	1.9	–
1687	Germacra-4(15),5,10(14)--trien-1-al	T	a,b	–	–	0.2	–	–	–	–	–
1690	2,3-Dihydrofarnesol	T	a,b	–	–	0.7	–	–	–	–	–
1692	3-Hydroxy-5,6-epoxy--*β*-ionone	CR	a,b	1.5	–	–	–	0.5	–	–	–
1714	(2*E*,6*E*)-Farnesol	T	a,b	–	–	0.3	–	–	–	–	–
1731	7,8-Dihydro-3-oxo-*α*-ionol	CR	a,b	1.0	–	–	–	–	–	0.3	–
1766	Methyl (2*E*,6*E*)-farnesate	T	a,b	0.5	–	–	–	–	–	–	–
1779	(*Z*)-7-Hexadecenal	FAD	a,b	–	–	tr	–	0.1	–	–	–
1785	(*E*)-7-Hexadecenal	FAD	a,b	–	–	–	–	0.1	–	–	–
1794	Antracene	O	a,b	–	–	–	–	0.2	–	0.3	–
1803	(2*Z*,6*E*)-Farnesyl acetate	T	a,b	–	–	0.1	–	0.1	–	–	–
1823	Hexadecanal	FAD	a,b	–	–	–	–	0.3	–	–	–
1844	Neophytadiene, isomer I	T	a,b	–	1.1	1.4	0.3	2.7	0.6	2.6	2.8
1845	Hexahydrofarnesylacetone	CR	a,b	3.5	–	–	–	–	–	–	–
1865	Neophytadiene, isomer II	T	a,b	–	0.2	0.1	–	0.3	–	0.3	0.2
1869	(*E*)-Nuciferyl acetate	T	a,b	0.8	–	0.2	–	–	–	–	–
1880	Neophytadiene, isomer III	T	a,b	0.5	0.4	0.5	0.1	0.6	–	0.5	0.6
1890	(*Z*)-Nuciferyl propionate	T	a,b	–	–	0.1	–	–	–	–	–
1900	Nonadecane	FAD	a,b,c	1.2	–	0.3	–	0.1	–	0.2	–
1902	Farnesyl acetone	CR	a,b	–	0.4	–	–	–	–	–	–
1905	Isopimara-8,15-diene	T	a,b	–	–	–	–	0.2	–	–	–

TABLE I-S. Continued

RI[a]	Compound	Class	Method[b]	*S. germanica*		*S. iva*		*S. plumosa*		*S. scardica*	
				DE[c]	EA[d]	DE	EA	DE	EA	DE	EA
1910	Methyl hexadecanoate (*syn.*[h] methyl palmitate)	FAD	a,b	1.2	0.2	0.1	–	0.3	–	0.5	–
1922	Cembrene	T	a,b	–	–	0.2	–	–	–	–	–
1929	1-Methylphenanthrene	O	a,b	–	–	–	–	–	1.2	–	–
1940	Isophytol	T	a,b	–	–	–	–	tr	–	0.3	–
1944	(*Z*)-Nuciferyl isobutyrate	T	a,b	4.5	0.2	15.3	1.2	0.1	–	–	–
1965	Labda-7,13(16),14-triene	T	a,b	–	–	0.2	–	–	–	–	–
1968	*n*-Hexadecanoic acid	FAD	a,b,c	–	–	–	–	6.0	–	–	–
1979	Ethyl hexadecanoate (*syn.* Ethyl palmitate)	FAD	a,b	1.7	0.1	0.3	–	6.1	–	4.8	–
2000	Eicosane	FAD	a,b,c	0.5	–	–	–	–	–	1.9	–
2001	Octadecanal (*syn.* stearaldehyde)	FAD	a,b	–	–	–	0.1	–	–	–	0.1
2007	13-*epi*-Manoyl oxide	T	a,b	–	–	–	–	2.4	–	–	–
2013	Methyl heptadecanoate	FAD	a,b	–	–	0.1	–	–	–	0.9	–
2039	Abieta-8,11,13-triene	T	a,b	0.3	–	0.1	–	13.6	17.8	5.0	0.8
2054	(*Z*)-Nuciferyl isovalerate	T	a,b	0.9	–	0.4	–	–	–	–	–
2073	Methyl-(*Z*,*Z*,*Z*)-9,12,15--octadecatrienoate (*syn.* methyl linolenate)	FAD	a,b	1.5	–	0.1	–	1.1	–	0.8	–
2076	(*Z*)-Nuciferyl 2-methylbutyrate	T	a,b	0.9	–	0.1	–	–	–	–	–
2079	Methyl-(*Z*,*Z*)-9,12-octadecanoate (*syn.* methyl linoleate)	FAD	a,b	–	0.4	–	–	–	–	–	–
2083	(*Z*)-9-Octadecenoic acid (*syn.* Oleic acid)	FAD	a,b	–	0.6	–	–	1.7	–	0.2	0.5
2084	Methyl-(*Z*)-9-octadecenoate (*syn.* methyl oleate)	FAD	a,b	1.0	–	0.2	–	–	–	0.4	–
2093	Isoabienol	T	a,b	–	–	3.6	1.2	–	–	–	–
2100	Heneicosane	FAD	a,b,c	2.2	0.4	–	0.4	0.2	–	0.5	0.1
2105	*trans*-Phytol	T	a,b	5.2	0.7	4.0	0.8	7.9	–	3.8	0.9
2127	Methyl octadecanoate (*syn.* Methyl stearate)	FAD	a,b	1.5	–	3.2	–	0.4	0.9	0.4	0.1
2140	Ethyl (*Z*,*Z*)-9,12-octadecadienoate (*syn.* ethyl linoleate)	FAD	a,b	1.4	–	0.3	–	2.9	–	0.4	–
2145	Ethyl (*Z*,*Z*,*Z*)-9,12,15-octadecatrienoate (*syn.* ethyl linolenate)	FAD	a,b	0.5	–	0.3	–	4.4	–	0.2	–
2151	Ethyl (*Z*)-9-octadecenoate (*syn.* ethyl oleate)	FAD	a,b	0.8	0.4	0.6	0.4	–	–	0.2	–
2170	Thunbergol	T	a,b	–	–	–	–	2.3	–	0.9	–
2170	Abieta-8(14),13(15)-diene	T	a,b	–	–	0.2	–	–	–	–	–

TABLE I-S. Continued

RI[a]	Compound	Class	Method[b]	*S. germanica*		*S. iva*		*S. plumosa*		*S. scardica*	
				DE[c]	EA[d]	DE	EA	DE	EA	DE	EA
2178	Ethyl octadecanoate	FAD	a,b	0.2	–	0.2	–	1.5	–	0.4	–
2200	Docosane	FAD	a,b,c	1.6	0.6	0.3	tr	–	–	0.6	0.2
2209	Sclareol	T	a,b	–	–	0.3	0.1	–	1.5	–	–
2223	*cis*-Totarol	T	a,b	–	–	–	0.9	3.0	–	–	–
2266	2-Methyldocosane	FAD	a,b	–	0.7	–	–	–	–	–	–
2270	Dehydroabietal	T	a,b	–	–	–	–	3.5	–	0.9	–
2271	1-Eicosanol	FAD	a,b	2.8	0.4	–	–	–	–	–	–
2274	3- Methyldocosane	FAD	a,b	–	–	–	0.4	–	–	–	–
2300	Tricosane	FAD	a,b,c	5.5	1.8	3.8	0.5	6.6	–	17.6	1.4
2328	11-Methyltricosane	FAD	a,b	–	–	–	–	–	–	–	4.4
2329	δ-Eicosanolactone (*syn.* meadowlactone)	FAD	a,b	–	–	0.5	0.3	0.7	–	0.7	–
2338	Dehydroabietic acid methyl ester	T	a,b	–	–	–	–	2.8	–	1.4	1.2
2347	Dehydroabietol	T	a,b	–	–	–	–	1.3	6.2	–	–
2361	Butyl octadecanoate	FAD	a,b	–	–	0.5	0.2	1.4	–	0.8	–
2365	2-Methyltricosane	FAD	a,b	–	0.2	–	–	–	–	–	–
2378	Ethyl eicosanoate	FAD	a,b	0.6	–	tr	–	0.4	–	2.1	–
2398	Labd-13(*E*)-en-8α,15-diol	T	a,b	–	–	14.3	–	–	–	–	–
2400	Tetracosane	FAD	a,b,c	1.0	0.6	tr	–	0.9	–	0.8	0.5
2408	Methyl heneicosanoate	FAD	a,b	–	–	–	–	0.6	–	0.5	–
2431	Methyl neoabietate	T	a,b	–	–	0.3	9.6	0.2	–	–	–
2465	2-Methyltetracosane	FAD	a,b	–	–	–	0.7	–	–	0.4	0.3
2468	1-Docosanol	FAD	a,b	1.2	0.4	–	–	–	–	–	–
2474	3-Methyltetracosane	FAD	a,b	–	0.3	–	–	–	–	–	–
2500	Pentacosane	FAD	a,b,c	3.6	2.5	0.6	0.8	1.2	2.6	1.3	1.4
2544	Tricosanoic acid	FAD	a,b	–	–	–	–	–	–	0.3	–
2564	2-Methylpentacosane	FAD	a,b	0.1	–	–	–	–	13.2	–	–
2573	3-Methylpentacosane	FAD	a,b	–	0.3	–	1.5	–	–	–	–
2576	Ethyl docosanoate	FAD	a,b	–	–	–	–	0.8	6.1	0.2	–
2600	Hexacosane	FAD	a,b,c	0.3	–	0.2	–	0.3	–	0.2	0.7
2615	3,7-Dimethylpentacosane	FAD	a,b	–	0.1	–	–	–	–	–	–
2636	10-Methylhexacosane	FAD	a,b	–	–	–	–	–	–	–	0.6
2664	2-Methylhexacosane	FAD	a,b	–	–	–	–	0.1	–	0.4	–
2667	2,6,10,15,19,23-Hexa-methyltetracosane (squalane)	T	a,b	0.2	–	–	–	–	–	0.6	0.2
2674	3-Methylhexacosane	FAD	a,b	–	0.5	–	–	–	–	–	–
2700	Heptacosane	FAD	a,b,c	4.9	7.2	2.9	5.3	4.3	27.7	4.3	5.0
2771	3-Methylheptacosane	FAD	a,b	0.2	1.0	–	0.1	0.1	–	–	–
2800	Octacosane	FAD	a,b,c	0.8	1.9	0.8	1.4	0.5	2.8	0.3	1.1
2808	Squalene	T	a,b	0.8	1.1	0.1	0.2	0.2	–	0.5	1.6
2835	10-Methyloctacosane	FAD	a,b	–	0.2	–	–	–	–	–	–
2864	2-Methyloctacosane	FAD	a,b	–	0.4	–	0.7	–	–	–	–

TABLE I-S. Continued

Compound		Class	Method[b]	*S. germanica*		*S. iva*		*S. plumosa*		*S. scardica*	
				DE[c]	EA[d]	DE	EA	DE	EA	DE	EA
2859	10-Demethylsqualene	T	a,b	0.1	0.2	0.5	–	0.3	–	1.0	0.4
2900	Nonacosane	FAD	a,b,c	17.0	36.9	18.0	28.3	–	6.5	3.6	19.3
2934	10-Methylnonacosane	FAD	a,b	–	2.7	–	12.0	–	–	–	–
2973	3-Methylnonacosane	FAD	a,b	–	0.3	–	–	–	3.2	–	0.6
3000	Triacontane	FAD	a,b,c	0.6	2.1	–	2.1	–	3.6	8.0	5.9
3033	10-Methyltriacontane	FAD	a,b	–	0.3	–	–	–	0.5	–	–
3038	3,7,15-Trimethyl-nonacosane	FAD	a,b	–	0.1	–	–	–	0.1	–	–
3100	Hentriacontane	FAD	a,b	–	20.9	–	23.3	–	–	–	43.7
Total				96.4	88.8	98.1	93.2	91.9	96.7	97.5	94.7
Yield, mass %				1.4	10.0	1.5	4.0	1.4	8.0	1.5	5.8
Grouped components											
Terpenoids (T)				36.5	3.9	64.7	14.7	47.3	28.3	43.0	8.8
Monoterpene hydrocarbons				–	–	tr	0.1	0.6	2.2	0.3	–
Oxygenated monoterpenes				0.4	–	–	–	2.5	–	0.1	–
Sesquiterpene hydrocarbons				6.5	–	6.0	tr	0.8	–	12.6	tr
Oxygenated sesquiterpenes				22.5	0.2	32.9	1.4	2.1	–	12.7	0.1
Diterpenes				6.0	2.4	25.2	13.0	40.8	26.1	15.7	6.5
Triterpenes				1.1	1.3	0.6	0.2	0.5	–	2.1	2.2
Fatty acid derived compounds (FAD)				59.9	84.9	33.4	78.5	44.6	68.4	54.5	85.9
n-Alkanes				39.2	74.9	26.9	62.1	14.1	43.2	39.3	79.3
Branched alkanes				0.3	7.1	–	15.4	0.2	17.0	0.8	5.9
Alcohols				4.0	0.8	–	–	–	–	–	–
Aldehydes				–	–	tr	0.1	0.5	–	–	0.1
Fatty acids and fatty acid esters				10.4	1.7	6.4	0.9	28.3	7.0	13.8	0.6
Carotenoid derived compounds				6.0	0.4	0.1	–	1.3	–	0.3	–
Others (O)				–	–	–	–	0.2	1.2	0.3	–

[a]Components listed in order of elution from an SPB-1 column (*RI* – experimentally determined retention indices on the mentioned column by co-injection of a homologous series of *n*-alkanes C_8–C_{31}); [b]a – constituent identified by retention index matching; b – constituent identified by mass spectra comparison; c – constituent identified by co-injection of an authentic sample; [c]diethyl ether extract; [d]ethyl acetate extract; [e]not detected; [f]trace (<0.05 %); [g]correct stereoisomer not determined; [h]synonym

Journal of the Serbian Chemical Society
JSCS-info@shd.org.rs • www.shd.org.rs/JSCS
J. Serb. Chem. Soc. *75* (10) 1361–1368 (2010)
JSCS–4058
UDC 635.71:581.46:665.5/.54
Original scientific paper

Inflorescence and leaves essential oil composition of hydroponically grown *Ocimum basilicum* L.

MOHAMMAD BAGHER HASSANPOURAGHDAM[1]*, GHOLAM REZA GOHARI[2], SEIED JALAL TABATABAEI[2] and MOHAMMAD REZA DADPOUR[2]

[1]*Department of Horticultural Sciences, Faculty of Agriculture, University of Maragheh, Maragheh 55181-83111 and* [2]*Department* of *Horticultural Sciences, Faculty of Agriculture, University of Tabriz, Tabriz 51666, Iran*

(Received 11 March, revised 30 April 2010)

Abstract: In order to characterize the essential oils of leaves and inflorescences, water distilled volatile oils of hydroponically grown *Ocimum basilicum* L. were analyzed by GC/EI-MS. Fifty components were identified in the inflorescence and leaf essential oils of the basil plants, accounting for 98.8 and 99.9 % of the total quantified components respectively. Phenylpropanoids (37.7 % for the inflorescence *vs*. 58.3 % for the leaves) were the predominant class of oil constituents, followed by sesquiterpenes (33.3 *vs*. 19.4 %) and monoterpenes (27.7 *vs*. 22.1 %). Of the monoterpenoid compounds, oxygenated monoterpenes (25.2 *vs*. 18.9 %) were the main subclass. Sesquiterpene hydrocarbons (25 *vs*. 15.9 %) were the main subclass of sesquiterpenoidal compounds. Methyl chavicol, a phenylpropane derivative, (37.2 *vs*. 56.7 %) was the principle component of both organ oils, with up to 38 and 57 % of the total identified components of the inflorescence and leaf essential oils, respectively. Linalool (21.1 *vs*. 13.1 %) was the second common major component followed by *α*-cadinol (6.1 *vs*. 3 %), germacrene D (6.1 *vs*. 2.7 %) and 1,8-cineole (2.4 *vs*. 3.5 %). There were significant quantitative but very small qualitative differences between the two oils. In total, considering the previous reports, it seems that essential oil composition of hydroponically grown *O. basilicum* L. had volatile constituents comparable with field grown counterparts, probably with potential applicability in the pharmaceutical and food industries.

Keywords: *Ocimum basilicum* L.; Lamiaceae; essential oil; hydroponic; methyl chavicol; linalool.

INTRODUCTION

Hydroponics, the method of growing plants without soil, has long been the subject of much public interest in most parts of the world.[1] This method of plant

* Corresponding author. E-mail: hassanpouraghdam@gmail.com
doi: 10.2298/JSC100311113H

production is an efficient alternative for countries short on water supply and limited in agricultural soil. Furthermore, in the last three decades, hydroponic culture has been employed as an economic and environmentally viable means for the mass production of vegetables and potting and/or cut flowers in most parts of the world.[1] Hydroponic production of medicinal and aromatic plants is a new trend in agricultural systems, particularly in organic and intensive agriculture.[2–4] High yields, cleaner and off-season production, balanced nutrient availability, adequate aeration and high water use efficiency have been defined as the main advantages of hydroponics production systems.[2–6]

Common basil (*Ocimum basilicum* L.), a herbaceous annual fragrant herb, belongs to the Lamiaceae family.[7,8] Basil is a cosmopolitan herb and aromatic plant with abundant applications in pharmaceutical, food and fragrance Industries.[8.9] In Iran, basil is a herb with great use in food products and gastronomy.[9] Furthermore, basil production occupies large areas of land, especially near crowded cities. Hydroponic production is a competent alternative for contending with the high demands for this crop.

Pharmaceutically, this plant and its preparations have been used for a long time as immunostimulant, sedative, hypnotic, local anesthetic, anticonvulsant, diuretic, carminative, galactogogue, stomachic, spasmodic and vermifuge purposes.[7,10–15] Additionally, several biological activities have been reported for its secondary metabolites, such as nematicidal, fungistatic, antifungal, insecticidal, pesticidal, antiviral, insect repellent and antioxidant.[10,11,13,14] Owing to aforementioned biological and healing activities, sweet basil plant and its preparations have been used to treat nausea, dysentery, mental fatigue, cold, rhinitis, increased plasma lipid content, soothe the nerves and as a first aid treatment for wasp stings and snake bites.[10,13–15]

The chemical analysis of basil essential oil has been investigated since the 1930s.[16] Lawrence[17] reported that the main components of basil volatile oil are synthesized *via* two distinct biochemical pathways, *i.e.*, the shikimic acid pathway leading to phenylpropane derivatives and the mevalonic acid pathway leading to terpenoid compounds. A substantial number of studies conducted on the composition of the essential oil of basil revealed a huge diversity in the constituents of its oil with different chemotypes from many regions of the world. Estragol, linalool, methyl eugenol, geraniol, methyl cinnamate, bergamotene, α-cubebene, germacrene D, β-elemene, 1,8-cineole, methyl cinnamate, α-cadinol and limonene are considered as the main constituents and chemotypes of basil from different parts of the world.[10–15,18–27] As mentioned above, there are several reports on the composition of the volatile oil of wild and field grown basil. In a recent study, menthone and estragol were reported to be major components of field grown basil plants from Iran.[9] However, to the best of our knowledge, there is scarce information on the chemical composition of the volatile oil of hydroponi-

cally grown *O. basilicum*. The objective of the present study was to comparatively characterize the composition of leaves and inflorescence essential oil of hydroponically grown *O. basilicum* L. plant from Iran.

EXPERIMENTAL

This experiment was conducted at the Research Greenhouse of Horticultural Sciences Department, Tabriz University, Iran, during spring–summer of 2009.

Plant material

Seeds of a native *O. basilicum* L. plants were directly sowed in 5 L pots. During the germination period and first two weeks of plantlet growth, they were irrigated with tap water. A quarter-strength modified Hoagland nutrient solution was used for regular irrigation of the plants for the following two weeks. Then after, the established plants were daily irrigated with half-strength Hoagland solution until harvest time. The pH and *EC* of the nutrient solution were adjusted to 6–6.5 and 2 dS m^{-1} using H_2SO_4 or KOH and water, respectively.[2-4]

This experiment was realized in a one-layer polyethylene covered greenhouse at ambient temperature, humidity and light intensity, *i.e.*, 15–30 °C, 40–50 % and 500 µmol m^{-2} s^{-1}, respectively. The pots were regularly watered with tap water in 10-day intervals for prevention of salinity accumulation in the growing media.[2] The aerial parts of 30 plants (3 plants per each pot, equally distanced for optimum light interception) were harvested at the flowering stage, dissected to leaves and inflorescences and dried at room temperature for 4–5 days.

Volatile oil extraction

Pooled samples (50 g) of air-dried powdered plant materials (inflorescence and leaves) were extracted by the hydrodistillation technique for 3 h in an all-glass Clevenger type apparatus. The extracted crude essential oils were dried over anhydrous sodium sulfate and stored in hermetically sealed glass flasks with a rubber lid, covered with aluminum foil to protect the contents from the light and air conversion and kept in a refrigerator at 4 °C until analysis.

Instrumentation

A GC/MS instrument (Agilent 6890N GC and Agilent 5973 mass selective detector operating in the EI mode, USA) was used for the volatile oil analysis. Ultra pure helium (99.99 %, Air Products, UK) passed through a molecular sieve trap and an oxygen trap (Chromatography Research Supplies, USA) was used as the carrier gas at a constant velocity of 1 ml min^{-1}. The injection port was held at 300 °C and used in the split mode; split ratio 1:100, volume injected: 5 µl of the pure volatile oil. The detector temperature was 200 °C. Separation was realized on an apolar HP5MS (5 %-phenyl methyl poly siloxane; 30 m×0.25 mm i.d. and 0.25 µm film thickness) capillary column (Hewllet-Packard, USA). The oven temperature was programmed as follows: 50 °C (held 2 min), raised to 110 °C at a rate of 10 °C min^{-1}, then heated to 200 °C at a rate of 10 °C/min and finally increased to 280 °C at 20 °C min^{-1}, isothermal at this temperature for 2 min. The mass operating parameters were as follows: ionization potential: 70 eV, interface temperature: 200 °C and acquisition mass range: 50–800.

Identification and quantification of volatile oil components

The relative percentage amounts of the volatile oil constituents were evaluated from the total peak area (TIC) using instrument software. The components of the essential oil were identified by comparing their mass spectral fragmentation patterns with those of similar

compounds from the NIST and WILEY library databases, as well as by comparing their Kovats gas chromatographic retention indices with those of the literature.[10-15,18-28]

RESULTS AND DISCUSSION

The hydrodistillation of the inflorescence and leaves of *O. basilicum* L. gave pale yellow liquids with a yield of 0.6 and 0.5 (v/w) based on the dry weight. The chemical composition of the studied oils, their retention indices, molecular formulae and percentage composition are presented in Table I. The main classes and subclasses of the identified components are reported in Table II as well. Fifty components were identified in the essential oil of inflorescence and leaves of hydroponically grown *O. basilicum*, accounting for 98.8 and 99.9 % of total identified components, respectively (Tables I and II). Phenylpropanoids were the main class of constituents with methyl chavicol (37.2 % in the inflorescence *vs*. 56.7 % in leaves) as their main representatives (Tables I and II). Sesquiterpenoids (33.3 *vs*. 19.4 %) were characterized as the second major class of volatile components and then monoterpenoids (27.7 *vs*. 22.1 %). Sesquiterpene hydrocarbons (25 *vs*. 15.9 %) were assigned as the main subclass of the volatile oil components (Table II). Another major subclass of components was oxygenated monoterpenes (25.2 *vs*. 18.9 %). Monoterpene hydrocarbons and oxygenated sesquiterpenes had a minor share in the essential oil profile (Table II). Considering the main classes and subclasses, there were quantitative differences between the leaves and inflorescence essential oil. In light of the major class of volatile oil components, *i.e*., phenylpropanoids, the leaf essential oil was superior to the inflorescence essential oil (Table II). Contrarily, the inflorescence essential oil was richer in sesquiterpenoids subclasses and oxygenated monoterpenes (Table II). Methyl chavicol, a phenylpropanoid pathway product, was the principal common constituent of both organs oils. Linalool, a highly appreciated oxygenated monoterpene, (21.1 *vs*. 13.1 %) was ranked as the second most abundant common component (Table I). α-Cadinol (6.1 *vs*. 3 %), germacrene D (6.1 *vs*. 2.7 %), 1,8-cineole (2.4 *vs*. 3.5 %), γ-cadinene (2.5 *vs*. 2 %), α-(*Z*)-bergamotene (1.8 *vs*. 2.6 %), bicyclogermacrene (1.8 *vs*. 1.4 %), (*E*)-β-farnesene (1.7 *vs*. 1.6 %), (*E*)-caryophyllene (1.4 *vs*. 1.0 %) and camphor (1.1 *vs*. 1.1 %) were the other common components of the oils (Table I). α-Guaiene (5.4 *vs*. 0.4 %) and β-elemene (2.1 *vs*. 0.7 %) were defined as two other common components with superiority of the inflorescence oil. (*E*)-β-Ocimene (0.9 *vs*. 1.2 %) and eugenol (0.3 *vs*. 1 %) were common components with higher amounts in the leaf oil than in the inflorescence oil (Table I). Spathulenol (1.3 %) and α-bulnesene (1.2 %) were constituents exclusive to the inflorescences and leaves, respectively (Table I). From chemical standpoint, alcohols were the highlighted components of both oils with notable amounts of linalool and α-cadinol. Taking into account the major volatile oil constituents, there was a significant quantitative but no strong qualitative difference between the two oils.

TABLE I. Chemical composition of the essential oil of hydroponically grown *O. basilicum* L. (compounds are reported according to their elution order on a non-polar column)

No.	Compound	*RI*	Molecular formula	Peak area, %	
				Inflorescence	Leaves
1	*α*-Pinene	0939	$C_{10}H_{16}$	0.1	0.2
2	Camphene	0954	$C_{10}H_{16}$	0.1	0.1
3	Sabinene	0975	$C_{10}H_{16}$	0.1	0.1
4	*β*-Pinene	0979	$C_{10}H_{16}$	0.4	0.6
5	Myrcene	0991	$C_{10}H_{16}$	0.3	0.7
6	*α*-Terpinene	1017	$C_{10}H_{16}$	–	0.1
7	Limonene	1029	$C_{10}H_{16}$	0.2	–
8	1,8-Cineole	1031	$C_{10}H_{18}O$	2.4	3.5
9	(*Z*)-*β*-Ocimene	1037	$C_{10}H_{16}$	–	0.1
10	(*E*)-*β*-Ocimene	1050	$C_{10}H_{16}$	0.9	1.2
11	*γ*-Terpinene	1060	$C_{10}H_{16}$	0.1	0.1
12	(*Z*)-Sabinene hydrate	1070	$C_{10}H_{18}O$	–	0.1
13	Fenchone	1087	$C_{10}H_{16}O$	–	0.8
14	Terpinolene	1089	$C_{10}H_{16}$	0.3	–
15	Linalool	1097	$C_{10}H_{18}O$	21.1	13.1
16	Camphor	1146	$C_{10}H_{16}O$	1.1	1.1
17	Borneol	1169	$C_{10}H_{18}O$	0.4	0.2
18	Terpinene-4-ol	1177	$C_{10}H_{18}O$	0.1	0.1
19	Methyl chavicol	1196	$C_{10}H_{12}O$	37.2	56.7
20	Geraniol	1253	$C_{10}H_{18}O$	0.1	–
21	*α*-Cubebene	1351	$C_{15}H_{24}$	0.1	0.8
22	Eugenol	1359	$C_{10}H_{12}O_2$	0.3	1
23	*α*-Copaene	1377	$C_{15}H_{24}$	0.4	0.2
24	*β*-Bourbonene	1388	$C_{15}H_{24}$	–	0.1
25	*β*-Cubebene	1388	$C_{15}H_{24}$	–	0.5
26	*β*-Elemene	1391	$C_{15}H_{24}$	2.1	0.7
27	Methyl eugenol	1404	$C_{11}H_{14}O_2$	0.2	0.6
28	*α*-Cedrene	1412	$C_{15}H_{24}$	0.1	–
29	*α*-(*Z*)-Bergamotene	1413	$C_{15}H_{24}$	1.8	2.6
30	(*E*)-Caryophyllene	1419	$C_{15}H_{24}$	1.4	1
31	*α*-Guaiene	1440	$C_{15}H_{24}$	5.4	0.4
32	Aromadendrene	1441	$C_{15}H_{24}$	0.3	0.1
33	(*E*)-*β*-Farnesene	1457	$C_{15}H_{24}$	1.7	1.6
34	Germacrene D	1485	$C_{15}H_{24}$	6.1	2.7
35	*β*-Selinene	1490	$C_{15}H_{24}$	0.2	–
36	*α*-Zingiberene	1494	$C_{15}H_{24}$	0.3	–
37	Bicyclogermacrene	1500	$C_{15}H_{24}$	1.8	1.4
38	*α*-Bulnesene	1510	$C_{15}H_{24}$	–	1.2
39	*γ*-Cadinene	1514	$C_{15}H_{24}$	2.5	2
40	*δ*-Cadinene	1523	$C_{15}H_{24}$	0.7	0.1
41	(*Z*)-Nerolidol	1533	$C_{15}H_{26}O$	0.2	0.1
42	*α*-Cadinene	1539	$C_{15}H_{24}$	0.1	0.1
43	(*Z*)-Calamenene	1540	$C_{15}H_{22}$	–	0.4
44	Spathulenol	1578	$C_{15}H_{24}O$	1.3	–

TABLE I. Continued

No.	Compound	*RI*	Molecular formula	Peak area, %	
				Inflorescence	Leaves
45	Caryophyllene oxide	1583	$C_{15}H_{24}O$	0.1	0.1
46	Alloaromadendrene	1641	$C_{15}H_{24}O$	–	0.1
47	β-Eudesmol	1651	$C_{15}H_{26}O$	0.3	0.1
48	α-Cadinol	1654	$C_{15}H_{26}O$	6.1	3
49	α-Bisabolol	1686	$C_{15}H_{26}O$	0.3	0.1
50	Phytol	1943	$C_{20}H_{40}O$	0.1	0.1
	Total	–	–	98.8	99.9

Comparison of the volatile constituents of hydroponically grown *O. basilicum* with data published on the oil composition of this plant from wild habitats and field and open-air grown plants shows that there are some qualitative and quantitative discrepancy and/or similarity between the essential oil profiles of different plant production systems.[10–14,18–27] Moreover, there was a significant difference between the chemical profile of our present and previous work on field grown basil plants, when menthone and estragole were identified as the principal volatile oil components.[9]

TABLE II. Main classes and subclasses of hydroponically grown *Ocimum basilicum* L. essential oil constituents

Class and subclass of compounds	Content, %	
	Inflorescence	Leaves
Monoterpenoids	27.7	22.1
Monoterpene hydrocarbons	2.5	3.2
Oxygenated monoterpenes	25.2	18.9
Sesquiterpenoids	33.3	19.4
Sesquiterpene hydrocarbons	25	15.9
Oxygenated sesquiterpenes	8.3	3.5
Phenylpropanoids	37.7	58.3
Total identified	98.8	99.9

Overall, regarding the major essential oil components of the present study and reports of other scientists from elsewhere, it seems that the hydroponic production system has potential application for basil production. Furthermore, the acceptable volatile oil content along with volatile oil richness in methyl chavicol and linalool make the studied oil worthy of consideration in commercial markets. The minor chemical variations from different plant origins and production systems seems to be due to the impact of divergent climatological and geographical conditions (light quality and quantity, soil characteristics, water and nutrient (subspecies, natural hybridization and chemovariety), diverse growing conditions (wild habitats, common greenhouse production and different soil-less culture sys-

tems) as well as agronomic parameters (fertilization, irrigation regime and weed control). Those different variables dependently modify the assimilation capacity and hence interactive relationship between primary and secondary metabolism of aromatic plants in favor of the biosynthesis and accumulation of distinct volatile components.

CONCLUSIONS

The essential oil content and composition of hydroponically grown *O. basilicum* L. were comparable with those of previously reported wild and cultivated plants. In conclusion, the hydroponics system can be a promising production method for the yearly growth of this phenylpropane- and monoterpene-rich plant in order to satisfy the high demands of the pharmaceutical, fragrance and food industries.

ИЗВОД

САСТАВ ЕТАРСКОГ УЉА ЦВАСТИ И ЛИСТОВА БОСИЉКА ГАЈЕНОГ ХИДРОПОНИЧНО

M. B. HASSANPOURAGHDAM[1], G. R. GOHARI[2], S. J. TABATABAEI[2] и M. R. DADPOUR[2]

[1]*Department of Horticultural Sciences, Faculty of Agriculture, University of Maragheh, Maragheh 55181-83111 и* [2]*Department of Horticultural Sciences, Faculty of Agriculture, University of Tabriz, Tabriz 51666, Iran*

Одређиван је састав етарског уља листа и цвасти хидропонично гајеног босиљка *Ocimum basilicum* L. методом дестилације воденом паром и GC/EI-MS. Идентификовано је педесет састојака који су чинили укупно 98,8 % садржаја уља цвасти, односно 99,9 % уља листа. Фенилпропаноиди (37,7 % уља цвасти и 58,3 % уља листа) чине доминантну класу једињења, а затим следе сесквитерпени (33,3 и 19,4 %) и монотерпени (27,7 и 22,1 %). Од монотерпена, једињења са кисеоником су главна потклаcа (25,2 и 18,9 %). Угљоводоници (25,0 и 15,9 %) су чинили главну поткласу сесквитерпенских једињења. Метил-чавикол, дериват фенилпропана, (37,2 и 56,7 %) основни је састојак оба уља, чинећи 38,0 % уља цвасти и 57,0 % уља листа. Линалол (21,1 и 13,1 %), *α*-кадинол (6,1 и 3,0 %), гермакрен D (6,1 и 2,7 %) и 1,8-цинеол (2,4 и 3,5 %) су, такође, међу основним састојцима уља. Значајна је квантитативна, али не и квалитативна разлика између етарских уља два биљна органа. Састав етарског уља хидропонично гајеног босиљка *O. basilicum* L. је сличан саставу уља биљке гајене на земљи, што може бити од значаја за фармацеутску и прехрамбену индустрију.

(Примљено 11. марта, ревидирано 30. априла 2010)

REFERENCES

1. M. Schwarz, *Soilless Culture Management*, Springer-Verlag, Berlin, 1995, p. 197
2. M. B. Hassanpouraghdam, S. J. Tabatabaie, H. Nazemiyeh, A. Aflatuni, *J. Food Agric. Environ.* **6** (2008) 145
3. M. B. Hassanpouraghdam, S. J. Tabatabaie, H. Nazemiyeh, L. Vojodi, M. A. Aazami, *J. Essent. Oil-Bear. Plants.* **11** (2008) 649
4. M. B. Hassanpouraghdam, *Nat. Prod. Res.* **23** (2009) 672

5. M. Dorais, A. P. Papadopoulos, X. Lou, S. Leonhart, A. Gosselin, K. Pedneault, P. Angers, L. Gaudreau, *Acta Hort.* **554** (2001) 297
6. S. K. Mairapetyan, *Acta Hort.* **502** (1999) 33
7. A. Zarghari, *Medicinal Plants*, Tehran University Publications, Iran, 1997, p. 921 (in Persian)
8. V. Mozaffarian, *A Dictionary of Iranian Plant Names*, Farhang Moaaser Publishing Company, Iran, 2004, p. 671 (in Persian)
9. M. B. Hassanpouraghdam, A. Hassani, M. S. Shalamzari, *Chemija* **21** (2010) 59
10. K. Koba, P. W. Poutouli, C. Raynaud, J. P. Chaumont, K. Sanda, *Bangladesh J. Pharmacol.* **4** (2009) 1
11. M. M. Zamfirache, I. Burzo, Z. Olteanu, S. Dunca, S. Surdu, E. Truta, M. Stefan, C. M. Rosu, *An. St. Univ. Al. L. Cuza. Iasi* **4** (2008) 35
12. M. Ismail, *Pharm. Biol.* **44** (2006) 619
13. S. E. Sajjadi, *Daru* **14** (2006) 128
14. M. Ozcan, J. C. Chalchat, *Czech J. Food Sci.* **20** (2002) 223
15. J. W. Zhang, S. K. Li, W. J. Wu, *Molecules*. **14** (2009) 273
16. X. Chang, P. G. Alderson, C. J. Wright, *Environ. Exper. Bot.* **63** (2008) 216
17. B. M. Lawrance, in *Developments in Food Sciences, Flavour and Fragrances: A World Perspective*, B. M. Lawrance, B. D. Mokheyee, B. J. Willis, Eds., Elsevier, Amsterdam, 1988
18. A. H. N. Abduelrahman, E. A. Alhussein, N. A. I. Osman, A. H. Nour, *Int. J. Chem. Technol.* **1** (2009) 1
19. V. D. Zheljazkov, A. N. Callahan, C. L. Cantrell, *J. Agric. Food Chem.* **56** (2007) 241
20. M. Marotti, R. Piccaglia, E. Giovanelli, *J. Agric. Food Chem.* **44** (1996) 3926
21. E. Werker, E. Putievsky, U. Ravid, N. Dudai, I. Katzir, *Ann. Bot.* **71** (1993) 43
22. O. Politeo, M. Jukic, M. Milos, *Croat. Chem. Acta* **79** (2006) 545
23. S. M. Keita, C. Vincent, J. P. Schmit, A. Belanger, *Flavour Fragrance J.* **15** (2000) 339
24. A. A. Kasali, A. O. Eshilokun, S. Adeola, P. Winterhalter, H. Knapp, B. Bonnlander, *Flavour Fragrance J.* **20** (2004) 45
25. A. J. Hussein, F. Anwar, S. T. H. Sherazi, R. Prybylski, *Food Chem.* **108** (2008) 986
26. J. C. Chalchat, M. M. Ozcan, *Food Chem.* **110** (2008) 501
27. S. R. Vani, S. F. Cheng, C. H. Chuah, *Am. J. Appl. Sci.* **6** (2009) 523
28. R. P. Adams, *Identification of Essential Oil Components by Gas Chromatography/Quadrupole Mass Spectroscopy*, Allured Publishing Corporation, Carol Stream, IL,, 2004, p. 456.

Journal of the Serbian Chemical Society
JSCS-info@shd.org.rs • www.shd.org.rs/JSCS
J. Serb. Chem. Soc. 75 (10) 1369–1380 (2010)
JSCS–4059
UDC 546.732'742'562'472'482.004.12:
615.281/.282:66.097.8–914.7
Original scientific paper

Synthesis, characterization and antibacterial and antifungal studies of some tetraazamacrocyclic complexes

DHARAM PAL SINGH[1]*, VANDNA MALIK[1], RAMESH KUMAR[1], KRISHAN KUMAR[1] and SAURABH SUDHA DHIMAN[2]

[1]*Department of Chemistry, National Institute of Technology, Kurukshetra-136 119 and* [2]*Department of Biotechnology, Kurukshetra University, Kurukshetra-136 119, India*

(Received 29 January, revised 28 April 2010)

Abstract: A new series of complexes was synthesized by template condensation of malonyl dihydrazide and glyoxal in methanolic medium in the presence of divalent cobalt, nickel, copper, zinc and cadmium salts, whereby complexes of the type: $[M(C_5H_6N_4O_2)X_2]$ where M = Co(II), Ni(II), Cu(II), Zn(II) and Cd(II), and X = Cl^-, NO_3^- and OAc^-, were formed. The complexes were characterized with the aid of elemental analyses, conductance measurements, magnetic susceptibility measurements, and electronic, NMR and infrared spectral studies. Based on these studies, a six coordinate octahedral geometry is proposed for these complexes. The complexes were tested for their *in vitro* antibacterial and antifungal activities. The minimum inhibitory concentration shown by complexes was compared with that of standard drugs.

Keywords: antibacterial; antifungal; macrocyclic complexes; minimum inhibitory concentration.

INTRODUCTION

During the past few decades, a great deal of interest has been devoted to macrocyclic complexes containing oxygen and nitrogen atoms. Macrocyclic complexes are of great interest due to their resemblance to naturally occurring macrocycles and analytical, industrial and medical applications.[1–6] Macrocyclic metal complexes of lanthanides, *e.g.* Gd(III), are used as MRI contrast agents.[7] Macrocyclic metal chelating agents (DOTA) are useful for detecting tumour lesions.[8] The chemistry of macrocyclic complexes is also important due to their use as dyes and pigments,[9] as well as NMR shift reagents.[10] Additionally, some macrocyclic complexes have been found to exhibit potential antibacterial activities.[11] Prompted by these applications, in the present paper, the syntheses of macrocyc-

* Corresponding author. E-mail: dpsinghchem@yahoo.co.in
doi: 10.2298/JSC100129110S

lic complexes of Co(II), Ni(II), Cu(II), Zn(II) and Cd(II) obtained by template condensation reaction of malonyl dihydrazide and glyoxal are reported. The complexes were characterized with the aid of IR, NMR and electronic spectral studies, and magnetic susceptibilities, elemental analysis and molar conductance measurements. These complexes were also tested for their *in vitro* antibacterial and antifungal activities.

EXPERIMENTAL

Isolation of the complexes

The complexes were synthesized by the template method, *i.e.*, by condensation of malonyl dihydrazide and glyoxal in the presence of a divalent metal salt. To a hot stirred methanolic solution (≈50 mL) of malonyl dihydrazide (10 mmol) was added a divalent cobalt, nickel, copper, zinc or cadmium salt (Cl^-, NO_3^-, CH_3COO^-) (10 mmol) dissolved in the minimum quantity of methanol (≈20 mL). The resulting solution was boiled under reflux for 0.5 h. Subsequently, glyoxal (10 mmol) was added to the refluxing mixture and refluxing was continued for 8–10 h. The mixture was concentrated to half its volume and kept in a desiccator overnight. The complexes were then filtered, washed with methanol, acetone and ether and dried *in vacuo*; yield ≈50–60 %. The complexes were soluble in DMF and DMSO, but insoluble in other common organic solvents and water. They were found to be thermally stable up to ≈225–260 °C, after which they decomposed.

The template condensation of malonyl dihydrazide and glyoxal in the presence of divalent cobalt, nickel, copper, zinc and cadmium salts may be represented by the following scheme:

$$C_3H_8N_4O_2 + C_2H_2O_2 + MX_2 \xrightarrow[8\text{-}10\ h]{MeOH} [M(C_5H_6N_4O_2)X_2] + 2H_2O$$

where M = Co(II), Ni(II), Cu(II), Zn(II) or Cd(II) and X = Cl^-, NO_3^- or CH_3COO^-.

Analytical and physical measurements

The microanalyses for C, H, and N were realized at SAIF, CDRI, Lucknow. The metal contents were determined by standard EDTA methods. The electronic spectra (DMF) were recorded on a Cary 14 spectrophotometer. The magnetic susceptibility measurements were performed at SAIF, IIT Roorkee. The IR spectra were recorded on an FT-IR spectrophotometer (Perkin Elmer) in the range 4000–200 cm^{-1} using the Nujol Mull method at SAIF, Punjab University, Chandigarh, India. The NMR spectra were recorded on a Bruker NMR spectrometer (300 MHz). The conductivity was measured on a digital conductivity meter (HPG System, G-3001).

In-vitro *antibacterial activity*

Primary screening. The antibacterial activities of the newly synthesized complexes were evaluated by the Agar Well Diffusion Assay Technique against two Gram-positive bacteria, *i.e.*, *Bacillus subtilis* (MTCC 8509) and *Bacillus stearothermophilus* (MTCC 8508) and two Gram-negative bacteria, *i.e.*, *Escherichia coli* (MTCC 51) and *Pseudomonas putida* (MTCC 121). The bacterial cultures were maintained on the nutrient agar media by sub-culturing them on fresh slants after every 4–6 weeks and incubating them at the appropriate temperature for 24 h. All stock cultures were stored at 4 °C. For the evaluation of antimicrobial activity of the synthesized complexes, a suspension of each test microorganism was prepared. The turbidity

of each suspension was adjusted to 0.5 McFarland units by suspending the cultures in sterile distilled water. The size of final inoculum was adjusted to 5×10^7 CFU ml^{-1}. A volume of 20 ml of agar media was poured into each Petri plate and the plates were swabbed with broth cultures of the respective micro-organisms and kept for 15 min for adsorption to occur. Using a punch, ≈8 mm diameter wells were bored in the seeded agar plates and a 100 µl volume of each test compound reconstituted in DMSO was added into the wells. DMSO was used as the control for all the test complexes. After holding the plates at room temperature for 2 h to allow diffusion of the compounds into the agar, the plates were incubated at 37 °C for 24 h. Antibacterial activity was determined by measuring the diameter of the inhibition zone. The entire tests were performed in triplicate and the mean of the diameter of inhibition was calculated. The antimicrobial activities of the complexes were compared against standard drugs.

*Minimum Inhibitory Concentration (*MIC*).* Nutrient broth was adjusted to pH 7.0 for the determination of the *MIC* of synthesized complexes.[12] The *MIC* is the lowest concentration of an antimicrobial agent that prevents the development of visible growth of microorganism after overnight incubation. The inoculum of the test microorganisms were prepared using 16 h-old cultures adjusted by reference to the 0.5 McFarland standards (10^8 cells ml^{-1}).[13] These cultures were further diluted up to 10-fold with nutrient broth to obtain an inoculum size of 1.2×10^7 CFU ml^{-1}. A positive control (containing inoculum but no complex) and a negative control (containing complex but no inoculum) were also prepared. A stock solution of 4 mg ml^{-1} of each compound was prepared in DMSO and further appropriately diluted to obtain final concentrations ranging from 250 to 0.03 µg ml^{-1}.[14] The requisite quantity of antifungal drug (cyclohexamide) was added to the broth to obtain its desirable final concentration of 100 µg ml^{-1}. Separate flasks were taken for each test dilution. To each flask was added 100 µl of inoculum. Then the appropriately diluted test sample was added to each flask having broth and microbial inoculum. The contents of the flask were mixed and incubated for 24 to 48 h at 37 °C. The test bacterial cultures were spotted in a predefined pattern by aseptically transferring 5 µl of each bacterial culture onto the surface of solidified agar-agar plates and incubated at 37 °C for 24 h for determining the *MIC* value.

In-vitro *antifungal activity*

Potato dextrose medium (PDA) was prepared in a flask and sterilized. To check the growth of bacterial culture in the medium, the requisite quantity of the standard antibiotic (ampicillin) was added to obtain the desired final concentration of 100 µg ml^{-1} of the medium. Test samples were prepared in different concentrations (10, 50 and 100 µg/ml*)* in dimethyl sulphoxide and 200 µl of each sample was spread on the PDA media contained in sterilized Petri plates. Mycelial discs taken from the standard cultures of fungi (*Aspergillus flavus* and *A. niger*) were grown on the PDA medium for 5–7 days. These cultures were used for the aseptic inoculation in the sterilized Petri dish. Standard cultures inoculated at 28±1 °C were also used as the control. The efficacy of each sample was determined by measuring the radial mycelial growth. The radial growth of the colony was measured in two directions at right angle to each other and the average of two replicates was recorded in each case. The data are expressed as percent inhibition over the control obtained from the size of colonies. The percent inhibition was calculated using the formula:

$$\% \text{ Inhibition} = 100(C–T)/C$$

where C is the diameter of fungus colony in the control plate after incubation for 96 h and T is the diameter of the fungus colony in the tested plate after the same incubation period.

RESULTS AND DISCUSSION

The analytical data show the formula for macrocyclic complexes as: $[M(C_5H_6N_4O_2)X_2]$; where M = Co(II), Ni(II), Cu(II), Zn(II) or Cd(II) and X = = Cl^-, NO_3^- or CH_3COO^-. The tests for the anions were positive only after decomposition of the complexes, indicating their presence inside the coordination sphere. All macrocyclic complexes were dark-coloured solids, which were soluble in DMF and DMSO. The measurements of molar conductance (conductance ≈10–20 S cm^2 mol^{-1}) in DMSO showed that these chelates are non-electrolytes.[15] All complexes gave satisfactory elemental analyses results, as shown in Table I.

TABLE I. Analytical data of the divalent Co, Ni, Cu, Zn and Cd complexes derived from malonyl dihydrazide and glyoxal

No.	Complex	Found (Calcd.), %				Colour	MW g mol^{-1}
		M	C	H	N		
1	$[Co(C_5H_6N_4O_2)Cl_2]$	20.56 (20.77)	21.09 (21.12)	2.02 (2.11)	19.63 (19.71)	Light brown	284
2	$[Co((C_5H_6N_4O_2)(NO_3)_2]$	17.42 (17.50)	17.71 (17.80)	1.65 (1.78)	24.76 (24.92)	Light brown	337
3	$[Co(C_5H_6N_4O_2)(OAc)_2]$	17.65 (17.82)	36.51 (36.62)	3.52 (3.62)	16.87 (16.91)	Shiny black	331
4	$[Ni(C_5H_6N_4O_2)Cl_2]$	20.43 (20.49)	21.17 (21.20)	2.06 (2.12)	19.53 (19.78)	Brown	283
5	$[Ni(C_5H_6N_4O_2)(NO_3)_2]$	17.23 (17.26)	17.88 (17.85)	1.76 (1.78)	24.89 (25.00)	Dark brown	336
6	$[Ni(C_5H_6N_4O_2)(OAc)_2]$	17.51 (17.56)	32.73 (32.72)	3.60 (3.63)	16.91 (16.96)	Shiny black	330
7	$[Cu(C_5H_6N_4O_2)Cl_2]$	21.89 (21.87)	20.81 (20.83)	2.03 (2.08)	19.46 (19.44)	Brown	288
8	$[Cu(C_5H_6N_4O_2)(NO_3)_2]$	18.41 (18.47)	17.51 (17.59)	1.72 (1.75)	24.69 (24.63)	Dark brown	341
9	$[Cu(C_5H_6N_4O_2)(OAc)_2]$	18.85 (18.80)	32.21 (32.23)	3.60 (3.58)	16.75 (16.71)	Greyish black	335
10	$[Zn(C_5H_6N_4O_2)(OAc)_2]$	19.26 (19.28)	32.02 (32.04)	3.55 (3.56)	16.64 (16.61)	Yellowish orange	337
11	$[Cd(C_5H_6N_4O_2)(OAc)_2]$	28.45 (29.16)	30.09 (28.12)	3.23 (3.12)	13.98 (14.58)	Reddish brown	384

IR Spectra

In the IR spectrum of malonyl dihydrazide, a pair of bands corresponding to ν(NH_2) was present at ≈3210 and ≈3270 cm^{-1}, but absent in the IR spectra of all the complexes.[16] However, a single broad medium band at 3360–3450 cm^{-1} was observed in the spectra of all the complexes, which may be assigned to ν(NH) stretching vibrations.[17,18] A strong peak at ≈1660 cm^{-1} in the IR spectrum of

malonyl dihydrazide is assigned to the >C=O group of the CONH moiety. This peak is shifted to lower frequencies (≈1620–1640 cm^{-1}) in the spectra of all the complexes,[19,20] suggesting the coordination of the oxygen of the carbonyl group with the metal. Furthermore, no strong absorption band was observed near 1700 cm^{-1} in the IR spectra of the complexes but was observed in the spectrum of glyoxal. This indicates the absence of >C=O groups of the glyoxal moiety in the complexes. These facts confirm the condensation of carbonyl groups of glyoxal and the amino groups of malonyl dihydrazide.[21,22] The IR spectra of the complexes showed a new strong absorption band in the region ≈1595–1610 cm^{-1}, which may be attributed to the ν(C=N) group.[23,24] These results provide strong evidence for the formation of the macrocyclic frame.[25] The lower value of ν(C=N) indicates coordination of the nitrogen of azomethine to the metal.[26] The bands present at ≈1300–1000 cm^{-1} are assigned to ν(C–N) vibration. The bands presents at ≈3040 cm^{-1} may be assigned to ν(C–H) vibrations of the glyoxal moiety. The IR spectra of the nitrate complexes display three (N–O) stretching bands at ≈1410–1455 cm^{-1} (ν_5), ≈1305–1315cm^{-1} (ν_1) and ≈1015–1030 cm^{-1} (ν_2). The separation of the two highest frequency bands ($\nu_5 - \nu_1$) suggest that both the nitrate groups are coordinated in a unidentate manner.[27] The acetate complexes showed two bands at ≈1630–1640 cm^{-1} (ν_1) and ≈1380–1390 cm^{-1} (ν_2). These indicate that the acetate group is coordinated in a unidentate manner.[28]

The far IR spectra show bands in the region ≈420–450 cm^{-1}. corresponding to ν(M–N) vibrations in all the complexes.[29–31] The presence of a band in all the complexes in the ≈420–450 cm^{-1} region originate from (M–N) azomethine vibration modes and support the coordination of azomethine nitrogen with the metal.[32] The bands present at ≈310–315 cm^{-1} in the chloride complexes are due to ν(M–Cl).[29,31] and bands present at ≈210–240 cm^{-1} in all the nitrate complexes to ν(M–O).[29]

NMR Spectra

The ^{1}H-NMR spectrum of the zinc complex showed a broad singlet at 8.6 ppm due to protons of the –CONH moiety.[17,33] The singlet at 2.34 ppm may be due to $-CH_2$ protons.[19] The singlet in the region of 7.8 ppm may be assigned to protons of the glyoxal moiety.[34]

Magnetic measurements and electronic spectra

Cobalt complexes. The magnetic moments of the cobalt complexes were measured at room temperature and lie in the range 4.85–4.90 μ_B, which corresponds to 3 unpaired electrons. The solution spectra of the cobalt(II) complexes exhibited absorption in the region *ca*. 8100–9160 (ν_1), 12500–15700 (ν_2) and 18600–20500 cm^{-1} (ν_3). The spectra resemble those of complexes reported to be octahedral.[35] Thus, the various bands can be assigned to: $^4T_{1g} \rightarrow {}^4T_{2g}(F)$ (ν_1);

$^4T_{1g} \rightarrow {}^4A_{2g}(F)$ (ν_2) and $^4T_{1g} \rightarrow {}^4T_{1g}(P)$ (ν_3) transitions, respectively. It appears that the symmetry of these complexes is not idealized O_h but D_{4h}. The assignment of the first spin-allowed band seems plausible since the first band appears approximately at half the energy of the visible band.[36] Various ligand field parameters, *Dq*, *B*, β and β% were calculated for the complexes and are listed in Table II (malonyl dihydrazide and glyoxal). *B* for a free cobalt(II) ion is 971 cm^{-1}. The values of β lie in the range 0.606–0.629. These values indicate the presence of covalent character in the metal–ligand "σ"' bond. The value of the ν_2/ν_1 ratio lies between 1.76–1.79, which identify the complexes as possessing a distorted octahedral structure.[37]

TABLE II. Ligand field parameters of the divalent cobalt and nickel complexes derived from malonyl dihydrazide and glyoxal

No.	Complexes	*Dq* cm^{-1}	*B* cm^{-1}	β	β%	ν_2/ν_1	μ_{eff} μ_B
1	$[Co(C_5H_6N_4O_2)Cl_2]$	1016	588	0.605	39.1	1.78	4.90
2	$[Co(C_5H_6N_4O_2)(NO_3)_2]$	1066	590	0.607	39.3	1.77	4.89
3	$[Co(C_5H_6N_4O_2)(OAc)_2]$	1071	591	0.608	39.2	1.78	4.93
4	$[Ni(C_5H_6N_4O_2)Cl_2]$	1185	540	0.519	48.1	1.41	2.88
5	$[Ni(C_5H_6N_4O_2)(NO_3)_2]$	1190	538	0.517	48.5	1.41	2.87
6	$[Ni(C_5H_6N_4O_2)(OAc)_2]$	1195	536	0.515	48.3	1.40	2.89

Nickel complexes. The magnetic moment of the nickel complexes at room temperature lie in the range 2.91–2.95 μ_B showing an octahedral environment around the Ni(II) ion in all complexes. The solution spectra of the Ni(II) complexes exhibited a well-discernable band with a shoulder on the low energy side. The other two bands generally observed in the region at *ca.* 16570–17240 cm^{-1} (ν_2), and 26860–28000 cm^{-1} (ν_3) are assigned to $^3A_{2g} \rightarrow {}^3T_{1g}(F)$ (ν_2) and $^3A_{2g} \rightarrow$ $\rightarrow {}^3T_{1g}(P)$ (ν_3) transitions, respectively. The first two bands result from the splitting of one band, ν_1, are in the range ≈9700–10000 and 11800–12440 cm^{-1}, which can be assigned to $^3B_{1g} \rightarrow {}^3E_g$ and $^3B_{1g} \rightarrow {}^3B_{2g}$ transitions, respectively, assuming the effective symmetry to be D_{4h} (component of $^3T_{2g}$ in O_h symmetry).[36] The intense higher energy band at *ca.* 34000 cm^{-1} may be due to a π–π* transition of the (C=N) group. The various bands do not follow any regular pattern and seem to be anion independent. The spectra are consistent with the distorted octahedral nature of these complexes. Various ligand field parameters, *Dq*, *B*, β and β% were calculated for the complexes and are listed in Table II (malonyl dihydrazide and glyoxal). *B* for a free nickel(II) ion is 1040 cm^{-1}. The values of β lie in the range 0.509–0.519. These values indicate the presence of covalent character in the metal–ligand "σ" bond. The value of the ν_2/ν_1 ratio lies between 1.37–1.41 and shows that the complexes possess a distorted octahedral structure.[37]

Copper complexes. The magnetic moment of the copper complexes lie in the range 1.77–1.82 μ_B. The electronic spectra of the copper complexes exhibit bands in the region *ca*. 17780–19000 cm^{-1} with a shoulder on the low energy side at ≈14600–16000 cm^{-1}, which show that these complexes have a distorted octahedral geometry.[35,36] Assuming tetragonal distortion in the molecule, the d-orbital energy level sequence for these complexes may be: $x^2 - y^2 > z^2 > xy > xz > yz$ and the shoulder can be assigned to: $z^2 \rightarrow x^2 - y^2$ ($^2B_{1g} \rightarrow {}^2B_{2g}$) and the broad band contains both $xy \rightarrow x^2 - y^2$ ($^2B_{1g} \rightarrow {}^2E_g$) and $xz, yz \rightarrow x^2 - y^2$ ($^2B_{1g} \rightarrow \rightarrow {}^2A_{2g}$) transitions.[38] The band separation of the spectra of the complexes is of the order 2500 cm^{-1}, which is consistent with the proposed geometry of the complexes.[35] Therefore, it may be concluded that all the complexes formed by the macrocycles with Cu(II) metals are distorted octahedral.

Biological results and discussion

In this study, all the chemically synthesized complexes were evaluated against Gram-positive and Gram-negative bacteria. The *MIC* values of the synthetic complexes were determined by the method given by Andrews[39]. Standard antibiotics, namely streptomycin and chloramphenicol, were used for comparison with the antibacterial activities exhibited by these complexes. All the complexes of the tested series possessed some antibacterial activity against Gram-positive bacteria as well as Gram-negative bacteria (Table III). In the whole series, complexes **1** and **5** were found to be most effective against all the tested bacterial strains, showing zone of growth inhibition in the range from 46.2–49.2 mm

TABLE III. *In-vitro* antibacterial activity of the complexes determined by the agar well diffusion method for a concentration of 100 μg ml^{-1} (A – *Bacillus subtilis* (MTCC 8509), B – *Bacillus stearothermophilus* (MTCC 8508), C – *Escherichia coli* (MTCC 51), D – *Pseudomonas putida* (MTCC 121))

No.	Complex	Diameter of zone of growth inhibition[a], mm			
		A	B	C	D
1	$[Co(C_5H_6N_4O_2)Cl_2]$	48.2	46.2	49.2	47.3
2	$[Co((C_5H_6N_4O_2)(NO_3)_2]$	13.3	16.2	29.6	28.1
3	$[Co(C_5H_6N_4O_2)(OAc)_2]$	11.3	15.6	9.9	11.5
4	$[Ni(C_5H_6N_4O_2)Cl_2]$	10.3	19.2	16.5	21.4
5	$[Ni(C_5H_6N_4O_2)(NO_3)_2]$	36.3	37.1	38.2	36.2
6	$[Ni(C_5H_6N_4O_2)(OAc)_2]$	10.4	12.3	21.5	19.2
7	$[Cu(C_5H_6N_4O_2)Cl_2]$	13.7	24.8	26.4	23.2
8	$[Cu(C_5H_6N_4O_2)(NO_3)_2]$	15.4	13.5	14.8	21.4
9	$[Cu(C_5H_6N_4O_2)(OAc)_2]$	21.2	27.3	23.4	21.7
10	$[Zn(C_5H_6N_4O_2)(OAc)_2]$	10.3	19.2	12.4	13.9
11	$[Cd(C_5H_6N_4O_2)(OAc)_2]$	28.8	21.4	21.9	23.3
	Chloramphenicol[b]	64.2	77.2	65.4	71.2
	Streptomycin[b]	63.2	77.2	79.4	82.2

[a]Mean of three replicates; [b]standard drugs

and 36.2–38.2 mm, respectively. Complexes **9** and **11** exhibited good activity against all the tested bacterial strains with a zone of inhibition in the range from 21.2–
–27.3 mm and 21.4–28.8 mm, respectively. Complex **2** showed the highest zone of inhibition (29.6 and 28.1 mm) against *E. coli* and *P. putida*, respectively. Complex **7** showed the highest zone of inhibition 23.2–26.4 mm against *B. subtilis*, *E. coli* and *P. putida* (Table III).

Based on the *MIC* values shown by these complexes against all the bacterial strains, complex **1** was found to be most effective by showing a *MIC* of 4 μg ml^{-1} for *E. coli*, which is equal to the *MIC* shown by the standard antibiotic chloramphenicol and streptomycin against the same bacterial strain. Complex **1** also exhibited *MIC* values in the range from 4 to 8 μg ml^{-1} for the other bacterial strains. In the whole series, the *MIC* value of complex **5** was found to be 16 μg ml^{-1} for *E. coli* and 32 μg ml^{-1} for *B. subtilis*, *B. stearothermophilus* and *P. putida*. Complex **11** showed an *MIC* of 64 μg ml^{-1} for *B. subtilis* (Table IV).

TABLE IV. Minimum inhibitory concentration (*MIC*) shown by the complexes against the test bacteria determined by agar dilution assay (A – *Bacillus subtilis* (MTCC 8509), B – *Bacillus stearothermophilus* (MTCC 8508), C – *Escherichia coli* (MTCC 51), D – *Pseudomonas putida* (MTCC 121))

No.	Complex	*MIC* / μg ml^{-1}			
		A	B	C	D
1	$[Co(C_5H_6N_4O_2)Cl_2]$	4	8	4	8
2	$[Co((C_5H_6N_4O_2)(NO_3)_2]$	>128	>128	64	64
3	$[Co(C_5H_6N_4O_2)(OAc)_2]$	>128	>128	>128	>128
4	$[Ni(C_5H_6N_4O_2)Cl_2]$	>250	>250	>250	>250
5	$[Ni(C_5H_6N_4O_2)(NO_3)_2]$	32	32	16	32
6	$[Ni(C_5H_6N_4O_2)(OAc)_2]$	>250	>250	128	>128
7	$[Cu(C_5H_6N_4O_2)Cl_2]$	>250	>128	>128	>128
8	$[Cu(C_5H_6N_4O_2)(NO_3)_2]$	>250	>250	>250	>128
9	$[Cu(C_5H_6N_4O_2)(OAc)_2]$	>128	128	>128	>128
10	$[Zn(C_5H_6N_4O_2)(OAc)_2]$	>250	>250	>250	>250
11	$[Cd(C_5H_6N_4O_2)(OAc)_2]$	64	>128	>128	>128
	Chloramphenicol[a]	2	2	4	2
	Streptomycin[a]	2	2	4	4

[a]Standard drugs

The antifungal activities of all the complexes were determined against two fungal strains, *i.e.*, *A. flavus* and *A. niger*, and then compared with the standard antifungal drug cyclohexamide (Table V). In the whole series, complex **1** showed the highest percentage inhibition (41–43 %) against both fungal strains but none of the tested complex restricted fungal growth excellently. However, of all the tested complexes, complex **5** showed nearly 30–31 % inhibition of mycelial growth against both fungal strains *i.e.*, *A. flavus* and *A. niger*, whereas complexes **10** and

11 showed nearly 15–24 % inhibition of mycelial growth against *A. flavus* and *A. niger* (Table V).

TABLE V. Antifungal activities of the complexes against the fungal strains for a concentration of 100 μg ml^{-1}

No.	Complex	Inhibition, %	
		Aspergillus flavus	*Aspergillus niger*
1	$[Co(C_5H_6N_4O_2)Cl_2]$	43.29	41.18
2	$[Co((C_5H_6N_4O_2)(NO_3)_2]$	10.69	11.07
3	$[Co(C_5H_6N_4O_2)(OAc)_2]$	11.68	15.31
4	$[Ni(C_5H_6N_4O_2)Cl_2]$	10.52	14.49
5	$[Ni(C_5H_6N_4O_2)(NO_3)_2]$	30.66	31.42
6	$[Ni(C_5H_6N_4O_2)(OAc)_2]$	12.33	10.66
7	$[Cu(C_5H_6N_4O_2)Cl_2]$	19.33	10.33
8	$[Cu(C_5H_6N_4O_2)(NO_3)_2]$	13.81	10.20
9	$[Cu(C_5H_6N_4O_2)(OAc)_2]$	16.77	12.62
10	$[Zn(C_5H_6N_4O_2)(OAc)_2]$	15.33	18.71
11	$[Cd(C_5H_6N_4O_2)(OAc)_2]$	23.77	16.66
	Cyclohexamide[a]	87.34	89.91

[a]Standard drug

CONCLUSIONS

Based on elemental analyses, conductivity and magnetic measurements, and electronic, IR and NMR spectral studies, the structure shown in Fig. 1 may be proposed for all the synthesized complexes.

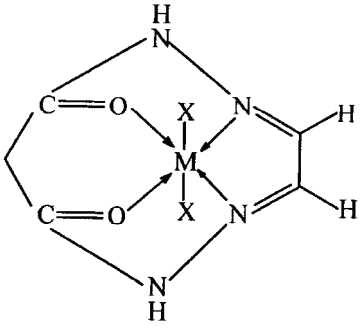

Fig. 1. Structure of the synthesized complexes (M = = Co(II), Ni(II), Cu(II), Zn(II) or Cd(II) and X = Cl^-, NO_3^- or CH_3COO^-).

However, none of the synthesized macrocyclic metal complexes showed good antibacterial and antifungal activities against all the bacterial and fungal strains, but some of the complexes, such as **1** and **5**, were found to be most effective against various bacterial and fungal strains. It is suggested that chelation/coordination reduces the polarity of the metal ion, mainly because of the partial sharing of its positive charge with a donor group within the whole chelate ring system.[39] This process of chelation thus increases the lipophilic nature of the

central metal atom, which in turn, favours its permeation through the lipoid layer of the membrane, thus causing the metal complex to cross the bacterial membrane more effectively, thus increasing the activity of the complexes. In addition to this, many other factors, such as solubility, dipole moment and conductivity, which are influenced by the metal ion may be the possible reasons for the antibacterial activities of these metal complexes.[40] It was also observed that some moieties, such as azomethine linkage or heteroaromatic nucleus introduced into such compounds exhibit extensive biological activities that may be responsible for the increase in hydrophobic character and liposolubility of the molecules in crossing the cell membrane of the microorganism and enhance the biological utilization ratio and activity of the complexes.[41]

Acknowledgements. DPS thanks the University Grants Commission, New Delhi, India, for financial support in the form of Major Research Project (MRP-F. No. 32-196/2006(SR)) and Krishan Kumar for the award of Project Fellowship under the above project. Thanks are also due to the authorities of N.I.T., Kurukshetra, India, for providing the necessary research facilities.

Abbreviations

MIC – Minimum inhibitory concentration; MTCC – microbial type culture collection; CFU – colony forming unit; DMF – *N*,*N*-dimethylformamide; DMSO – dimethyl sulphoxide; PDA – potato dextrose medium.

ИЗВОД

СИНТЕЗА, КАРАКТЕРИСАЊЕ, АНТИБАКТЕРИЈСКА И АНТИФУНГАЛНА ИЗУЧАВАЊА НЕКИХ ТЕТРААЗАМАКРОЦИКЛИЧНИХ КОМПЛЕКСА

DHARAM PAL SINGH[1], VANDNA MALIK[1], RAMESH KUMAR[1], KRISHAN KUMAR[1] и SAURABH SUDHA DHIMAN[2]

[1]*Department of Chemistry, National Institute of Technology, Kurukshetra-136 119 и* [2]*Department of Biotechnology, Kurukshetra University, Kurukshetra-136 119, India*

Применом темплатне кондензационе методе полазећи од малонилдихидразида и глиоксала у метанолу као растварачу у присуству соли Co(II), Ni(II), Cu(II), Zn(II) и Cd(II) јона синтетизовани су нови комплекси $[M(C_5H_6N_4O_2)X_2]$-типа (M = неки од наведених јона метала; X = Cl^-, NO_3^- и OAc^-). За карактеризацију ових комплекса употребљени су елементарна микроанализа, магнетна и кондуктометријска мерења. Поред тога, за карактеризацију комплекса употребљена је електронска, NMR и инфра црвена спектроскопија. На бази ових изучавања за добивене комплексе претпостављена је октаедарска геометрија. Приказани су резултати *in vitro* испитивања антибактеријске и антифунгалне активности изолованих комплекса.

(Примљено 29. јануара, ревидирано 28. априла 2010)

REFERENCES

1. D. P. Singh, R. Kumar, V. Malik, P. Tyagi, *Transition Met. Chem.* **32** (2007) 1051
2. L. F. Lindoy, *The Chemistry of Macrocyclic Ligand Complexes*, Cambridge University Press, Cambridge, 1989

3. W. Ma, Y. Tian, S. Zhang, J. Wu, *Transition Met. Chem.*,**31** (2006) 97
4. *Current Trends and Future Perspectives*, K. Gloe, Ed., Springer, Amsterdam, 2005
5. *Coordination Chemistry of Macrocyclic Compounds*, E. C. Constable, Ed., Oxford University Press, Oxford, 1999
6. D. P. Singh, R. Kumar, V. Malik, P. Tyagi, *J. Enzym. Inhib. Med. Chem.* **22** (2007) 177
7. *Magnetic Resonance Imaging of the Body*, A. D. Watson, S. M. Rockladge, Eds., Raven Press, New York, 1992
8. C. Kosmas, D. Snook, C. S. Gooden, N. S. Courtenay-Luck, M. J. McCall, F. Claude, C. F. Meares, A. A. Epenetos, *Cancer Res.* **52** (1992) 904
9. J. Seto, S. Tamura, N. Asai, N. Kishii, Y. Kijima, N. Matsuzawa,, *Pure Appl. Chem.* **68** (1996) 1429
10. W. Dong, R Yang, L. Yan, *Indian J. Chem.* **40A** (2001) 202
11. D. P. Singh, R. Kumar, P. Tyagi, *Transition Met. Chem.* **31** (2006) 970
12. D. Greenwood, R. Slack, J. Peutherer, *Medical Microbiology: A Guide to Microbial Infections: Pathogenesis, Immunity, in Laboratory Diagnosis and Control*, 15th ed., ELST Publishers, Edinburgh, 1997
13. J. McFarland, *J. Am. Med. Assoc.* **14** (1907) 1176
14. NCCLS, *Method for dilution antimicrobial susceptibility test for bacteria that grow aerobically, in Approved Standards*, 5th ed., M7-A5, National Committee for Clinical Laboratory Standards, Villanova, PA, 2000
15. S. Chandra, S. D. Sharma, *Transition Met. Chem.* **27** (2002) 732
16. R. N. Prasad, M. Mathur, A. Upadhyay, *J. Indian Chem. Soc.* **84** (2007) 1202
17. T. A. Khan, M. A. Rather, N. Jahan, S. P. Varkey, M. Shakir, *Transition Met. Chem.* **23** (1998) 283
18. A. K. Singh, A. Panwar, R. Singh, S. Beniwal, *Transition Met. Chem.* **28** (2003) 160
19. D. L. Pavia, G. M. Lampman, G. S. Kriz, *Introduction to Spectroscopy*, Harcourt College Publishers, New York, 2001
20. N. Nishat, Rahis-ud-din, M. M. Haq, K. S. Siddiqi, *Transition Met. Chem.* **28** (2003) 948
21. R. N. Prasad, M. Mathur, *J. Indian. Chem. Soc.* **83** (2006) 1208
22. Q. Zeng, J. Sun, S. Gou, K. Zhou, J. Fang, H. Chen, *Transition Met. Chem.* **23** (1998) 371
23. A. K. Singh, R. Singh, P. Saxena, *Transition Met. Chem.* **29** (2004) 867
24. L. K. Gupta, S. Chandra, *Transition Met. Chem.* **31** (2006) 368
25. A. K. Mohamed, K. S. Islam, S. S Hasan, M. Shakir, *Transition Met. Chem.* **24** (1999) 198
26. C. Lodeiro, R. Bastida, E. Bertolo, A. Macias, R. Rodriguez, *Transition Met. Chem.* **28** (2003) 388
27. a) S. Chandra, L. K. Gupta, *Spectrochim. Acta A* **60** (2004) 2767; b) M. Shakir, S. P. Varkey, P. S. Hameed, *Polyhedron* **12** (1993) 2775
28. K. Nakamoto, *Infrared & Raman Spectra of Inorganic & Coordination Compounds Part B*, 5th ed., Wiley Interscience, New York, 1997
29. M. Shakir, K. S. Islam, A. K. Mohamed, M. Shagufta, S. S. Hasan, *Transition Met. Chem.* **24** (1999) 577
30. M. Shakir, S. P. Varkey, *Polyhedron* **14** (1995) 1117
31. F. M. A. M. Aqra, *Transition Met. Chem.* **24** (1999) 337
32. S. Chandra, R. Kumar, *Transition Met. Chem.* **29** (2004) 269
33. Z. A. Siddiqi, S. M. Shadab, *Indian J. Chem.* **43A** (2004) 2274

34. D. M. Boghaei, S. Mohebi, *J. Mol. Catal. Chem.* **179** (2002) 41
35. V. B. Rana, D. P. Singh, P. Singh, M. P. Teotia, *Transition Met. Chem.* **6** (1981) 36
36. A. B. P. Lever, *Inorganic Electronic Spectroscopy*, Elsevier, Amsterdam, 1984
37. D. N. Sathyanarayana, *Electronic Absorption Spectroscopy and Related Techniques*, 1st ed., Universities Press, New Delhi, 2001
38. A. B. P. Lever, E. Mantovani, *Inorg. Chem.* **10** (1971) 817
39. J.M. Andrews, *J. Antimicrob. Chemother*. **48** (2001) 5
40. N. Raman, S. R. Johnson, A. Sakthivel, *J. Coord. Chem*. **62** (2009) 691
41. Z. H. Chohan, M. U. Hassan, K. M. Khan, C. T. Supuran, *J. Enzym. Inhib. Med. Chem*. **20** (2005) 183
42. K. Singh, D. P. Singh, M. S. Barwa, P. Tyagi, Y. Mirza, *J. Enzym. Inhib. Med. Chem.* **21** (2006) 749.

Journal of the Serbian Chemical Society
JSCS-info@shd.org.rs • www.shd.org.rs/JSCS
J. Serb. Chem. Soc. *75* (10) 1381–1389 (2010)
JSCS–4060
UDC 546.39+661.8'038+541.124:535–31
Original scientific paper

UV Radiation and the reaction between ammonium and thiocyanate under prebiotic chemistry conditions

HENRIQUE de SANTANA[1], LEIDIMARA PELISSON[1], DIOGO R. JANIASKI[1], CÁSSIA THAÏS B. V. ZAIA[2] and DIMAS A. M. ZAIA[1]*

[1]*Departamento de Química – CCE, Universidade Estadual de Londrina, 86051-990, Londrina-PR and* [2]*Departamento de Ciências Fisiológicas–CCB, Universidade Estadual de Londrina, 86051–990, Londrina–PR, Brazil*

(Received 19 February, revised 26 May 2010)

Abstract: The reaction between ammonium and thiocyanate under prebiotic chemistry conditions was studied using FT-IR spectroscopy. Ammonium thiocyanate (1.0×10^{-3} mol L^{-1}) was dissolved in sodium chloride solution (28.57 g L^{-1}) at two different pH values (5.30 and 7.20). FT-IR results showed that it was possible that some compound that resembles dithiooxamides was synthesized when samples of ammonium thiocyanate were exposed to UV radiation under a regular atmosphere, as UV radiation in the presence of oxygen leads to the formation of perchlorate ions (ClO_4^-) due to the presence of Cl^- as well. After acid hydrolysis of the samples of ammonium thiocyanate irradiated under a nitrogen atmosphere, yellow and white compounds were obtained, which could not be identified. These results were different from those reported in the literature, where other authors found methionine. However, they used higher concentrations of ammonium thiocyanate and a different type of UV lamp. On the other hand, in the present study, a lower concentration of ammonium thiocyanate was used, which probably resembled more the concentration of ammonium thiocyanate of primitive earth.

Keywords: ammonium thiocyanate; prebiotic chemistry; UV radiation; origin of life.

INTRODUCTION

Amino acids play an important role in the biochemistry of present living organisms, such as: inhibitory and excitatory neurotransmitters, glucose, hormone and neurotransmitters precursors and peptides and proteins subunits. It should be emphasized that proteins participate 18 % w/w to the composition of mammalian cells.[1] Thus, the study of their synthesis is relevant to an understanding of the origin of life on Earth. As pointed out by Zaia *et al.*,[2] when planning prebiotic

* Corresponding author. E-mail: damzaia@uel.br
doi: 10.2298/JSC100219112S

chemistry experiments, it is important to know what were the sources for amino acid synthesis on the primitive Earth and which amino acids were synthesized from these sources.

Ammonium and thiocyanate were synthesized in experiments under prebiotic chemistry conditions. They were also found in places that resemble these environments. Dowler and Ingmanson[3] determined the presence of thiocyanate in Atlantis II Deep Brine, located at the bottom of the sea in the Rift Valley. Thiocyanate was synthesized due to the reaction between HCN and H_2S. HCN, H_2S and nitrogen compounds (CNS^-, amines, amino acids – Arg, Ser, Thr, Gly, ABA, Phe) are found in sub-marine volcanoes.[4,5] Comets[6] could be a source of NH_3, HCN and H_2S, as well as of other sulfur and nitrogen compounds (NH_2CHO, HNC, HNCO, CH_3CN, HC_3N, CS_2, CS, SO_2, SO, OCS, H_2CS, NS). Summers[7] showed that nitrite could be reduced to ammonia by iron(II). As reviewed by Raulin and Toupance,[8] ammonium thiocyanate can be synthesized when a mixture of gases (CH_4–NH_3–$H_2O_{(vap)}$–H_2–N_2–CO_2–H_2S), resembling the primitive atmosphere of Earth, is submitted to electric discharges. Thus, ammonium and thiocyanate are substances that probably were easily found on the primitive Earth.

The reaction between ammonium and thiocyanate has been studied under different conditions, some of them resembling the environments of the primitive earth. For example, Holmes[9] irradiated a concentrated aqueous solution of ammonium thiocyanate (4.0 mol L^{-1}) and observed the formation of colloidal sulfur. Talreja *et al.*[10] heated/irradiated with UV radiation ammonium thiocyanate in the solid state and observed the formation of thiourea. Zaia *et al.*[11] also studied the reaction of ammonium thiocyanate in the solid state. They heated samples of ammonium thiocyanate, sand and transition metals and detected the formation of guanidine. Spheres were detected in samples of ammonium thiocyanate and formaldehyde with or without UV irradiation and ammonium thiocyanate with UV irradiation.[12,13] Steinman *et al.*[14] detected the formation of methionine when an aqueous solution of ammonium thiocyanate was exposed to UV radiation.

The climate of the primitive Earth is uncertain, there are models of hot and cold primitive Earth and both are plausible.[15,16] The atmosphere of the primitive Earth was probably neutral-redox (CO, CO_2, N_2, H_2) and the O_2 concentration was very low, it could have been about 0.10 % of the present atmospheric level.[17] The main extraterrestrial source of carbon compounds was interplanetary dust particles, IDPs.[18–20] The main proposed sources of energy on the primitive Earth are: UV radiation, electric discharges, volcanic heating, radioactivity, cosmic rays and meteor impacts. According to Kobayashi *et al.*,[21] UV radiation was the greatest source of energy for the synthesis of biomolecules on the primitive Earth. Thus in the present research, UV radiation was used as the source of energy for the synthesis of biomolecules from the reaction between ammonium and thiocyanate under prebiotic chemistry conditions. To simulate the action of UV

rays, a UV lamp was used. Ammonium thiocyanate (1.0 10^{-3} mol L^{-1}) was dissolved in a sodium chloride solution (28.57 g L^{-1}), which is the same concentration found in seawater, at two different pH values (5.30 and 7.20). It should be emphasized that, to the best of our knowledge, this reaction has not been studied before under conditions plausible to those of the primitive Earth.

EXPERIMENTAL

All employed reagents were of analytical grade. For all the experiments, a wooden box with the following dimensions (40 cm×40 cm×40 cm) was used. The box contained an Hg lamp with a 120 W bulb. The pH of the samples was adjusted to 5.30 and 7.20, because the former is found in hydrothermal environments and the latter is the average pH of seawater.[22]

Experiment 1: UV irradiation of ammonium thiocyanate solution

50 mL of a solution containing ammonium thiocyanate (1.0×10^{-3} mol L^{-1}) and sodium chloride (28.57 g L^{-1}) were added to four beakers. The pH of the samples was adjusted to 5.30 or 7.20 with HCl (0.10 mol L^{-1}) or NaOH (0.10 mol L^{-1}). The samples were irradiated for 0.5, 1.0, 3.0, 4.0, 6.0, 8.0, 10.0, 12.0, 14.0 and 15.0 h. During all the irradiation period (0–15 h), the beakers were kept on an ice bath. After irradiation, aliquots were withdrawn for ammonium and thiocyanate analysis, the samples were lyophilized, and the FT-IR spectra were recorded using the pressed KBr disc technique.

Experiment 2: UV irradiation of ammonium thiocyanate solution under a nitrogen atmosphere

A volume of 50 mL of ammonium thiocyanate (1.0×10^{-3} mol L^{-1}) dissolved in a sodium chloride solution (28.57 g L^{-1}) was added to four beakers. The pH of the samples was adjusted to 5.30 or 7.20 with HCl (0.10 mol L^{-1}) or NaOH (0.10 mol L^{-1}), respectively. The samples were irradiated for 3.0 h. During the irradiation period, the beakers were kept on an ice bath and under a nitrogen atmosphere. After irradiation, the samples were lyophilized and then were submitted to acid hydrolysis with an HCl solution (6.0 mol L^{-1}) at 120 °C for 24 h. The FT-IR spectra were recorded using the pressed KBr disc technique.

Experiment 3: UV irradiation of ammonium thiocyanate solution under a nitrogen atmosphere without sodium chloride[14]

The samples for Experiment 3 were prepared as described by Steinman *et al.*[14] A volume of 50 mL of ammonium thiocyanate (0.10 mol L^{-1}) was added to four beakers. The samples were irradiated for 3.0 h. During irradiation, the beakers were kept on an ice bath and under a nitrogen-saturated atmosphere. After irradiation, the samples were lyophilized and then were submitted to acid hydrolysis in 6.0 mol L^{-1} HCl at 120 °C for 24 h. The FT-IR spectra were recorded using the pressed KBr disc technique.

Acid hydrolysis of the samples from Experiments 2 and 3

An aliquot of 500 μL of each sample and 500 μL of concentrated HCl were added to tubes used for acid digestion of amino acids. The tubes were heated at 110 °C for 24 h. After cooling, the solids (white and yellow) were withdrawn and washed several times with distilled water. The solids, white and yellow aggregates, separated from each other and thus were separated manually.

Infrared spectrophotometric method

The IR spectra were recorded on a Shimadzu FT-IR 8300 instrument, using the pressed KBr disk technique. The spectral resolution was 4 cm^{-1} and each spectrum was determined

after acquiring 120 spectra. About 10 mg of samples plus 200 mg of KBr were weighed and then ground in an agate mortar until a homogeneous mixture was obtained. The disc pellets were prepared and the spectra were recorded from 400 to 4000 cm^{-1}. The FT-IR spectra were analyzed with the program Origin (version 5.0).

RESULTS AND DISCUSSION

Prebiotic chemistry studies require that the experiments must be performed under conditions plausible to those that prevailed on the primitive Earth.[23] The concentration of thiocyanate in present seawater is 1.0×10^{-5} mol L^{-1},[2] and the concentration of total nitrogen compounds around submarine volcanoes is 2.2×10^{-2} mol L^{-1}.[4] Thus, the concentration used in the experiments (1.0×10^{-3} mol L^{-1}) was close enough to real conditions and a reasonable value to perform prebiotic chemistry experiments. Seawater as described by Benetoli *et al.*[24] could not be used because sulfates and carbonates would interfere with the FT-IR experiments. Thus, ammonium thiocyanate was dissolved in distilled water with sodium chloride at the same concentration present in seawater (28.57 g L^{-1}). Experiments 1 and 2 were performed at pH 5.30 and 7.20 because the first is found in hydrothermal environments and the second is the average of seawater today.[22] Thus experiments 1 and 2 were realized under conditions of an ammonium thiocyanate concentration of 1.0×10^{-3} mol L^{-1}, control of pH (5.30 or 7.20) and NaCl (at the same concentration as in seawater), *i.e.*, under conditions more close to those of prebiotic Earth than any of the mentioned studies. It should also be emphasized that Experiment 1 simulated a primitive atmosphere with oxygen and Experiment 2 without it.

Experiments 1 and 2 showed a change in the solution and slight white suspension appeared in the solution after 2 h of irradiation. Smith *et al.*[12] irradiated aqueous solutions of ammonium thiocyanate (0.01–2.0 mol L^{-1}) and perceived the formation of an intense white suspension. After 10 min, the irradiation was stopped and formation of microspheres that aggregated to form large spheres and chains was observed. According to them, the formation of spheres depended on the time of irradiation and the concentration of ammonium thiocyanate (NH_4SCN). In the present experiments a white suspension appeared but the formation of microspheres was not observed. On the other hand, Holmes[9] studied the irradiation of a concentrated solution of NH_4SCN (4.0 mol L^{-1}) and observed the formation of solids believed to be colloidal sulfur. Experiments 1 and 2 did not show the formation of microspheres or colloidal sulfur and after a few hours, the irradiation was stopped and the white suspension disappeared. These results could be explained by the fact that a low concentration of ammonium thiocyanate (1.0×10^{-3} mol L^{-1}) compared to those employed in the experiments of Holmes[9] (4.0 mol L^{-1}) and Smith *et al.*[12] (0.01–2.0 mol L^{-1}) was used. In addition, it should be mentioned that the experimental conditions used by Holmes[9] and Smith *et al.*[12] were unrealistic from a prebiotic chemistry view point,

since they used a high concentration of ammonium thiocyanate that could never have existed on the primitive Earth.[3,4,25]

The FT-IR spectra of solid ammonium thiocyanate (lyophilized samples of ammonium thiocyanate dissolved in sodium chloride solution after ultraviolet irradiation for 2, 7 and 15 h at pH 7.20) are shown in Fig. 1. The experiment (Experiment 1) was performed under a regular atmosphere. The intensity of the bands was determined using the internal standard KIO_3 (784 cm^{-1}). The bands at 1400 and 3125 cm^{-1} are characteristic of the ammonium ion, attributed to NH_4 deformation and stretch, respectively, and the feature at 2065 cm^{-1} is due to the SCN^- group, assigned to the CN bond stretching. After ultraviolet irradiation, the bands at 2065 and 3125 cm^{-1} vanished and two new bands (at 1152 and 1633 cm^{-1}) were observed (Fig. 1). The intensity of the bands at 1152 and 1633 cm^{-1} increased with irradiation time. The same results were observed for the samples irradiated at pH 5.30. Besides the decomposition of SCN^- and NH_4^+, only the vanishing of the band at 2065 cm^{-1} occurred. The band at 1400 cm^{-1} did not disappear, thus suggesting a coupling between thiocyanates $[S=C=N]^-$. This coupling could explain the retention of the band at 1400 cm^{-1} and the new band at 1633 cm^{-1}. The product of the coupling of thiocyanates $[S=C=N]^-$ resembles dithiooxamides $[NH_2C(=S)C(=S)NH_2]$ which have characteristic bands at 1592 and 1434 cm^{-1} due to the groups NH_2 and H_2NCS.[26] The band at 1152 cm^{-1} could not be explained by the synthesis of compounds that resemble dithioox-

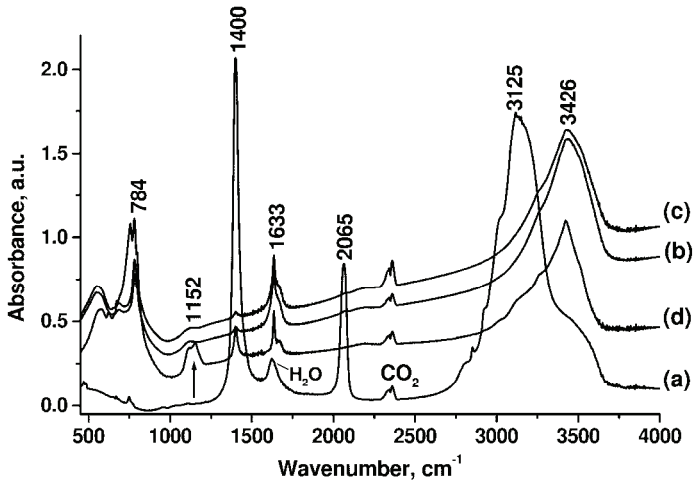

Fig. 1 FT-IR spectra: solid ammonium thiocyanate (a); lyophilized samples of ammonium thiocyanate (1.0×10^{-3} mol L^{-1}) dissolved in sodium chloride solution (28.57 g L^{-1}) after irradiation for 2 (b), 7 (c) and 15 h (d) at pH 7.20. The FT-IR spectra of the samples (b), (c) and (d) were recorded with an internal standard of KIO_3 (784 cm^{-1}). The FT-IR spectra of the samples were recorded in pressed KBr discs. The experiments were performed under a regular atmosphere, as described in the experimental section (Experiment 1).

amides. An explanation for this band is the synthesis of perchlorate (ClO_4^-); in fact, it is known to occur naturally through the formation of ozone (O_3) by UV radiation of oxygen and, subsequently, perchlorate is formed by the oxidation of chloride by ozone.[27] The FT-IR spectrum of sodium perchlorate showed a band at 1152 cm^{-1} due to Cl–O stretch (data not shown). However, it should be emphasized that this reaction probably did not play an important role in prebiotic chemistry, since the amount of oxygen was too low on the primitive Earth.[15]

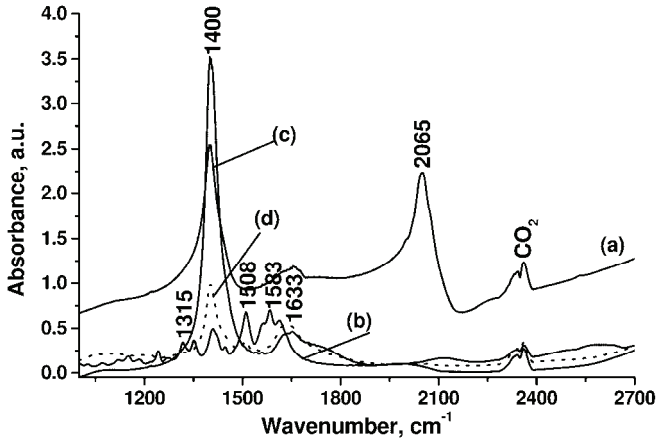

Fig. 2. FT-IR spectra of: solid ammonium thiocyanate (a); solid methionine (b); white solid (c) and yellow solid (d). The white and yellow solids were obtained in Experiment 3. The samples in Experiment 3 (50 mL of 0.10 mol L^{-1} ammonium thiocyanate) were irradiated for 3.0 h. During irradiation, the samples were kept on an ice bath and under a nitrogen saturated atmosphere. After irradiation, the samples were lyophilized, and then submitted to acid hydrolysis in 6.0 mol L^{-1} HCl at 120 °C for 24 h. The FT-IR spectra of the samples were recorded in pressed KBr discs.

Samples prepared as described in experiment 2 and 3 were irradiated for just 3 h under a nitrogen atmosphere. Experiment 3 was performed under the same conditions as described by Steinman *et al.*[14] In both experiments, two solids (white and yellow) were obtained after acid hydrolysis. The acid hydrolysis was performed to verify if the precursors of amino acids were synthesized.[28] The FT-IR spectra of solid ammonium thiocyanate, solid methionine and the observed white solid (Experiment 3) and yellow solid (Experiment 3) are shown in Fig. 2. The band at 2065^{-1} was absent in spectrum d (yellow solid) and bands at 1400 and 1633 cm^{-1} were again observed. However, these bands are not characteristic of methionine, which shows bands at 1315, 1508 and 1583 cm^{-1} (Fig. 2). The solids (white and yellow) obtained in experiment 2 showed the same FT-IR spectra as in Experiment 3. As shown by Lapinski *et. al.*,[29] the synthesis of the solids (white and yellow) could be attributed to phototautomeric compounds of dithiooxamides. However, this could be true only for the yellow solid because the S–H

stretch was observed in the FT-IR spectrum of this sample. As expected, the products in Experiments 2 and 3 did not show a band at 1152 cm^{-1}, because both experiments were carried out under a nitrogen atmosphere and in Experiment 3 there was also no sodium chloride present.

The experiments described in this paper (Experiments 1–3) did not show the presence of methionine, even when the experiment (Experiment 3) described by Steinman *et al.*[14] was reproduced. This failure to synthesize methionine could be due to the difference in UV lamps used here and by Steinman *et al.*[14] The radiation emitted by the UV lamp used in the present experiments has emission lines from 185 to 580 nm,[30] while the UV lamp used by Steinman *et al.*[11] had 90 % of intensity emission at 254 nm.[31] It should also emphasized that the only method used by Steinman *et al.*[14] to identify methionine was paper chromatography, which could not have been conclusive. However, this experiment was realized in 1969 and that time paper chromatography was best analytical tool available.

CONCLUSIONS

In conclusion, this paper showed the following results: a) UV radiation is an important source for the synthesis of biomolecules; b) a compound that resembled dithiooxamides was probably synthesized; c) perchlorate (ClO_4^-) was synthesized when the samples were irradiated with UV radiation in the presence of oxygen and Cl^-; d) two non-identified solids (white and yellow) were obtained after acid hydrolysis of the samples of ammonium thiocyanate irradiated under a nitrogen atmosphere; e) methionine was not obtained as reported other authors. However, they used higher concentrations of ammonium thiocyanate and a different type of UV lamp; f) the formation of microspheres was not observed, probably because of the low concentration of ammonium thiocyanate employed in the experiments; g) no biomolecules were found in this work.

Acknowledgments. LP and DRJ acknowledge the fellowships from PIBIC/CNPq/UEL. This research was supported by grants from CNPq (473076/2004) and Fundação Araucária (2421). Dr. A. Leyva helped with the English editing of the manuscript.

ИЗВОД

UV РАДИЈАЦИЈА И РЕАКЦИЈА ИЗМЕЂУ АМОНИЈАКА И ТИОЦИЈАНАТА ПРИ ПРЕБИОТИЧКИМ ХЕМИЈСКИМ УСЛОВИМА

HENRIQUE DE SANTANA[1], LEIDIMARA PELISSON[1], DIOGO R. JANIASKI[1], CÁSSIA THAÏS B. V. ZAIA[2] и DIMAS A. M. ZAIA[1]

[1]*Departamento de Química – CCE, Universidade Estadual de Londrina, 86051–990, Londrina–PR и* [2]*Departamento de Ciências Fisiológicas – CCB, Universidade Estadual de Londrina, 86051–990, Londrina–PR, Brazil*

Применом FT-IR спектроскопије изучавана је реакција између амонијака и тиоцијаната при пребиотичким хемијским условима. Амонијум-тиоцијанат ($1{,}0\times10^{-3}$ mol/dm^3) је растворен у раствору натријум-хлорида (28,57 g/dm^3) при две различите pH вредности (5,30 и 7,20).

На основу FT-IR спектроскопских резултата нађено је да у току UV радијације амонијум--тиоцијаната долази до грађења дитиооксимида, док у присуству Cl^- и киселоника настаје перхлорат (ClO_4^-). При радијацији у инертним условима (струја азота) и киселој хидролизи узорка амонијум-тиоцијаната долази до грађења производа жуте боје, чија структура није одређена. Приказани резултати се разликују од одговарајућих литературних података, где су аутори претпоставили да при наведеним условима долази до грађења метионина. Међутим, ови аутори су користили веће концентрације амонијум-тиоцијаната и различите UV лампе. Насупрот овоме, у овом раду коришћене су ниже концентрације амонијум-тиоцијаната, што више одговара његовом садржају у земљи.

(Примљено 19. фебруара, ревидирано 26. маја 2010)

REFERENCES

1. B. Alberts, D. Bray, J. Lewis, M. Raff, K. Roberts, J. D. Watson, *Molecular Biology of the Cell*, 3rd ed., Garland Publishing Inc., New York, 1994
2. D. A. M. Zaia, C. T. B. V. Zaia, H. de Santana, *Origins Life Evol. Biosph*ere **38** (2008) 469
3. M. J. Dowler, D. E. Ingmanson, *Nature* **279** (1979) 51
4. G. Aloisi, M. Drews, K. Wallmann, G. Bohrmann, *Earth Planet. Sci. Lett.* **225** (2004) 347
5. L. M. Mukhin, *Origins Life* **7** (1976) 355
6. J. Lhorca, *Int. Microbiol.* **8** (2005) 5
7. D. P. Summers, *Origins Life Evol. Biosphere* **29** (1999) 33
8. F. Raulin, G. Toupance, *J. Mol. Evol.* **9** (1977) 329
9. M. Holmes, *J. Chem. Soc.* (1926) 1690
10. S. T. Talreja, P. M. Oza, P. S. Rao, *Bull. Chem. Soc. Jpn.* **40** (1967) 2427
11. D. A. M. Zaia, H. de Santana, R. Toppan, C. T. B. V. Zaia, *J. Braz. Chem. Soc.* **15** (2004) 190
12. A. E. Smith, G. Steinman, C. Galand, *Experientia* **25** (1969) 255
13. A. E. Smith, J. J. Silver, G. Steinman, *Experientia* **24** (1968) 36
14. G. Steinman, A. E. Smith, J. J. Silver, *Science* **159** (1968) 1108
15. J. F. Kasting, M. T. Howard, *Philos. Trans. R. Soc. B* **361** (2006) 1733
16. J. F. Kasting, S. Ono, *Philos. Trans. R. Soc. B* **361** (2006) 917
17. I. H. Campbell, C. M. Allen, *Nat. Geosci.* **1** (2008) 554
18. C. Chyba, C. Sagan, *Nature* **355** (1992) 125
19. M. Bernstein, *Philos. Trans. R. Soc. B* **361** (2006) 1689
20. A. Brack, *Chem. Biodiversity* **4** (2007) 665
21. K. Kobayashi, H. Masuda, K. I. Ushio, A. Ohashi, H. Yamanashi, T. Kaneko, J. I. Takahashi, T. Hosokawa, H. Hashimoto, T. Saito, *Adv. Space Res.* **27** (2001) 207
22. N. G. Holm, E. Andersson, *Astrobiology* **5** (2005) 444
23. D. A. M. Zaia, *Quim. Nova* **26** (2003) 260
24. L. O. B. Benetoli, C. M. D. de Souza, K. L. da Silva, I. G. de Souza Jr, H. de Santana, A. Paesano Jr., A. C. S. da Costa, C. T. B. V. Zaia, D. A. M. Zaia, *Origins Life Evol. Biosphere* **37** (2007) 479
25. M. Pasek, D. Lauretta, *Origins Life Evol. Biosphere* **38** (2008) 5
26. N. B. Colthup, L. H. Daly, S. E. Wierly, *Introduction to Infrared and Raman Spectroscopy*, Academic Press, New York, 1964
27. P. K. Dasgupta, P. K. Martinelango, W. A. Jackson, T. A. Anderson, K. Tian, R. W. Tock, S. Rajagopalan, *Environ. Sci. Technol.* **39** (2005) 1569

28. K. Kobayashi, T. Kaneko, A. Kouchi, H. Hashimoto, T. Saito, *Adv. Space Res.* **23** (1999) 401
29. L. Lapinski, H. Rostkowska, A. Khvorostov, M. Yaman, R. Fausto, M. J. Novak, *J. Phys. Chem. A* **108** (2004) 5551
30. A. Cavicchioli, G. R. Gutz, *Quim. Nova* **26** (2003) 913
31. Pen-Ray UV lamps (2008), http://ridl.cis.rit.edu/products/manuals/Acton/old/MANUAL/ /MS-416.pdf (accessed on December 8, 2008).

Journal of the Serbian Chemical Society
JSCS-info@shd.org.rs • www.shd.org.rs/JSCS
J. Serb. Chem. Soc. 75 (10) 1391–1404 (2010)
JSCS–4061
UDC 547.538:532.14:532.74:541.4:615.214
Original scientific paper

Artificial neural network prediction of the psychometric activities of phenylalkylamines using DFT-calculated molecular descriptors

MINA HAGHDADI[1]* and MOHAMMAD H. FATEMI[2]

[1]*Department of Chemistry, Islamic Azad University, Babol Branch and*
[2]*Department of Chemistry, Mazandaran University, Babolsar, Iran*

(Received 8 April, revised 11 May 2010)

Abstract: In the present work, a quantitative structure–activity relationship (QSAR) method was used to predict the psychometric activity values (as mescaline unit, log *MU*) of 48 phenylalkylamine derivatives from their density functional theory (DFT) calculated molecular descriptors and an artificial neural network (ANN). In the first step, the molecular descriptors were obtained by DFT calculation at the 6-311G* level of theory. Then the stepwise multiple linear regression method was employed to screen the descriptor spaces. In the next step, an artificial neural network and multiple linear regressions (MLR) models were developed to construct nonlinear and linear QSAR models, respectively. The standard errors in the prediction of log *MU* by the MLR model were 0.398, 0.443 and 0.427 for training, internal and external test sets, respectively, while these values for the ANN model were 0.132, 0.197 and 0.202, respectively. The obtained results show the applicability of QSAR approaches by using ANN techniques in prediction of log *MU* of phenylalkylamine derivatives from their DFT-calculated molecular descriptors.

Keywords: density functional theory; artificial neural network; multiple linear regression; quantitative structure–property relationship; phenylalkylamines.

INTRODUCTION

Phenylalkyamines form a class of hallucinogenic agents which are pharmacologically diverse and a heterogeneous group of agents.[1] Different properties of phenylalkylamine derivatives, (which were known to display hallucinogenic, central stimulant, empathogenic activity, or a combination of activities) have been studied for a long time using different approaches.[1,2] Phenylalkylamines are one of the few types of psychotomimetic compounds whose structure–activity relationships (SAR) have been investigated.[3] Snyder and Merril first reported a cor-

* Corresponding author. E-mail: mhaghdadi2@yahoo.co.uk
doi: 10.2298/JSC100408116H

relation of hallucinogenic activity with a quantum index that was calculated using the Hückel molecular orbital theory.[4] They found that high activity is associated with the highest occupied molecular orbital (HOMO) energy in a small number of phenylalkylamines. Moreover, some quantitative structure–activity relationship (QSAR) studies were reported recently on this class of compounds.[5–7] Thakur and coworkers reported QSAR studies on a series of psychotomimetric phenylalkylamines by combining the minimum topological difference method and topological descriptors.[6] They developed a penta-parametric linear model, which had the statistics: correlation coefficient R = 0.932, standard error SE = 0.272 and Fisher value F = 56.77. They evaluated the predictive power of their model by a cross-validation test, which provided the statistics: R^2_{CV} = 0.864 and SPRESS = = 0.262. They used two experimentally determined parameters in their model, which were the octanol–water partition coefficient and the molar refraction. In another work, the structure-hallucinogenic activity relationships for a series of phenylethylamine and phenylisopropylamine derivatives was investigated by Altum *et al*. within the framework of electron-conformational methods.[7] In addition, B. W. Clare developed a QSAR model of a series of psychotomimetric phenylalkylamines by using CNDO/2 calculation to derive molecular the volume and electronic structure of the compounds of interest.[8] These QSAR studies were limited to the use of physicochemical descriptors and electronic structure or quantum chemical descriptors, which were obtained based on semi-empirical molecular orbital (MO) calculations. The latest development in computer technology and software for electronic structure theory allows the calculation of quantum chemical descriptors at first principal levels, such as the density functional theory (DFT), with a higher accuracy including some effective consideration of electron correlation effects.[9] DFT Methods are, in general, capable of calculating a variety of isolated molecular properties, such as ionization energies, dipole moment, electron affinities, electronegativities, hardness and softness, electrostatic potential *etc*., quite accurately.[10–17] In the present work, a quantitative structure–activity relationship method was used to predict the psychometric activities value of some phenylalkylamine derivatives from their DFT-calculated molecular descriptors and an artificial neural network.

METHODOLOGY

Data set

The psychometric activity of drugs are generally expressed in mescaline units (*MU*), defined as the ratio of the effective dose of mescaline to the effective dose of the tested compound. The potency is usually expressed as log *MU*, where *MU* is taken as mole of mescaline/mole of the tested phenylalkylamine. The data set in this work consisted of the log *MU* values of 48 phenylalkylamine derivatives, which were taken from the literature.[6] The structural features of these compounds and their experimental log *MU* values are presented in Table I. The values of log *MU* ranged from –0.67 to 2.72 for compounds 1 and 38, res-

pectively. The data set was split by y-ranking methods into training; internal and external test sets, which consisted of 38, 5 and 5 members, respectively. In this method, the data were sorted according to their log *MU* values and the training, internal and external test sets were chosen from these lists with desired distances from each other.[18] The training set was used to adjust the ANN parameters, the internal test set was used to prevent overtraining during ANN development and the external test set was used to evaluate the obtained models.

TABLE I. Data set and corresponding observed and calculated values of log *MU* (*MU* is taken as the moles of mescaline/moles of the tested phenylalkylamine)

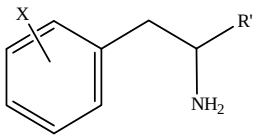

No.	X	R'	log *MU* Exp	log *MU* ANN	Residual	log *MU* MLR	Residual
1	3,5-OMe	H	–0.67	–0.52	0.15	–0.014	0.655
2	3,4-OMe	Me	–0.06	–0.13	–0.07	0.001	0.061
3	3,4,5-OMe	H	0.00	0.09	0.09	0.349	0.349
4	3-OEt,4,5-OMe	H	0.03	–0.15	–0.18	0.303	0.273
5	3,4-OEt,5-OMe	H	0.23	0.32	0.09	0.440	0.210
6	3,4,5-OMe	Me	0.33	0.43	0.10	0.525	0.195
7	3-Set,4-OEt,5-OMe	H	0.38	0.31	–0.07	0.697	0.317
8	3,4-OEt,5-OMe	H	0.38	0.34	–0.04	1.025	0.645
9	3-OCH_2O-4	Me	0.41	0.47	0.06	0.734	0.323
10	3-OMe,4-OCH_2O-5	Me	0.43	0.51	0.08	0.757	0.327
11	3,5-OMe,4-SBut	H	0.58	0.45	–0.13	1.482	0.901
12	4-Me	Me	0.59	0.67	0.08	–0.146	–0.736
13	3-OEt,4-SMe,5-OMe	H	0.66	0.57	–0.09	0.991	0.331
14	2,4-OMe	Me	0.67	0.61	–0.06	0.843	0.173
15	2.3-OMe,4-OCH_2O-5	Me	0.76	0.67	–0.09	0.829	0.069
16	3,4-OMe,5-SMe	H	0.81	0.85	0.04	1.072	0.262
17	3,5-OMe,4-OPr	H	0.83	0.93	0.10	1.073	0.243
18	3,5-OMe,5-SEt	H	0.84	0.89	0.05	0.457	–0.382
19	2,3,4,5-OMe	Me	0.86	0.94	0.08	1.216	0.356
20	3,5-OMe,4-OEt	H	0.87	0.75	–0.12	0.972	0.102
21	2-OMe,3-OCH_2O-4	Me	1.00	0.95	–0.05	0.575	–0.425
22	2-OMe,4-OCH_2O-5	Me	1.00	1.05	0.05	1.377	0.377
23	3,5-OMe,4-Phenyl	Me	1.10	1.24	0.14	1.261	0.161
24	3,5-OMe,4-SMe	H	1.11	1.21	0.10	1.311	0.201
25	2,5-OMe,3-CH_2O-4	Me	1.14	0.95	–0.19	0.631	–0.508
26	2,5-OMe,4-Et	H	1.25	1.35	0.10	1.354	0.104
27	3,5-OMe,4-SPr	H	1.29	1.12	–0.17	0.896	–0.394
28	2,4,5-OMe	Me	1.33	1.21	–0.12	1.188	–0.141
29	2,5-OMe,4-OEt	Me	1.36	1.25	–0.11	1.236	–0.123
30	3,5-OMe,4-SEt	H	1.36	1.44	0.08	1.368	0.008
31	2,5-OMe,4-SMe	Me	1.66	1.54	–0.12	1.317	–0.342
32	2,5-OMe,4-Bu	Me	1.68	1.76	0.08	1.391	–0.289

TABLE I. Continued

No.	X	R'	log *MU* Exp	log *MU* ANN	Residual		log *MU* MLR	Residual
33	2,5-OMe,4-Br	H	1.69	1.56	–0.13		2.275	0.585
34	2,5-OMe,4-Me	Me	1.90	1.81	–0.09		1.319	–0.581
35	3,5-OMe,4-Br	Me	1.91	2.24	0.33		1.484	–0.426
36	2,5-OMe,4-Pr	Me	1.95	1.67	–0.28		1.363	–0.586
37	2,5-OMe,4-Et	Me	2.02	2.24	0.22		2.078	0.058
38	2,5-OMe,4-Br	Me	2.72	2.56	–0.16		2.275	–0.444
			Internal test set					
39	2,3,5-OMe	H	–0.03	–0.12	–0.09		0.568	0.597
40	3,5-OMe,4-$CH_2C_6H_5$	Me	0.46	0.64	0.18		0.662	0.201
41	3-OMe,4-OEt,5-SMe	H	0.84	0.68	–0.16		1.176	0.336
42	2,5-OMe,4-Me	H	1.27	1.14	–0.13		0.920	–0.349
43	2,5-OMe,4-S-iPr	Me	1.71	1.92	0.21		1.191	–0.518
			External test set					
44	3,5-OMe,4-OBu	H	0.38	0.45	0.07		0.029	–0.350
45	3-OEt,4-SEt,5-OMe	H	0.68	0.88	0.20		1.040	0.360
46	3,5-OMe,4-OEt	Me	1.05	0.78	–0.27		0.409	–0.640
47	2,5-OMe,4-OPr	Me	1.38	1.22	–0.16		0.929	–0.450
48	2,5-OMe,4-SEt	Me	1.96	2.16	0.20		1.560	–0.399

Quantum chemical descriptors

The structures of the 48 substituted phenyalkylamine compounds were optimized using the Gaussian 2003W computational package.[19] The Becke three parameter exact exchange functional (B3)[20] combined with the gradient corrected correlation functional of Lee–Yang–Parr (LYP)[21] of the DFT methods implementing the 6-311G* basis sets were employed. The nature of optimized geometries at the B3LYP levels was checked with frequency calculations. The total energy and corrected zero point (*ZPE*) were calculated for all optimized structures. Then, the quantum chemical descriptors that were taken from the DFT calculations were used to analyze the variations in the biological activities of the studied compounds. The minimum energy conformations were used to calculate the electronic descriptors, such as the energy of the highest occupied molecular orbital, the lowest unoccupied molecular orbital (LUMO), hardness (η), softness (S), electronegativity (χ), electrophilicity (ω) and the dipole moment (*DP*). It was found that the stability of the molecules is related to their hardness and electronegativity, defined as the power of an atom in a molecule to attract electrons to it. The hardness and electronegativity are given as follow:

$$\eta = 1/2(\partial^2 E/\partial N^2)v(r) \quad (1)$$

$$\chi = -\mu = -(\partial E/\partial N)v(r) \quad (2)$$

where E and $v(r)$ are the electronic energy and the external potential of an N-electron system, respectively, and μ is the chemical potential. In addition, the operational definition of absolute hardness and electronegativity is given as:

$$\eta = 1/2(IP - EA) \quad (3)$$

$$\chi = -\mu = -1/2(IP + EA) \quad (4)$$

where *IP* and *EA* are the ionization potential and electron affinity, respectively. According to the DFT counterpart of the Koopman theorem, the *IP* is simply the eigenvalue of the HOMO

with a change of sign and *EA* is the eigenvalue of the LUMO with a change of sign;[22,23] hence Eqs. (3) and (4) may be written as:

$$\eta = \frac{1}{2}\left(\varepsilon\mathrm{LUMO} - \varepsilon\mathrm{HOMO}\right) \tag{5}$$

$$\chi = -\mu = \frac{1}{2}\left(\varepsilon\mathrm{LUMO} + \varepsilon\mathrm{HOMO}\right) \tag{6}$$

The other calculated molecular parameter is softness, which measures the extent of chemical reactivity and it is the reciprocal of hardness:

$$S = \frac{1}{\eta} \tag{7}$$

Parr *et al*. proposed an electrophilicity index (ω) as a measure of energy lowering due to maximal electron flow among donor and acceptor.[24] They defined the electrophilicity index as follow:

$$\omega = \frac{\mu^2}{2\eta} \tag{8}$$

These DFT calculated parameters can encode features of phenylalkylamines which could affect their psychometric activities.

Modeling

In the first step of feature screening, constant and near-constant variables were excluded from the pool of descriptors and the pair wise correlation cut off selection procedure was employed to exclude the correlated descriptors.[18] In the development of QSPRs, a major decision is when to stop adding descriptors to the model during the stepwise regression procedure. An excessive number of descriptors lead to overcorrelated equations that are difficult to interpret in terms of interaction mechanisms. A simple procedure used to control the model expansion is the so-called "break point procedure" in the improvement of the statistical quality of the model.[25] From analyses of the plot of the number of descriptors involved *vs*. the correlation coefficient (*R*), and also the standard error (*SE*) of model, it appears that the statistical improvement of the model is high until a point (the "break point") is reached after which the improvement is negligible. Consequently, the model corresponding to the break point is considered to be the best/optimum model (Fig. 1). This figure shows that no significant improvements in the *R* and *SE* values of the model appear after the addition of more than 5 parameters to the MLR model. Therefore, these five descriptors were considered as independent variable in the development of MLR and ANN models. These parameters are: hardness, chemical potential, lowest unoccupied molecular orbital energy, dipole moment and vibrational energy, the numerical values of which are given in Table II. The specifications of the obtained 5-parameter MLR model are presented in Table III.

TABLE II. The DFT- calculated values of the molecular descriptors

No.	LUMO eV	Hardness eV	Chemical potential eV	Vibrational energy Hartree	Dipole moment D
1	–0.346	2.953	–3.299	–595.42	1.252
2	–0.352	2.955	–3.307	–634.475	1.186
3	–0.198	2.875	–3.073	–709.969	2.366

TABLE II. Continued

No.	LUMO eV	Hardness eV	Chemical potential eV	Vibrational energy Hartree	Dipole moment D
4	–0.059	2.898	–2.957	–749.297	3.488
5	–0.165	2.879	–3.044	–788.63	2.282
6	–0.117	2.857	–2.974	–749.297	2.524
7	–0.606	2.653	–3.259	–1111.61	2.579
8	–0.239	2.703	–2.942	–1111.62	2.817
9	–0.353	2.723	–3.077	–594.224	1.526
10	–0.038	2.849	–2.887	–708.772	1.886
11	–0.487	2.512	–2.999	–1150.93	2.032
12	–0.324	2.977	–3.301	–444.976	1.258
13	–0.604	2.579	–3.184	–1072.29	2.273
14	–0.226	2.669	–2.896	–749.309	3.562
15	–0.214	2.724	–2.957	–823.316	2.869
16	–0.332	2.729	–3.062	–1032.96	0.965
17	–0.575	2.567	–3.142	–1111.6	2.411
18	–0.679	2.675	–3.354	–1072.28	2.768
19	–0.239	2.674	–2.913	–863.838	1.524
20	–0.606	2.574	–3.179	–1072.28	2.465
21	–0.019	2.902	–2.921	–708.772	2.036
22	–0.188	2.571	–2.579	–708.775	2.48
23	–0.231	2.612	–2.843	–788.627	2.359
24	–0.518	2.523	–3.041	–1032.96	2.172
25	–0.051	2.82	–2.872	–823.318	3.458
26	–0.201	2.609	–2.811	–674.076	1.774
27	–0.498	2.519	–3.016	–111.609	1.998
28	–0.26	2.61	–2.87	–749.298	2.455
29	–0.247	2.609	–2.856	–788.629	2.428
30	–0.511	2.52	–3.031	–1072.29	2.08
31	–0.686	2.447	–3.133	–1072.29	2.357
32	–0.294	2.585	–2.879	–792.052	1.623
33	–0.682	2.536	–3.218	–3208.29	1.586
34	–0.248	2.601	–2.849	–674.08	1.746
35	–0.444	2.789	–3.233	–3168.96	2.978
36	–0.296	2.586	–2.882	–752.728	1.624
37	–0.216	2.606	2.822	–713.402	1.821
38	–0.682	2.536	–3.218	–3208.29	1.585
39	–0.089	2.847	–2.936	–709.966	2.6
40	–0.204	2.848	–3.051	–980.405	1.876
41	–0.219	2.741	–3.046	–1072.29	1.266
42	–0.486	2.604	–2.838	–634.754	1.672
43	–0.783	2.445	–3.228	–1150.94	2.533
44	–0.437	2.901	–3.107	–827.947	1.856
45	–0.586	2.576	–3.161	–1111.61	2.322
46	–0.093	2.861	–2.954	–788.627	3.451
47	–0.435	2.614	–2.842	–788.627	2.359
48	–0.45	2.454	–2.803	–1111.61	2.876

TABLE III. Specification of the multiple linear regression model

Descriptor	Notation	Coefficient	S. E.
Lowest unoccupied molecular orbital	LUMO	1.588	0.530
Hardness	η	–3.605	0.619
Chemical potential	μ	1.019	0.079
Vibrational energy	*Ev*	–0.00053	0.000
Dipole moment	*DP*	–0.171	0.114
Constant		11.388	1.720

To examine the existence of any nonlinear relations among the selected molecular descriptors and the log *MU* values, an artificial neural network was used. Artificial neural networks are mathematical systems that simulate biological neural networks. Detail descriptions of the theory of ANNs are presented in the literature.[26–28] In the first step in the development of an ANN, a model of a three-layer network with a sigmoid transfer function was designed both for the hidden and output nodes. This ANN program was coded in MATLAB 7 for windows.[29] In this network, the number of nodes in the input layer was the number of descriptors that were selected by the stepwise multiple linear variable selection method. The adjustable weights among neurons have a random distribution between –0.3 and 0.3. The ANN parameters, including the number of nodes in the hidden layer, the weights of the learning rate, the biases of the learning rate and the momentum should be optimized to find the most accurate results. The procedure of optimizing these parameters is given in previous papers.[30,31] The optimized values of these terms and the ANN topology are given in Table IV. The network was then trained using the training set by the back propagation strategy for optimization of the weights and bias values. The goal in the training of the network is to change the weights between the layers to minimize output errors. The root-mean-square error (*RMSE*) value was calculated to measure how good the outputs were in comparison with the target values. To prevent over fitting, the training of the network had to be stopped when the *RMSE* in the prediction of log *MU* of the internal test set commenced to increase. Then the trained network was used to predict the log *MU* values of the external test set.

TABLE IV. Architecture and specifications of optimized ANN model

Parameter	Value
Number of nodes in the input layer	5
Number of nodes in the hidden layer	4
Number of nodes in output layer	1
Weights learning rate	0.6
Biases learning rate	0.8
Momentum	0.4

RESULTS AND DISCUSSION

Molecular diversity analysis

In this study, diversity analysis was performed on the data set to ensure that the structures of the training or test sets can represent those of the whole ones.[32] A data base of n compounds generated from m highly correlated chemical descriptors $\{x_j\}_{j=1}^{m}$. Each compound X_i is represented as a vector of:

$$X_i = (x_{i1}, x_{i2}, x_{i3},..., x_{im}) \text{ for } i = 1, 2,..., n \quad (9)$$

where x_{ij} denotes the value of descriptor j of compound X_i. The collective database, $X = \{X_i\}_{i=1}^{N}$ is represented by the $n \times m$ matrix **X** as follow:

$$\mathbf{X} = \begin{bmatrix} x_{11} & x_{12} & \cdots & x_{1m} \\ x_{21} & x_{22} & \cdots & x_{2m} \\ \vdots & \vdots & \ddots & \vdots \\ x_{m1} & x_{m2} & \cdots & x_{nm} \end{bmatrix} \quad (10)$$

A distance score for two different compounds X_i and X_j can be measured from their Euclidean distance norm, d_{ij}, based on the compound descriptors:

$$d_{ij} = \left\| X_I - X_J \right\| = \sqrt{\sum_{k=1}^{m} \left(x_{ik} - x_{jk} \right)^2} \quad (11)$$

The mean distances $\overline{d_i}$ of one sample to the remaining ones were computed as follows:

$$\overline{d_i} = \frac{\sum_{j=1}^{n} d_{ij}}{n-1}, \; i = 1, 2,....., n \quad (12)$$

Then the mean distances were normalized within the interval (0,1). The closer to one the distance is, the more diverse from each other the compounds are. The mean distances of samples *vs*. experimental log *MU* of data set are plotted in Fig. 2. Inspection to this figure illustrates the good distribution of test set throughout the whole of data set. The training set with a broad representation of the chemistry space was adequate to ensure the stability of the models and the diversity of test set can prove the predictive capability of the model.

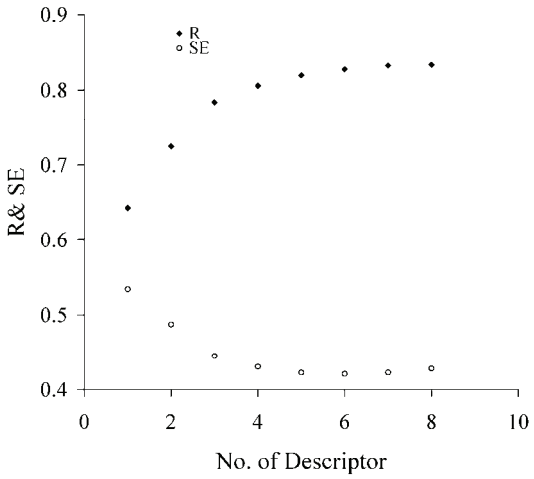

Fig. 1. The results of the break point procedure.

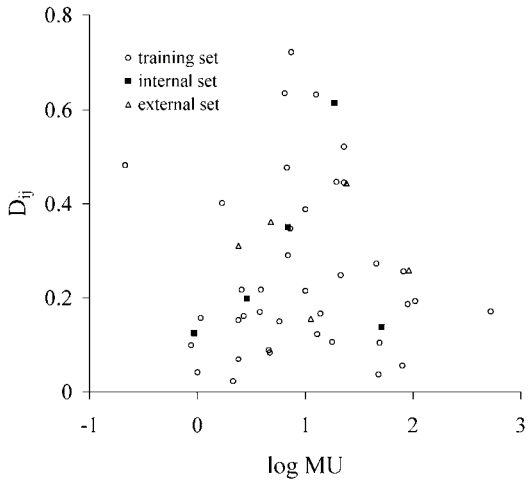

Fig. 2. The results of diversity analysis (the unit of *MU* is mmol of mescaline/mmol of the tested phenylalkylamine with the same effect).

Model development

The descriptors which were selected by the stepwise variable subset selection were chemical potential, hardness, lowest unoccupied molecular orbital energy, dipole moment and vibrational energy. The appearances of these descriptors in the model can represent different aspects of a molecule which affected the absorption, distribution, metabolism, and excretion (ADEME) properties of the molecule.

The inter-correlations among these descriptors are shown in Table V, from which it can be seen that there are no high correlations between the descriptors. These descriptors were used as independent variables and log *MU* was considered as a dependent variable to develop the MLR model. The obtained MLR model was used to calculate the log *MU* values for the test and training sets. The MLR calculated values of log *MU* are given in Table I. The average error (*AE*), average absolute error (*AAE*) and standard error (*SE*) of this calculation were *AE* = –0.051, *AAE* = 0.334 and *SE* = 0.396 for training set; *AE* = –0.054, *AAE* = = 0.408 and *SE* = 0.475 for the internal test set and *AE* = 0.296, *AAE* = 0.440 and *SE* = 0.506 for the external test set. Other statistical parameters of the MLR model are given in Table VI.

TABLE V. Correlation matrix between selected descriptors

	LUMO	η	μ	*Ev*	*DP*
LUMO	1.000	0.62	0.21	0.45	0.143
η	–	1.000	–0.17	0.237	–0.32
μ	–	–	1.000	0.136	–0.44
Ev	–	–	–	1.000	–0.15
DP	–	–	–	–	1.000

TABLE VI. Statistical parameters obtained using the ANN and MLR models

Set	MLR							ANN						
	R	*F*	*SE*	*AE*	*AAE*	Q^2	*SPRESS*	*R*	*F*	*SE*	*AE*	*AAE*	Q^2	*SPRESS*
Training	0.82	74	0.398	–0.05	0.334	0.62	0.372	0.98	968	0.132	0.0065	0.113	0.91	0.147
External	0.82	6	0.443	–0.05	0.408	–	–	0.97	54	0.197	–0.002	0.154	–	–
Internal	0.80	5	0.427	0.296	0.44	–	–	0.96	33	0.202	0.072	0.180	–	–

Since the MLR model was unable to accurately predict the log *MU* values of the data set, an ANN model as a non-linear feature mapping technique was developed. After training this 5:4:1 network, its prediction power was examined on an independent data set which was named the external test set. The ANN predicted values of log *MU* for this set as well as for the training and internal test sets are given in Table I. The statistics of this calculation are: *AE* = 0.006, *AAE* = = 0.113 and *SE* = 0.130 for the training set; *AE* = –0.002, *AAE* = 0.154 and *SE* = = 0.178 for the internal test set and *AE* = 0.072, *AAE* = 0.180 and *SE* = 0.210 for the external test set. Other statistical parameters of the developed ANN model are given in Table VI. In the next step, the sensitivity analysis was carried out on the ANN model to determine the relative importance of each descriptor in the model. The procedure of this approach is based on the sequential removal of variables by zeroing the specific connection weights for that specific input variable in the first layer of the ANN.[33] For each sequentially zeroed input variable, the root mean square error of the prediction set (*RMSEP*), as the prediction error of this network, was calculated. Generally, the *RMSEP* value increases in this way. Then, differences between the *RMSEP* and the root mean square error (*RMSE*) of the established ANN was calculated and shown as *DRMSE*. Each variable which causes a greater value of *DRMSE* is important. The results of this test showed that the order of the importance of the selected molecular descriptors is $Ev > \mu >$ $> dp > \eta >$ LUMO.

Model validation

Validation techniques constitute a fundamental tool for the assessment of the validity of models. They are used to check the prediction power of the models, that is, to give a measure of their capability to perform reliable predictions of the modeled response for new cases for which the response is unknown. Cross-validation is a popular technique used to explore the predictive ability of statistical models.[34] Presuming that a data set consisting of *n* compounds is available, then several modified data sets are created by deleting in each case one or a small group (leave-some-out) of the objects.[23] For each data set, an input-output model is developed, based on the used modeling technique. The model is evaluated by measuring its accuracy in predicting the responses of the remaining data (the ones that have not been used in the development of the model). In particular, the leave-five-out (L5O) procedures were utilized in this study, which produce seve-

ral models, by deleting five objects, respectively from the data set. The maximum numbers of models produced by the L5O procedure is equal to $n!/5!(n-5)!$, where n is the number of molecules in the data set. The squared differences among the true response and the predicted response for each object left out are added to calculate the standardized prediction error sum of squares (*SPRESS*). In addition, the value of Q^2 was calculated from the following equation:

$$Q^2_{\mathrm{Imo}} = 1 - \frac{\Sigma\left(y_0 - y_i\right)^2}{\Sigma\left(y_i - y_m\right)^2} \tag{13}$$

where y_i, y_0 and y_m are the experimental, predicted and average experimental value of log *MU*, respectively. The statistical results of this test on the examined data set was Q^2 = 0.628 and *SPRESS* = 0.472 for the MLR model, while Q^2 = = 0.916 and *SPRESS* = 0.147 for the ANN model, which revealed the reliability of ANN model. In addition, a *Y*-randomization test was applied to examine the chance correlation among log *MU* and selected molecular descriptors.[35] In this method, a dependent variable vector is randomly shuffled and a new QSAR model is developed using the original independent variable. The result of 30 times randomization of log *MU* vectors gave $\overline{R}^2 = 0.111$, which revealed that there was no chance correlation in the data set. Comparison of the statistical results in the prediction of log *MU* using the ANN and the MLR models in Table VI reveals the superiority of the ANN over the MLR model. These observations show that there are some non-linear relation between the selected molecular descriptors and log *MU*. The ANN predicted values of log *MU* are plotted against their experimental values for the training, internal and external test sets in Fig. 3, which shows good correlation among these values. In addition, the residuals of this calculation are plotted against their experimental log *MU* value in Fig. 4. The random propagation of the residuals over the zero line shows that no systematic error existed in the developed ANN model.

As mentioned earlier, Thakur and coworkers proposed a QSAR model on the same data set.[6] The leave-one-out cross-validation test on their model provided the statistics Q^2 =0.7154 and *SPRESS* =0.87, while these statistics for the presented model are Q^2 =0.841 and *SPRESS* =0.34, which revealed the superiority of the present work. In addition, they used two experimentally determined parameters (log P_{ow} and *MR*) as independent parameter in their proposed model while it is preferred to use theoretically derived molecular descriptors in QSAR models. In contrast to their work, the present model uses only theoretically derived molecular descriptors.

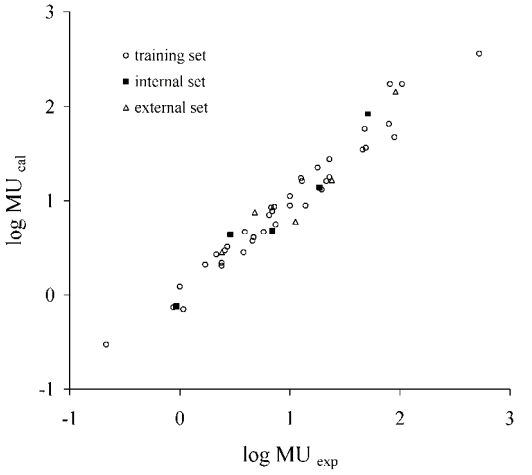

Fig. 3. The plot of ANN calculated *vs.* experimental value of log *MU*.

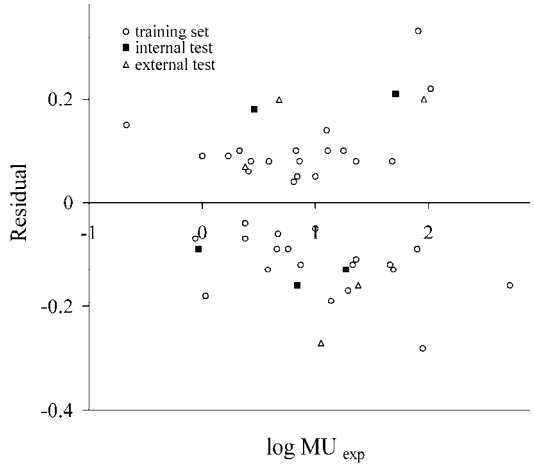

Fig. 4. The plot of ANN calculated residuals *vs.* experimental value of log *MU*.

CONCLUSIONS

The results of this study show that there are some non-linear relationships between the DFT calculated molecular descriptors and the psychometric activities of phenylalkylamines. The high correlation coefficients and low prediction errors of the developed ANN model confirm the good predictive ability of this QSAR model. Finally, the descriptors used in this work can encode some electronic and topological aspect of phenylalkylamines, which could affect on their steric and lipophilic interaction with target cell.

Acknowledgments. The authors wish to acknowledge Anna Ranson, Casa Latinoamericana, London, UK, for reading the manuscript and providing valuable suggestions. This work was supported by the Islamic Azad University, Babol Branch.

ИЗВОД

ПРЕДВИЂАЊЕ ПСИХОМЕТРИЈСКЕ АКТИВНОСТИ ФЕНИЛАЛКИЛАМИНА ПОМОЋУ НЕУРОНСКИХ МРЕЖА ПРИМЕНОМ МОЛЕКУЛСКИХ ДЕСКРИПТОРА РАЧУНАТИХ DFT МЕТОДОМ

MINA HAGHDADI[1] и MOHAMMAD H. FATEMI[2]

[1]*Department of Chemistry, Islamic Azad University, Babol Branch и* [2]*Department of Chemistry, Mazandaran University, Babolsar, Iran*

У раду је примењена метода QSAR за предвиђање психометријске активности (у мескалинским јединицама, log *MU*) за 48 фенилалкиламинских деривата, применом њихових молекулских дескриптора рачунатих DFT методом и помоћу вештачких неуронских мрежа (ANN). У првом кораку молекулски дескриптори су одређени DFT израчунавањима на нивоу теорије 6-311G*. Затим је примењена метода вишеструке линеарне регресије (MLR). У следећем кораку разрађена је метода базирана на ANN, одн. MLR, да би се добили нелинеарни одн. линеарни QSAR модели. Стандардне грешке за log *MU* у MLR-моделу су 0,398, 0,443 и 0,427 за тренинг, унутрашњи и спољашњи сет, док одговарајуће вредности за ANN модел износе 0,132, 0,197 и 0,202. Добијени резултати показују да се ANN-технике могу применити за QSAR предвиђања log *MU* вредности деривата фенилалкиламина на основу њихових молекулских дескриптора израчунатих DFT методом.

(Примљено 8. априла, ревидирано 11. маја 2010)

REFERENCES

1. R. A. Glennon, *Pharmacol. Biochem. Behav.* **64** (1999) 251
2. O. E. Taurian, R. H. Contreras, *J. Mol. Struct. (Theochem)* **504** (2000) 119
3. K. A. Nieforth, *J. Pharm. Sci.* **60** (1971) 655
4. S. H. Synder, C. R. Merril, *Natl. Acad. Sci. U.S.A.* **54** (1965) 258
5. M. Mracec, M. Mracec, L. Kurunczi, T. Nussar, Z. Simon, G. Naray-Szabo, *J. Mol. Str. (Theochem)* **367** (1996) 139
6. M. Thakur, A. Thakur, P. V. Khadikar, *Bioorg. Med. Chem.* **12** (2004) 825
7. A. Altun, K. Golcuk, M. Kumru, A. F. Jalbout, *Bioorg. Med. Chem.* **11** (2003) 3861
8. B. W. Clare, *J. Med. Chem.* **33** (1990) 687
9. R. R. Ruffolo, *Drug Design Discov.* **9** (1993) 351
10. P. K. Chattaraj, A. Cedillo, R. G. Parr, *J. Chem. Phys.* **103** (1995) 7645
11. P. W. Ayers, R. G. Parr, *J. Am. Chem. Soc.* **122** (2000) 2010
12. F. De Proft, J. M. L. Martin, P. Geerlings, *Chem. Phys. Lett.* **250** (1996) 393
13. P. Geerlings, F. De Proft, J. M. L Martin, *Recent Developments in Density Functional Theory*, Elseveir, Amsterdam, 1996, p. 773
14. P. Geerlings, F. De Proft, W. Langenaeker, *Adv. Quantum Chem.* **33** (1999) 303
15. R. G. Parr, R. A. Donnelly, M. Levy, W. E. Palke, *J. Chem. Phys.* **68** (1978) 3801
16. F. De Proft, J. M. L. Martin, P. Geerlings, *Chem. Phys. Lett.* **256** (1996) 400
17. F. De Proft, P. Geerlings, *J. Chem. Phys.* **106** (1997) 3270
18. R. Todeschini, V. Consonni, *Molecular Descriptors for Chemoinformatics*. Wiley-VCH, Weinheim, 2009
19. *Gaussian 98*, Revision A. 6, Gaussian. Inc., Pittsburgh, PA, 2003
20. C. Lee, W. Yang, R. G. Parr, *Phys. Rev. B* **37** (1988) 785
21. A. D. Becke, *J. Chem. Phys.* **98** (1993) 1372

22. R. G. Parr, R. A. Donnelly, M. Levy, W. E. Palke, *J. Chem. Phys.* **68** (1978) 3801
23. P. Politzer, A. Fakher, *Theor. Chim. Acta* **99** (1998) 83
24. A. R. Katritzky, D. C. Fara, H. Yang, M. Karelson, T. Suzuki, V. P. Solov'ev, A. Varnek, *J. Chem. Inf. Comput. Sci.* **44** (2004) 529
25. J. Zupan, J. Gasteiger, *Anal. Chim. Acta* **248** (1991) 1
26. N. K. Bose, P. Liang, *Neural Network-Fundamentals*, McGraw-Hill, New York, 1996
27. B. J. Wytho, *Chemom. Intell. Lab. Syst.* **18** (1993) 115
28. MATLAB version 7.0. The MathWorks, Inc., 2004 (www.mathworks.com)
29. M. Jalali-Heravi, M. H. Fatemi, *Anal. Chim. Acta* **415** (2000) 95
30. M. Jalali-Heravi, M. H. Fatemi, *J. Chromatogr. A* **897** (2000) 227
31. A. G. Maldonado, J. P. Doucet, M. Petitjean, B. T. Fan, *Mol. Divers.* **10** (2006) 39
32. L. I. Nord, S. P. Jacobsson, *Chemometr. Intell. Lab. Syst.* **44** (1998) 153
33. D. W. Osten, *J. Chemom.* **2** (1998) 39
34. B. Walczak, D. L. Massart, *Chemom. Intell. Lab. Sys.* **27** (1995) 2741.

Journal of the Serbian Chemical Society
JSCS-info@shd.org.rs • www.shd.org.rs/JSCS
J. Serb. Chem. Soc. *75* (10) 1405–1412 (2010)
JSCS–4062
UDC 539.6+535.51:548.3
Original scientific paper

The Wiener polarity index of molecular graphs of alkanes with a given number of methyl groups

HANYUAN DENG* and HUI XIAO

College of Mathematics and Computer Science, Hunan Normal University, Changsha, Hunan 410081, P. R. China

(Received 20 March, revised 13 April 2010)

Abstract: The Wiener polarity index of a graph G is the number of unordered pairs of vertices $\{u,v\}$ of G such that the distance between u and v is equal to 3. In this paper, the maximum Wiener polarity index of molecular graphs of alkanes with a given number of methyl groups is studied.

Keywords: topological index; Wiener polarity index; distance; alkane with k methyl groups.

INTRODUCTION

Among various topological indices considered in chemical graph theory, only a few have been widely studied in mathematical and chemical literatures. However, it seems that less attention has been paid to the Wiener polarity index. It was introduced by Harold Wiener[1] for acyclic molecules in 1947. The Wiener polarity index of an organic molecule the molecular graph of which is $G = (V,E)$ is defined as:[2,3]

$$W_p(G) = |\{\{u, v\}|d_G(u, v) = 3, u, v \in V\}|$$

which is the number of unordered pairs of vertices $\{u,v\}$ of G such that $d_G(u,v) = 3$, where $d_G(u,v)$ is the distance between two vertices u and v in G.

Using the Wiener polarity index, Lukovits and Linert[4] demonstrated quantitative structure–property relationships in a series of acyclic and cycle-containing hydrocarbons. Hosoya[5] found a physico-chemical interpretation of $W_p(G)$. Very recently, Du, Li and Shi[2] described a linear time algorithm APT for computing the index of trees and characterized the trees maximizing the index among all trees of a given order. Deng *et al.*[3] characterized the extremal trees with respect to this index among all trees of order n and diameter k. Deng[6] gave the extremal Wiener polarity indices of all chemical trees of order n.

* Corresponding author. E-mail: hydeng@hunnu.edu.cn
doi: 10.2298/JSC100320114D

In this paper, the Wiener polarity index of molecular graphs of alkanes with k methyl groups will be studied. For an alkane with k methyl groups, its graph representation can be considered as a chemical tree with k pendents in which a pendent vertex corresponds to a methyl group. Thus, the maximum Wiener polarity index of chemical trees with n and k pendents will be discussed.

SOME PROPERTIES OF THE WIENER POLARITY INDEX

Let T be a tree with its vertex set $V(T)$ and edge set $E(T)$. The degree of a vertex $v \in V(T)$ is denoted by $d_T(v)$.

A path P in T is called an i-degree pendent chain if all of its internal vertices are of degree 2 and its ends of degree 1 and I, respectively, where $i \geq 3$. In particular, P is called an i-degree pendent edge if P is an edge. Here, only chemical trees are considered.

For convenience, let $\mathbf{C}_n$ be the set of chemical trees (*i.e.*, trees for which every vertex has a degree at most of 4) of order n and $\mathbf{C}_{n,k}$ the set of chemical trees of order n with k pendents.

The degree sequence (n_1, n_2, n_3, n_4) is associated to $T \in \mathbf{C}_{n,}$ where n_i denotes the number of vertices of T with degree i ($1 \leq i \leq 4$). In particular, n_1 is the number of pendents. Recall the relations:

$$n_1 + n_2 + n_3 + n_4 = n \text{ and } n_1 + 2n_2 + 3n_3 + 4n_4 = 2n - 2$$

which implies

$$n_3 + 2n_4 + 2 = n_1 \text{ and } n = 2 + n_1 + n_2 + 2n_3 + 3n_4$$

First, a formula for computing the Wiener polarity index of trees is given.

Lemma 1.[2,3] Let $T = (V,E)$ be a tree. Then

$$W_p(T) = \sum_{uv \in E} (d_T(u) - 1)(d_T(v) - 1)$$

Let m_{ij} be the number of edges in T between vertices of degrees i and j. By Lemma 1, one has

$$W_p(T) = \sum_{uv \in E} (d_T(u) - 1)(d_T(v) - 1) = \sum_{1 \leq i \leq j \leq 4} (i-1)(j-1)m_{ij}$$

Especially, if T is a chemical tree, then

$$W_p(T) = m_{22} + 2m_{23} + 3m_{24} + 4m_{33} + 6m_{34} + 9m_{44}$$

Now, two graph transformations are introduced, which will be used in the next section.

An edge $e = uv$ is said to be subdivided when it is deleted and replaced by a path of length two connecting u and v, the internal vertex w of this path being a new vertex. The converse of subdividing is called smoothing the vertex w of degree 2. This is illustrated in Fig. 1.

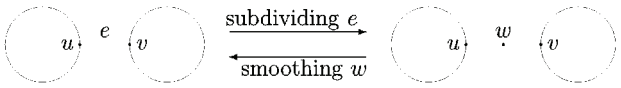

Fig. 1. The operations in subdividing and smoothing.

The following two lemmas can be proved by immediately computing from Lemma 1.

Lemma 2. Let $T \in \mathbf{C}_n$. $e = uv$ is an edge of T with $d_T(u) \le d_T(v)$. T' is the tree obtained by subdividing e. Then:

$$W_p(T') - W_p(T) = \begin{cases} 1, & d_T(u) = 1, \quad d_T(v) = 2; \\ 2, & d_T(u) = 1, \quad d_T(v) = 3; \\ 3, & d_T(u) = 1, \quad d_T(v) = 4; \\ 1, & d_T(u) = 2, \quad d_T(v) = 2,3,4; \\ 0, & d_T(u) = 3, \quad d_T(v) = 3; \\ -1, & d_T(u) = 3, \quad d_T(v) = 4; \\ -3, & d_T(u) = 4, \quad d_T(v) = 4; \end{cases}$$

Lemma 3. Let $T \in \mathbf{C}_n$. w is a vertex of degree 2 of T with the neighbors u and v, $d_T(u) \le d_T(v)$. T' is the tree obtained by smoothing w. Then

$$W_p(T') - W_p(T) = \begin{cases} -1, & d_T(u) = 1, \quad d_T(v) = 2; \\ -2, & d_T(u) = 1, \quad d_T(v) = 3; \\ -3, & d_T(u) = 1, \quad d_T(v) = 4; \\ -1, & d_T(u) = 2, \quad d_T(v) = 2,3,4; \\ 0, & d_T(u) = 3, \quad d_T(v) = 3; \\ 1, & d_T(u) = 3, \quad d_T(v) = 4; \\ 3, & d_T(u) = 4, \quad d_T(v) = 4; \end{cases}$$

Lemma 4. Let $T \in \mathbf{C}_{n,k}$ ($n \ge 7$) with the degree sequence (n_1, n_2, n_3, n_4), and all the vertices of degree 2 in T are on the pendent chains. If $n_3 \ge 2$, then there exists $T' \in \mathbf{C}_{n,k}$ with the degree sequence (n_1, n_2+1, n_3-2, n_4+1) such that $W_p(T') \ge W_p(T)$.

Proof. $x,y \in V(T)$ can be chosen such that $d_T(x) = d_T(y) = 3$ and there is neither a vertex of degree 3 nor a vertex of degree 2 between them since all the vertices of degree 2 in T are on the pendent chains. Let $T' = T - xa + ya$. Obviously, $T' \in \mathbf{C}_{n,k}$ has the degree sequence (n_1, n_2+1, n_3-2, n_4+1).

i) If $x,y \in E(T)$, see Fig. 2i. Without loss of generality, it is assumed that $d_T(a) \ge d_T(b)$ and $d_T(a) + d_T(b) \le d_T(c) + d_T(d)$. By Lemma 1:

$$W_p(T')-W_p(T) =[3(d_T(a)-1)+(d_T(b)-1)+3+3(d_T(c)-1)+3(d_T(d)-1)] -$$
$$-[2(d_T(a)-1)+2(d_T(b)-1)+4+2(d_T(c)-1)+2(d_T(d)-1)] =$$
$$= (d_T(a)-1)-(d_T(b)-1)-1+(d_T(c)-1)+(d_T(d)-1) =$$
$$= (d_T(a)-d_T(b))+(d_T(c)+d_T(d)-3)$$

If $d_T(a) > 1$, then $d_T(c)+d_T(d) \geq d_T(a)+d_T(b) \geq 3$; thus $W_p(T') \geq W_p(T)$. If $d_T(a) = 1$, then $d_T(b) = 1$ since $d_T(a) \geq d_T(b)$, and $d_T(c)+d_T(d) \geq 3$ since $n \geq 7$; thus, $W_p(T') \geq W_p(T)$.

ii) Otherwise, x,y may be chosen as in Fig. 2ii. Notice that $x_1 = y_1$ is possible. Without loss of generality, it is assumed that $d_T(a) \geq d_T(b)$. By Lemma 1:

$$W_p(T') - W_p(T) = [3(d_T(a)-1)+(d_T(b)-1)+3+9+3(d_T(c)-1)+3(d_T(d)-1)] -$$
$$-[2(d_T(a)-1)+2(d_T(b)-1)+6+6+2(d_T(c)-1)+2(d_T(d)-1)] =$$
$$= (d_T(a)-1)-(d_T(b)-1)+(d_T(c)-1)+(d_T(d)-1) =$$
$$= (d_T(a)-d_T(b))+(d_T(c)+d_T(d)-2) \geq 0$$

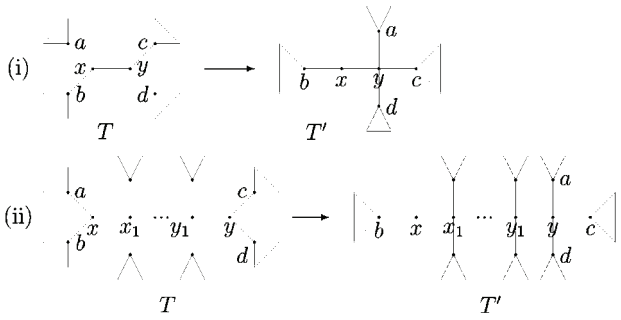

Fig. 2. Proof cases of Lemma 4.

THE MAXIMUM WIENER POLARITY INDEX OF CHEMICAL TREES WITH *n* VERTICES AND *k* PENDENTS

In this section, maximum Wiener polarity index of chemical trees with n vertices and k pendents will be discussed.

First, some special cases are considered. Let T be a chemical tree with n vertices and k pendents.

If $k = 2$, then T is the path P_n of length $n-1$, and $W_p(P_2) = 0$, $W_p(P_n) = n-3$ for $n \geq 3$.

If $k = 3$, then $n_3 = 1$, $n_4 = 0$ and $m_{14} = m_{24} = m_{33} = m_{34} = m_{44} = 0$, $0 \leq m_{23} \leq 3$. Since

$$\sum_{j=1}^{4} m_{1j} = n_1 = k \text{ and } \sum_{i=1}^{4}\sum_{j=i}^{4} m_{ij} = n-1,\ m_{22} + m_{23} = n-1-k = n-4$$

and

$$W_p(T) = m_{22} + 2m_{23} = n - 4 + m_{23} \leq \begin{cases} 0, n = 4; \\ 2, n = 5; \\ 4, n = 6; \\ n-1, n \geq 7. \end{cases}$$

with equality if and only if T is one of the graphs in Fig. 3.

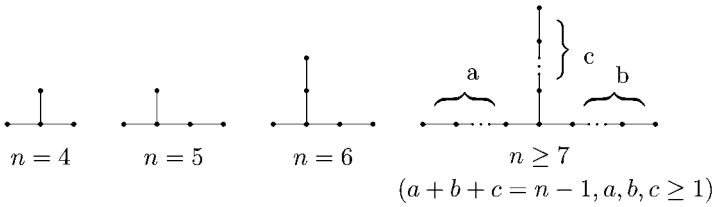

Fig. 3. The extremal tree with 3 pendents.

If $k = 4$ and $n = 5$, then T is a star with 5 vertices and $W_p(T) = 0$. If $k = 4$ and $n = 6$, then there are only two chemical trees with 6 vertices and 4 pendents. One can immediately obtain that $W_p(T) = 3$ or $W_p(T) = 4$.

In the following, it is assumed that $k \geq 4$ and $n \geq 7$.

Let $\mathbf{C}^{*}_{n,k}$ be the set of chemical trees T with n vertices and k pendents satisfying the following conditions:

i) there is at most one vertex of degree 3 in T;

ii) all the vertices of degree 2 in T are on the pendent chains;

iii) if P is a path in T with ends of degree 4, then all internal vertices of P are of degree 4;

iv) if $n_2 \geq k$, then there is neither a 4-degree pendent edge nor a 3-degree pendent edge.

Remark. Let $T \in \mathbf{C}^{*}_{n,k}$ with a degree sequence (n_1, n_2, n_3, n_4).

I) If k is even, then $n_3 = 0$, the induced subgraph T' by the vertices of degree 4 in T is also a tree, and $m_{44} = n_4 - 1$. By the relations:

$$\begin{cases} k + n_2 + n_4 = n, \\ k + 2n_2 + 4n_4 = 2n - 2 \end{cases}$$

one has $n_2 = n + 1 - 3k/2$ and $n_4 = k/2 - 1$.

i) If $n_2 \leq k$, *i.e.*, $k \geq 2(n+1)/5$, then $m_{24} = n_2$, $m_{22} = 0$ and

$$W_p(T) = 3m_{24} + 9m_{44} = 3n_2 + 9(n_4 - 1) = 3n - 15$$

ii) If $n_2 \geq k$, *i.e.*, $k \leq 2(n+1)/5$, then $m_{24} = k$, $m_{22} = n - 1 - (k + m_{24} + m_{44}) = n + 1 - 5k/2$ and $W_p(T) = m_{22} + 3m_{24} + 9m_{44} = n + 5k - 17$.

II) If k is odd, then T has only a vertex v of degree 3, *i.e.*, $n_3 = 1$. The induced subgraph T' by the vertices of degree 3 or 4 in T is also a tree and v is a pendent of T'. Thus, $m_{44} = n_4–1$, $m_{34} = 1$ and $m_{33} = 0$. By the relations:

$$\begin{cases} k + n_2 + n_3 + n_4 = k + n_2 + n_4 = n, \\ k + 2n_2 + 3n_3 + 4n_4 = k + 2n_2 + 3 + 4n_4 = 2n - 2 \end{cases}$$

one has $n_2 = n + 1/2 - 3k/2$ and $n_4 = k/2 - 3/2$.

i) If $n_2 \le k–2$, *i.e.*, $k \ge 2n/5 + 1$, then $m_{24} = n_2$, $m_{23} = m_{22} = 0$ and

$$W_p(T) = 3m_{24} + 6m_{34} + 9m_{44} = 3n_2 + 6 + 9(n_4–1) = 3n–15$$

ii) If $n_2 = k–1$, *i.e.*, $k = 2n/5 + 3/5$, then $m_{23} = 1$, $m_{24} = n_2–1 = k–2$, $m_{22} = 0$ and

$$W_p(T) = 2m_{23} + 3m_{24} + 6m_{34} + 9m_{44} = 3n–16$$

iii) If $n_2 \ge k$, *i.e.*, $k \le 2n/5 + 1/5$, then $m_{23} = 2$, $m_{24} = k–2$,

$$m_{22} = n–1 – (k + m_{23} + m_{24} + m_{34} + m_{44}) = n+1 – 5/2k$$

and

$$W_p(T) = m_{22} + 2m_{23} + 3m_{24} + 6m_{34} + 9m_{44} = n + 5k – 18$$

Hence, for any $T \in \mathbf{C}^{*}_{n,k}$, one has:

$$W_p(T) = \begin{cases} n + 5k - 17, & k \text{ is even and } 4 \le k \le \frac{2}{5}(n+1); \\ 3n - 15, & k \text{ is even and } k \le \max\{4, \frac{2}{5}(n+1)\}; \\ n + 5k - 18, & k \text{ is odd and } 5 \le k \le \frac{2}{5}n + \frac{1}{5}; \\ 3n - 16, & k \text{ is odd and } k = \frac{2}{5}n + \frac{3}{5} \ge 5; \\ 3n - 15, & k \text{ is odd and } k \ge \max\{5, \frac{2}{5}n + 1\} \end{cases}$$

Theorem 1. For any $T \in \mathbf{C}^{*}_{n,k}$, there is $T^{*} \in \mathbf{C}^{*}_{n,k}$ such that $W_p(T^{*}) \ge W_p(T)$.

Proof. *i*) First, if there is a vertex of degree 2 in T which is not on any pendent chain. Let Q be the set of all vertices of degree 2 in T which are not on any pendent chain. T_1 is obtained from T by smoothing the vertices in Q, then $W_p(T_1)–W_p(T) \ge –|Q|$ by Lemma 3. Now, let T_2 be obtained from T_1 by subdividing a pendent edge $|Q|$ times, then $T_2 \in \mathbf{C}^{*}_{n,k}$ and $W_p(T_2)–W_p(T_1) \ge |Q|$ by Lemma 2, and $W_p(T_2) \ge W_p(T)$, *i.e.*, there is $T_2 \in \mathbf{C}^{*}_{n,k}$ such that all its vertices of degree 2 are on the pendent chains and $W_p(T_2) \ge W_p(T)$.

ii) Secondly, if there are at least two vertices of degree 3 in T_2, then, by Lemma 4, there exists a tree $T_3 \in \mathbf{C}^{*}_{n,k}$ with at the most one vertex of degree 3 such that $W_p(T_3) \ge W_p(T)$. Furthermore, it can be assumed that all the vertices of

degree 2 in T_3 are on the pendent chains since process *i*) can be repeated without changing its degree sequence.

iii) Next, we consider $T_3 \in \mathbf{C}^*_{n,k}$ with exactly one vertex of degree 3 and with all its vertices of degree 2 on the pendent chains. If there is a path P in T_3 with ends of degree 4 and one of its internal vertices is of degree 3, see Fig. 4 (case 1), where $d_{T_3}(v) = 3$, it may be assumed that P is maximal, then

$$d_{T_3}(a), d_{T_3}(b), d_{T_3}(c) < 4 \text{ and } d_{T_3}(a), d_{T_3}(b), d_{T_3}(c) \le 2$$

since v is the unique vertex of degree 3. Let $T_4 = T_3 - ya + va$, see Fig. 4 (case 2), then $T_4 \in \mathbf{C}^*_{n,k}$. Notice that $z = y$ is possible. By Lemma 1, one obtains:

$$W_p(T_4) - W_p(T_3) = [3(d_{T_3}(u) - 1) + 3(d_{T_3}(x) - 1) + 3(d_{T_3}(z) - 1) + 3(d_{T_3}(a) - 1) +$$
$$+ 2(d_{T_3}(w) - 1) + 2(d_{T_3}(b) - 1) + 2(d_{T_3}(c) - 1)] - [2(d_{T_3}(u) - 1) + 2(d_{T_3}(x) - 1) +$$
$$+ 2(d_{T_3}(z) - 1) + 3(d_{T_3}(a) - 1) + 3(d_{T_3}(w) - 1) + 3(d_{T_3}(b) - 1) + 3(d_{T_3}(c) - 1)] =$$
$$= [9 + 3(d_{T_3}(x) - 1) + 9 + 3(d_{T_3}(a) - 1) + 6 + 2(d_{T_3}(b) - 1) + 2(d_{T_3}(c) - 1)] -$$
$$- [6 + 2(d_{T_3}(x) - 1) + 6 + 3(d_{T_3}(a) - 1) + 9 + 3(d_{T_3}(b) - 1) + 3(d_{T_3}(c) - 1)] =$$
$$= 4 + d_{T_3}(x) - d_{T_3}(b) - d_{T_3}(c) > 0$$

and $W_p(T_4) > W_p(T_3)$.

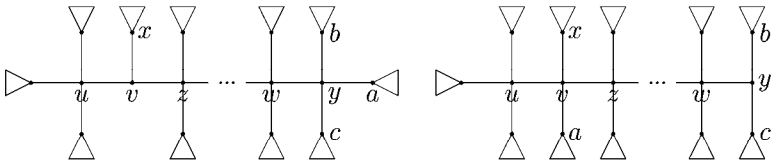

(1) T_3 (2) T_4

Fig. 4. Proof cases for Theorem 1.

iv) Finally, if $n \ge k$ and there is an *i*-degree pendent edge e in T_4 (i = 3 or 4), then there is a pendent chain P with length at least 3. Let T_5 be the tree obtained from T_5 by smoothing a vertex of degree 2 on the path P and subdividing the edge e. By Lemmas 2–3, $W_p(T_5) > W_p(T_4)$.

Hence, there is $T^* \in \mathbf{C}^*_{n,k}$ such that $W_p(T^*) \ge W_p(T)$ for any $T \in \mathbf{C}^*_{n,k}$.

In order to obtain the maximum Wiener polarity index of trees in $\mathbf{C}_{n,k}$, one only needs to find the Wiener polarity index of trees in $\mathbf{C}^*_{n,k}$. By Theorem 1 and the Remark, one has

Theorem 2. Among all chemical trees with $n \ge 7$ vertices and $k \ge 2$ pendents, the maximum Wiener polarity index is $W_p(T)_{max}$, where:

$$W_{\mathrm{p}}(T)_{\max}=\begin{cases} n-3, & k=2; \\ n-1, & k=3; \\ n+5k-17, & k \text{ is even and } 4\le k\le \frac{2}{5}(n+1); \\ 3n-15, & k \text{ is even and } k\ge \max\{4,\ \frac{2}{5}(n+1)\}; \\ n+5k-18, & k \text{ is odd and } 5\le k\le \frac{2}{5}n+\frac{1}{5}; \\ 3n-16, & k \text{ is odd and } k=\frac{2}{5}n+\frac{3}{5}\ge 5; \\ 3n-15, & k \text{ is odd and } k\ge \max\{5,\ \frac{2}{5}n+1\}. \end{cases}$$

From Theorem 2 and the result in the literature,[6] an interesting fact is found, *i.e.*, the maximum Wiener polarity index of chemical trees with $n\ge 7$ vertices and $k\ge 4$ pendents is the same as that of chemical trees with n vertices when $k\ge 2n/5+1$.

Acknowledgements. This work was supported by the Hunan Provincial Natural Science Foundation of China (09JJ6009) and the Scientific Research Fund of the Hunan Provincial Education Department (09A057).

ИЗВОД

WIENER-ОВ ИНДЕКС ПОЛАРНОСТИ МОЛЕКУЛСКИХ ГРАФОВА АЛКАНА СА ЗАДАНИМ БРОЈЕМ МЕТИЛ ГРУПА

HANYUAN DENG и HUI XIAO

College of Mathematics and Computer Science, Hunan Normal University, Changsha, Hunan 410081, P. R. China

Wiener-ов индекс поларности графа G је број парова чворова $\{u,v\}$ графа G таквих да је растојање између u и v једнако 3. У раду је испитан максимални Wiener-ов индекс поларности молекулских графова алкана са заданим бројем метал група.

(Примљено 20. марта, ревидирано 13. априла 2010)

REFERENCES

1. H. Wiener, *J. Am. Chem. Soc.* **69** (1947) 17
2. W. Du, X. Li, Y. Shi, *MATCH Commun. Math. Comput. Chem.* **62** (2009) 235
3. H. Deng, H. Xiao, F. Tang, *MATCH Commun. Math. Comput. Chem.* **63** (2010) 257
4. I. Lukovits, W. Linert, *J. Chem. Inf. Comput. Sci.* **38** (1998) 715
5. H. Hosoya, in: D. H. Rouvray, R. B. King, Eds., *Topology in Chemistry – Discrete Mathematics of Molecules*, Horwood, Chichester, 2002, p. 57
6. H. Deng, *MATCH Commun. Math. Comput. Chem.*, 2010, accepted

Journal of the Serbian Chemical Society
JSCS-info@shd.org.rs • www.shd.org.rs/JSCS
J. Serb. Chem. Soc. 75 (10) 1413–1420 (2010)
JSCS–4063
UDC 546.96–31+546.93–31+621.3.032.22–882:667.6:544.4
Original scientific paper

Differences in the electrochemical behavior of ruthenium and iridium oxide in electrocatalytic coatings of activated titanium anodes prepared by the sol–gel procedure

VLADIMIR V. PANIĆ[1*#], ALEKSANDAR B. DEKANSKI[1#], VESNA B. MIŠKOVIĆ-STANKOVIĆ[2#], SLOBODAN K. MILONJIĆ[3#] and BRANISLAV Ž. NIKOLIĆ[2#]

[1]*ICTM – Department of Electrochemistry, University of Belgrade, Njegoševa 12, 11000 Belgrade,* [2]*Faculty of Technology and Metallurgy, University of Belgrade, P. O. Box 350, 11001 Belgrade and* [3]*Vinča Institute of Nuclear Science, P. O. Box 522, 11001 Belgrade, Serbia*

(Received 10 March, revised 1 June 2010)

Abstract: The electrochemical characteristics of $Ti_{0.6}Ir_{0.4}O_2$/Ti and $Ti_{0.6}Ru_{0.4}O_2$/Ti anodes prepared by the sol–gel procedure from the corresponding oxide sols, obtained by force hydrolysis of the corresponding metal chlorides, were compared. The voltammetric properties in H_2SO_4 solution indicate that $Ti_{0.6}Ir_{0.4}O_2$/Ti has more pronounced pseudocapacitive characteristics, caused by proton-assisted, solid state surface redox transitions of the oxide. At potentials negative to 0.0 V_{SCE}, this electrode is of poor conductivity and activity, while the voltammetric behavior of the $Ti_{0.6}Ru_{0.4}O_2$/Ti electrode is governed by proton injection/ejection into the oxide structure. The $Ti_{0.6}Ir_{0.4}O_2$/Ti electrode had a higher electrocatalytical activity for oxygen evolution, while the investigated anodes were of similar activity for chlorine evolution. The potential dependence of the impedance characteristics showed that the $Ti_{0.6}Ru_{0.4}O_2$/Ti electrode behaved like a capacitor over a wider potential range than the $Ti_{0.6}Ir_{0.4}O_2$/Ti electrode, with fully-developed pseudocapacitive properties at potentials positive to 0.60 V_{SCE}. However, the impedance characteristics of the $Ti_{0.6}Ir_{0.4}O_2$/Ti electrode changed with increasing potential from resistor-like to capacitor-like behavior.

Keywords: activated titanium anodes; sol–gel procedure, ruthenium and iridium oxide; electrochemical impedance spectroscopy; pseudocapacitance.

INTRODUCTION

Titanium anodes coated with noble metal oxides (activated titanium anodes, ATA), being electrocatalytically active for the chlorine evolution and oxygen re-

* Corresponding author. E-mail: panic@ ihtm.bg.ac.rs
# Serbian Chemical Society member.
doi: 10.2298/JSC100310078P

action,[1] are commercially applied in industrial electrochemistry for chlor–alkali electrolysis, cathodic protection and metal electrowinning processes.[2] ATA coatings with RuO_2 and/or IrO_2 undergo degradation due to the electrochemical dissolution of noble metal oxide species.[3–6] Since these products of noble metal oxide degradation are soluble, the anode coating is gradually enriched in insulating TiO_2 during operation, since not only is this oxide already present as a stabilizing component of binary and/or ternary coatings, but it also comes from the coating substrate. These processes lead to anode passivation.[3–5]

The anode activity for the oxygen evolution reaction plays a key role in the process of anode degradation.[5,6] It is known that ATA with iridium oxide in the coating is more stable against passivation in the electrolysis of NaCl solutions than a binary RuO_2–TiO_2 coating.[7,8] This is due to the slower dissolution rate of IrO_2 with respect to RuO_2, especially when a considerable portion of the current is related to the oxygen evolution reaction. For this reason, commercially available ATAs contain iridium oxide in small amounts, in addition to ruthenium and titanium oxide. A recent investigation showed that a RuO_2–IrO_2–TiO_2 anode is an ideal anti-fouling electrode material in the electrolysis process of brine.[9]

Previous studies[6,10,11] postulated a higher activity for the chlorine and oxygen evolution reaction, as well as greater stability to passivation of $Ti_{0.6}Ru_{0.4}O_2$ coatings on titanium prepared by the sol-gel procedure in comparison to the same coating prepared by the usual thermal decomposition of metal chlorides.[5,11] This improvement was assigned to the larger real surface area of the sol–gel-prepared coating.[6]

The activity and stability of a ternary $Ti_{0.6}Ru_{0.3}Ir_{0.1}O_2$ coating on titanium prepared by the sol–gel procedure were investigated under conditions of chlorine and oxygen evolution.[12,13] The anode characteristics were compared to the characteristics of a binary $Ti_{0.6}Ru_{0.4}O_2$ coating. The investigation showed that finely dispersed iridium oxide was produced by the sol–gel procedure.[13] It was found by an accelerated stability test in sea water that the ternary coating was considerably more stable during exploitation than the binary one.[12] This was assigned to the greater stability of nano-sized IrO_2 under vigorous oxygen and chlorine evolution in comparison to sol–gel processed RuO_2.

The aim of this study was to investigate the differences in electrochemical properties of $Ti_{0.6}Ir_{0.4}O_2$/Ti and $Ti_{0.6}Ru_{0.4}O_2$/Ti anodes prepared by the sol–gel procedure, in order to obtain further insight into the differences between the noble oxides, which result in the beneficial behavior of IrO_2-containing coatings.

EXPERIMENTAL

Colloidal dispersions of ruthenium, iridium and titanium oxide were obtained by the forced hydrolysis of the corresponding metal chlorides in boiling 0.27 mol dm^{-3} HCl.[11,13] The dispersions of RuO_2, IrO_2 and TiO_2 (oxide sols) were formed during 46, 20 and 10 h (ageing times), respectively. These ageing times were chosen since $Ti_{0.6}Ru_{0.4}O_2$ coatings with the best

electrochemical properties were obtained from sols of these ageing times,[9] while the ageing time of IrO_2 was set in-between. The prepared oxide sols were mixed to form binary dispersions for the preparation of a coating with the desired compositions of $Ti_{0.6}Ir_{0.4}O_2$ and $Ti_{0.6}Ru_{0.4}O_2$. The dispersions were painted over Ti plates (1 cm×1 cm×0.89 mm), previously sand-blasted, degreased in saturated NaOH/ethanol solution and etched in hot 20 mass % HCl for 20 min. The coatings were applied in two layers, each converted into the gel phase at 90 °C and annealed at 450 °C; the first layer was annealed for 10 min and the second for 20 min. This procedure developed the crystal structure of the oxide and provided good coating adhesion. The total coating mass was 1.0 mg cm^{-2} (calculated to the overall oxide).

The capacitive behavior of the prepared anodes was investigated by cyclic voltammetry (CV) in 1.0 mol dm^{-3} H_2SO_4 and by electrochemical impedance spectroscopy (EIS) in the same solution at the characteristic potentials indicated by the CV behavior of the prepared anodes. The polarization characteristics of the prepared oxide coatings in 1.0 mol dm^{-3} H_2SO_4 and in 0.50 mol dm^{-3} NaCl, pH 2, were registered by anodic linear sweep voltammetry at a scan rate of 0.50 mV s^{-1}. A Pt plate electrode was used as the counter electrode, while the reference electrode was a SCE, and all potentials are referred to the SCE.

RESULTS AND DISCUSSION

Colloidal dispersions of ruthenium, iridium and titanium oxide of different degrees of polydispersity were obtained.[13] The TiO_2 sol consisted of particles of size around 100 nm with a weak tendency to agglomerate. The RuO_2 particle size fell in the range 3–10 nm; however, the sporadic presence of agglomerates of sizes of several hundreds of nm was also evidenced.[13] The agglomeration was more pronounced upon dilution due to the increase in pH of the dispersion. A high affinity for agglomeration was also registered in the case of the IrO_2 particles, which were prepared as ultra-small (around 1 nm)[13] but, upon dilution, the stable iridium oxide agglomerates had sizes of 50–90 nm.

The capacitive cyclic voltammograms of $Ti_{0.6}Ir_{0.4}O_2$/Ti and $Ti_{0.6}Ru_{0.4}O_2$/Ti electrodes in H_2SO_4 solution, registered at different sweep rates, are shown in Figs. 1A and 1B, respectively. The voltammograms for the different coatings are of different shape, with much more pronounced pseudocapacitive reversible peaks for the $Ti_{0.6}Ir_{0.4}O_2$/Ti electrode, which are to be ascribed to proton-assisted, solid state surface redox transitions (SSRTs) of the noble metals (Me):[1,11,14]

$$MeO_x(OH)_y + \delta H^+ + \delta e^- \rightarrow MeO_{x-\delta}(OH)_{y+\delta},\ 0 \le \delta \le 2 \qquad (1)$$

In the case of the $Ti_{0.6}Ru_{0.4}O_2$/Ti electrode (Fig. 1B), the SSRTs are overlapped in the investigated potential range and form a single broad peak around 0.55 V, while at least three well-resolved SSRTs are seen for $Ti_{0.6}Ir_{0.4}O_2$/Ti as peaks at 0.35, 0.74 and 1.02 V (Fig. 1A, 50 mV s^{-1}). The most negative and positive peaks showed appreciable dependence on the sweep rate; the first one diminishes and the last one shifts cathodically with increasing sweep rate, and finally (at 300 mV s^{-1}) emerges with an SSRT peak at 0.74 V. In addition to the better separation of the SSRTs in the case of $Ti_{0.6}Ir_{0.4}O_2$/Ti, the associated capacitance values were much higher than for $Ti_{0.6}Ru_{0.4}O_2$/Ti.

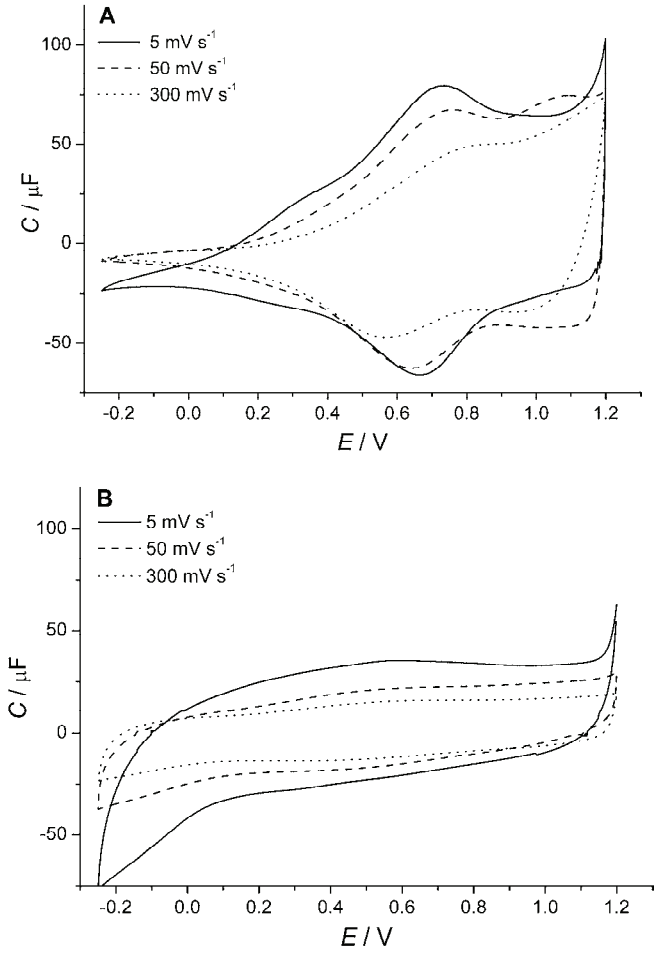

Fig. 1. Capacitance–potential curves of the $Ti_{0.6}Ir_{0.4}O_2$/Ti (A) and $Ti_{0.6}Ru_{0.4}O_2$/Ti (B) electrodes registered in 1.0 mol dm^{-3} H_2SO_4 at the sweep rates shown in the graph; room temperature.

The most remarkable difference in the CV behavior of the investigated electrodes is seen in the potential region below 0.0 V. The capacitance of $Ti_{0.6}Ir_{0.4}O_2$/Ti considerably decreases, which indicates poor conductivity in the cathodic direction, while $Ti_{0.6}Ru_{0.4}O_2$/Ti exhibits a considerable increase in the cathodic capacitance, due to pronounced proton injection according to Eq. (1). Hence, the data shown in Fig. 1 introduce iridium oxide as good anodic capacitor, while ruthenium oxide has desirable capacitive properties at more negative potentials.

The polarization curves of $Ti_{0.6}Ir_{0.4}O_2$/Ti and $Ti_{0.6}Ru_{0.4}O_2$/Ti anode in oxygen and chlorine evolution are shown in Fig. 2. The anodes showed different Tafel slopes for O_2 evolution (40 and 60 mV dec^{-1}, for the $Ti_{0.6}Ir_{0.4}O_2$/Ti and

$Ti_{0.6}Ru_{0.4}O_2$/Ti anodes, respectively), which promotes iridium oxide as a much better catalyst for this reaction. Only below 1.25 V were higher currents registered for the $Ti_{0.6}Ru_{0.4}O_2$/Ti anode. In the case of Cl_2 evolution, a slope close to 40 mV was registered for both anodes. The currents were higher for the $Ti_{0.6}Ru_{0.4}O_2$/Ti anode up to a potential close to the onset of O_2 evolution (near 1.15 V). These data show that the anode containing iridium oxide should behave beneficially from the standpoint of anode stability, as was already evidenced by comparison of $Ti_{0.6}Ru_{0.3}Ir_{0.1}O_2$/Ti and $Ti_{0.6}Ru_{0.4}O_2$/Ti anodes during their operation in sea water.[12]

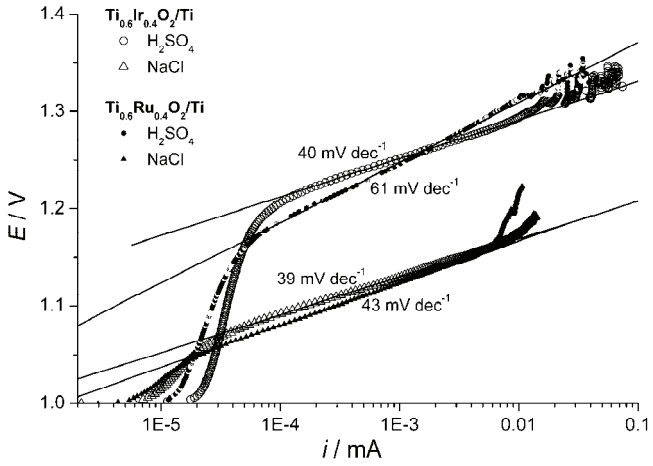

Fig. 2. Polarization curves of the $Ti_{0.6}Ir_{0.4}O_2$/Ti and $Ti_{0.6}Ru_{0.4}O_2$/Ti anodes registered in 1.0 mol dm^{-3} H_2SO_4 and in 0.50 mol dm^{-3} NaCl, pH 2; room temperature.

The EIS characteristics of $Ti_{0.6}Ir_{0.4}O_2$/Ti and $Ti_{0.6}Ru_{0.4}O_2$/Ti electrodes, registered at the characteristic potentials (–0.10, 0.35 and 0.74 V) related to CV behavior of the $Ti_{0.6}Ir_{0.4}O_2$/Ti electrode (Fig. 1A), are shown in Figs. 3 and 4, respectively.

The EIS data for the $Ti_{0.6}Ru_{0.4}O_2$/Ti electrode showed a much less pronounced dependence on potential (Fig. 4) than the $Ti_{0.6}Ru_{0.4}O_2$/Ti electrode. At all investigated potentials, the former electrode behaved like a capacitor and the changes of the EIS characteristics with potential were registered in the low frequency region (below 1 Hz). A low frequency capacitive loop clearly developed at 0.74 V, while at lower potentials the low frequency data indicate diffusion limitations. Since SSRTs dominate in the capacitive behavior of ruthenium oxide at the potentials positive to 0.60 V (Fig. 2B), it can be concluded that the low frequency capacitive loop at 0.74 V corresponds to a fully-developed pseudocapacitive behavior caused by SSRTs. At lower potentials, the SSRTs are controlled by proton injection/ejection through the porous structure of the coating.

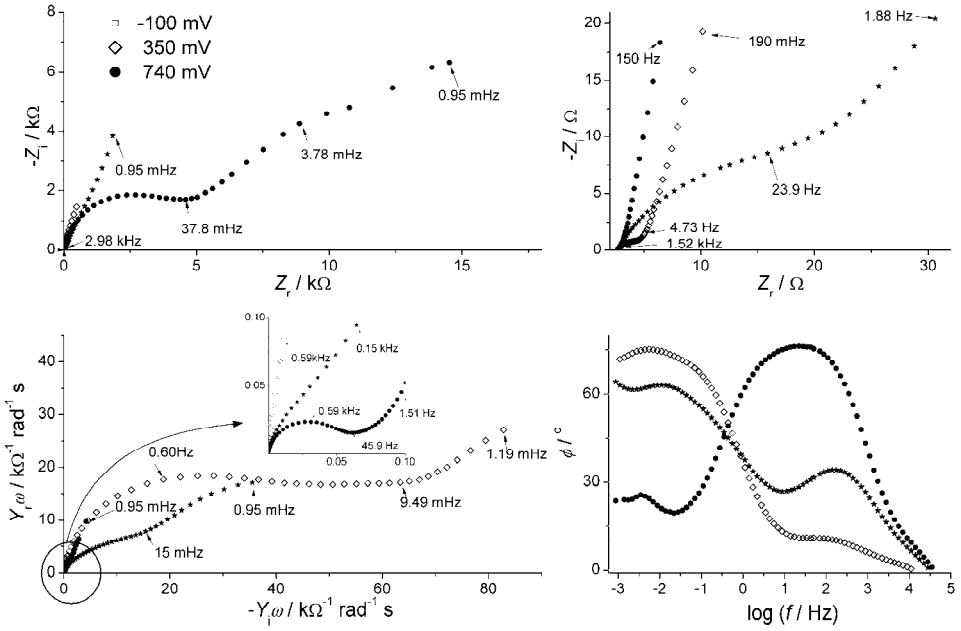

Fig. 3. The EIS characteristics of the $Ti_{0.6}Ir_{0.4}O_2$/Ti electrode registered at different potentials in 1.0 mol dm^{-3} H_2SO_4 at room temperature.

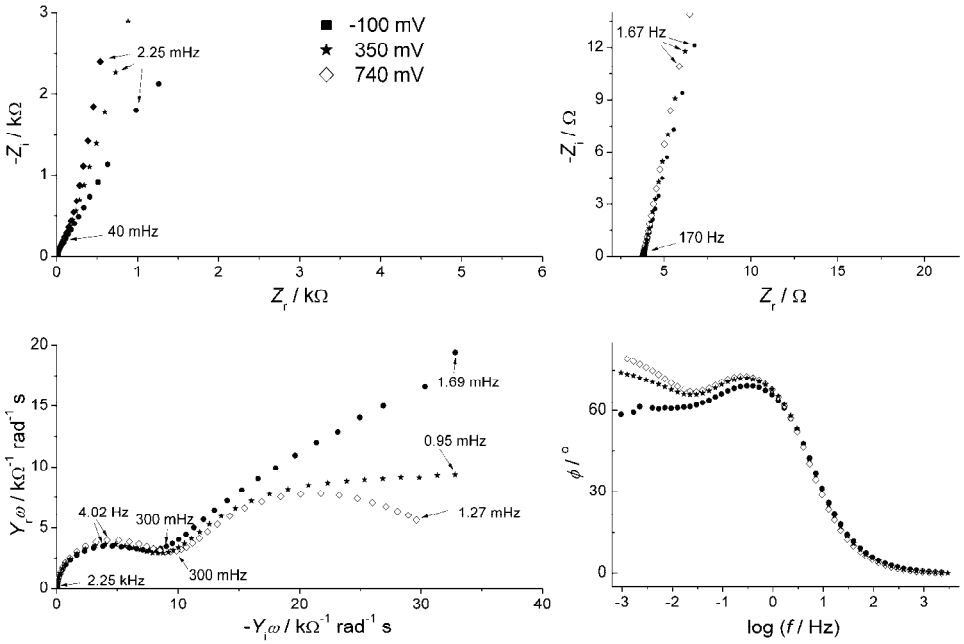

Fig. 4. The EIS characteristics of the $Ti_{0.6}Ru_{0.4}O_2$/Ti electrode registered at different potentials in 1.0 mol dm^{-3} H_2SO_4 at room temperature.

The $Ti_{0.6}Ir_{0.4}O_2$/Ti electrode behaved much like a resistor at –0.10 V (Fig. 3), as is indicated by the appearance of a semicircle in the complex plane plot, which corresponds to a considerably lower capacitance in comparison to the $Ti_{0.6}Ru_{0.4}O_2$/Ti electrode (also registered by CV measurements, Fig. 1). As the potential increases, SSRTs are involved and the semicircle diminishes (the associated resistance decreases from ≈ 5 kΩ (–0.10 V) to ≈ 5 Ω (0.74 V)). At 0.74 V, a capacitive loop clearly developed and the electrode behaved much like capacitor upon the onset of SSRTs. The associated capacitance is much higher in comparison to that of the $Ti_{0.6}Ru_{0.4}O_2$/Ti electrode, as was also indicated by CV measurements (Fig. 1).

CONCLUSIONS

The electrochemical properties of $Ti_{0.6}Ir_{0.4}O_2$/Ti and $Ti_{0.6}Ru_{0.4}O_2$/Ti anodes were investigated and compared, in order to obtain further insight into the differences between the two noble metal oxides, whereby iridium oxide was shown to be more stable in electrolysis processes involving simultaneous oxygen evolution. Cyclic voltammetry and electrochemical impedance spectroscopy showed that the $Ti_{0.6}Ir_{0.4}O_2$/Ti electrode changed its behavior with the potential from resistor-like to capacitor-like due to the suppression of the proton injection/ejection process (resistor-like behavior). The $Ti_{0.6}Ru_{0.4}O_2$/Ti electrode behaved as capacitor over the whole potential window of water stability. Proton-assisted, solid state surface redox transition processes, responsible for the pseudocapacitive behavior of noble oxides, were more pronounced in the case of the iridium oxide-containing electrode. Additionally, the $Ti_{0.6}Ir_{0.4}O_2$/Ti anode was more active for oxygen evolution and of similar activity for chlorine evolution in comparison to the $Ti_{0.6}Ru_{0.4}O_2$/Ti anode. It appears that the higher activity for oxygen evolution and greater stability of the $Ti_{0.6}Ir_{0.4}O_2$/Ti anode are closely connected to the much better resolved redox transition process of iridium oxide. The state of the oxide formed prior to the oxygen evolution is more stable and active than the appropriate state of ruthenium oxide.

Acknowledgement. This work was financially supported by the Ministry of Science and Technological Development of the Republic of Serbia, Project Nos. 142048 and 142060.

И З В О Д

РАЗЛИКЕ У ЕЛЕКТРОХЕМИЈСКОМ ПОНАШАЊУ ОКСИДА РУТЕНИЈУМА И ИРИДИЈУМА У ЕЛЕКТРОКАТАЛИТИЧКИМ ПРЕВЛАКАМА АКТИВИРАНИХ ТИТАНСКИХ АНОДА ДОБИЈЕНИХ СОЛ–ГЕЛ ПОСТУПКОМ

ВЛАДИМИР В. ПАНИЋ[1], АЛЕКСАНДАР Б. ДЕКАНСКИ[1], ВЕСНА Б. МИШКОВИЋ-СТАНКОВИЋ[2], СЛОБОДАН К. МИЛОЊИЋ[3] и БРАНИСЛАВ Ж. НИКОЛИЋ[2]

[1]ИХТМ – Центар за електрохемију, Универзитет у Београду, Његошева 12, 11000 Београд, [2]Технолошко–металуршки факултет, Универзитет у Београду, п. пр. 3503, 11001 Београд и [3]Институт за нуклеарне науке "Винча", п. пр. 522, 11001 Београд

У раду су испитиване електрохемијске карактеристике $Ti_{0,6}Ir_{0,4}O_2$/Ti и $Ti_{0,6}Ru_{0,4}O_2$/Ti анода добијених сол–гел поступком из оксидних солова синтетисаних форсираном хидроли-

зом одговарајућих хлорида метала. Волтаметријске карактеристике у раствору H_2SO_4 указују на више изражено псеудокапацитивно понашање $Ti_{0,6}Ir_{0,4}O_2$/Ti електроде које је последица површинских редокс прелаза у чврстом стању уз учешће протона. На потенцијалима негативнијим од 0,0 V_{ZKE} ова електрода показује слабу проводност и активност, док волтаметријским понашањем $Ti_{0,6}Ru_{0,4}O_2$/Ti електроде доминира продор протона у структуру оксида. $Ti_{0,6}Ir_{0,4}O_2$/Ti анода је електрокаталитички активнија за реакцију издвајања кисеоника, док су аноде сличних активности за реакцију издвајања хлора. Импедансне карактеристике формираних анода показују да се $Ti_{0,6}Ru_{0,4}O_2$/Ti електрода понаша слично кондензатору у ширем опегу потенцијала него што је то случај са $Ti_{0,6}Ir_{0,4}O_2$/Ti електродом, са потпуно развијеним псеудокапацитивним својствима на потенцијалима позитивнијим од 0,60 V_{ZKE}. С друге стране, за $Ti_{0,6}Ir_{0,4}O_2$/Ti електроду се уочава прелаз са карактеристика сличних отпорнику на карактеристике сличне кондензатору са порастом потенцијала електроде.

(Примљено 10. марта, ревидирано 1. јуна 2010)

REFERENCES

1. S. Trasatti, in *Interfacial Electrochemistry – Theory, Experiment and Applications*, A. Wieckowski, Ed., Marcel Dekker Inc., New York, 1999, p. 769
2. De Nora elettrodi network, http://www.denora.com/Products/tabid/66/Default.aspx (February, 2009)
3. F. Beck, *Electrochim. Acta* **34** (1992) 811
4. L. M. Gajić-Krstajić, T. L. Trišović, N. V. Krstajić, *Corr. Sci*. **46** (2004) 65
5. V. Jovanović, A. Dekanski, P. Despotov, B. Nikolić, R. Atanasoski, *J. Electroanal. Chem*. **339** (1992) 147
6. V. Panić, A. Dekanski, V. B. Mišković–Stanković, S. Milonjić, B. Nikolić, *J. Electroanal. Chem*. **579** (2005) 67
7. V. V. Gorodetskii, V. A. Neburchilov, V. I. Alyab'eva, *Russ. J. Electrochem*. **41** (2005) 1111
8. T.-X. Cai, H. Chen, H. Ju, L.-N. Lu, *Corr. Prot.* **27** (2006) 522
9. C. Liang, N. Huanga, *Mater. Chem. Phys.* **111** (2008) 244–248
10. V. Panić, A. Dekanski, S. Milonjić, R. Atanasoski, B. Nikolić, *Electrochim. Acta* **46** (2000) 415
11. V. V. Panić, B. Ž. Nikolić, *J. Serb. Chem. Soc*. **73** (2008) 1083
12. V. V. Panić, B. Ž. Nikolić, *J. Serb. Chem. Soc*. **72** (2007) 1393
13. V. V. Panić, A. B. Dekanski, M. Mitrić, S. K. Milonjić, V. B. Mišković-Stanković, B. Ž. Nikolić, *Phys. Chem. Chem. Phys.* **12** (2010) 7521
14. V. V. Panić, *J. Serb. Chem. Soc*. **73** (2008) 661.

Journal of the Serbian Chemical Society
JSCS-info@shd.org.rs • www.shd.org.rs/JSCS
J. Serb. Chem. Soc. *75* (10) 1421–1434 (2010)
JSCS–4064
UDC 542.97+544.6.076.32–033.5:
665.7.035.7.000.57
Original scientific paper

Preparation and electrochemical application of rutin biosensor for differential pulse voltammetric determination of NADH in the presence of acetaminophen

HAMID R. ZARE*, REZA SAMIMI, NAVID NASIRIZADEH and MOHAMMAD MAZLOUM-ARDAKANI

Department of Chemistry, Yazd University, Yazd, 89195-741, Iran

(Received 9 February, revised 14 May 2010)

Abstract: The electrocatalytic behavior of reduced nicotinamide adenine dinucleotide (NADH) was studied at the surface of a rutin biosensor, using various electrochemical methods. According to the results, the rutin biosensor had a strongly electrocatalytic effect on the oxidation of NADH with the overpotential being decreased by about 450 mV as compared to the process at a bare glassy carbon electrode, GCE. This value is significantly greater than the value of 220 mV that was reported for rutin embedded in a lipid-cast film. The kinetic parameters of the electron transfer coefficient, α, and the heterogeneous charge transfer rate constant, k_h, for the electrocatalytic oxidation of NADH at the rutin biosensor were estimated. Furthermore, the linear dynamic range; sensitivity and limit of detection for NADH were evaluated using the differential pulse voltammetry method. The advantages of this biosensor for the determination of NADH are excellent catalytic activity and reproducibility, good detection limit and high exchange current density. The rutin biosensor could separate the oxidation peak potentials of NADH and acetaminophen present in the same solution while at a bare GCE, the peak potentials were indistinguishable.

Keywords: electrocatalytic behavior; rutin; NADH; biosensor, acetaminophen.

INTRODUCTION

The electrochemical oxidation of dihydronicotinamide adenine dinucleotide (NADH) to the corresponding oxidized form (NAD^+) in aqueous solution has received considerable attention. This is due to its significance both as a cofactor for dehydrogenase enzymes and its role in the NAD^+/NADH redox couple of the electron transfer chain. A great number of NADH-dependent dehydrogenases are often used in biochemical analysis, mostly in enzymatic assays.[1,2] However, the

* Corresponding author. E-mail: hrzare@yazduni.ac.ir
doi: 10.2298/JSC100209111Z

direct oxidation of NADH at an unmodified electrode surface is highly irreversible and occurs at a considerable overpotential.[3] Moreover, possible side-products formed during the NADH redox process can be adsorbed on the electrode surface, leading to electrode fouling.[4] A decrease occurs in the overpotential of the oxidation of NADH through immobilization of some redox compounds on an electrode surface.[5–18] The compounds are able to mediate the electron transfer between NADH and the electrode. The strategy of electrode modification is to decrease the overvoltage for NADH and have good catalytic properties. Various inorganic and organic materials, such as transition metal hexacyanoferrates,[5–7] phenazines,[8,9] phenoxazines,[10–12] thionine derivatives,[13] hydroquinone derivatives[14–20] and carbon nanotubes,[21] showed interesting catalytic properties for the electro-oxidation of NADH.

Acetaminophen (N-acetyl-*p*-aminophenol or parcetamol) is used widely all over the world as a pharmaceutical analgesic and antipyretic agent. Hence, it is necessary to develop a rapid, precise and reliable method for the determination of acetaminophen. Recently, multiwall carbon nanotubes,[22] hematoxylin,[23] cobalt hydroxide nanoparticles[24] and nano-TiO_2[25] modified electrodes were fabricated and applied to the electrochemical determination of acetaminophen.

The electrochemical behavior of rutin,[26,27] the preparation of a few rutin modified electrodes and the investigation of their electrocatalytic effect for some important species[28–31] were reported. Rutin, as a biological important molecule, is a derivative of catechol and has the basic structure of many natural products with physiological activities. Thus, it seems that the use of rutin as a modifier could be important and could yield some new information concerning the catalysis of slow reactions. In continuation of studies into the preparation of biosensors for the determination of NADH,[14–18] the present study focuses on the fabrication of a rutin biosensor and its electrocatalytic effect on the oxidation of NADH. Cyclic voltammetry was used to characterize the electrocatalytic behavior of the rutin biosensor toward NADH oxidation. To evaluate the utility of the rutin biosensor for analytical application, it was used for the differential pulse voltammetric detection of NADH. The findings indicate that the rutin biosensor had several distinct advantages, including excellent catalytic activity and reproducibility, good detection limit, and high exchange current density for NADH. Differential pulse voltammetry was also used to evaluate the analytical performance of the biosensor in the quantification of NADH in the presence of acetaminophen.

EXPERIMENTAL

All the electrochemical experiments were realized using a potentiostat PGSTAT 30 model from Autolab (Netherland) equipped with GPES 4.9 software. The geometric area of the glassy carbon-working electrode (Azar Electrode, Iran), was 0.031 cm^2. A platinum electrode and a saturated calomel electrode (SCE) were used as the counter and reference electrodes, respectively. All the potentials are reported with respect to this reference electrode.

NADH-Na_2 (92 % purity), acetaminophen and the chemicals required for the preparation of the buffer solution were obtained from Merck and used as received. Rutin was purchased from Fluka and used without further purification. All the employed chemical reagents were of analytical grade. All the solutions were prepared with doubly distilled water. The NADH and the rutin solutions were prepared immediately prior to use.

For the preparation of the rutin biosensor, a glassy carbon electrode, GCE, was first polished mechanically with 0.05 μm alumina in a water slurry using a polishing cloth. Then, the electrode was rinsed with doubly distillated water. The electrochemical activation of the GCE was performed by continuous potential cycling from –1.1 to 1.6 V at a sweep rate of 100 mV s^{-1} in a sodium bicarbonate (0.10 M) solution until a stable voltammogram was obtained. For the construction of the biosensor, an activated electrode was placed in a 1.0 mM solution of rutin in 0.10 M phosphoric acid (pH 2.0). Then it was modified by 6 potential sweep cycles between 300 and 650 mV at 25 mV s^{-1}. Subsequently, the modified electrode was rinsed with water and placed in a buffer solution (pH 7.0) to test its electrocatalytic behavior.

RESULTS AND DISCUSSION

Properties of the electrodeposited rutin layer at the activated glassy carbon electrode

To investigate the possible mechanism of rutin electrodeposition on the activated glassy carbon electrode (AGCE), the effect of the number of potential recycling during the preparation of the biosensor on its cyclic voltammetric responses was studied. For this propose, electrodeposited rutin layers were prepared from a 1.0 mM solution of rutin at pH 2.0 using a different number of potential cycles. The effect of the number of potential cycles used for surface modification on the voltammetric response of the modified electrode is illustrated in Fig. 1A. The resulting surface coverage of rutin on the AGCE surface was then monitored as function of number of potential cycles. The surface coverage was evaluated from the cyclic voltammograms recorded at 100 mV s^{-1} in 0.1 M phosphate buffer (pH 7.0), using the equation $\Gamma = Q/nFA$, where Q is the charge obtained by integrating the anodic peak under the background correction and other symbols have their usual meanings. Figure 1B shows that both the anodic and cathodic surface coverage increased with increasing the number of potential cycles in the range of 1–6 cycles and then started to level off for more than six potential cycles.

Studies of the mechanism of electrodeposition of *o*- and *p*-quinone derivatives onto AGCE indicated that the immobilization of such compounds is based on a nucleophilic attack of the quinones resulting from the oxidation of the parent hydroquinone.[18,19] When AGCE is used as the platform for the electro-oxidation of rutin, carboxyl and hydroxyl groups on the activated surface of the GCE[18] behave as nucleophiles against the *o*-quinone formed from rutin oxidation. Indeed, the surface active functional groups, as nucleophiles, attack the position 6' of the oxidized form of rutin[30] that plays the role of a Michael acceptor.[32] Such a process leads to chemical bond formation between the oxidized form of rutin and the surface active groups and, hence, to the deposition of rutin on the AGCE surface.

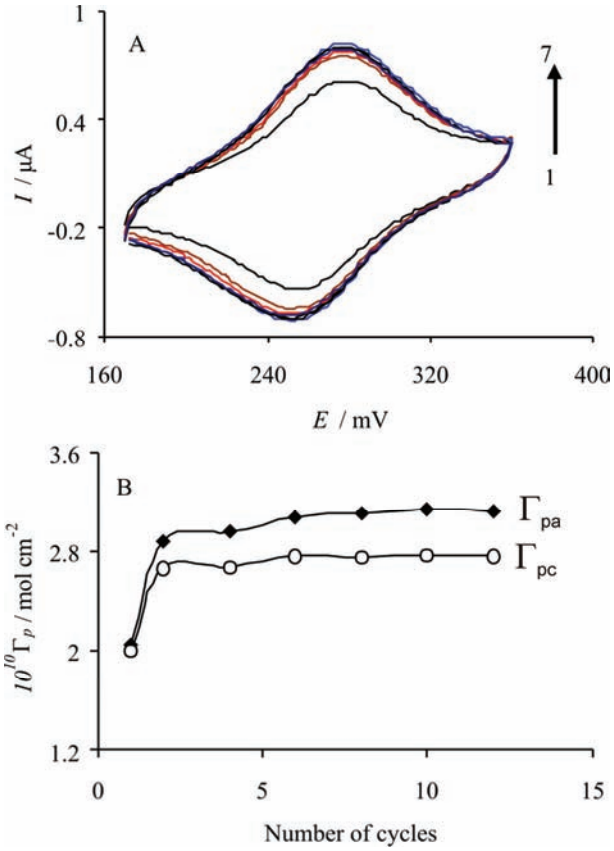

Fig. 1. A) Cyclic voltammetric responses of the rutin biosensor in 0.10 M phosphate buffer (pH 7.0) at 25 mV s^{-1}. The biosensor was modified under the conditions 1.0 mM rutin concentration, pH 2.0, scan rate 25 mV s^{-1} and different numbers of potential cycling. The numbers of 1–7 correspond to 1, 2, 4, 6, 8, 10 and 12 potential cycles which used during for the preparation of the biosensor. B) Variation of the anodic and cathodic peak surface coverage as a function of number of potential cycle sweeps.

Electrocatalytic oxidation of NADH at the rutin biosensor

The electrocatalytic effect of the rutin biosensor on the oxidation of NADH is shown in Fig. 2. The cyclic voltammetry responses of the rutin biosensor in 0.1 M phosphate buffer (pH 7.0) without and with 0.50 mM NADH in the solution are shown by curves a and b, respectively. Under the same experimental conditions, the direct oxidation of NADH at a bare GCE shows an irreversible wave at a more positive potential (curve c).

It can be seen that the oxidation peak potential of NADH at the rutin biosensor surface was shifted by about 450 mV toward negative values as compared with that at a bare GCE, which is significantly greater than the value of 220 mV previously reported for rutin embedded in a lipid-cast film.[29] The higher electrocatalytic oxidation overpotential of NADH at rutin embedded in a lipid-cast film might arise due to non-ideal behavior caused by the effects of charge transfer and an uncompensated ohmic drop of the lipid film.[33] In addition, an enhancement of the peak current was achieved with the biosensor. This behavior is consistent with

a very strong electrocatalytic effect. According to an EC catalytic mechanism ($E_rC'_i$), the process can be expressed as follows:

$$RB_{red} \rightleftharpoons RB_{ox} + 2H^+ + 2e^- \quad (1)$$

$$RB_{ox} + NADH \xrightarrow{k_h} RB_{red} + NAD^+ \quad (2)$$

The overall oxidation of NADH by the biosensor is given by Eq. (3).

$$NADH \longrightarrow NAD^+ + 2H^+ + 2e^- \quad (3)$$

where RB_{ox} and RB_{red} stand for the oxidized and reduced form of the rutin bonded on the biosensor, respectively.

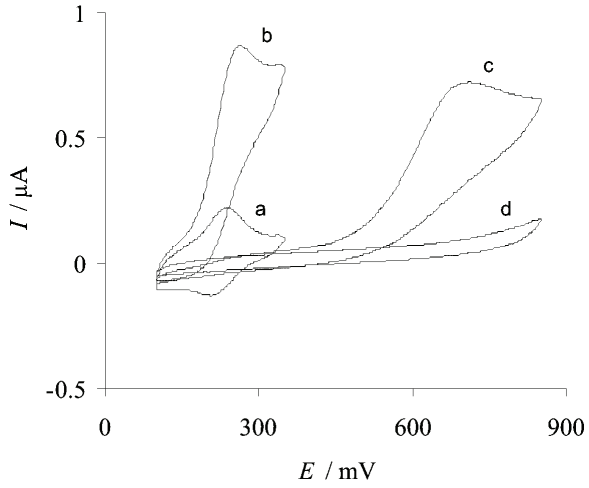

Fig. 2. Cyclic voltammetric responses of a) the rutin biosensor in 0.10 M phosphate buffer solution (pH 7.0) and b) the same biosensor in the same solution containing 0.50 mM NADH. Curves d as a and c as b for a bare GCE. In all cases, the scan rate was 25 mV s^{-1}.

Kinetics studies of NADH electrocatalytic oxidation at the rutin biosensor

The scan rate dependence of the cyclic voltammograms for the rutin biosensor in 0.10 M phosphate buffer (pH 7.0) solution containing 0.25 mM NADH (Fig. 3, inset) was used for studies of the electrocatalytic reaction kinetics of NADH. Fig. 3, curve a, shows that the peak potential, E_p, is proportional to log v.

The Tafel slope (b in Eq. (4)) may be estimated according to Eq. (4) for a totally irreversible diffusion-controlled process:[34]

$$E_p = (b \log v)/2 + \text{constant} \quad (4)$$

Considering $dE_p/d(\log v) = 39$ mV (Fig. 3, curve a), it can be indicated that a one-electron transfer is the rate-limiting step, assuming an electron transfer coefficient of $\alpha = 0.24$ between the rutin biosensor and NADH. One of the important parameters in electrocatalytic applications is the heterogeneous catalytic electron transfer rate constant, k_h, in the reaction of the catalyst (deposited modifier) with

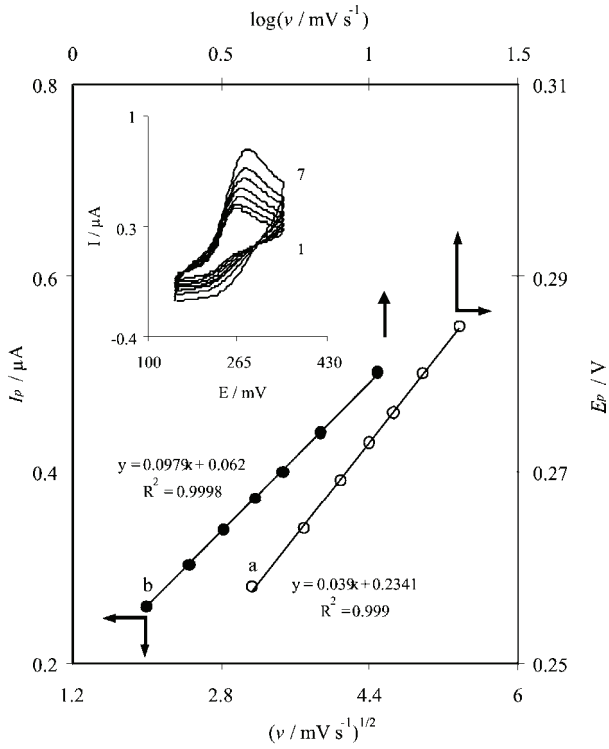

Fig. 3. Variation of a) the of peak potential *vs.* logarithm scan rate and b) the electrocatalytic peak current *vs.* the square root of scan rate, which was obtained from cyclic voltammetric responses of the rutin biosensor in 0.10 M phosphate buffer (pH 7.0) containing 0.25 mM NADH. The inset shows the cyclic voltammograms of the rutin biosensor in 0.10 M phosphate buffer (pH 7.0) containing 0.25 mM NADH at different scan rates. The numbers of 1 to 7 correspond to scan rates of 4, 6, 8, 10, 12, 15 and 20 mV s^{-1}.

the substrate. Fig. 3, curve b, shows the electrocatalytic oxidation currents for NADH increase linearly with the square root of the scan rate, indicating that, at a sufficient overpotential, the reaction is diffusion controlled. In addition, as previously mentioned, the oxidation of NADH at the rutin biosensor exhibits the characteristic of a catalytic reaction mechanism ($E_rC'_i$). Under these conditions, k_h can be calculated using the theoretical model which was developed by Andrieux and Saveant.[35] For large values of the catalytic rate constant parameter defined in their paper, the electrocatalytic current can be expressed by Eq. (5):

$$I_{cat} = 0.496nFAc_0(DnFv)^{1/2}(RT)^{-1/2} \quad (5)$$

where A is the electrode surface, c_0 the bulk concentration of the substrate, v the scan rate, D the diffusion coefficient of the substrate (obtained by chronoamperometry), and the other symbols have their usual meanings. Small values of the kinetic parameter result in a prefactor lower than 0.496. The slope of the plot of I_p *versus* $v^{1/2}$ (Fig. 3, curve b) was used to evaluate the prefactor. For low scan rates of 4 to 20 mV s^{-1}, the average value of this prefactor was found to be 0.3 for the rutin biosensor with a surface coverage of 3.1×10^{-10} mol cm^{-2} in the presence of 0.25 mM NADH. According to the approach adopted by Andrieux and Saveant and using Fig. 1 of their paper, the average value of k_h was found to be 1.9×10^3

M^{-1} s^{-1}. In addition, the slope of curve b of Fig. 3 was used to estimate the total number of electrons involved in the electrocatalytic oxidation of NADH at the biosensor. According to the following equation for a totally irreversible process:[36]

$$I_P = 3.01\times10^5 n[(1-\alpha)n_\alpha]^{1/2} Ac_0 D^{1/2} v^{1/2} \quad (6)$$

and by considering $(1–\alpha)n_\alpha$ = 0.74 and $D = 6.04\times10^{-7}$ cm^2 s^{-1} (see below), it was estimated that the total number of electrons involved in the electrocatalytic oxidation of NADH was n = 1.95, *i.e.*, ≈ 2. The Tafel slope, b, was obtained by another method. Fig. 4, inset, shows the linear sweep voltammograms of the biosensor in 0.10 M phosphate buffer (pH 7.0) containing 0.25 mM NADH at two scan rates, *i.e.*, 15 and 20 mV s^{-1}. The Tafel plots were drawn using the data of the rising part of the current-voltage curves at the two scan rates (Fig. 4). An average Tafel slope of 0.012 mV^{-1} was obtained, indicating that a one-electron process was involved in the rate-determining step, assuming a charge transfer coefficient of α = 0.27. This result is similar to that obtained for α using the first method. In addition, the average value of the current density, j_0, was found to be 0.014 μA cm^{-2} from the intercept of the Tafel plot.

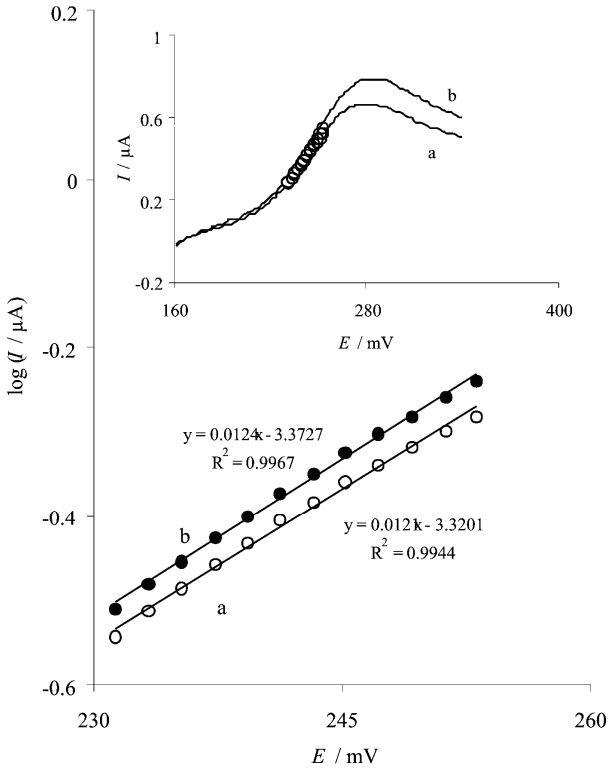

Fig. 4. The Tafel plots derived from the linear sweep voltammograms shown in the inset. The inset shows the linear sweep voltammetric responses of the rutin biosensor at scan rates of a) 15 and b) 20 mV s^{-1}. The solution conditions were the same as those given in the caption to Fig. 3.

Chronoamperometric and amperometric studies

The catalytic oxidation of NADH by the rutin biosensor was also studied by chronoamperometry. In this study, the diffusion coefficient of NADH was determined at the biosensor surface. The chronoamperograms of the biosensor in 0.10 M phosphate buffer (pH 7.0) containing different concentrations of NADH, which were obtained at a potential step of 260 mV, are shown in Fig. 5. The inset to Fig. 5, shows the experimental plots of I *versus* $t^{-1/2}$ with the best straight lines shown for the different concentrations of NADH employed. From the slopes of the resulting straight lines and using the Cottrell Equation,[37] an average diffusion coefficient of 6.04×10^{-7} cm^2 s^{-1} was calculated for NADH.

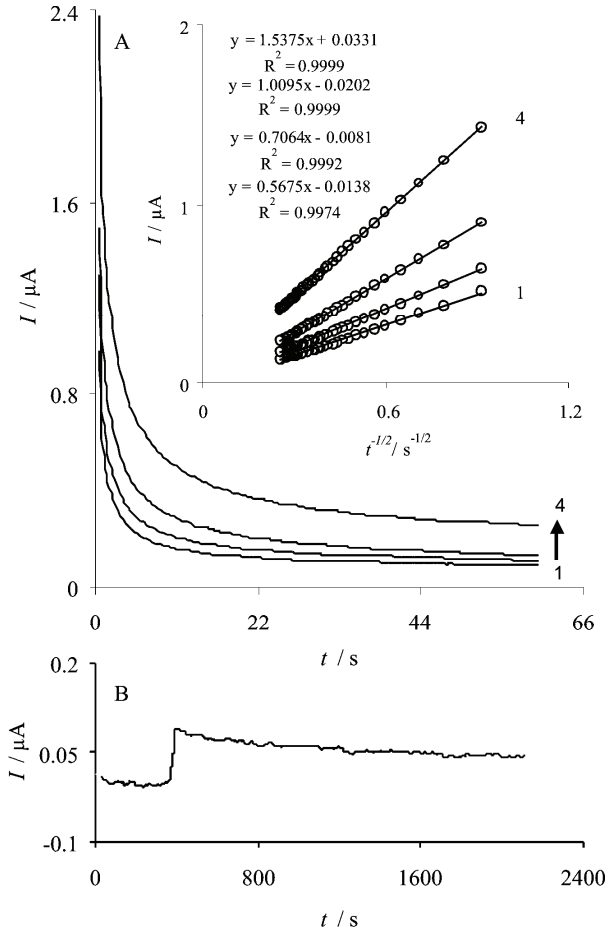

Fig. 5. A) The chronoamperometric responses of the rutin biosensor in 0.10 M phosphate buffer (pH 7.0) containing different concentrations of NADH at potential step of 260 mV. The numbers 1 to 4 correspond to the concentrations of 0.29, 0.32, 0.36 and 0.45 mM NADH, respectively. The inset shows the plots of I *vs.* $t^{-1/2}$ obtained from the chronoamperograms. B) Stability of the amperometric response of the rutin biosensor (rotation 2000 rpm) held at 260 mV in 0.10 M phosphate buffer (pH 7.0) containing 0.20 mM NADH.

This value of the diffusion coefficient is in good agreement with some values reported in the literature[16,38,39] but differs from those reported by others.[14,40,41]

In addition, amperometry under stirring conditions was employed to estimate the long-term stability of the biosensor. The amperometric response of 0.20 mM NADH as recorded over a continuous 2110 s period is shown in Fig. 5B. As can be seen, the response of the biosensor after an initial decrease remained almost stable throughout the experiment. This fact indicates that there was no inhibition effect of NADH and its oxidation products on the rutin biosensor.

Differential pulse voltammetric detection of NADH at the rutin biosensor

Differential pulse voltammetric, DPV, measurements were used to determine the linear range and to estimate the detection limit of NADH at the rutin biosensor. The voltammograms obtained for different concentrations of NADH are depicted in Figs. 6A and 6B. These figures show voltammograms in the NADH concentration ranges of 8.3–46.3 μM (Fig. 6A) and 55.5–833 μM (Fig. 6B). As shown in Fig. 6A, during the addition of even 1.7 μM NADH, a well-defined response was observed. The dependence of the electrocatalytic peak current, corrected for any background current of the biosensor in the supporting electrolyte, on the NADH concentration is shown in Figs. 6C and 6D.

These figures clearly show that the plot of the peak current *versus* NADH concentration is constituted of two linear segments with different slopes, corresponding to two different NADH concentration ranges of 8.3–151.5 μM (Fig. 6C) and 151.5–833.3 μM (Fig. 6D). The linear least square calibration curves over the two linear ranges indicate that the regression lines fit very well with the experimental data and the regression equations can be applied for the determination of NADH in unknown samples. Since DPV method has a much higher current sensitivity than the cyclic voltammetry method, the slope (m) of the calibration plot in the first linear range (Fig. 6C) was used to estimate the detection limit of NADH at the rutin biosensor. According to the method mentioned in reference,[42] the lower detection limit, c_m, was obtained using the equation $c_m = 3s_{bl}/m$, where s_{bl} is the standard deviation of the blank response (μA). From an analysis of these data, the limit of detection of NADH was estimated to be 1.6 μM. The analytical parameters of the electrocatalytic determination of NADH in this work are compared in Table I with the corresponding values previously reported for some biosensors.[14–18,20,29,43] As can be seen, the responses of the proposed biosensor are comparable and even better than those obtained using several modified electrodes. In addition, a small variation in the sensitivity was observed when the concentration of NADH was changed in the two calibration ranges. The average voltammetric peak current for 18 repeated measurements (n = 18) of 55.5 μM NADH at the biosensor was 0.055±0.001 μA, which indicate that the biosensor is stable and also the results obtained are reproducible.

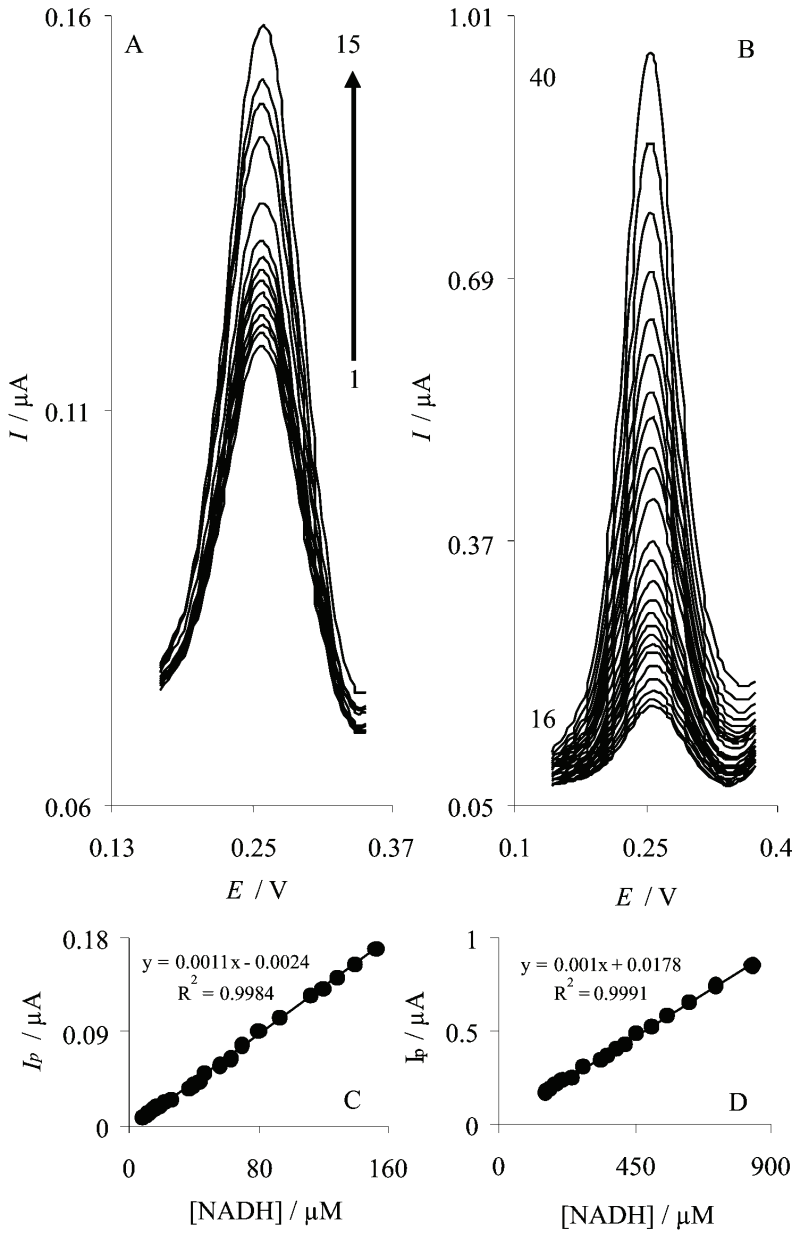

Fig. 6. A) and B) show differential pulse voltammetric responses of the rutin biosensor in 0.10 M phosphate buffer (pH 7.0) containing different concentrations of NADH. The numbers of 1–15 and 16–40 correspond to NADH concentration ranges of 8.3–46.3 μM and 55.5–833 μM, respectively. C) and D) show the dependence of the electrocatalytic peak current, corrected for any background current of the biosensor in the supporting electrolyte, on the NADH concentrations in the ranges of 8.3–152 μM and 151.5–833 μM, respectively.

TABLE I. Comparison of the analytical parameters of the several biosensors for the determination of NADH (CFA: caffeic acid; PCV: pyrocatechol violet; CGA: chlorogenic acid; PDA: *o*-phenylenediamine; DPPC: dipalmitoylphosphatidylcoline; GCE: glassy carbon electrode; CPE: carbon paste electrode; DPV: differential pulse voltammetry; CV: cyclic voltammetry)

Modifier	Electrode	Method	Linear range μM	Detection limit μM	Sensitivity μA μM^{-1}	Ref.
CFA	GCE	CV	50.0–1000	–	0.0022	14
PCV	GCE	Amperometry	2.5–200	1.03	0.000029	15
			200.0–1500		0.00034	
Coumestan	CPE	DPV	1.0–10	0.1	0.0103	16
			10–400		0.0028	
Hematoxylin	GCE	DPV	0.40–600	0.08	0.0028	17
CGA	GCE	CV	100–1000	–	–	18
An imine derivative	Pt	CV	200–2000	–	0.0012	20
Rutin	GCE-DPPC	CV	–	–	–	25
PDA	CPE	Amperometry	40.0–800	7.1	0.0242	40
Rutin	GCE	DPV	8.3–152	1.6	0.0011	This
			152–833		0.0010	work

Simultaneous determination of NADH and acetaminophen

At most bare solid electrodes, NADH is usually oxidized at a potential close to the potential of acetaminophen (AC) oxidation. The differential pulse voltammograms obtained with increasing concentrations of NADH in the presence of different concentrations of AC at the rutin biosensor are shown in Fig. 7A and the inset shows the DPV of a mixture of 500.0 μM NADH and 125.0 μM AC at a bare GCE. As can be seen, the bare electrode shows poorly-defined oxidation peaks for the mixture of NADH and AC (Fig. 7A, inset). However, the rutin biosensor separates the voltammetric signals of NADH and AC and two well-distinguished anodic peaks at potentials of 254 and 364 mV, corresponding to the oxidation of NADH and AC, respectively, are observed.

Furthermore, substantial increases in peak currents were also observed with increasing concentrations of NADH and AC. The calibration curves for NADH and AC are shown in Fig. 7B–7E. These figures clearly show that the plot of peak current *versus* NADH or AC concentration is constituted of two linear segments with different slopes, corresponding to two different ranges of substrate concentration. The peak current of NADH was linear with respect to the concentration in the ranges of 42.7–166 μM (Fig. 7B) and 166.5–625.0 μM (Fig. 7C) with linear equations of I_p (μA) = 0.0325 + 0.0021[NADH] (μM) and I_p (μA) = = 0.2512 + 0.0009[NADH] (μM). Similarly, the current intensity corresponding to the oxidation of AC increased linearly with increasing AC concentration in the ranges of 13.9–55.5 (Fig. 7D) and 55.5–214 μM (Fig. 7E). The linear regression

equations of the two calibration plots were expressed as I_p (μA) = 0.1922 + + 0.0091[AC] (μM) and I_p (μA) = 0.4799 + 0.0041[AC] (μM), respectively.

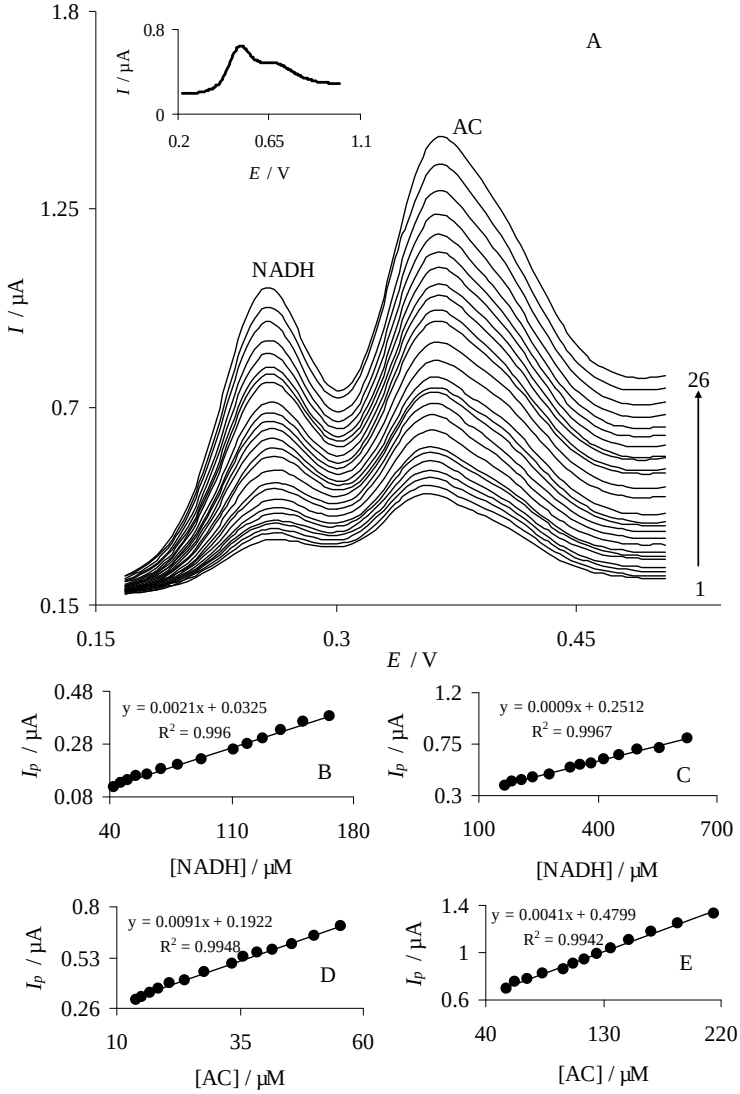

Fig. 7. A) Differential pulse voltammetric responses of the rutin biosensor in 0.10 M phosphate buffer (pH 7.0) in mixed solutions of NADH and acetaminophen (AC). The numbers 1–26 correspond to the different concentrations of 42.7–625.0 μM NADH and 13.9–214.3 μM AC that were present in the various mixtures. The inset shows the response of a mixed solution of 500.0 μM NADH and 125.0 μM AC at a bare GCE. Plots of the peak currents as concentration of B) NADH in the range of 42.7–166.5 μM, C) NADH in the range of 166.5–625.0 μM, D) AC in the range of 13.9–55.5 μM and E) AC in the range of 55.5–214.3 μM.

CONCLUSIONS

The obtained results show that a rutin biosensor exhibits excellent electrocatalytic activity and reproducibility for NADH oxidation. The diffusion coefficient of NADH was calculated using chronoamperometric results as 6.04×10^{-7} cm^2 s^{-1} under the employed experimental conditions. For the oxidation of NADH at the rutin biosensor, average values for the electron transfer coefficient, α, current density, j_0, and the heterogeneous charge transfer rate constant, k_h, of 0.27, 0.014 μA cm^{-2} and 1.9×10^3 M^{-1} s^{-1} were obtained, respectively. Linear sweep and cyclic voltammetric methods were used for this purpose. The differential pulse voltammetric method was used for the determination of the detection limit, sensitivity and the linear range of NADH at the rutin biosensor. The most important advantages of the rutin biosensor for NADH determination are excellent catalytic activity and reproducibility, good detection limit, and high exchange current density. Unlike bare GCE, the rutin biosensor could separate the oxidation peaks of NADH and acetaminophen when present in the same solution.

ИЗВОД

ПРИПРЕМА И ПРИМЕНА БИОСЕНЗОРА НА БАЗИ РУТИНА ЗА ЕЛЕКТРОХЕМИЈСКО ОДРЕЂИВАЊЕ NADH У ПРИСУСТВУ АЦЕТАМИНОФЕНА ДИФЕРЕНЦИЈАЛНОМ ПУЛСНОМ ВОЛТАМЕТРИЈОМ

HAMID R. ZARE, REZA SAMIMI, NAVID NASIRIZADEH и MOHAMMAD MAZLOUM-ARDAKANI

Department of Chemistry, Yazd University, Yazd, 89195-741, Iran

Коришћењем различитих електрохемијских метода испитивано је електрокаталитичко понашање редукованог никотинамид аденин динуклеотида (NADH) на површини биосензора на бази рутина. Резултати су показали да биосензор на бази рутина испољава јак каталитички ефекат на оксидацију NADH уз смањење пренапетости за око 450 mV у односу на реакцију на стакластом угљенику. Ово смањење пренапетости је знатно веће од 220 mV, што је вредност објављена за случај рутина који је био уграђен у липидни филм. У раду су одређени кинетички параметри електрокаталитичке оксидације NADH – коефицијент прелаза, α, и константа брзине хетерогеног преноса наелектрисања, k_h. Диференцијалном пулсном волтаметријом је одређен линеарни динамички опсег, затим осетљивост и граница детекције NADH. Предности биосензора на бази рутина за одређивање NADH су одлична каталитичка активност и репродуктивност, ниска граница детекције и висока густина струје измене. Биосензор на бази рутина може да раздвоји пикове оксидације NADH и ацетаминофена из истог раствора, док се на чистом стакластом угљенику поменути пикови преклапају.

(Примљено 9. фебруара, ревидирано 14. маја 2010)

REFERENCES

1. R. D. Braun, *J. Electrochem. Soc.* **124** (1977) 1342
2. R. Blonder, E. Katz, I. Willner, V. Wray, A. F. Buckmann, *J. Am. Chem. Soc.* **119** (1997) 11747
3. C.-X. Cai, K.-H. Xue, *Microchem. J.* **64** (2000) 131
4. M. Aizawa, R. W. Coughlin, M. Charles, *Biochim. Biophys. Acta* **385** (1975) 362
5. C. X. Cai, H. X. Ju, H. Y. Chen, *J. Electroanal. Chem.* **397** (1995) 185

6. C. X. Cai, H. X. Ju, H. Y. Chen, *Anal. Chim. Acta* **310** (1995) 145
7. M. Somasundrun, J. Hall, J. V. Bannister, *Anal. Chim. Acta* **295** (1994) 47
8. J. J. Kulys, *Anal. Lett.* **14** (1981) 377
9. A. Torstensson, L. Gorton, *J. Electroanal. Chem.* **130** (1981) 199
10. B. Persson, L. Gorton, *J. Electroanal. Chem.* **292** (1990) 115
11. F. Ni, H. Feng, L. Gorton, T. M. Cotton, *Langmuir* **6** (1990) 66
12. L. Gorton, A. Torestensson, H. Jaegfeldt, G. Johansson, *J. Electroanal. Chem.* **161** (1984) 103
13. K. Hajizadeh, H. T. Tang, H. B. Halsall, W. R. Heinemann, *Anal. Lett.* **24** (1991) 1453
14. H. R. Zare, S. M. Golabi, *J. Solid. State Electrochem.* **4** (2000) 87
15. S. M. Golabi, H. R. Zare, M. Hamzehloo, *Electroanalysis* **14** (2002) 611
16. H. R. Zare, N. Nasirizadeh, S. M. Golabi, M. Namazian, M. Mazloum-Ardekani, D. Nematollahi, *Sens. Actuators B* **114** (2006) 610
17. H. R. Zare, N. Nasirizadeh, M. Mazloum-Ardakani, M. Namazian, *Sens. Actuators B* **120** (2006) 288
18. H. R. Zare, S. M. Golabi, *J. Electroanal. Chem.* **464** (1999) 14
19. F. Pariente, E. Lorenzo, H. D. Abruna, *Anal. Chem.* **66** (1994) 4337
20. E. Lorenzo, L. Sanchez, F. Pariente, J. Tirado, H. D. Abruna, *Anal. Chim. Acta* **309** (1995) 79
21. M. Musameh, J. Wang, A. Merkoci, Y. Lin, *Electrochem. Commun.* **4** (2002) 743
22. Z. A. Alothman, N. Bukhari, S. M. Wabaidur, S. Haider, *Sens. Actuators B* **146** (2010) 314
23. N. Nasirizadeh, H. R. Zare, *Talanta* **80** (2009) 656
24. M. Houshmand, A. Jabbari, H. Heli, M. Hajizadeh, A. A. Moosavi-Movahedi, *J. Solid State Electrochem.* **12** (2008) 1117
25. S. A. Kumar, C.-F. Tang, S.-C. Chen, *Talanta* **76** (2008) 997
26. H. R. Zare, R. Samimi, M. Mazloum-Ardakani, *Int. J. Electrochem. Sci.* **4** (2009) 730
27. M. E. Ghica, A. M. O. Brett, *Electroanalysis* **17** (2005) 313
28. J. Tang, Z. Wu, J. Wang, E. Wang, *Electroanalysis* **13** (2001) 1315
29. J. Tang, Z. Wu, J. Wang, E. Wang, *Electrochem. Commun.* **2** (2000) 796
30. H. R. Zare, Z. Sobhani, M. Mazloum-Ardakani, *Sens. Actuators B* **126** (2007) 641
31. H. R. Zare, Z. Sobhani, M. Mazloum-Ardakani, *J. Solid. State Electrochem.* **11** (2007) 971
32. S. M. Golabi, D. Nematollahi, *J. Electroanal. Chem.* **430** (1997) 141
33. H. Jaegfeldt, A. B. C. Torstensson, L. G. O. Gorton, G. Johansson, *Anal. Chem.* **53** (1981) 1979
34. J. A. Harrison, Z. A. Khan, *J. Electroanal. Chem.* **28** (1970) 131
35. C. P. Andrieux, J. M. Saveant, *J. Electroanal. Chem.* **93** (1978) 163
36. S. Antoniadou, A. D. Jannakoudakis, E. Theodoridou, *Synth. Met.* **30** (1989) 295
37. A. J. Bard, L. R. Faulkner, *Electrochemical methods: Fundamentals and Applications*, Wiley, New York, 2001.
38. Z. Y. Wu, W. G. Jing, E. Wang, *Electrochem. Commun.* **1** (1999) 545
39. S. M. Golabi, L. Irannejad, *Electroanalysis* **17** (2005) 985
40. J. Moiroux, P. J. Elving, *J. Am. Chem. Soc.* **102** (1980) 6533
41. F. Pariente, E. Lorenzo, F. Tobalina, H. D. Abruna, *Anal. Chem.* **67** (1995) 3936
42. D. A. Skoog, F. J. Holler, T. A. Nieman, *Principles of Instrumental Analysis*, 5th ed., Saunders College Publishing, London, 1998
43. A. C. Pereira, A. S. Santos, L. T. Kubota, *Electrochim. Acta* **48** (2003) 3541.

Journal of the Serbian Chemical Society
JSCS-info@shd.org.rs • www.shd.org.rs/JSCS
J. Serb. Chem. Soc. 75 (10) 1435–1439 (2010)
JSCS–4065
UDC 539.12:66.094.1:544.6.004.12
Extended abstract

EXTENDED ABSTRACT

The electrochemical properties of carbon nanotubes and carbon XC-72R and their application as Pt supports•

MAJA D. OBRADOVIĆ

Institute of Chemistry, Technology and Metallurgy, University of Belgrade, Njegoševa 12, 11000 Belgrade, Serbia

(Received 20 May 2010)

Abstract: The results of an investigation of two samples of commercial multi--walled carbon nanotubes and a sample of carbon black, in the raw and activated state, were presented in the lecture. The activation of the carbon materials led to the formation of an abundance of oxygen-containing functional groups on the surface, an increased electrochemically active surface area, an enhanced charge storage ability and a promotion of the electron-transfer kinetics. It was presented that the morphology of the carbon nanotubes is important for the electrochemical properties, because nanotubes with a higher proportion of edge and defect sites showed faster electron transfer and pseudocapacitive redox kinetics. Modification of oxidized nanotubes by ethylenediamine and wrapping by poly(diallyldimethylammonium chloride) led to a decrease in the electrochemically active surface area and to reduced electron-transfer kinetics. Pt nanoparticles prepared by the microwave-assisted polyol method were deposited at the investigated carbon materials. A much higher efficiency of Pt deposition was observed on the modified CNTs than on the activated CNTs. The activity of the synthesized catalyst toward electrochemical oxygen reduction was almost the same as the activity of the commercial Pt/XC-72 catalyst.

Keywords: carbon nanotubes; morphology; electrochemical properties; Pt nanoparticles; electrocatalyst for oxygen reduction.

Carbon nanotubes (CNTs) have attracted enormous attention because of their unique structure, excellent chemical and thermal stability, mechanical properties and, in some cases, even metallic conductivity.[1,2] The tubular structure of carbon

obradovic@ihtm.bg.ac.rs
Serbian Chemical Society member.
• Lecture at the Meeting of the Electrochemical Section of the Serbian Chemical Society, held 2 February, 2010.
doi: 10.2298/JSC100520081O

nanotubes makes them unique among different forms of carbon and they have proven themselves as extremely promising nanostructured materials for electrochemical application, such as catalysis,[3] chemical sensing,[4,5] and gas and energy storage.[6] The structure of the carbon material can play an important role in the dispersion of a catalyst, in its crystallographic characteristics and, consequently, in its electrochemical properties.[7,8]

In this lecture, a survey of the results of an investigation of the physicochemical and electrochemical properties of two types of commercial carbon nanotubes (Sigma-Aldrich and Sun Nanotech) and carbon black (Vulcan XC-72R), in the raw and acid-activated state, was presented. The carbon powders were activated by treating the samples with concentrated H_2SO_4 + HNO_3 in an ultrasonic bath. Changes in the chemical composition of the carbon surfaces upon activation were investigated by Fourier transform infrared spectroscopy and the Boehm titration method.[9–11] The results indicated that the groups formed on the surface were dominantly acid groups. The stability of water suspensions of the carbon powders before and after activation was investigated by UV–visible spectroscopy and it was registered that an abundance of oxygen-containing functional groups made the carbon surfaces more hydrophilic. The structural characterization of the carbon nanotubes, performed by atomic force microscopy, indicated that activated Sigma-Aldrich nanotubes were straight with the corrugated walls (bamboo-like structure), while the Sun Nanotech nanotubes are tortuous with smooth walls.

The influence of activation and morphology on the electrochemical properties of the carbon powders, applied on a gold substrate in the form of a thin-film, was investigated by cyclic voltammetry and electrochemical impedance spectroscopy in 0.10 M H_2SO_4 and in 1.0 M KCl. The steady-state capacitive potentiodynamic curves of the raw CNT feature a rectangular-shaped profile with a rather low specific capacitance. After activation, the capacitance increased and a pair of broad peaks appeared at around 0.6 V, which is commonly attributed to surface oxidation/reduction processes of the hydroquinone/quinone groups.[1,12,13]

The electron-transfer properties of the investigated carbons were probed by the simple redox transition of the $Fe(CN)_6^{3-}/Fe(CN)_6^{4-}$ couple in 1.0 M KCl + + 5.0 mM $K_4[Fe(CN)_6]$. The voltammograms of $Fe(CN)_6^{3-}/Fe(CN)_6^{4-}$ on the thin films of raw carbons show rather low currents with not well resolved redox peaks, while the activated carbons show an almost reversible currents transition superposed on high capacitance currents. The currents for the straight CNTs with corrugated walls were the highest and the peak separation was the closest to that of reversible kinetics. The results of a detailed interpretation of the EIS measurements were consistent with the properties of the carbons established by cyclic voltammetry. It was concluded that the nanotubes with the higher proportion of edge and defect sites were the most active for electron transfer processes, when compared to XC and tortuous nanotubes with smooth walls.

Modification of the CNTs with covalently attached ethylenediamine (eda)[8] and poly(diallyldimethylammonium chloride) (polymer), adsorbed on the surface of the nanotubes by electrostatic interaction[14] led to a certain agglomeration of the CNTs, a decrease in the capacitance of the material, and a reduced rate of electron transfer between the nanotubes and solution species. Addition of a nitrogen heteroatom to active carbon was used to form an electrode material with intermediate acid–base properties.[15] An investigation of the $Fe(CN)_6^{3-}/Fe(CN)_6^{4-}$ redox process on CNTs modified with diethylenetriamine, triethylenetetramine and 1,6-hexanediamine[11] indicated even more hindered electron transfer than on eda-CNT.[8]

A colloidal Pt solution was prepared in a microwave oven from H_2PtCl_6 with ethylene glycol as the reducing agent[7] and the Pt nanoparticles were supported on the investigated carbons. The Pt content was determined by thermogravimetric analysis of the deposited Pt/C in an oxygen atmosphere. The deposition of Pt nanoparticles on the oxidized CNTs resulted in a Pt/CNTs material with a very low Pt content. However, modification of oxidized CNTs with either eda or the polymer prior to mixing with the colloidal Pt solution increased the amount of deposited Pt. The much higher efficiency of Pt deposition on the modified CNTs than on the oxidized CNTs was ascribed to a decrease of the negative charge on the surface of the CNTs that was formed by dissociation of acidic oxygen-containing groups. An investigation by transmission electron microscopy (TEM) revealed that the mean diameter of Pt particles in Pt/eda-CNT was 2.5±0.5 nm and that their distribution on the support was homogenous with no evidence of pronounced agglomeration of the particles.

The electrochemical properties of the synthesized catalyst were investigated in 0.10 M H_2SO_4 by using cyclic voltammetry and compared to the results obtained with the commercial Pt/XC-72 catalyst manufactured by E-TEK. The real Pt surface was determined from the desorption charge of underpotentially deposited hydrogen. The polarization curves for oxygen reduction on all the investigated catalysts almost overlapped. The Tafel plots exhibited two distinct linear regions with a slope of $-2.3RT/F$ in the low current densities region and $-2.3\times2RT/F$ in the high current densities region, which are the same as those observed on polycrystalline Pt and Pt/C catalyst in acidic solution.[16] Although noble metal catalysts supported on CNTs were found to be more active for methanol oxidation than catalysts supported on other high area carbons,[7] a recent study[17] and the present results showed that the carbon support has no influence on the activity of the electrocatalysts for oxygen reduction.

Acknowledgements. The results presented in the lecture were obtained with the financial support of the Ministry of Science and Technological Development of the Republic of Serbia, Projects No. 142048 and 142056.

ИЗВОД

ЕЛЕКТРОХЕМИЈСКЕ КАРАКТЕРИСТИКЕ УГЉЕНИЧНИХ НАНОЦЕВИ И УГЉЕНИКА XC-72R И ЊИХОВА ПРИМЕНА У СИНТЕЗИ Pt КАТАЛИЗАТОРА

МАЈА Д. ОБРАДОВИЋ

Институт за хемију, технологију и металургију, Универзитет у Београду, Његошева 12, 11000 Београд, Србија

У оквиру предавања су приказани резултати испитивања две врсте комерцијалних вишеслојних угљеничних наноцеви и узорка угљеничног праха развијене површине пре и након активације хемијском оксидацијом. Оксидација узорака доводи до израженог формирања кисеоничних група на површини угљеничних материјала, повећања електрохемијски активне површине као и до убрзања преноса наелектрисања. Показано је да морфологија угљеничних наноцеви има значајан утицај на њихове електрохемијске карактеристике. Узорак са већим уделом ивица и дефеката показао је бржу кинетику преноса наелектрисања и већу псеудокапацитивност. Модификовање оксидованих наноцеви етилендиамином и полимером поли(диалилдиметиламонијум-хлоридом) доводи до смањења активне површине и до споријег преноса наелектрисања. Наночестице платине, синтетисане у раствору етиленгликола у микроталасној пећници, нанете су на испитиване угљеничне материјале. Количина нанете Pt је много већа на модификованим него на оксидованим наноцевима. Активност синтетисаних узорака за електрохемијску редукцију кисеоника је упоређена са активношћу комерцијалног катализатора Pt/XC-72 за исту реакцију и показало се да су њихове специфичне активности приближно једнаке.

(Примљено 20. маја 2010)

REFERENCES

1. J. J. Gooding, *Electrochim. Acta* **50** (2005) 3049
2. S. N. Marinković, *J. Serb. Chem. Soc*. **73** (2008) 891
3. K. Kinoshita, *Carbon, Electrochemical and Physicochemical Properties*, Wiley, New York, 1987
4. H. Tang, J. Chen, K. Cui, L. Nie, Y. Kuang, S. Yao, *J. Electroanal. Chem.* **587** (2006) 269
5. H. Yaghoubian, H. Karimi-Maleh, M. Ali Khalilzadeh, F. Karimi, *J. Serb. Chem. Soc.* **74** (2009) 1443
6. B. E. Conway, *Electrochemical Supercapacitors*, Kluwer Academic/Plenum Publishing, New York, 1999
7. X. Li, W. X. Chen, J. Zhao, W. Xing, Z. D. Xu, *Carbon* **43** (2005) 2168
8. G. D. Vuković, M. D. Obradović, A. D. Marinković, J. R. Rogan, P. S. Uskoković, V. R. Radmilović, S. L. Gojković, *Mater. Chem. Phys.*, submitted for publication
9. H. P. Boehm, *Carbon* **32** (1994) 759
10. M. D. Obradović, G. D. Vuković, S. I. Stevanović, V. V. Panić, P. S. Uskoković, A. Kowal, S. L. Gojković, *J. Electroanal. Chem.* **634** (2009) 22
11. G. Vuković, A. Marinković, M. Obradović, V. Radmilović, M. Čolić, R. Aleksić, P. S. Uskoković, *Appl. Surf. Sci*. **255** (2009) 8067
12. H. A. Andreas, B. E. Conway, *Electrochim. Acta* **51** (2006) 6510
13. E. Fuente, J. A. Menéndez, D. Suárez, M. A. Montes-Morán, *Langmuir* **19** (2003) 3505
14. K. Jiang, A. Eitan, L. S. Schandler, P. M. Ajayan, R. W. Siegel, N. Grobert, M. Mayne, M. Reyes-Reyes, H. Terrones, M. Terrones, *Nano Lett.* **3** (2003) 275

15. S. C. Roy, A. W. Harding, A. E. Russell, K. M. Thomas, *J. Electrochem. Soc.* **144** (1997) 2323
16. N. R. Elezović, B. M. Babić, N. V. Krstajić, S. L. Gojković, L. M. Vračar, *J. Serb. Chem. Soc.* **73** (2008) 641
17. E. K. Tuseeva, N. A. Mayorova, V. E. Sosenkin, N .F. Nikol'skaya, Y. M. Vol'fkovich, A. V. Krestinin, G. I. Zvereva, V. A. Grinberg, O. A. Khazova, *Russ. J. Electrochem.* **44** (2008) 884.

Journal of the Serbian Chemical Society
JSCS-info@shd.org.rs • www.shd.org.rs/JSCS
J. Serb. Chem. Soc. 75 (10) 1441–1452 (2010)
JSCS–4066
UDC *Methylprednisolone:615.451.1:615.015.1:543.612
Original scientific paper

Methylprednisolone and its related substances in freeze-dried powders for injections

LJILJANA SOLOMUN[1], SVETLANA IBRIĆ[2], VLATKA VAJS[3#], IVAN VUČKOVIĆ[3#] and ZORICA VUJIĆ[2*]

[1]*Hemofarm, A.D. Vršac,* [2]*Faculty of Pharmacy, Belgrade and* [3]*Faculty of Chemistry, Belgrade, Serbia*

(Received 15 January, revised 24 May 2010)

Abstract: In this work, the behavior of the active pharmaceutical substances methylprednisolone (in a form of methylprednisolone sodium succinate) in finished pharmaceutical dosage form, *i.e.*, freeze-dried powder for injections, was examined. The goal was to evaluate the chemical stabilities of methylprednisolone sodium succinate packaged in a dual chamber vial, as a specific container closure system. The effect of different parameters: temperature, moisture and light were monitored. The method proposed by United States Pharmacopeia was used to determine concentrations of methylprednisolone, as the sum of the concentration of methylprednisolone esters (17-hydrogen succinate and 21-hydrogen succinate) and free methylprednisolone. The HPLC method was used for stability evaluation of the active substance and determination of related substances. Four main degradation products were registered. Temperature has a major impact on the degradation process with the appearance of 3 degradation products (impurities **B**, **C** and **D**), while the presence of light caused an increasing content of impurity **A**. Identification of impurity **B**, **C** and **D** has been realized using mass and NMR spectroscopy. All three substances are substances related to methylprednisolone.

Keywords: methylprednisolone sodium succinate; freeze-dried powder; container closure system; stability; impurities.

INTRODUCTION

Methylprednisolone (MP) is a synthetically produced glucocorticoid with a structure similar to that of a natural hormone produced by the adrenal glands. Like most adrenocortical steroids, MP is typically used in replacement therapy for adrenal insufficiency and as an anti-inflammatory and immunosuppressant agent.

* Corresponding author. E-mail: zvujic@pharmacy.bg.ac.rs
# Serbian Chemical Society member.
doi: 10.2298/JSC100115087S

MP (Fig. 1A) belongs to the group of corticosteroids which are hydroxyl compounds (alcohols). Both, free alcohol and ester (Fig. 1B) occur as odorless, white or almost white, crystalline powder. They are practically insoluble in water and sparingly soluble in alcohol. The sodium salt of the phosphate or succinate ester is generally used to provide water-soluble forms for injections or solutions.

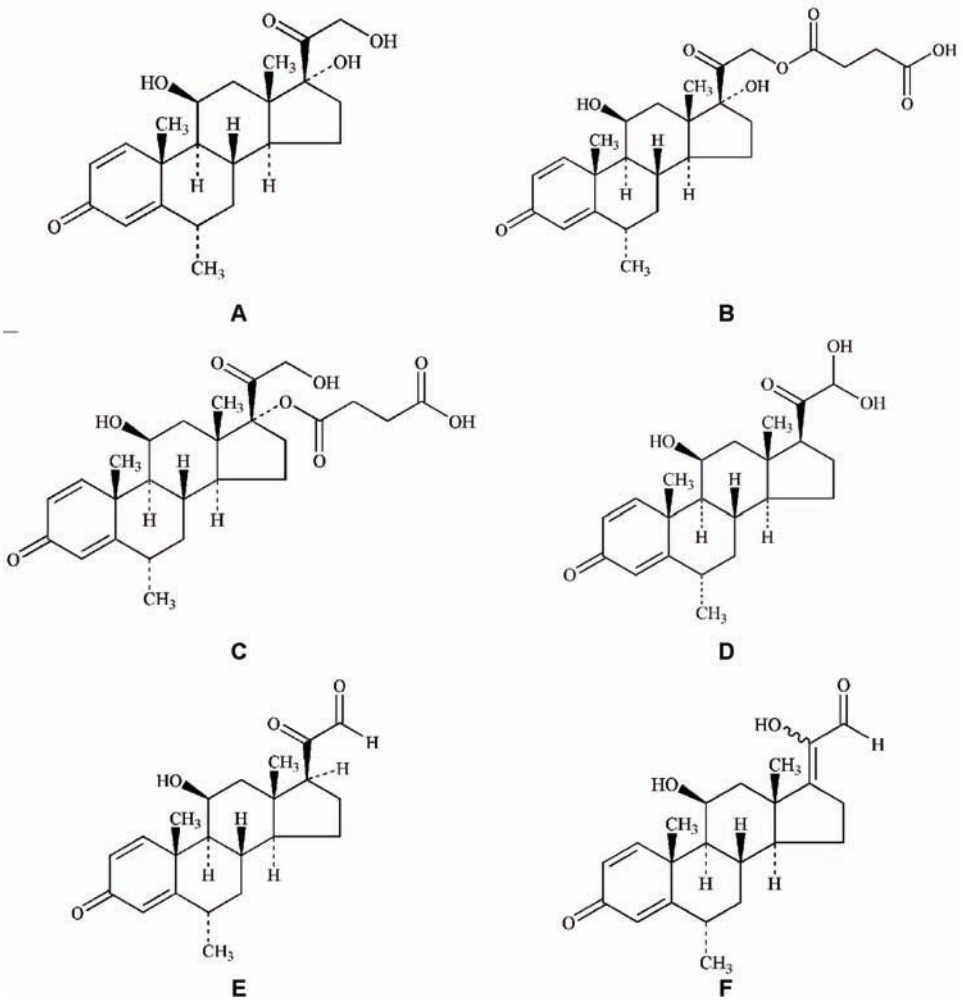

Fig. 1. Structure of MP (A), MP 21-HS (B), MP 17-HS (C), impurity **B** (D), impurity **B1** (E), and impurities **C** and **D** (F).

In pharmacopeias there are several referenced chemical substances: MP, methylprednisolone acetate, methylprednisolone hydrogen succinate (MP 21-HS)[1–4] and methylprednisolone sodium succinate (MPNaS).[3]

Among all the cited substances, only MPNaS may be given intravenously. MPNaS is so extremely soluble in water[3] that it may be administered in a small volume of diluents and is especially well suited for intravenous use in situations in which high blood levels of MP are required rapidly and oral therapy is not possible.[5] The chemical name for MPNaS is (6α,11β)-11,17,21-trihydroxy-6-methyl--pregna-1,4-diene-3,20-dione-monosodium salt and the molecular weight is 496.53 g mol^{-1}.

MP is a very unstable substance, especially in the presence of moisture.[6–10] This is the main reason for using the lyophilization process for production of injections. A problem associated with this type of injection is the storage of the medications (powder and solution for reconstitution) that should be administered as separate component parts and mixed prior to injection. Therefore, dual chamber vials have been developed to facilitate the storage and mixing of such two-component medications. This container closure system consists of a glass vial with two chambers separated by an intermediate rubber closure and an upper closure on the top. The specific feature of this type of the products is that both the lyophilized active ingredient (in the lower chamber) and the solution for reconstitution (in the upper chamber) are in the same vial.

MP and its derivatives are well known and defined, not only in Pharmacopeias, but in official documentations of the manufacturers and in the literature as well.[11–13] Although a number of studies of the physical and chemical stabilities of MPNaS have been reported,[14–19] no published information is available on its stability in a dual chamber vial.

The objective of this work was to evaluate the chemical stability of lyophilized injectable preparation of MPNaS. The last step to reach our goal was to check the influence of all critical points on the degradation profile of MP. Special consideration was given to changes in the concentration of the active substance (total MP), the concentration of free MP, determination of related substances as possible degradation products and also their identification.

EXPERIMENTAL

Materials

A lyophilized injectable preparation of MPNaS was purchased by Hemofarm, Vršac, Serbia. The solution for reconstitution was water for injection/ 0.9 % benzyl alcohol. Two milliliters of reconstituted solution contained MPNaS equivalent to 125 mg MP, phosphate buffer and benzyl alcohol. This product was tested in the early development phase in accordance with relevant guidelines.[20–26]

All solvents, *n*-butyl chloride (Merck, Germany), tetrahydrofuran (Sigma-Aldrich, Germany) methanol (Merck, Germany), glacial acetic acid (Sigma-Aldrich, Germany) and chloroform (Merck, Germany) were of a grade suitable for high-performance liquid chromatography (HPLC) analysis. MP 21-HS (Aventis Pharma, France), MP and fluorometholone reference standards (RS) were obtained commercially. The reference standard was used without further purification.

All samples were conditioned according to the requirements of the International Conference on Harmonization Standards for Stability (Q1A)[21] and Photostability (Q1B UV).[26] The following chambers were used: Weiss 2000, Weiss Gallenkamp, Weiss 600, Weiss Gallenkamp, Sanyo PSC 062, Sanyo Gallenkamp (Great Britain) and Weiss Umwelttechnik 140, Weiss Umwelttechnik, Germany.

Procedure for stability testing

A stability study was designed to increase the rate of chemical degradation of the finished pharmaceutical product (FPP) by using exaggerated storage conditions as part of the formal stability studies. The acceleration conditions used in this study are presented in Table I. During the study, the vials were kept in an upright or in a horizontal position. The horizontal position was chosen for compatibility assessment, in other words to ensure maximal contact of the diluent of the subject drug product with the elastomeric closures.

TABLE I. Storage conditions and testing frequencies

Storage conditions		Storage orientation	Testing time points, months
Accelerated	40±2 °C/75±5 % RH[a]	Upright	0, 1, 2, 3 and 6
		Horizontal	0, 3 and 6
Intermediate	30±2 °C/65±5 % RH	Upright	0, 3, 6, 9 and 12
		Horizontal	0, 6 and 12
Long-term	25±2 °C/60±5 % RH	Horizontal	0, 12, and 24

[a]Relative humidity

The in-use stability[24,25] was evaluated by examining the quality parameters of the subject drug product susceptible to change at the end of the proposed in-use shelf life (*i.e.*, 48 h after reconstitution, kept at room temperature). The samples were tested immediately after production (initial test point), at the end of the accelerated and intermediate conditions and at 12 and 24 month-testing points during long-term testing.

Photostability testing was performed using a light source – Option 2.[26] This means that a cool white fluorescent lamp and a near UV fluorescent lamp were used. The vials were exposed to light providing a defined energy (1.2×10^6 lx h) and then reconstituted. At the same time, protected samples (vials wrapped in aluminum foil or kept in a cardboard box) were used as the dark controls. At the end of this phase, the concentration of MP and related substances was determined.

Methods

HPLC Method for MP determination. Analytical procedures for the determination of both the total MP and free MP were in accordance with USP 32. The concentration of total MP is expressed as the sum of the concentration of free MP, MP 21-HS and MP 17-HS. The concentration of free MP is separately expressed as it is an important degradation product. The analyses were performed on an HPLC system, Agilent Technology 1100 Series, equipped with a 254 nm detector and a column packed with porous silica particles (L3). The flow rate was 1.0 mL min^{-1}. The mobile phase was prepared by mixing butyl chloride, water-saturated butyl chloride, tetrahydrofuran, methanol and glacial acetic acid (95:95:14:7:6; volume ratio).

An internal standard solution of concentration 3 mg mL^{-1} was obtained by dissolving the required amount of fluorometholone (RS) in tetrahydrofuran.

An MP solution was prepared by transferring an accurately weighed amount of MP RS (about 7.5 mg) to a 25-mL volumetric flask and dissolving to the mark with solvent. The solvent was 3 % glacial acetic acid in chloroform.

A standard solution was prepared by transferring an accurately weighed amount of MP 21-HS RS (about 32.5 mL) to a 50-mL volumetric flask. 5 mL of internal standard solution and 5 mL of MP solution were added. Solvent was added up to 50 mL.

A test solution was prepared as follows. The tested product was reconstituted according to the manufacturer's directions. Aliquots of 10 vials were collected and 0.8 mL of this solution was transferred to a 100-mL volumetric flask. The internal standard solution (10 mL) was added and the mixture was diluted with solvent to the mark. After 5 minute shaking, the layers were separated and the upper one was discarded.

The injection volume was 10 µL of each sample.

HPLC Method for determination of related substances. The related substances were determined by an isocratic HPLC method using an Agilent 1100 Series instrument with a variable wavelength UV–Vis detector. Separation was realized on a C18 column (250 mm×4.6 mm, 5 µm) column at a flow rate of 1.2 mL min^{-1}. The mobile phase was prepared by combining acetic acid, acetonitrile, and purified water (2:30:75, volume ratio).

A test solution was prepared as follows. Reconstituted solutions prepared from the contents of 10 vials of MPNaS for injection were mixed and 0.4 mL was transferred to a 20-mL volumetric flask and diluted with mobile phase up to 20 mL. The concentration of the obtained solution was 0.1 % w/v.

A standard solution was prepared by transferring 1 mL of test solution to a 100-mL volumetric flask and diluting with mobile phase. Then 1 mL of this solution was diluted with mobile phase to 10 mL. The concentration of the standard solution was 0.0001 % w/v.

The injection volume was 20 µl of each sample.

Methods for identification of related substances. Samples were treated with 5 mol L^{-1} HCl for 30 min at 80 °C in order to force degradation and obtain higher concentrations of the degradation products.

The samples of the degradation products were obtained from the reaction mixture by semi-preparative HPLC. The same apparatus was used (Agilent 1100 Series), with a variable wavelength UV–Vis detector, but a semi-preparative Zorbax Eclipse XDB-C18 (250 mm×9.4 mm; 5 µm) column was used; the flow rate was 4.0 mL min^{-1} and the injection volume was 1000 µL. The mobile phase was prepared by combining formic acid and acetonitrile (7:3, v/v).

The high resolution electrospray ionization in a time of flight (HR-ESI-TOF) mass spectra of MP and three degradation products were measured on an Agilent 6210 LC/MS instrument. The mass spectrometer was operated under the following conditions: source – ESI in the positive/negative mode, dry gas: 12.0 L min^{-1}, dry temperature: 350 °C, nebulizer: 45 psig, scan: 100–1500 *m*/*z*, fragmentor: 140 V, capillary voltage: 4000 V.

The ^{1}H-NMR spectra of impurities **C** and **D** were measured on a Varian Gemini 2000 instrument at 200 MHz in $CDCl_3$. The NMR spectra of MP and impurity **B** (^{1}H-, ^{13}C-, DEPT--135, COSY, NOESY, HSQC and HMBC) were measured on a Bruker Avance III instrument at 500 MHz in $CDCl_3$ (a few drops of CD3OD were added for MP).

RESULTS AND DISCUSSION

Assay MP and related substances determination

A chromatogram of the test solution obtained during assay determination is presented in Fig. 2. The order of the elution of peaks is the internal standard

peak, MP 21-HS peak and successive smaller peaks of free MP and methylprednisolone 17-hydrogen succinate (MP 17-HS). The concentration of total MP is expressed as the sum of the concentration of free MP, MP 21-HS and MP 17-HS (Fig. 1C). The concentration of total MP in the initial sample (in the form of sodium succinate) was defined as 100 %, and subsequent sample concentrations were expressed as percentage of the initial concentration.

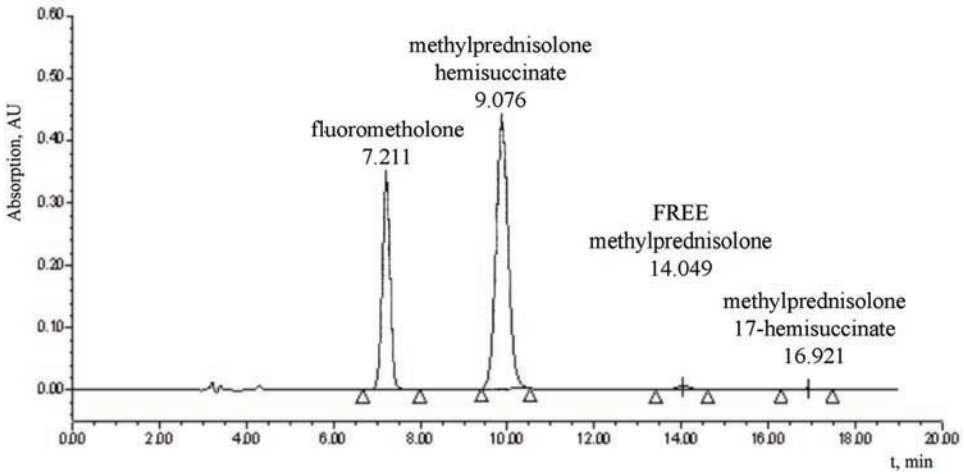

Fig. 2. Chromatogram of the MP test solution; fluorometholone was used as the internal standard.

The HPLC method for the determination of related substances confirmed the existence of four specified and not identified impurities marked as impurity **A**, **B**, **C** and **D**. A typical chromatogram related to the impurities is presented in Fig. 3. The second part of this study was focused on the identification of these impurities.

The influences of different temperature in terms of the concentration of total MP, free MP and related substances are given in Tables II and III. All results are related to horizontal positioned vials. As can be seen, increasing the temperature was followed by an increase of free MP (because of hydrolysis) but it was still significantly below the maximum allowed level of 6.6 %. The obtained results indicated that there were no changes in the content of total MP, which could influence the shelf life.

An increase in the concentrations of the related substances was also registered. After 6 months conditioning at 40 °C/75 % relative humidity (RH), the concentrations of impurity **B** and impurity **D** were above 0.15 %, which is the identification level in accordance with relevant guidelines.[27] The increase in the concentration of impurity **A** was not significant.

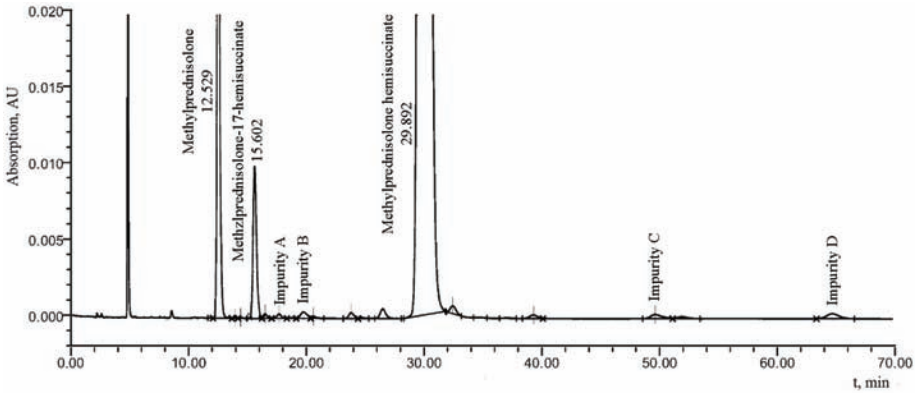

Fig. 3. Chromatogram of related substances – impurities **A**, **B**, **C** and **D** are considered as related substances: the sample was treated at 40 °C/75 % RH for 3 months and prepared as described in the method for determination of related substances (test solution).

TABLE II. Results for the concentration of total MP/free MP (percent of the labeled amount of MP) under different storage conditions

Storage conditions	Initial result	Intermediate result	Final result
40 °C/75 % RH[a]	101.9/1.51	101.3/2.70	100.4/3.12
30 °C/65 % RH	101.9/1.51	100.9/2.21	102.1/2.89
25 °C/60 % RH	101.9/1.51	101.8/2.04	101.3/2.68

[a]Relative humidity

TABLE III. Results of the determination of the related substances (presented as percent of labeled amount of MP)

Storage conditions	Related substance	Initial result	Intermediate result	Final result
40 °C/75 % RH[a]	**A**	<*LOD*[b]	0.03	0.04
	B	0.03	0.22	0.25
	C	0.03	0.11	0.14
	D	0.04	0.15	0.21
30 °C/65 % RH	**A**	<*LOD*	<*LOD*	0.05
	B	0.03	0.10	0.14
	C	0.03	0.06	0.08
	D	0.04	0.10	0.12
25 °C/60 % RH	**A**	<*LOD*	0.03	0.06
	B	0.03	0.10	0.13
	C	0.03	0.06	0.08
	D	0.04	0.09	0.12

[a]Relative humidity; [b]limit of detection

For the testing of the in-use stability, all samples are conditioned according to ICH requirements and reconstituted. The samples were analyzed initially (immediately after production in use) and at the end after conditioning under defined conditions. The measurements on day 0 served as the references. The obtained

results are presented in Table IV. There were no statistically significant changes in the tested parameters – if the solution was kept at room temperature, there was no influence of water during 48 h; hence, only the results immediately after production (initial test point) and after 6 months conditioning at 40 °C/75 % RH are presented.

TABLE IV. Results of the in-use testing

Tested parameters	Immediately after production (initial test point)		Final test (after 6 months conditioning at 40 °C/75 % RH)	
	0 h	48 h	0 h	48 h
Total MP concentration, %	101.9	99.6	100.4	100.2
Free MP concentration, %	1.51	3.62	3.12	4.98
Related substances, %				
Impurity **A**	<*LOD*[a]	0.01	0.04	0.03
Impurity **B**	0.03	0.04	0.25	0.25
Impurity **C**	0.03	0.04	0.14	0.14
Impurity **D**	0.04	0.06	0.21	0.20

[a]Limit of detection

The results of the photostability testing are summarized in Table V. It was concluded that there was a change in the tested parameters. It is obvious that impurity **A** increased while the concentration of total MP decreased. When vials are kept in the dark (wrapped in aluminum foil or kept in a cardboard box), the increase in the concentration of impurity **A** was not significant; hence, impurity **A** was not the subject of further identification.

TABLE V. Results of the photostability testing

Tested parameters	Initial	Directly exposed vials	Protected vials
Total MP concentration, %	101.9	96.3	100.3
Free MP concentration, %	1.51	1.58	1.64
Related substances, %			
Impurity **A**	<*LOD*[a]	0.32	0.01
Impurity **B**	0.03	0.03	0.05
Impurity **C**	0.03	0.04	0.04
Impurity **D**	0.04	0.07	0.06

[a]Limit of detection

Identification of the structures of the degradation products

From the retention times of the impurities, it was concluded that impurity **B** was less polar then MP, and impurities **C** and **D** were significantly less polar.

Previous investigations of impurity **B** by MS showed that this compound has a mass of 374 amu, *i.e.*, the same as MP. The most abundant ion in HR-ESI-TOF mass spectra of MP is the ion at *m*/*z* 375.2464 ($M+H^+$), followed by 771.4071 ($2M+Na^+$) and 357.2057 ($M+H^+–H_2O$). The same ions appear in the mass spec-

trum of impurity **B**, which means that impurity **B** and MP have the same molecular formula, *i.e.*, they are isomers. The presence of other ions (343, 345, 387...) in the mass spectrum of **B** showed that impurity **B** was impure and started to decompose. Hence, additional analyses (*i.e.*, ^{1}H-, ^{13}C-, DEPT-135, COSY, NOESY, HSQC and HMBC NMR spectroscopy) were required in order to elucidate the structure of impurity **B**.

Compound **B** had same mass and similar polarity as MP, so its structure could be 17-deoxy-21,21-dihydroxy-6α-methylprednisolone (Fig. 1D). The same compound was defined as impurity **B** of MP in EP.[1] In the European Pharmacopoeia this compound was defined as an impurity of MP and designated as **B**.

It was assumed that MP initially gave impurity **B**, which was later transformed (by standing and/or solvent exchange) into impurity **B1**. Since the structure of impurity **B1** was not compatible with the chromatographic behavior and mass spectra of impurity **B**, the structure of impurity **B1** was determined unequivocally by NMR spectroscopy.

The ^{1}H-NMR spectrum of **B1** (Fig. 4) is similar to that of MP, showing that they have the same basic structure. Based on all the spectra, it can be concluded that instead of a –CH_2OH group at 21 and an –OH group at 17 in MP, impurity **Bl** has a –CHO group at 21 and an H-atom at 17. Thus **Bl** has the structure of 17--deoxy-21-dehydro-6α-methylprednisolone (Figure 1E). The same impurity is known in the literature as an impurity of 6α-methylprednisolone acetate.[28]

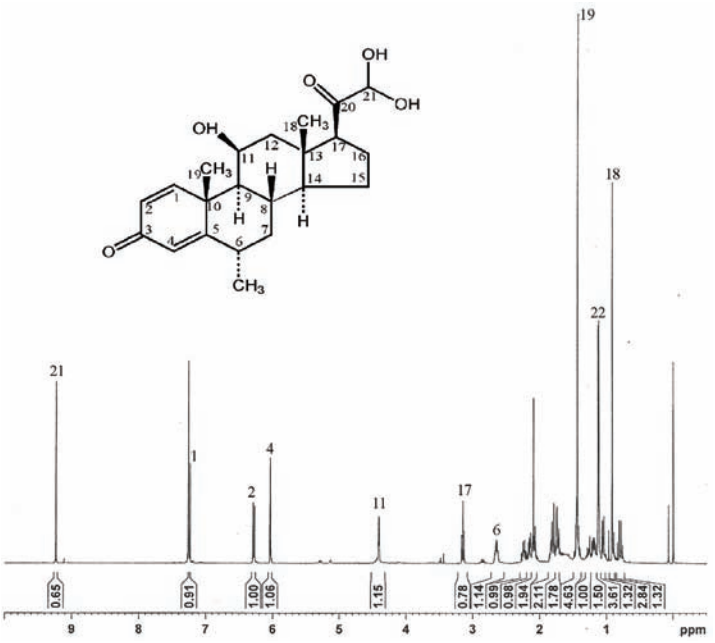

Fig. 4. ^{1}H-NMR Spectrum of impurity **B**.

The ^{1}H-NMR spectra of impurities **C** and **D** were very similar; they differed slightly in their chemical shifts. Compared to the proton spectrum of MP, the signals from the diastereotopic protons at C-21 were missing and a new signal appeared at 9.71 ppm in the spectrum of **C** and at 9.56 in the spectrum of **D**. This means that **C** and **D** are isomeric aldehydes (Fig. 1 F). The spectral data of **C** and **D** are in very good agreement with data for isomeric enol aldehydes obtained from prednisolone. Thus **C** and **D** can be identified as the *E* and *Z* (respectively) 20-hydroxy-17(20) *E*-ene-21-al derivatives of 6α-methylprednisolone, which was defined as impurity **D** of MP in EP.[1]

According to the obtained results, the proposed degradation profile of MP is shown in Fig. 5.

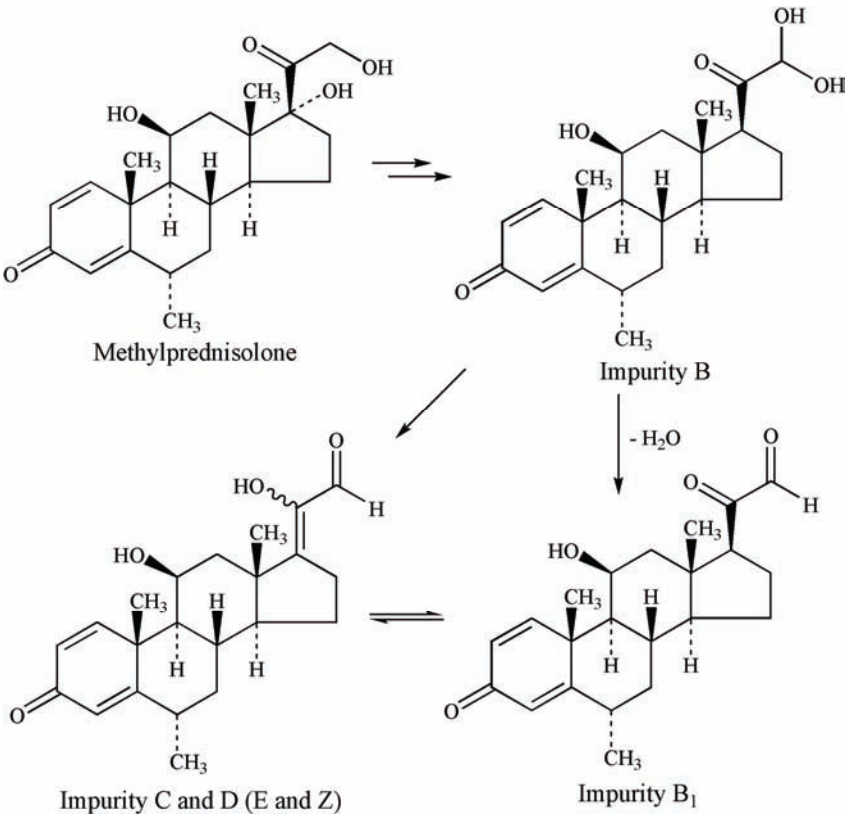

Fig. 5. Proposed degradation profile of MP.

CONCLUSIONS

Even if MP is a well known substance, it is still a subject of many studies especially regarding stability. In this work degradation profile in the freeze-dried product is presented. It is obviously clear that the temperature has influence on

degradation process, as well as light. Three of four detected degradation products are increasing under the temperature treatment. During this study it is confirmed that they are derivatives of the MP and at the same time defined as MP impurities in the Monograph in EP. The concentration of impurity **A** increases in the presence of light.

Acknowledgment. We gratefully acknowledge the financial support of the Ministry of Sciences and Technological Development of the Republic of Serbia (Grant No. 142072).

И З В О Д

МЕТИЛПРЕДНИЗОЛОН И ЊЕГОВЕ СРОДНЕ СУПСТАНЦЕ У ЛИОФИЛИЗАТУ ЗА РАСТВОР ЗА ИНЈЕКЦИЈЕ

ЉИЉАНА СОЛОМУН[1], СВЕТЛАНА ИБРИЋ[2], ВЛАТКА ВАЈС[3], ИВАН ВУЧКОВИЋ[3] и ЗОРИЦА ВУЈИЋ[2]

[1]Хемофарм, А.Д. Вршац [2]Фармацеутски факултет, Београд и [3]Хемијски факултет, Београд

У овом раду испитиване су особине фармаколошки активне супстанце метилпреднизолона (у облику метилпреднизолон-натријум-сукцината) у готовом производу – лиофилизату за раствор за инјекције. Циљ рада је испитивање хемијске стабилности метилпреднизолон-натријум-сукцината у двокоморној бочици, као специфичном систему контактног паковања. Испитан је ефекат различитих параметара: температуре, влаге и светлости. За одређивање концентрације метилпреднизолона, као збирне концентрације метилпреднизолон естара (17-хидроген-сукцината и 21-хидроген-сукцината) и слободног метилпреднизолона, коришћена је метода описана у Америчкој фармакопеји. За испитивање сродних супстанци примењена је HPLC метода. Уочена су 4 деградациона производа. Доказано је да повећање температуре има највећи значај на процес деградације и утиче на повећање садржаја нечистоћа **B**, **C** и **D**, док присуство светлости доводи до повећања садржаја нечистоће **A**. Нечистоће **B**, **C** и **D** су идентификоване применом масене и NMR спектроскопије. Све три нечистоће су идентификоване као сродне супстанце метилпреднизолона.

(Примљено 15. јануара, ревидирано 24. маја 2010)

REFERENCES

1. *European Pharmacopoeia*, 6th ed., European Directorate for the Quality of Medicines, Council of Europe, Strasbourg, 2008, p. 2397
2. *British Pharmacopoeia*, British Pharmacopoeia Commission, The Stationery Office, London, 2009, p. 1348
3. *USP – NF*, 32nd ed., United States Pharmacopeia Convention, Inc., Rockville, MD, on-line version (www.uspnf.com/uspnf/display?cmd=jsp&page=chooser), 2009 (accessed October, 2010)
4. *Japanese Pharmocopoeia*, 15th ed., Ministry of Health, Labour and Welfare Ministerial Notification, Society of Japanese Pharmacopoeia, Tokyo, 2006
5. *Martindale, The Complete Drug Reference*, Thomson Micromedex, Pharmaceutical Press, London, 2005, on-line (www.medicinescomplete.com/mc/martindale/current/), 2009 (accessed October, 2010)
6. S. Gőrőg, *Quantitative analysis of Steroids*, Elsevier, Amsterdam, 1983, pp. 184-246
7. S. L. Alli, *Analytical Profiles of Drug Substances and Excipients*, Academic Press, San Diego, CA, 1992, p. 432

8. T. L. Herzog, M. J. Gentles, H. Marshall, E. B. Hershberg, *J. Am. Chem. Soc*. **83** (1961) 4073
9. M. L. Di Gioia, A. Leggio, A. Le Pera, A. Liguori, A. Napoli, C. Siciliano, G. Sindona, *Tetrahedron Lett*. **42** (2001) 7413
10. M. L. Lewbart, C. Monder, W. J. Boyko, C. J. Singer, F. Iohan, *J. Org. Chem.* **54** (1989) 1332
11. G. Ulsaker, G. Teien, *Am. J. Health Syst. Pharm.* **59** (2002) 2456
12. L. A. Trissel, Y. Zhang, *J. Am. Pharm. Assoc.* **42** (2002) 868
13. M. I. Amin, J. T. Bryan, *J. Pharm. Sci*. **62** (1973) 1768
14. J. G. Strom, S. W. Miller, *Am. J. Hosp. Pharm.* **48** (1991) 1237
15. R. J. Townsend, A. H. Puchala, S. L. Nail, *Am. J. Hosp. Pharm.* **38** (1981) 1319
16. R. A. Pyter, L. C. C. Hsu, J. D. Buddenhagen, *Am. J. Hosp. Pharm.* **40** (1983) 1329
17. J. T. Stewart, F. W. Flynn, A. D. King, *Am. J. Hosp. Phar*. **51** (1994) 1802
18. V. D. Gupta, *Int. J. Pharm. Compound* **5** (2001) 148
19. C. Gellis, V. Sautou-Miranda, A. Arvouet, M.-P. Vasson, J. Chopineau, *Am. J. Health Syst. Pharm.* **58** (2001) 1139
20. The European Medicines Agency, *Note for Guidance on Pharmaceutical Development*, 2006, http://www.ema.europa.eu/pdfs/human/ich/16706804enfin.pdf (18 May 2010)
21. ICH Steering Committee, *ICH Q 1A (R2), Stability Testing of New Drug Substances and Products*, 2003, http://www.ich.org/lob/media/MEDIA419.pdf (18.May 2010)
22. The European Medicinal Agency, *Guideline on Stability Testing: Stability Testing of Existing Active Substances and Related Finished Products*, 2004; http:// www.ema.europa.eu/ /pdfs/human/qwp/012202en.pdf (18.may 2010)
23. U.S. Department of Health and Human Services, *FDA Draft Guidance for Industry "Stability Testing of Drug Substances and Drug Products"*, Rockville, MD, 1998
24. The European Medicines Agency, *Note for Guidance on In-use Stability Testing of Human Medicinal Products*, London, 2001
25. Note for guidance on in-use stability testing of human medicinal product, http:// //www.ema.europa.eu/pdfs/human/qwp/293499en.pdf (18 May 2010)
26. The European Medicines Agency, *Note for Guidance on Maximum Shelf–life for Sterile Products for Human Use after First Opening or Following Reconstitution*, London, 1998
27. Note for guidance on maximum shelf-life for sterile products for human use after first opening or following reconstitution, http://www.ema.europa.eu/pdfs/human/qwp/ /015996en.pdf (18 May 2010)
28. ICH Steering Committee, *ICH Q1B, Stability Testing: Photostability Testing of New Drug Substances and Products*, 1996, http://www.ich.org/LOB/media/MEDIA412.pdf (18 May 2010)
29. The European Medicines Agency, *ICH Q3B (R2), Impurities in New Drug Products*, 2006, http://www.ema.europa.eu/pdfs/human/ich/273899en.pdf (18 May 2010)
30. E. Ciranni Signoretti, L. Valvo, A. L. Savella, G. Cavina, *J. Pharm. Biom. Anal.* **11** (2003) 587.

Journal of the Serbian Chemical Society
JSCS-info@shd.org.rs • www.shd.org.rs/JSCS
J. Serb. Chem. Soc. 75 (10) 1453–1461 (2010)
JSCS–4067
UDC 582.795–035.27:546.19+546.881+546.48:66–914(497.11)
Original scientific paper

Urban deciduous tree leaves as biomonitors of trace element (As, V and Cd) atmospheric pollution in Belgrade, Serbia

KATARINA M. ŠUĆUR[1], MIRA P. ANIČIĆ[2], MILICA N. TOMAŠEVIĆ[2]*, DAVOR Z. ANTANASIJEVIĆ[3], ALEKSANDRA A. PERIĆ-GRUJIĆ[3#] and MIRJANA DJ. RISTIĆ[3#]

[1]*National Library of Serbia, Skerlićeva 1, 11000 Belgrade,* [2]*Institute of Physics, University of Belgrade, Pregrevica 118, 11080 Zemun and* [3]*Faculty of Technology and Metallurgy, University of Belgrade, Karnegijeva 4, 11120 Belgrade, Serbia*

(Received 19 March, revised 18 May 2010)

Abstract: Leaves of common deciduous trees: horse chestnut (*Aesculus hippocastanum*) and linden (*Tilia spp*.) from three parks within the urban area of Belgrade were studied as biomonitors of trace element (As, V, and Cd) atmospheric pollution. The May–September trace element accumulation in the leaves, and their temporal trends, were assayed in a multi-year period (2002––2006). Significant accumulation in the leaves was evident for As and V, but not so regularly for Cd. Slightly decreasing temporal trends of V and As accumulated in the leaf tissues were observed over the years. During the time span, the concentrations of Cd remained approximately on the same level, except in May 2002 and September 2005, when a rapid increase was observed. The May–September accumulations of As and V were higher in horse chestnut than in linden, although both may be used as biomonitors for these elements, and optionally for Cd in conditions of its high atmospheric loadings.

Keywords: trace elements; tree leaves; biomonitoring; *Aesculus hippocastanum*; *Tilia spp.*; ICP-MS.

INTRODUCTION

Increasing industrialization and human activities intensify the emission of various pollutants, including trace elements, into the atmosphere and introduce harmful substances into the environment.[1,2] Particulate pollution is a matter of great concern due to its adverse effects on human and living plant populations. Road traffic contributes significantly to air pollution in urban areas, generating particulate matter, aerosols and trace elements around roads.[3,4]

* Corresponding author. E-mail: milica.tomasevic@ipb.ac.rs
# Serbian Chemical Society member.
doi: 10.2298/JSC100319079S

Trees are very efficient at trapping atmospheric particles, and they have a special role in reducing the level of fine, "high risk" respirable particulates, which have the potential to cause serious human health problems.[5] Therefore, tree leaves have been used for biomonitoring of particulate pollutants, which are often associated with trace elements, in air quality studies.[3,6] Leaves of different evergreen and deciduous tree species and their validity for the biomonitoring of trace elements have been assessed in urban and industrial areas.[7–9]

Previous investigation showed that common tree species in the Belgrade urban area had distinguishable seasonal accumulations of some elements, especially horse chestnut, for which the Pb accumulation in the leaves reflected changes of atmospheric Pb concentrations.[10]

The purpose of this study was to extend these investigations by applying horse chestnut (*Aesculus hippocastanum*) and linden (*Tilia spp*.) leaves for the biomonitoring of atmospheric contamination with V, As and Cd, present at low concentrations in air but with high health risk potentials.[11] Vanadium is required for the activity of enzymes, while As and Cd do not have any known physiological function in plants and can be toxic. The aim was to evaluate the accumulation during the growing season (May–September) and the temporal accumulation of the elements in a multi-year period (2002–2006).

EXPERIMENTAL

The study was conducted in Belgrade, the capital of Serbia, which is located in south-eastern Europe, on the Balkan Peninsula (φ = 44° 49' N, λ = 20° 27' E, H_s = 117 m). Belgrade has a moderate continental climate, with four seasons (cold winters and hot, humid summers, with well-distributed rainfall). By the end of 2004, Belgrade had about 1.6 million urban inhabitants, which is 20 % of the total population of Serbia. The samples were collected from three urban parks exposed to the exhaust of heavy traffic: Karadjordjev Park (KP), Botanička bašta – Botanical Garden (BG) and Studentski Park (SP). Tree species with broad leaves *Aesculus hippocastanum* L. and *Tilia sp*. L. were chosen since they are common in Belgrade city parks. The leaf samples were collected at the beginning (May) and the end (September) of the vegetation cycles from 2002–2006. The leaves were cut off with stainless steel scissors from a height of about 2 m (polyethylene gloves were worn to prevent contamination). Five subsamples (10 to 15 fully developed leaves) were taken randomly from all sides of a crown. The subsamples were packed in polyethylene bags. The leaf samples were carefully washed with bidistilled, deionized water to remove adhering coarse particles, dried in an oven at 40 °C for 24 h, pulverized using agate mortars, packed in polyethylene bags and kept under stable laboratory conditions until chemical analyses. Approximately 0.4 g leaf (dry weight) was digested with 3 ml of 65 % HNO_3 and 2 ml of 30 % H_2O_2 using a microwave oven (Speedwave^{TM} MWS-3$^+$, Berghof). After digestion, the solution was diluted with distilled water to a total volume of 25 ml. Trace elements in the extracts were analyzed by inductively coupled plasma-mass spectrometry (ICP-MS) using an Agilent 7500ce spectrometer equipped with an Octopole Reaction System (ORS). With this method, low detection limits can be obtained for elements present in low concentration and for metalloid elements, such as As, with high ionization energies. Prior to the ICP-MS analysis, all the samples were filtered

through a 0.45 μm pore diameter membrane filter. Calibration was performed with external standards obtained by appropriate dilution of a Fluka multi-element standard solution IV. The blank and calibration standards were prepared in 2 % nitric acid for all the measurements except for those used to determine the detection limits. A tuning solution containing 1 μg L^{-1} Li, Mg, Co, Y, Ce and Tl (Agilent) was used for all instrument optimizations. Details of the ICP MS operating conditions are summarized in Table I.

TABLE I. Optimal instrument (Agilent 7500ce) operating conditions

Parameter	Value
RF frequency, MHz	27
RF power, W	1500
Plasma gas flow, L min^{-1}	15
Nebulizer gas flow, L min^{-1}	0.9
Sample uptake rate, rps	0.3
Data acquisition	
Acquisition mode	Peak hopping
Dwell time, ms	100
Integration time, s/point	0.1–0.3
Repetition	3 (FullQ)

The determination of the method detection limit (MDL) was based on seven replicate measurements of a series of spiked calibration blanks. Each blank solution was spiked with analytes at concentrations between 2 and 5 times the calculated IDL (instrument detection limit). The MDL was calculated by multiplying the standard deviation of the seven replicate measurements by the appropriate Student's test value based on a 99 % confidence level (t = = 3.14 for six degrees of freedom).

The analytical quality control included daily analyses of standards and triplicate analysis of samples and blanks. The accuracy and precision of the analytical procedures were verified through analysis of the standard reference material lichen-336 (IAEA). The recovery range was 90–95 %. All results were calculated on a dry weight basis.

RESULTS AND DISCUSSION

The concentrations (μg g^{-1}) of As, Cd, and V in the leaves of horse chestnut (*A. hippocastanum*) and linden (*Tilia spp.*) from three parks (KP, BG and SP), representative for the urban area of Belgrade, are presented in Table II (mean concentration of triplicate analysis, *RSD* less than 3 %). The leaves were sampled at the beginning (May) and at the end (September) of the vegetation periods from 2002 to 2006. For the investigated species, the concentrations of V and As in the leaves increased at a significant level $p < 0.05$ from May to September. In case of Cd, the May–September increase of this element in the leaves was not significant (except for 2005). This is in agreement with a previous study on *A. hippocastanum* leaves, in which no clear Cd accumulation in leaves was found within a single season.[12]

In general, the ratio of the September/May concentrations of the elements in the leaves were higher in horse chestnut than in linden, over the multi-year period, suggesting a better accumulative ability of the former species.

TABLE II. Concentration (μg g^{-1}) of V, As and Cd in *Tilia spp*. (linden) and *A. hippocastanum* (chestnut) leaves from the Belgrade urban area during the vegetation periods from 2002–2006

Year	KP				BG				SP			
	Linden		Chestnut		Linden		Chestnut		Linden		Chestnut	
	Month											
	May	Sept.	May	Sept.	May	Sept.	May	Sept.	May	Sept.	May	Sept.
	V											
2002	0.728	1.483	0.515	1.764	0.269	0.324	0.448	0.881	0.405	0.745	0.286	1.104
2003	0.200	0.873	0.364	0.405	0.044	0.381	0.158	0.332	0.089	0.408	0.123	0.858
2004	0.322	0.841	0.258	1.080	0.235	0.480	0.378	0.664	0.118	0.661	0.277	0.416
2005	0.110	0.463	0.765	1.154	0.080	0.460	0.336	0.298	0.082	0.372	0.179	0.494
2006	0.556	0.999	0.694	0.633	0.162	0.235	0.339	0.518	0.135	0.229	0.141	0.493
	As											
2002	0.193	0.293	0.166	0.313	0.121	0.274	0.252	0.530	0.281	0.754	0.313	0.913
2003	0.063	0.177	0.142	0.176	0.054	0.294	0.098	0.296	0.169	0.360	0.223	0.704
2004	0.065	0.181	0.071	0.346	0.077	0.213	0.133	0.265	0.100	0.388	0.289	1.217
2005	0.050	0.207	0.102	0.352	0.060	0.233	0.146	0.201	0.106	1.144	0.189	0.691
2006	0.105	0.249	0.110	0.108	0.078	0.193	0.216	0.244	0.138	0.486	0.544	0.670
	Cd											
2002	0.758	0.023	0.119	0.031	0.074	0.019	0.302	0.032	1.963	0.054	0.614	0.096
2003	0.040	0.018	0.015	0.076	0.025	0.029	0.014	0.035	0.012	0.056	0.007	0.075
2004	0.014	0.023	0.011	0.027	0.035	0.052	0.024	0.026	0.011	0.118	0.020	0.030
2005	0.062	0.016	0.046	0.150	0.038	0.554	0.297	1.577	0.013	2.777	0.066	0.271
2006	0.017	0.025	0.014	0.049	0.016	0.014	0.020	0.018	0.010	0.020	0.006	0.033

Considering a physiological significance of the studied elements, only V is beneficial for higher plants, *i.e.*, it may be involved in lipid metabolism and nitrogen fixation. Cadmium and arsenic may interfere with protein synthesis, and thus exhibit toxic effects.[13,14] Although, according to some authors, these elements are regarded as beneficial for some plants (algae and fungi) at low concentration, but toxic at higher concentrations.[3]

It is widely accepted that higher plants, including trees, take up elements mostly *via* the roots, although some uptake is considered possible through the leaves from atmospheric deposition. The foliar uptake and atmospheric origin has been clearly proven only for Pb.[15] However, topsoil analyses showed no serious contamination with the examined elements at the studied sites during the investigated period, *i.e.*, the values were: As ,7.2,[16] V, 1.4,[10] and Cd, 1.8[17] and 8.9 mg kg^{-1}.[18]

Moreover, the soil pH at the studied sites was mostly alkaline (> 8.0),[10,17] causing a decrease in the solubility of the trace elements. Trace element avail-

ability depends on several factors, such as, organic matter content, redox potential and pH. In the literature, it is emphasized that as a rule, the axial transport of elements from the roots (or other assimilation organ) to the bark can be assumed to be negligible. In fact, leaves are the main sink for many pollutants.[3] According to the previous assumption, the V, As, and Cd contents in the leaves of horse chestnut and linden are most likely of atmospheric origin. Furthermore, trace elements deposited on leaves are often present in the fine particle fraction, as was also shown previously for horse chestnut in Belgrade, with the majority of the particles observed on leaves belonging to the class of fine particles ($d < 2$ μm).[19] Most of elements in fine particles are considered as water soluble, as was also recently confirmed for Cd.[20]

The concentrations of the elements in the leaves of the investigated species, obtained for the Belgrade urban areas (2002–2006) (Table II) were compared to the values of the "reference plant" (*RP*) given by Markert (V: 0.5, As: 0.1, and Cd: 0.05 μg g^{-1}).[21]

In all the leaf samples from Botanical Garden and Studentski Park, and most of the samples from Karadjordjev Park, the concentration of V in May was even below the reference plant value (RP = 0.5 μg g^{-1}) and in most samples had increased to about this level by September. The highest c(measured)/c(RP) ratio was obtained for September 2002 (Fig. 1a), indicating vanadium accumulation in the leaves, probably as a consequence of atmospheric pollution. Considering the temporal accumulation trend, a decreasing V content in the leaves of the investigated species (September 2002/September 2006) was observed and its content at two locations (Botanical Garden and Studentski Park) decreased from a level about two times higher in 2002 to the level of the "reference plant"; even below this value in 2006. Examining the site dependence, the highest concentration of V was evident in both horse chestnut and linden leaves sampled from the KP site (Fig. 1a). This sampling site is located in an area with a high traffic density with a highway in the vicinity.

The arsenic concentration in most samples was higher than the reference plant value (RP = 0.1 μg g^{-1}), indicating a continuous source of emission at all locations in all the examined years (Fig. 1b). The accumulation of this element during the vegetation period was evident in the leaves of both tree species, linden and horse chestnut, which can be related to increasing deposits from aerosol arsenic and the increase was enough to offset the dilution effect by leaf material which increase during the growing period. The highest As concentration, about twelve times the RP value were found in the leaves from Studentski Park, a small park with a bus terminal and surrounded by many high buildings.

During the investigated time span, the Cd concentrations at all sites were mostly at about the same level, except for a few extremely high values in 2002 and 2005 registered for both horse chestnut and linden, (Fig. 1c). It should be em-

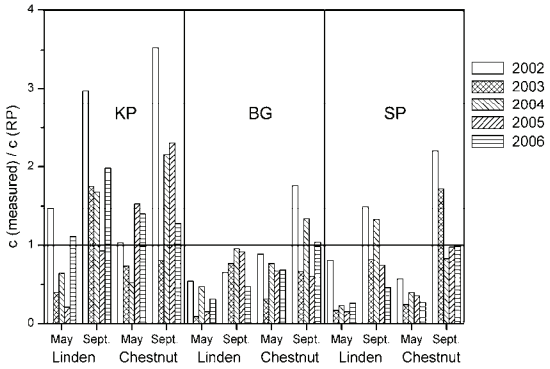

(a)

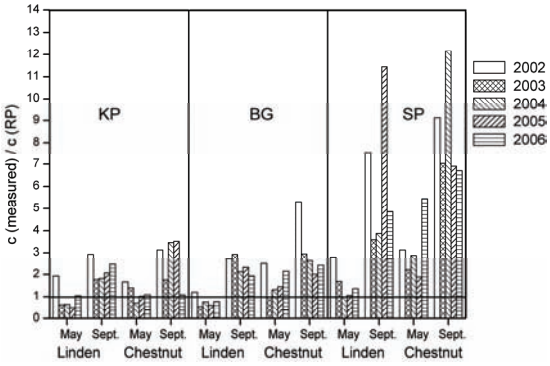

(b)

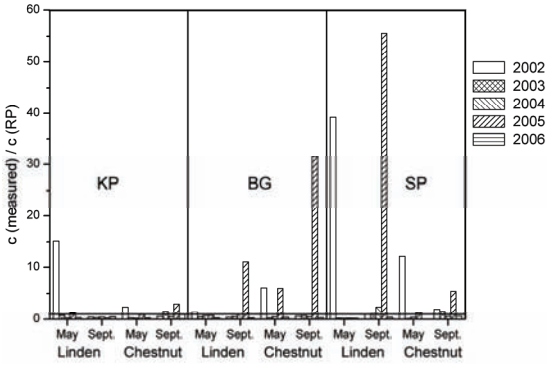

(c)

Fig. 1. The ratio of measured concentration of V (a), As (b), and Cd (c) in the leaves of *Tilia spp.* (linden) and *A. hippocastanum* (chestnut) and the relevant concentration in the "reference plant".

phasized that at all locations in May 2002, the cadmium concentration was higher than the background level proposed by Markert.[21] However, no accumulation of Cd was observed until September in these samples from 2002, which probably indicates a decreasing cadmium concentration in the air and dilution by leaf material. An accumulation of cadmium in the leaves was observed from September 2005 for all samples, except in linden from Karadjordjev Park. Five times higher

level than the RP value was determined in samples from the Botanical Garden from May 2005, and even more than 30 times in samples from the same location taken in September 2005. At all locations, it seems that higher concentrations of cadmium compared with other years resulted in increased accumulation of this element. Cadmium is emitted into the atmosphere by several sources and it is highly volatile, thus undergoing long-range transport.

As suggested in a previous investigation of element concentrations in $PM_{2.5}$ (particles smaller than 2.5 μm in diameter) in central Belgrade, vanadium and cadmium had a common source, traffic, with a considerable portion of resuspended road dust, and products of other fossil fuel combustion processes.[4] The relatively low concentrations of vanadium and cadmium found in leaves in the present study could be explained by a lack of heating sources during the vegetation period because the dominant source of PM in Belgrade is stationary combustion.[22] In addition, most of the coarse particulates were removed by the procedure of washing the leaves before chemical analyses, which diminished the contribution of road dust resuspension on the surface of the leaves. Consequently, the V, As and Cd found in the leaves originated mainly from traffic, motor exhaust and also metallic parts of cars.

CONCLUSIONS

This study gives evidence for the accumulation of As and V during the growing season (May–September) in the leaves of horse chestnut and linden sampled in the Belgrade urban area. During the studied time span (2002–2006), the concentrations of As and V in the leaves showed slightly decreasing trends. In general, Cd showed no significant May–September accumulation over the years, except in 2005 when higher concentration around the parks resulted in increased accumulations. The highest vanadium and cadmium contents were found in the leaves sampled from Karadjordjev Park, while the highest As concentration was detected in the leaves sampled in Studentski Park. The contents of As and V in September were mostly higher than those May, especially in horse chestnut, although both studied trees may be used as biomonitors for these elements, and optionally for Cd under conditions of its high atmospheric loading.

Acknowledgements. The authors acknowledge funding from the Ministry of Science and Technological Development of the Republic of Serbia, Fundamental Science Project No. 141012 and Fundamental Science Project No. 142002.

ИЗВОД

ИСПИТИВАЊЕ ЗАГАЂЕНОСТИ ВАЗДУХА У БЕОГРАДУ ЕЛЕМЕНТИМА У ТРАГОВИМА (As, V, Cd) ИЗ ЛИСТОВА ЛИСТОПАДНОГ ДРВЕЋА

КАТАРИНА М. ШУЋУР[1], МИРА П. АНИЧИЋ[2], МИЛИЦА Н. ТОМАШЕВИЋ[2], ДАВОР З. АНТАНАСИЈЕВИЋ[3], АЛЕКСАНДРА А. ПЕРИЋ-ГРУЈИЋ[3] и МИРЈАНА Ђ. РИСТИЋ[3]

[1]*Народна библиотека Србије, Скерлићева 1, 11000 Београд,* [2]*Институт за физику, Универзитет у Београду, Прегревица 118, 11080 Земун и* [3]*Технолошко–металуршки факултет, Универзитет у Београду, Карнегијева 4, 11120 Београд*

Једна од последица интензивног економског и индустријског развоја је повећана емисија загађујућих супстанција у атмосферу. Дрвеће, посебно у урбаним срединама, веома је значајно са аспекта пречишћавања ваздуха; поред тога, уочено је да постоји корелација између концентрације појединих загађујућих материја у ваздуху и у лишћу дрвећа, што је искоришћено за биомониторинг квалитета ваздуха. У овом раду је испитивана могућност биомониторинга елемената у траговима у ваздуху помоћу две врсте листопадног дрвећа, дивљег кестена (*Aesculus hippocastanum*) и липе (*Tilia spp.*), које су веома заступљене у Београду. Узорци су сакупљани на почетку вегетационог периода, у мају, као и на крају вегетационог периода, у септембру, током пет година, од 2002. до 2006. године. У експерименталном делу извршена је анализа садржаја елемената у траговима (арсен, ванадијум, кадмијум) у листовима наведених врста дрвећа сакупљеним са три локације у Београду (Карађорђев парк, Студентски парк и Ботаничка башта), које су одабране због интензивног саобраћаја. Поређењем добијених вредности са концентрацијама испитиваних елемената у суспендованим честицама у ваздуху одређен је степен акумулације и закључено је да се испитиване врсте могу користити за биомониторинг квалитета ваздуха, односно његове загађености испитиваним елементима у траговима, при чему је дивљи кестен имао боље акумулативне способности.

(Примљено 19. марта, ревидирано 18. маја 2010)

REFERENCES

1. J. H. Seinfeld, S. N Pandis, *Atmospheric Chemistry and Physics: From Air Pollution to Climate Change*, Wiley, New York, 1998, pp. 21, 97
2. E. G. Pacyna, J. M. Pacyna, J. Fudala; E. Strzelecka-Jastrzab, S. Hlawiczka, D. Panasiuk, *Atmos. Environ.* **41** (2007) 8557
3. R. Bargagli, *Trace Elements in Terrestrial Plants: An Ecophysiological Approach to Biomonitoring and Biorecovery*, Springer-Verlag, Berlin, 1998
4. S. Rajšić, Z. Mijić, M. Tasić, M. Radenković, J. Joksić, *Environ. Chem. Lett.* **6** (2008) 95
5. K. P. Beckett, P. H. Freer-Smith, G. Taylor, *J. Arboric.* **26** (2000) 12
6. B. A. Markert, *Water Air Soil Pollut.* **64** (1992) 533
7. A. Alfani, G. Maisto, P. Iovieno, F. A. Rutigliano, G. Bartoli, *J. Plant Physiol.* **148** (1996) 243
8. G. Baycu, D. Tolunay, H. Ozden, G. Sureyya, *Environ. Pollut.* **143** (2006) 545
9. F. DeNicola, G. Maisto, M. V. Prati, A. Alfani, *Environ. Pollut.* **153** (2008) 376
10. M. Tomašević, Z. Vukmirović, S. Rajšić, M. Tasić, B. Stevanović, *Environ. Monit. Assess.* **137** (2008) 393
11. *WHO, Air Quality Guidelines for Europe*, 2nd ed., World Health Organization Regional Office for Europe, Copenhagen, 2000
12. N. D. Kim, J. E. Fergusson, *Environ. Pollut.* **86** (1994) 89

13. P. Kieffer, P. Schröder, J. Dommes, L. Hoffmann, J. Renaut, J.-F. Hausman, *J. Proteomics* **72** (2009) 379
14. N. Singh, L. Q. Maa, J. C. Vu, A. Raj, *Environ. Pollut.* **157** (2009) 2300
15. M. F. Hovmand, S. P. Nielsen, I. Johnsen, *Environ. Pollut.* **157** (2009) 404
16. D. Crnković, M. Ristić, D. Antonović, *Soil Sediment Contam.* **15** (2006) 581
17. M. D. Marjanović, M. M. Vukčević, D. G Antonović, S. I. Dimitrijević, Đ. M. Jovanović, M. N. Matavulj, M. Đ. Ristić, *J. Serb. Chem. Soc*. **74 (**2009) 697
18. I. Gržetić, R. H. A. Ghariani, *J. Serb. Chem. Soc*. **73 (**2008) 923
19. M. Tomašević, Z. Vukmirović, S. Rajšić, M. Tasić, B. Stevanović, *Chemosphere* **61** (2005) 753
20. E. Schneidemesser, E. A. Stone, T. A. Quraishi, M. M Shafer, J. J. Schauer, *Sci. Total Environ.* **408** (2010) 1640
21. B. Markert, *Water Air Soil Pollut.* **64 (**1992) 533
22. A. M. Žujić, B. B. Radak, D. A. Marković, *J. Serb. Chem. Soc*. **72** (2007) 889.